Synthesis of Value-Added Intermediates by Continuous Flow Technology

SMITH, LAURA,KATHERINE

Synthesis of Value-Added Intermediates by Continuous Flow Technology

Laura Katherine Smith

A thesis presented for the degree of

Doctor of Philosophy at Durham University

Department of Chemistry

12 November 2017

Abstract

We present three projects linked by our use of continuous flow chemistry in the synthesis of organic intermediates. The first is the synthesis of 1,1'-spirobiindane-7,7'-diol (SPINOL) in 6 steps and 32% overall yield. The synthesis has been improved over the previous literature protocols as it is safer, scalable, and higher-yielding, with better robustness and reproducibility. We introduce two attempts towards the enantioselective synthesis of SPINOL. In the second project, we have developed a flow process based on the Vapourtec reactor to synthesise coumalic acid and methyl coumalate from malic acid in concetrated sulfuric acid. A new heated rotating flow reactor is also presented for the intensified synthesis of coumalic acid, a valuable intermediate in organic synthesis derived from biorenewable sources of malic acid. Methyl coumalate has been used in two Diels-Alder reactions where the products have applications in molecular electronics and organic light-emitting diodes. Finally, the Darzens reaction for the synthesis of epoxides is presented here for the first time in flow, providing access to a range of benzaldehyde-derived products, including precursors to the pharmaceutical compound ibuprofen.

Contents

Declaration

The work in this thesis is based on research carried out within the Baxendale laboratory, in the Department of Chemistry at Durham University, UK. No part of this thesis has been submitted elsewhere for any other degree or qualification and it is all the author's own work unless stated otherwise in the text.

Acknowledgements

The author was sponsored by the Engineering and Physical Sciences Research Council, UK and the Royal Society, UK.

I would like to thank my supervisor, Prof Ian Baxendale, for his support during this challenging project. I would also like to thank the members of the Baxendale research group for their assistance and advice, in particular Dr Marcus Baumann, Dr Christian Stanetty and Dr Paolo Filipponi. Thanks must also go to students Joshua Goswell, Hubert Abberton and Lauriane Peyrical for their collaborative work on several projects, and my co-supervisor Prof Graham Sandford. I would particularly like to thank the staff of the Analytical Services at Durham University (NMR, Mass Spectrometry, Elemental Analysis, Chromatography and X-Ray Crystallography), the mechanical and glass-blowing workshops, and members of the Integrated Chemical Reaction Facility in the Department of Chemistry.

Finally, I would like to thank my family and friends for their unending support throughout the whole of my PhD.

List of Abbreviations

3D	three-dimensional	LUMO	lowest-unoccupied molecular orbital
Å	10^{-10} metres	m	medium intensity (IR spectroscopy)
Ac	acetyl	m	multiplet (NMR spectroscopy)
Ar	aryl	*m*	meta
ASAP	Atmospheric Solids Analysis Probe (mass spectrometry)	M	moles per litre
atm	atmospheres	MA	malic acid
BINAP	2,2-*bis*(diphenylphosphino)-1,1-binaphthalene	MC	methyl coumalate
BINOL	1,1'-bi-2-naphthol	MCA	methyl chloroacetate
Bn	benzyl	MDMP	methyl-3,3-dimethoxypropionate
Boc	*tert*-butyloxycarbonyl	Me	methyl
BOX	*bis*(oxazoline)	MeOD	deuterated methanol
usbr	broad (NMR and IR spectroscopies)	MHz	megahertz
Br-SPINOL	4,4'-dibromo-2,2',3,3'-tetrahydro-1,1'-spirobi[indene]-7,7'diol	mins	minutes
Br-SPINOMe	4,4'-dibromo-7,7'-dimethoxy-1,1'-spirobiindane	mL	millilitres
Bu	butyl	mm	millimetres
CA	coumalic acid	mmol	millimoles
CBS	Corey-Bakshi-Shibata catalyst	mol	moles
cm^{-1}	inverse centimetre	mol.	molecular
COD	cycloocta-1,5-diene	mp	melting point
conc.	concentrated	Ms	mesyl
COSY	correlation spectroscopy (NMR spectroscopy)	NBLP	*N*-Boc-l-phenylglycine
CSA	camphorsulfonic acid	NBS	*N*-bromosuccinimide

d	days	NCS	*N*-chlorosuccinimide
d	doublet (NMR spectroscopy)	nm	nanometres
DABCO	1,4-diazabicyclo[2.2.2]octane	NMR	nuclear magnetic resonance
DBSPINOL	4,4'-dibromo-2,2',3,3'-tetrahydro-1,1'-spirobiindene-7,7'-diol	NOESY	Nuclear Overhauser Effect Spectroscopy (NMR spectroscopy)
DBU	1,8-diazabicycloundec-7-ene	NSAID	non-steroidal anti-inflammatory drug
DCE	1,2-dichloroethane	*o*	ortho
DCM	dichloromethane	OD	outer diameter
dd	doublet of doublets (NMR spectroscopy)	OLEDs	organic light-emitting diodes
ddd	doublet of doublet of doublets (NMR spectroscopy)	o/n	overnight
ddt	doublet of doublet of triplets (NMR spectroscopy)	*o*-SPINOMe	7,7'-dimethoxy-1,1'-spirobiindane
DEPT	distortionless enhancement through polarisation transfer	*o*-SPINOMs	7,7'-dimesylate-1,1'-spirobiindane
dm	decimetres	*p*	para
DMAP	4-dimethylaminopyridine	pd	pentet of doublets (NMR spectroscopy)
DME	dimethoxyethane	pet.	petroleum
DMF	dimethylformamide	Ph	phenyl
DMSO	dimethylsulfoxide	Phe	phenylalanine
d_6−DMSO	deuterated dimethylsulfoxide	pin	pinacol
DOE	Design of Experiments	PMHS	polymethylhydrosiloxane
dppe	1,2-*bis*(diphenylphosphino)ethane	POM	polyoxometalate
dq	doublet of quartets (NMR spectroscopy)	ppb	parts per billion
dr	diastereomeric ratio	ppm	parts per million
dt	doublet of triplets (NMR spectroscopy)	Pr	propyl

e^-	electron	*p*-SPINOL	1,1'-spirobiindane-5,5'-diol
ECA	ethyl chloroacetate	*p*-SPINOMe	5,5'-dimethoxy-1,1'-spirobiindane
EDG	electron-donating group	*p*-SPINOMs	5,5'-dimesylate-1,1'-spirobiindane
ee	enantiomeric excess	PTFE	polytetrafluoroethylene
EG	ethylene glycol	*p*-TsOH	*p*-toluenesulfonic acid
Eqn.	equation		
equiv.	equivalents	PTTL	*N*-phthaloyl-(*S*)-tert-leucinate
et al.	*et alia*	Pyr	pyridine
ES	electrospray	q	quartet (NMR spectroscopy)
Et	ethyl	QP-DMA	QuadraPure dimethylamine
EWG	electron-withdrawing group	qq	quartet of quartets (NMR spectroscopy)
FEP	fluorinated ethylene propylene		
FT-IR	Fourier-transform infrared	RBF	round-bottomed flask
g	grams	rpm	rotations per minute
h	hours	R_t	retention time
h	heptet (NMR spectroscopy)	RT	room temperature
HeRo	heated rotating reactor	RTP	room temperature and pressure
Hex	hexanes	s	singlet (NMR spectroscopy)
HMAF	hydroxymethylacylfulvene	s	strong intensity (IR spectroscopy)
HOMO	highest-occupied molecular orbital	sat.	saturated
HPA	heteropoly acid	sp.	species
HPLC	high performance liquid chromatography	SPINOL	1,1'-spirobiindane-7,7'-diol
HPMoV	$H_5PMo_{10}V_2O_{40} \cdot xH_2O$	t	triplet (NMR spectroscopy)

HRMS	high resolution mass spectroscopy	TBAB	*tetra*-butylammonium bromide
HWE	Horner-Wadsworth-Emmons	TBS	*tert*-butyldimethylsilyl
Hz	Hertz	THF	tetrahydrofuran
IBBA	isobutylbenzaldehyde	Tf	triflate
ID	inner diameter	TLC	thin layer chromatography
IPA	isopropyl acetate	TPA	*tris*-(2-pyridylmethyl)amine
IR	infrared	Ts	tosyl
IUPAC	International Union of Pure and Applied Chemistry	Val	valine
J	coupling constant (NMR spectroscopy)	wt	weight
JMP	Statistical software	μW	microwave
L*	chiral ligand	ν	wavenumber (IR spectroscopy)
LCMS	liquid chromatography mass spectrometry	w	weak intensity (IR spectroscopy)
LD_{50}	median lethal dose	δ	chemical shift (NMR spectroscopy)
LDA	Lithium diisopropylamide	Δ	error (mass spectrometry)
Leu	leucine		

Part I

Synthesis of Spirocyclic Compounds

Chapter 1

Literature Review

Spirocycles are two rings that share a common atom. The spiro motif is increasingly found in drug candidates, and has historically been observed in many natural products.[1] They are also a key structural component in several promising classes of privileged chiral ligands used in asymmetric synthesis, such as 1,1'-spirobiindane-7,7'-diol (SPINOL). Restricted rotation and high rigidity at the spiro centre can assist in improving enantiomeric excess in asymmetric reactions. However, it is very challenging to synthesise quaternary carbon centres asymmetrically,[2] and the stereocontrolled preparation of spiro products[3–5] adds further difficulty.

Up until very recently,[6] the synthesis of SPINOL has been achiral and inefficient, due to several poorly-yielding steps and the resolution into enantiomers at the end of the synthesis.[7–10] In this literature review, we will examine how the use of continuous flow technology may improve the efficiency of this process. We will also outline several strategies towards an asymmetric synthesis of SPINOL, which we will re-visit in the Results and Discussion section.

1.1 Flow chemistry

Flow chemistry uses a series of pumps (HPLC, peristaltic or syringe) connected to tubing to mix reagents in a continuous fashion. Systems can incorporate reactors, which are coils of tubing or reactor chips which can be temperature-controlled. It is also possible to customise systems to incorporate glass columns containing, for example, solid-supported reagents or catalyst-packed bed reactor units. Systems can be on a micro- (sub-millimetre capillary flow path), meso- (millimetre to centimetre) or macrofluidic (super-centimetre) scale, with controlled mixing in chips, static mixers, T-pieces or other mixing elements.[11] Flow chemistry is complementary to traditional batch chemistry, and can offer many advantages.[12] For example, photochemistry is a particular beneficiary due to the increased surface-

to-volume ratio, exposing reagents to more focused light than can be achieved in a batch set-up. Chemistry can be more sustainable and systems can be run in continuous flow mode, facilitating easy scale-up. Flow can enhance reaction optimisation by reducing reaction times (often minutes compared to hours, for example) and work-up procedures, by incorporating scavenging systems or columns for purification.[13] In-line analysis assists in the monitoring and control of reactions. One particularly important advantage is increased safety: hazardous or volatile chemicals such as azides,[14–17] diazoketones[18] or bromine[19–23] can be contained within the system, reducing the user's exposure. Reactive intermediates can be taken forward in multi-step processes without isolation, allowing long reaction sequences to be built up.

Catalysis in flow

A brief overview of asymmetric catalysis in flow systems will be given below.

Homogeneous catalysis in flow

Homogeneous catalysis requires a catalyst to be dissolved in a solution with the substrates. It has several advantages over heterogeneous catalysis, including better activity and enantioselectivity, and easier preparation and monitoring. However, the major drawback is the difficulty in removing the catalyst at the end of a reaction. This can lead to large-scale production problems due to separation and recycling of the catalyst, as well as product contamination by leaching of the metal and/ or ligand into the product. Attempting homogeneous catalysis in flow can speed up catalyst screening and process optimisation. In batch, enantioselective reactions are typically run at lower temperatures to improve enantiomeric excess whereas flow reactions are typically run at higher temperatures, which in theory should lead to poorer enantioselectivity. Integrated analysis using IR spectroscopy[24] or mass spectrometry[25] is possible, enabling rapid profiling of reaction conditions, although monitoring enantioselectivity is still a challenging area and requires much more research.

Another advantage of homogeneous catalysis in flow is the possibility of performing multi-step transformations without isolating unstable intermediates, as found in the asymmetric carbolithiation of conjugated enynes, where an organolithium intermediate is generated in a flow microreactor and reacted with an electrophile before it epimerises (Scheme 1.1).[26]

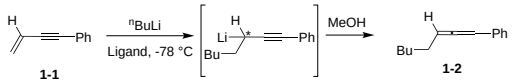

Scheme 1.1 Carbolithiation of a conjugated enyne.

A further example is highlighted by a tube-in-tube gas-liquid flow reactor which has been used for homogeneous asymmetric hydrogenation (Scheme 1.2).[27]

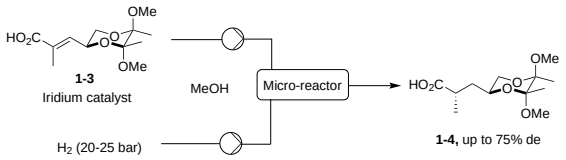

Scheme 1.2 Tube-in-tube gas-liquid reactor for asymmetric hydrogenation.

Homogeneous catalysis when used in flow can require lower catalyst loadings compared to batch reactions, as illustrated in the case of an organocatalysed asymmetric aldol reaction (Scheme 1.3).[28]

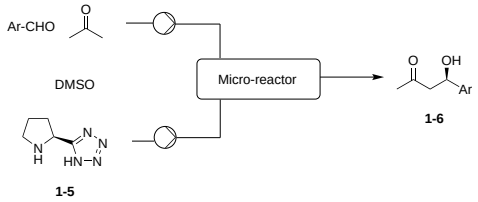

Scheme 1.3 5-(Pyrrolidin-2-yl)tetrazole-catalysed asymmetric aldol reaction.

Heterogeneous catalysis in flow

Many homogeneous catalysts can potentially be immobilised to form a heterogeneous catalyst, whilst attempting to retain selectivity and catalyst activity which are often reduced by immobilisation. Heterogeneous catalysts can be polymer-supported by covalent bonding between the ligand and the support, self-supported, or attached to a medium *via* adsorption, hydrogen bonding or electrostatic interactions. Other media include ionic liquids[29] and supercritical fluids.[30] Advantages over homogeneous catalysts include simultaneous reaction and separation, as well as improved recyclability which helps reduce costs. In flow, there is no mechanical stirring, so that the support material is not mechanically degraded. Crucially, the product will not be contaminated by the catalyst if it is immobilised.

The most common immobilisation strategy is attachment to a polymer support, which forms a covalent bond between the ligand and the polymer backbone support. This requires functionality that can interact with the support, which can create synthetic challenges in ligand design. An example is a

polystyrene-supported proline derivative used in an organocatalytic asymmetric α-aminoxylation of an aldehyde (Scheme 1.4).[31] The immobilised catalyst was prepared by the Cu(I)-catalysed cycloaddition of azidomethylpolystyrene and a propargyloxyproline derivative.

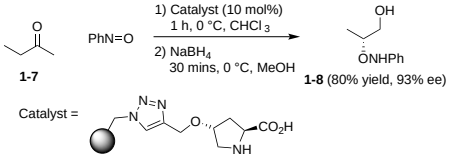

Scheme 1.4 α-Aminoxylation of aldehyde with a polystyrene-supported catalyst. Step 1 is in flow.

Metal-organic frameworks can also be used as heterogeneous catalysts. Mixing BINOL-phosphoramidite ligands with $[Rh(COD)_2]BF_4$ leads to self-assembly to form a catalyst which has been used in asymmetric flow hydrogenation (Scheme 1.5).[32]

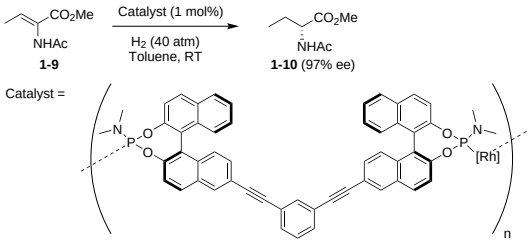

Scheme 1.5 Asymmetric hydrogenation with a self-supported Rh-monoPhos catalyst.

Asymmetric hydrogenation can also be achieved by using a rhodium catalyst immobilised on Al_2O_3, held in place by simple electrostatic interactions (Scheme 1.6).[33]

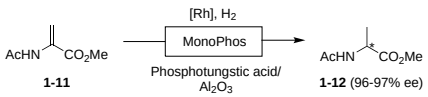

Scheme 1.6 Asymmetric hydrogenation using a Rh-monoPhos catalyst immobilised on Al_2O_3.

Weaker van der Waals' interactions can be used to hold the support and catalyst together. This makes immobilisation straightforward, but since binding is weak, increased catalyst leaching into the product is observed. An example of this mode of binding is media other than polymers. This increases the ease of separation and catalyst recovery. These media have been used in hydrogenation, cyclopropanation and hydroformylation reactions (Scheme 1.7).[34,35]

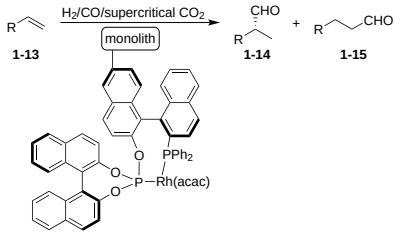

Scheme 1.7 Asymmetric alkene hydroformylation using a supported Rh-BINAPhos catalyst in supercritical CO_2.

1.2 Asymmetric synthesis in organic chemistry

Strategies for the synthesis of chiral compounds

Enantioselective synthesis is defined by IUPAC as a reaction which creates at least one new element of chirality in a substrate, to give stereoisomeric products in unequal amounts.[36] There are several methods that can be employed to achieve these results, and these are summarised below.

Chiral pool

The chiral pool approach uses cheap and readily available, mainly naturally-occurring starting materials such as amino acids or sugars. The chirality of the starting material is incorporated in full or part into the product.

Chiral auxiliaries

An enantiomerically pure compound is covalently attached to a substrate, which is followed by a diastereoselective reaction which ideally gives only one enantiomer of the product. The chiral auxiliary is then removed, and it is sometimes possible to recycle this auxiliary. Examples include Evans' oxazolidinone and ephedrine derivatives (Fig. 1.1).

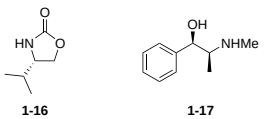

Fig. 1.1 An Evans' oxazolidinone and an ephedrine derivative.

Myers *et al.* used enolates of pseudoephedrine amides as chiral auxiliaries in a diastereoselective alkylation with alkyl halides.[37] Following asymmetric alkylation, pseudoephedrine could be regenerated in excellent yields by a simple extractive work-up (Scheme 1.8).

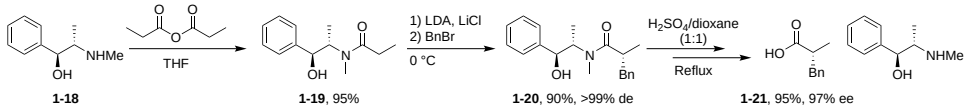

Scheme 1.8 A pseudoephedrine derivative as a chiral auxiliary in an asymmetric alkylation.

Chiral reagents

A chiral reagent is reacted with an achiral substrate to give a chiral product. The advantage of this method over the use of chiral auxiliaries is that there are no addition/ cleavage steps. However, it requires stoichiometric amounts of a chiral reagent which can be expensive.

An example of a widely-used chiral reagent is L-aspartic acid, which is used in diastereoselective alkylations.[38] An example is shown below (Scheme 1.9).[39]

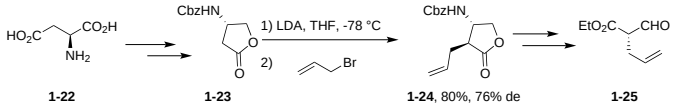

Scheme 1.9 L-Aspartic acid as a chiral reagent in a diastereoselective alkylation reaction.

Asymmetric catalysis

The preferred method to achieve enantioselective synthesis is asymmetric catalysis, where one chiral molecule is used to effect an enantioselective reaction that gives many molecules of the chiral product, known as chiral amplification. A chiral catalyst can be formed by the coordination of chiral ligands to a metal atom.

The Corey-Bakshi-Shibata catalyst, a chiral oxazaborolidine, is a well-known example. It has been used in an enantioselective catalytic reduction of an achiral chloromethyl ketone, with borane as a stoichiometric reductant (Scheme 1.10).[40]

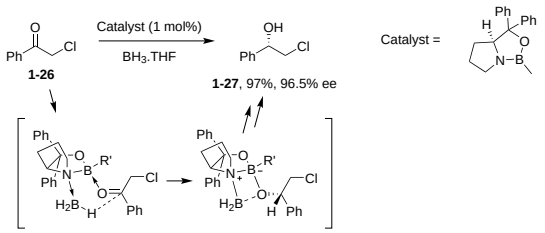

Scheme 1.10 The Corey-Bakshi-Shibata oxazaborolidine as a catalyst in an asymmetric reduction of a ketone.

Privileged ligand classes

Ligands that catalyse a broad range of enantioselective reactions with high selectivity, requiring little or no change in the ligand structure are also known as privileged ligands. Many possess a rigid chiral backbone and an axis of chirality (atropisomerism). The conditions for atropisomerism are the possession of a rotationally stable axis and different substituents on both sides of the axis. Examples of privileged ligands include chiral salen derivatives, *bis*(oxazoline)s, cinchona alkaloid derivatives and the binapthalenes BINAP and BINOL (Fig. 1.2).

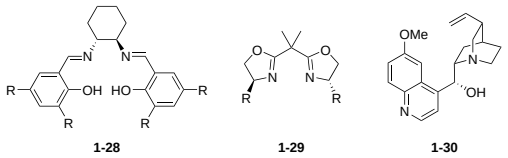

Fig. 1.2 Chiral salen, *bis*(oxazoline)s and cinchona alkaloid derivatives.

BINOL and BINAP

BINOL and BINAP are biaryl compounds with *ortho* substituents that are large enough to prevent free rotation around the C-C single bond. They are highly versatile ligands for asymmetric synthesis, and their structures are shown below (Fig. 1.3).

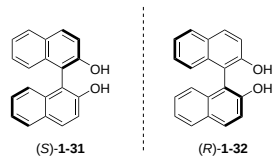

Fig. 1.3 Structures of (*R*)- and (*S*)-BINOL.

BINOL and BINAP can be synthesised *via* the following route (Scheme 1.11).[41]

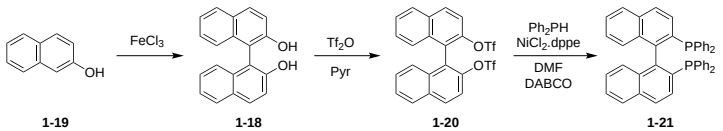

Scheme 1.11 Synthesis of BINOL and BINAP.

BINOL can be resolved into its enantiomers by three different methods. The first is the addition of *N*-benzylcinchonidium chloride. The (*S*)-enantiomer is a crystalline inclusion compound which dissolves in MeCN whereas the (*R*)-enantiomer is not. Alternatively, BINOL can be reacted with pentanoyl chloride and the enzyme cholesterol esterase added. The enzyme can hydrolyse the

(*S*)-diester but not the (*R*)-diester. Finally, preparative HPLC with a chiral stationary phase can be used to separate the enantiomers.

BINOL is capable of catalysing a wide variety of reactions, whether as a ligand attached to a metal or as an organocatalyst on its own.[42,43] Its derivatives can also be used in reduction and oxidation reactions, and can be used as Lewis or Brønsted acid catalysts in C-C bond formation (Scheme 1.12), as well as bifunctional acid/ base catalysts.

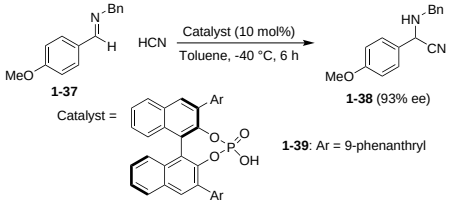

Scheme 1.12 An example of using a (*R*)-BINOL derivative as a Brønsted acid in an asymmetric Strecker reaction.[44]

Binapthyl phosphoric acids have been particularly well studied, and their chirality-inducing behaviour is derived from the steric environment that the two bulky napthyl groups provide. Viewing from two different angles demonstrates this perspective in terms of quadrants (Fig. 1.4).[45]

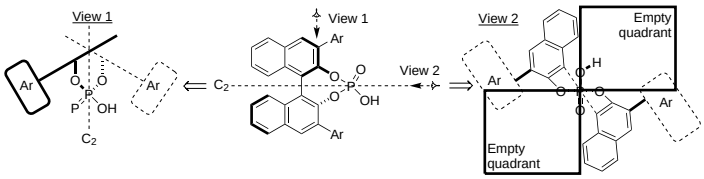

Fig. 1.4 Structures of (View 1: top-down view of BINOL-phosphoric acid; View 2: quadrant view of BINOL phosphoric acid.

This quadrant view can similarly describe BINAP. Examples of reactions catalysed by BINAP are more common, and include hydrogenations of olefins and ketones (Scheme 1.13), isomerisation of allylamines, hydroboration, allylic alkylation, Heck reaction, aldol and Mannich reactions, Michael-type reactions, conjugate additions using organoboron and Grignard reactions, Diels-Alder reactions, ene reactions, cyclisations and ring-opening reactions.[46]

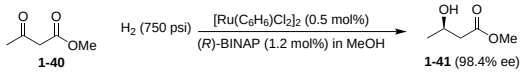

Scheme 1.13 An example of using (*R*)-BINAP as a chiral ligand in an asymmetric hydrogenation of β keto-esters.[47]

Axial chirality and bite angles

Many of the privileged ligand classes discussed above exhibit axial chirality, where the molecules possess an axis of chirality rather than a stereogenic centre. Biaryl compounds must have *ortho* substituents that are sufficiently large to prevent rotation around the C-C single bond, such as in BINOL and BINAP to maintain their chirality. The two atropisomers of BINOL, (*R*)- and (*S*)-BINOL are illustrated below (Fig. 1.5).

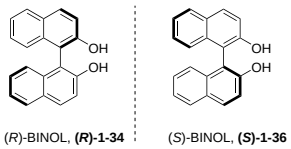

Fig. 1.5 Enantiomers (atropisomers) of a an axially chiral binapthyl ligand, BINOL.

The X-ray crystal structure of (*R*)-BINOL is shown below (Fig. 1.6).[48]

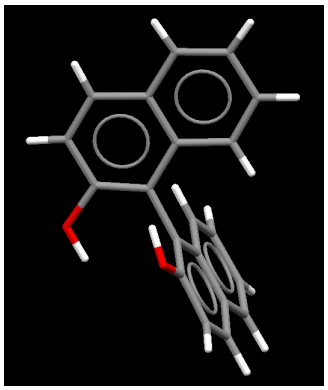

Fig. 1.6 (*R*)-BINOL X-ray crystal structure.

Spirobiindanes also require substituents to restrict rotation and thus render them chiral. (±)-SPINOL has been re-drawn in 3D to emphasise its rigidity and lack of rotational ability (Fig. 1.7).

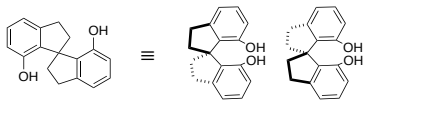

Fig. 1.7 Racemic SPINOL re-drawn in 3D, with its (*R*)- and (*S*)-enantiomers.

The X-ray crystal structure of SPINOL is shown below (Fig. 1.8).[49]

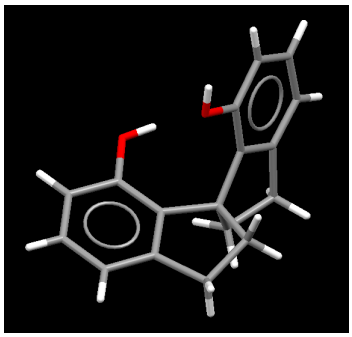

Fig. 1.8 SPINOL X-ray crystal structure.

The bite angle, β_n, of a bidentate ligand is measured by the X-metal-X angle (Fig. 1.9).[50]

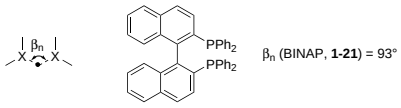

Fig. 1.9 The bite angle, β_n, and the bite angle of the BINAP ligand.

A wide bite angle has both steric and electronic effects on a complex: it increases the bulk of the bidentate ligand, and favours or disfavours certain geometries of transition metal complexes. BINAP has a relatively wide bite angle. SPINOL systems have an altered bite angle of bidentate coordination compared to these binapthyl systems: for example, Zhou *et al.* reported a bite angle of 87.91° for the (*S*,*S*)-SIPHOX ligand shown below (Fig. 1.10).[51] Changing the bite angle of a complex can affect the enantioselectivity and rate of a reaction.[45,52]

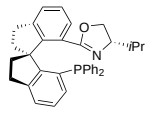

(*S*,*S*)-SIPHOX, **(*S*,*S*)-1-43**

Fig. 1.10 A phosphine-oxazoline ligand (SIPHOX) with a bite angle reported when chelated to an iridium complex.

1.3 1,1'-Spirobiindane-7,7'-diol (SPINOL)

1,1'-Spirobiindane-7,7'-diol (SPINOL) possesses a rigid spirobiindane backbone, with two phenol groups. When viewed in three dimensions, the phenol groups are relatively close to each other in space (Fig. 1.11).[9]

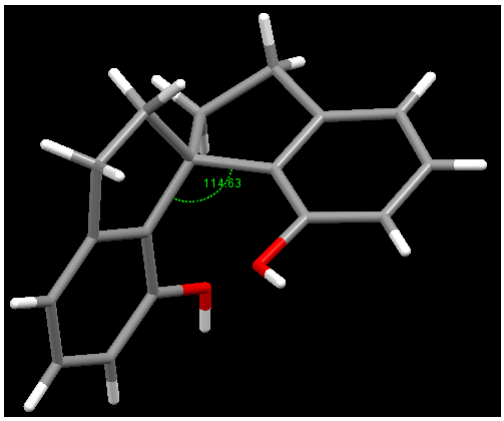

Fig. 1.11 X-ray crystal structure of 1,1'-spirobiindane-7,7'-diol.

This forms a relatively small bite angle and a sterically differentiated 3D site for catalysis. The pK_a of the phenol groups is substantially lower than that of free phenol and thus SPINOL is more Lewis acidic than phenol.[53]

Spirocarbocycles in natural products

Natural products containing the spirocycle motif are well-documented in the literature, for example as spirooxindoles.[54,55] They are also becoming more common in drugs due to their increased three-dimensionality for potential improved specificity, and novelty for patenting purposes.[56] The total synthesis of natural products containing spirocarbocycles utilises many reactions including the aldol, Diels-Alder, and Claisen reactions, as well as ring-closing metathesis and reactions promoted by acid, base and light.[1]

Ligands and organocatalysts derived from SPINOL

Once synthesised and resolved, SPINOL can be derivatised to form other useful compounds which can act as ligands and/ or organocatalysts in asymmetric processes. Several of the most common analogues are summarised in the diagram below (Fig. 1.12).

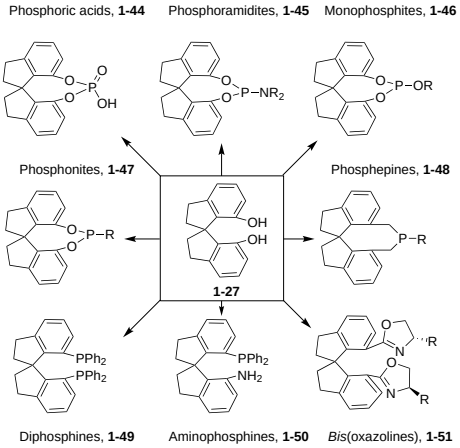

Fig. 1.12 Summary of selected derivatives of SPINOL.

Literature syntheses of SPINOL

In 1999, Birman *et al.* reported the first literature synthesis of SPINOL,[7] starting from 3-methoxybenzaldehyde and proceeding in 28% overall yield over 6 steps (Scheme 1.14).[7]

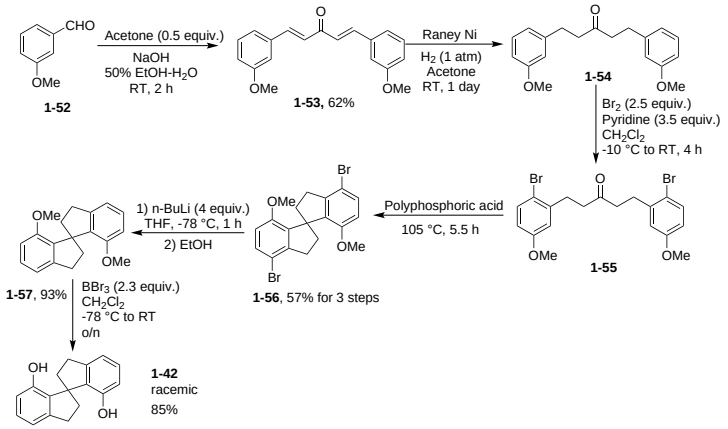

Scheme 1.14 The Birman synthesis of SPINOL.

Since then, there have been various incremental improvements to the synthesis process. Shan *et al.* used a range of heteropoly acids to spirocyclise various pentanones, and improved the yield of Br-SPINOMe from 66% to 80% (Scheme 1.15).[8]

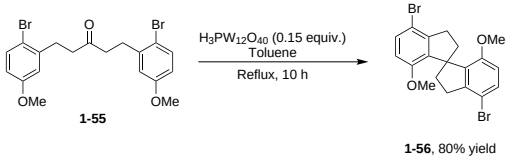

Scheme 1.15 Improved spirocyclisation of 1,5-*bis*(2-bromo-5-methoxyphenyl)pentan-3-one using phosphotungstic acid.

The original synthesis is not asymmetric, and thus requires a final resolving step to separate the (*R*)- and (*S*)-enantiomers of SPINOL. The original paper used (–)-menthyl chloroformate, followed by separation of the diastereomers by column chromatography (Scheme 1.16).

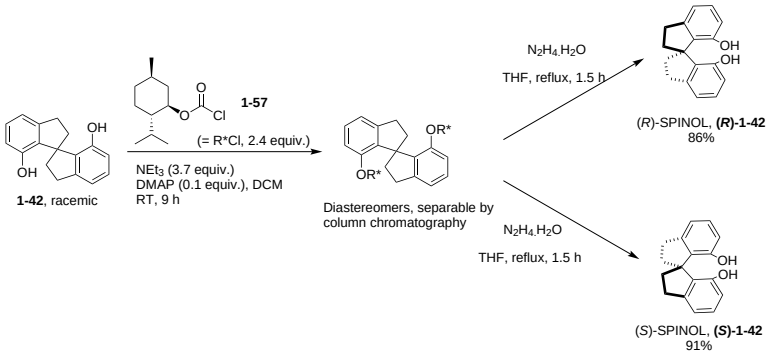

Scheme 1.16 Resolution of SPINOL using (–)-menthyl chloroformate.

In 2002, a simpler and more reproducible method was published by Zhou *et al.* that used the co-crystallisation of SPINOL with *N*-benzyl cinchonidium chloride (Scheme 1.17).[9]

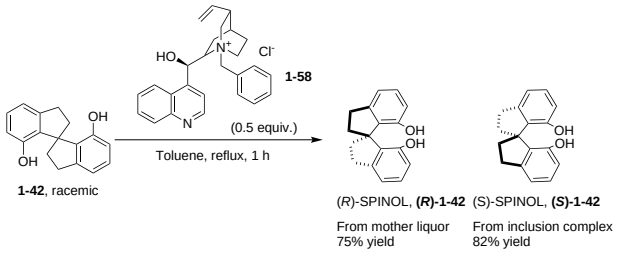

Scheme 1.17 Resolution of SPINOL with *N*-benzylcinchonidium chloride.

Two years later, a further method was used to separate the enantiomers of dibrominated SPINOL (DBSPINOL).[10] Transformation with (–)-menthyl chloroformate followed by recrystallisation permitted separation of the dibrominated products in high yields (Scheme 1.18).

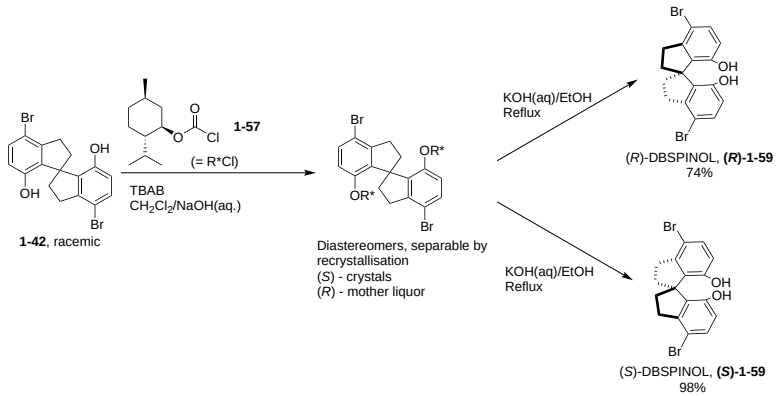

Scheme 1.18 Resolution of DBSPINOL with (–)-menthyl chloroformate.

1.4 Asymmetric approaches to SPINOL

We were interested in investigating several routes to an asymmetric synthesis of SPINOL. These included the use of chiral auxiliaries and the asymmetric addition of an aryl ring to an alkene. A further suggestion not investigated in detail here is an approach involving the generation of a chiral tight-ion pair (Scheme 1.19).[57]

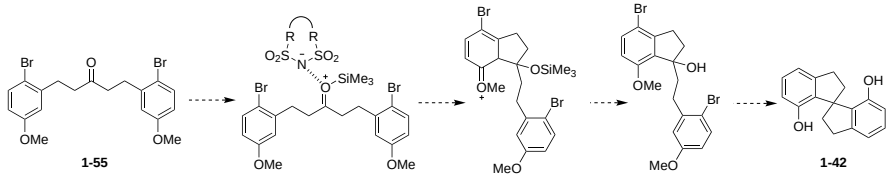

Scheme 1.19 Suggested tight-ion pair approach to SPINOL.

Enantioselective catalysis

There are four key activation modes for asymmetric catalysis: Lewis acid catalysis, hydrogen-bonding catalysis, Brønsted acid catalysis, and chiral anion catalysis.[57] In a tight ion pair, there are no solvent molecules between the anion and cation, and the individual ions keep their stereochemical configuration. In chiral anion catalysis, an achiral but catalytically active species is combined with a chiral counterion. In a non-polar medium, these species form a tight ion pair, and the counterion is able to influence the stereochemical outcome of a reaction.

Whether the transition state of the reaction is early or late according to Hammond's postulate is important in being able to control the stereochemistry of the product. There are two places to generate chirality in the synthesis of SPINOL: either through the attack on the original carbonyl in the ketone starting material, or by control of the attack on the enantiotopic faces of a carbocation formed during the reaction. One theoretical mechanism for the spirocyclisation

is through the formation of a very reactive tertiary benzylic alcohol intermediate (Scheme 1.20). This represents an earlier transition state.

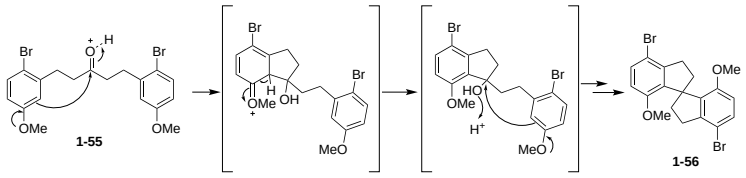

Scheme 1.20 Postulated tertiary alcohol intermediate in the synthesis of SPINOL.

This alcohol is itself a chiral centre which can act to influence the angle of the subsequent attack on the tertiary carbocation centre by potentially blocking one of the enantiotopic faces (Scheme 1.21).

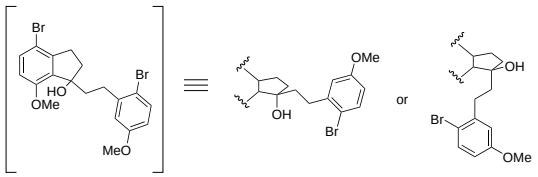

Scheme 1.21 Postulated 'blocking' of one face during addition in the synthesis of SPINOL.

However, this chiral information may be lost if the alcohol is highly labile. Its loss would form a tertiary carbocation which can be stabilised by resonance, through the involvement of the aromatic methoxy group (Scheme 1.22).

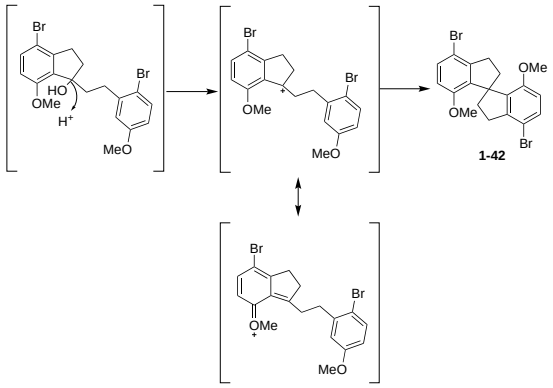

Scheme 1.22 Postulated tertiary carbocation transition state in the synthesis of SPINOL.

At this point, any stereochemical control would depend on being able to 'choose' which enantiotopic face of the carbocation is blocked.

Asymmetric alkene cyclisation

As discussed in the chiral auxiliary route above, we are interested in the tertiary intermediate during the spirocyclisation process (Fig. 1.13).

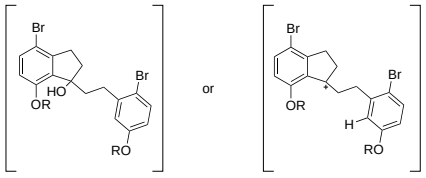

Fig. 1.13 Postulated tertiary intermediates in the synthesis of SPINOL.

We hypothesised that an alkene could be substituted for this intermediate, and that the subsequent cyclisation can be enantioselectively controlled (Scheme 1.23) through the use of a chiral acid catalyst. The carbocation can be stabilised through resonance. If the diphenolic groups are not protected as the dimethoxy equivalent, autocatalysis may even be possible by harnessing the enhanced acidity of the resultant diphenolic spiro product.

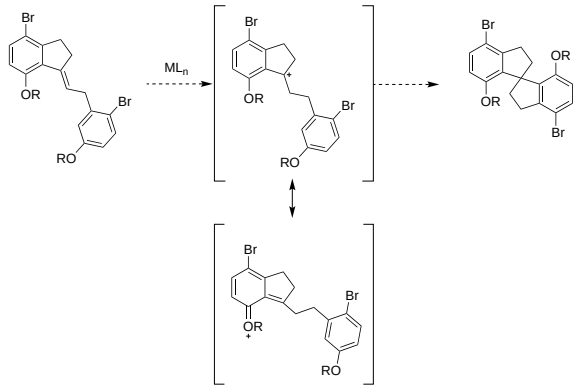

Scheme 1.23 Hypothesised cyclisation of an alkene intermediate in the synthesis of SPINOL.

This alkene could be protonated to generate a carbocation-like intermediate for cyclisation, for example by Brønsted acid catalysis (Scheme 1.24).[58–62]

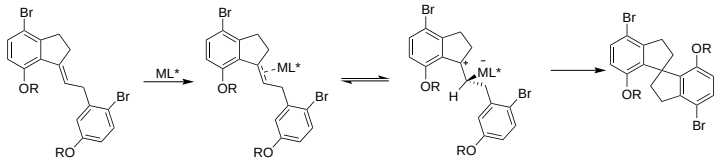

Scheme 1.24 Suggested Brønsted acid catalysis in the synthesis of SPINOL.

There is some literature precedent for asymmetric addition to an alkene in the presence of a chiral ligand.[63–65]

Toste *et al.* have used gold(I)-catalysis for the intramolecular addition of amines into unactivated alkenes (Scheme 1.25), first using an alkylgold complex,[64] and later using gold(I)/menthol cooperative catalysis.[63]

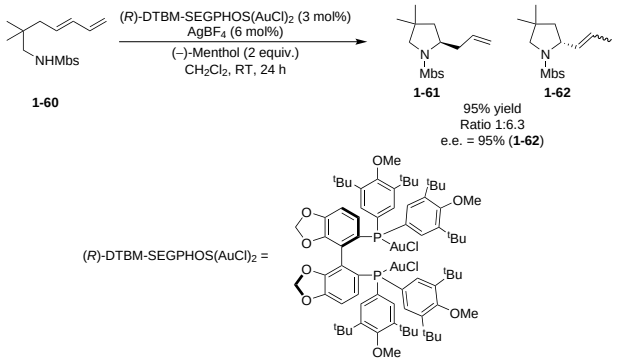

Scheme 1.25 Asymmetric Au(I)-catalysed hydroamination of a diene.

Additions to unactivated alkenes have been the topic of a recent review.[66]

We have seen how the incorporation of continuous flow technology is an important development in synthetic organic chemistry, and how it may be possible to influence the mechanism of SPINOL formation to give an asymmetric synthesis of this valuable compound.

Chapter 2

Project Aims

The first aim of the project was to synthesise (±)-SPINOL in batch, with the aim of eventually investigating an enantioselective synthesis.

It was first examined whether it was possible to improve the literature synthesis of SPINOL by incorporating continuous flow technologies. Several or all of the planned steps may be possible in flow, with a focus on bromination and hydrogenation as easily translated steps. Two key starting compounds will be considered, 3-hydroxybenzaldehyde and 3-methoxybenzaldehyde, and the necessity and efficiency of each step will be examined. The spirocyclisation step in particular will be investigated in detail, exploring the reagents and conditions required to optimise this crucial step.

Next, approaches to the asymmetric synthesis of SPINOL will be investigated. These will start with the use of diols derived from amino acids as chiral auxiliaries. The second route will be *via* an indanone intermediate, targeting an asymmetric alkene addition as the spirocyclisation step.

Finally, the chapter will end with the conclusions which can be drawn, and suggestions for future work.

Chapter 3

Attempted Synthesis of (±)-SPINOL from Hydroxybenzaldehydes

Retrosynthetic analysis of (±)-SPINOL implies that it may be directly synthesised in three steps from 3-hydroxybenzaldehyde and acetone (Scheme 3.1).

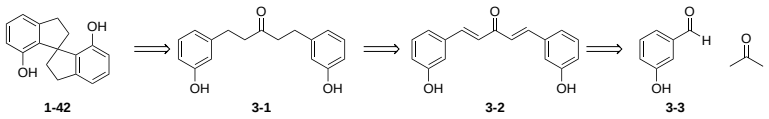

Scheme 3.1 Retrosynthetic analysis of (±)-SPINOL.

3.1 Starting from 3-hydroxybenzaldehyde

The first synthetic route attempted started from 3-hydroxybenzaldehyde. It was envisaged that the first step would comprise a double aldol condensation, followed by conjugate reduction and finally the desired spirocyclisation (Scheme 3.2).

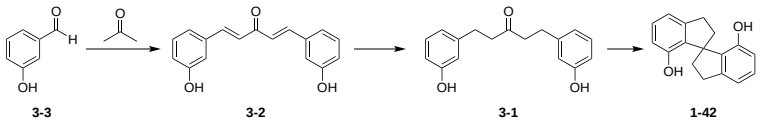

Scheme 3.2 Proposed synthetic route to (±)-SPINOL.

During the synthesis of 1,5-*bis*(3-hydroxyphenyl)penta-1,4-dien-3-one, a method was developed by adapting conditions for the synthesis of related compounds by Dolliver[67] and Ding.[68] This new method used 5 equivalents of 10% NaOH, and a solvent mixture of EtOH−H_2O (ratio 4:5) (Scheme 3.3). The aldehyde starting material and acetone were added in two portions, and the mixture

was heated at 25 °C for between 2-4 h, with a longer heating period required for larger scales. This maximised the conversion of 3-hydroxybenzaldehyde to the desired pentadienone product.

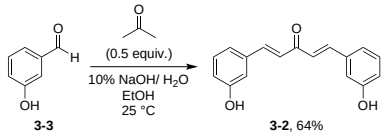

Scheme 3.3 Dolliver-Ding aldol condensation of 3-hydroxybenzaldehyde with acetone.

Recrystallisation of the crude product from IPA gave the pentadienone product in 64% overall yield (99% pure by ^{1}H NMR spectroscopy).

After screening many conditions for the conjugate reduction of the α,β-unsaturated ketone to the pentanone, the most successful was found to be treatment with Pd/C under a 1 bar H_2 atmosphere with Ph_2S as a catalyst poison (Scheme 3.5). Without the poison, the over-reduced pentane was observed as the major product (Scheme 3.4).

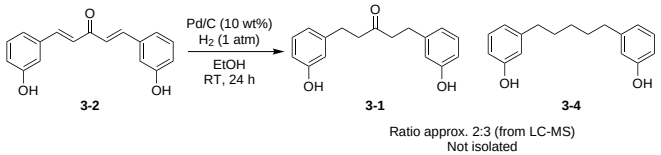

Scheme 3.4 Batch reduction of 1,5-*bis*(3-hydroxyphenyl)penta-1,4-dien-3-one using Pd/C.

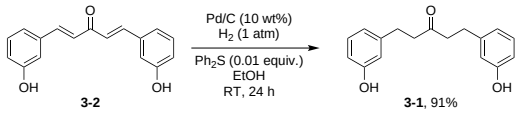

Scheme 3.5 Batch reduction of 1,5-*bis*(3-hydroxyphenyl)penta-1,4-dien-3-one using Pd/C and Ph_2S.

The pentanone was obtained as the sole product of hydrogenation, in excellent yield and with no need for further purification.

The reaction was next transferred to the H-Cube® reactor, with some screening of suitable conditions which are summarised in Table 3.1 below. The reaction was always run using the full H_2 production mode,* and with 1 bar pressure (Scheme 3.6). The conversion values were determined by ^{1}H NMR spectroscopy.

*Described as approx. 30 mL min^{-1} at atmospheric pressure in correspondence with ThalesNano Inc.

Table 3.1 Screening of conditions for the flow reduction of 1,5-*bis*(3-hydroxyphenyl)penta-1,4-dien-3-one, poisoned with Ph_2S (0.01 equivalents).

Scheme 3.6 Flow reduction of 1,5-*bis*(3-hydroxyphenyl)penta-1,4-dien-3-one.

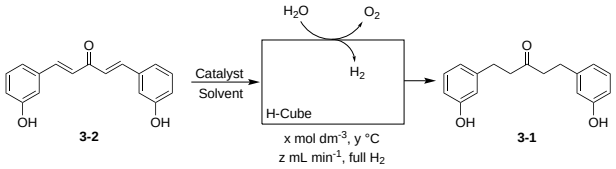

Entry	Catalyst	Solvent	Temp. /°C	Flow rate /mL min^{-1}	% Conversion	% Yield
1	10% Pd/C	EtOH	20	1.0	100%	81-93%
2	10% Pd/C	EtOH	25	1.5	100%	61%
3[a]	10% Pd/C	EtOH	20	2.0	100%	90%
4	10% Pd/C	EtOAc	20	2.0	83%	-
5[b]	Raney Ni	EtOAc	40	2.0	88%	-

[a]Catalyst leaching was observed as discolouration of the product solution, and the amount of leached palladium could be reduced by stirring with a thiourea immobilised metal scavenger resin.

[b]No catalyst poison used.

At only a few minutes, this reaction time is much shorter than the batch procedure. Furthermore, using the optimum conditions of 10% Pd/C, EtOH, 20 °C and a flow rate of 1.0 mL min^{-1} enabled the formation of the 1,5-*bis*(3-hydroxyphenyl)penta-1,4-dien-3-one in an efficient, safer, and slightly higher yield than the batch reduction.

An early theory was that it may be possible to spirocyclise the diphenol directly to the *o*-SPINOL, potentially avoiding the addition and removal of the bromides as blocking groups (Scheme 3.7). It should be noted that no mention of any attempts to previously conduct this chemistry were reported in the literature.

Scheme 3.7 Theoretical spirocyclisation without bromide blocking groups.

In reality, when investigating this route, the phenol groups were unintentionally 'protected' as the mesylates, and the regioselectivity observed was found to be exclusively for the *para* site of the aromatic ring (Scheme 3.8).

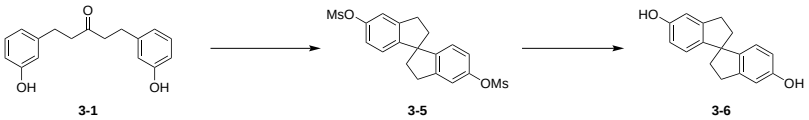

Scheme 3.8 *Para* spirocyclisation and mesylation.

The literature procedure from Birman *et al.*[69] used polyphosphoric acid whilst heating for 5.5 h at 105 °C to spirocyclise a similar starting material (Scheme 3.9).

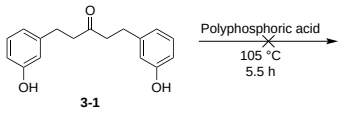

Scheme 3.9 Attempted spirocyclisation of 1,5-*bis*(3-hydroxylphenyl)pentan-3-one using polyphosphoric acid.

Several attempts were made to spirocyclise 1,5-*bis*(3-hydroxyphenyl)pentan-3-one using polyphosphoric acid, but no organic product was successfully extracted although some unreacted starting material was recovered.

Eaton's reagent is phosphorous pentoxide-methanesulfonic acid (1:10 by weight) and is a convenient alternative to phosphoric acid.[70] The spirocyclisation was repeated with Eaton's reagent at 80 °C (Scheme 3.10).

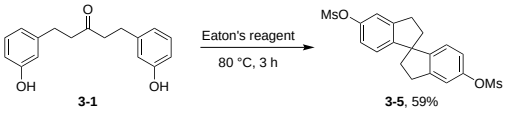

Scheme 3.10 Spirocyclisation of 1,5-*bis*(3-hydroxylphenyl)pentan-3-one using Eaton's reagent to (*p*)-SPINOMs.

Comparison with the literature data for (±)-(*o*)-SPINOL indicated that a spiro structure had indeed been formed, but the peaks in the aromatic region of the ^{1}H NMR spectrum did not match exactly. Some of the spectroscopic data matched the literature, but there were a few conflicting pieces of evidence. The ^{1}H NMR spectrum contained a peak at δ 3.36 ppm (6 protons) which would be consistent with the methyl protons of the mesyl group, but a D_2O shake caused a broad singlet at 3.57 ppm to disappear. An additional peak was also observed in the ^{13}C NMR spectrum at 37.8 ppm. The LC-MS spectrum implied that the compound may be mesyl-protected rather than the free phenol, due to the observation of a peak at 408 m/z (RT 3.38 mins). Later experiments to synthesise (*p*)-SPINOMs by a different route confirmed the identity of this product.

Various attempts were made to try to hydrolyse the mesylate using NaOH, but none were successful (Scheme 3.11). The ^{1}H NMR spectra of all crude products obtained matched the starting material in all cases.

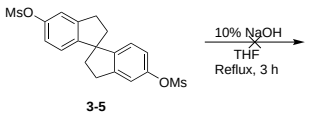

Scheme 3.11 Attempted demesylation of (*p*)-SPINOMs

The first step in the confirmation of the synthesis of *p*-SPINOMs was the deprotection of *p*-(±)-SPINOMe to form *p*-(±)-SPINOL, following the same procedure as for the deprotection of *o*-(±)-SPINOMe (Scheme 3.12).

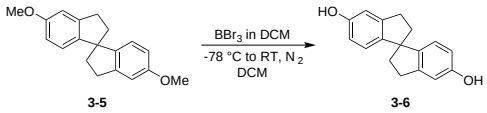

Scheme 3.12 Demethylation of *p*-SPINOMe to form *p*-SPINOL.

The ^{1}H NMR spectrum of the crude product revealed the absence of the signal from the methyl protons. The aromatic region of the ^{1}H NMR spectrum also did not match that of the previously synthesised product. The second step was the mesylation of the phenols, using mesyl chloride and pyridine (Scheme 3.13).

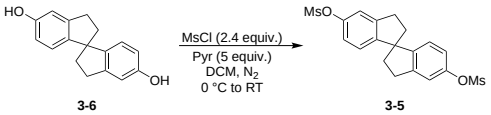

Scheme 3.13 Mesylation of *p*-SPINOL.

The ^{1}H NMR spectrum of the crude product showed that the aromatic region contained a doublet at 6.96 ppm, a doublet of doublets at 7.11 and another doublet at 7.29. This matched the data for the originally spirocyclised product, thus identifying the compound formed with Eaton's reagent as *para*-(±)-SPINOMs.

The spirobiindane product *o*-Br-SPINOMe contains two protecting groups which needed to be removed to furnish the desired end-product, *o*-(±)-SPINOL. The two bromine atoms were installed to act as blocking groups so that only one isomer of the spirobiindane could form. One literature synthesis of SPINOL removes these with *n*-BuLi.

3.2 Starting from 2-bromo-5-hydroxybenzaldehyde

One of the disadvantages of the previous route was the potential for α-bromination products to form from the ketone.[71] This was expected to become a more significant issue upon scale up due to the higher concentration

of HBr being generated, catalysing enol formation. It would also be possible for HBr-catalysed spirocyclisation to occur, leading to the *para* product. Since the literature procedure incorporates bromine atoms as blocking groups pre-spirocyclisation, the possibility of changing the order of the reactions starting from 3-hydroxybenzaldehyde was investigated.

The first step in the alternative sequence was the bromination of the benzaldehyde, which was attempted in both batch and flow.

Various batch methods were attempted for the synthesis of 2-bromo-5-hydroxybenzaldehyde. The method that gave the highest yield and greatest proportion of monobrominated product used molecular bromine in DCM (Scheme 3.14).

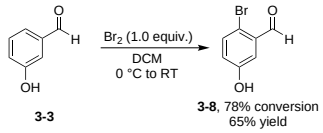

Scheme 3.14 Batch bromination of 3-hydroxybenzaldehyde.

The maximum conversion reached was 78% as determined by ^{1}H NMR spectroscopy, and the crude material was recrystallised from AcOH to give the pure product in 65% isolated yield.

To mitigate the risks associated with using molecular bromine in batch at scale, flow methods were also considered. Higher dilutions of solutions were used to prevent precipitation of product whilst in the flow reactor. DCM, AcOH and mixtures of these two solvents were considered (Scheme 3.15). The starting material was less soluble in DCM than AcOH, and the maximum conversion observed was only approximately 20% by ^{1}H NMR spectroscopy. This value did not vary according to the flow rate or residence time. It was therefore thought that the low concentration of starting material may be the limiting factor in improving the overall conversion.

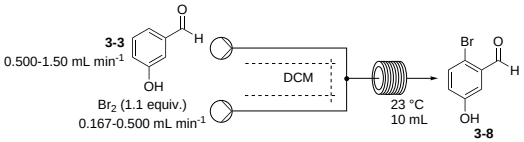

Scheme 3.15 Flow bromination of 3-hydroxybenzaldehyde in DCM.

AcOH was also considered as a suitable solvent since it was compatible with both bromine and the starting material (Scheme 3.16). Conversion to the monobrominated product peaked around 60%. As the flow rates were increased, the ratio of mono- to di-brominated product remained at around 2:1.

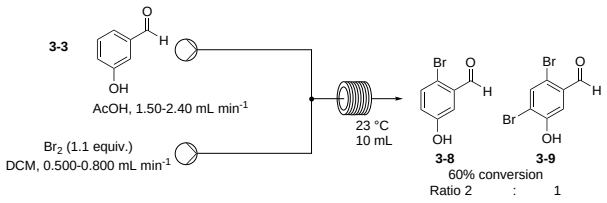

Scheme 3.16 Flow bromination of 3-hydroxybenzaldehyde in AcOH/DCM.

To improve the solubility of the starting material in DCM, 10% AcOH was added (Scheme 3.17). The flow rates were varied, and the composition of the resulting mixture was analysed by ^{1}H NMR spectroscopy. The results are summarised in Fig. 3.1 below.

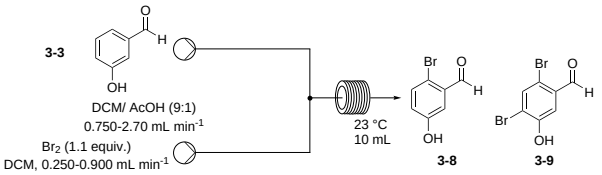

Scheme 3.17 Flow bromination of 3-hydroxybenzaldehyde in DCM/AcOH.

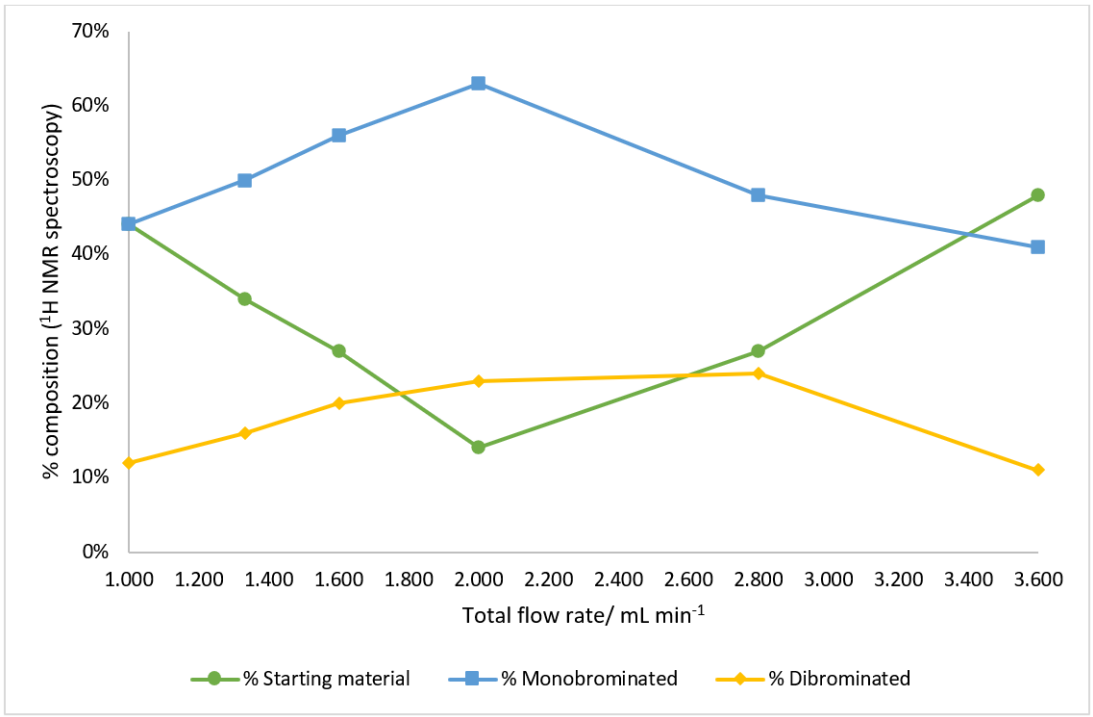

Fig. 3.1 Flow bromination of 3-hydroxybenzaldehyde; flow rate vs. composition.

The maximum conversion (88%) was observed at 2.0 mL min^{-1}, but at this flow rate dibromination was competitive with the desired monobromination.

In conclusion, the batch method of bromination gave the best yields of 2-bromo-5-hydroxybenzaldehyde. It would have been preferable to be able to use

flow chemistry, to reduce user exposure to bromine, but this method gave a higher proportion of the undesired dibrominated product. In the future, alternative solvents, dilutions, and reaction temperatures may be considered in flow. One of the causes of this dibromination may be due to the improved mixing in flow, which is normally an advantage. Different mixing pieces may reduce this over-bromination.

Although not optimised in flow, material was prepared allowing the next step to be tested. Hence the Dolliver-Ding conditions developed in the synthesis of 1,5-*bis*(3-hydroxyphenyl)penta-1,4-dien-3-one were applied to the condensation of 2-bromo-5-hydroxybenzaldehyde with acetone (Scheme 3.18).

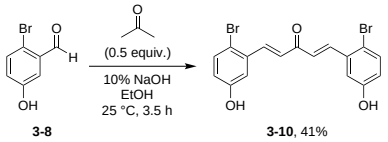

3-8 **3-10**, 41%

Scheme 3.18 Dolliver-Ding aldol condensation of 2-bromo-5-hydroxybenzaldehyde with acetone.

The reaction produced the crude product as an orange solid which was re-crystallised from IPA to give a bright yellow solid.

It was anticipated that the reduction of the brominated pentadienone may occur with simultaneous loss of the aromatic bromides.

Chemoselective reduction of the brominated pentadienone was attempted (Scheme 3.19) using the poisoned palladium-based conditions that had previously proved successful for the reduction of the corresponding 1,5-*bis*(3-hydroxyphenyl)penta-1,4-dien-3-one (Pd/C, H_2, Ph_2S, EtOH).

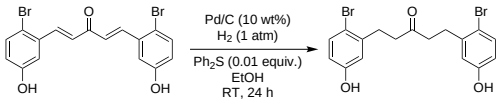

3-10 **3-11**, 80% purity
29% isolated yield

Scheme 3.19 Batch reduction of 1,5-*bis*(2-bromo-5-hydroxyphenyl)penta-1,4-dien-3-one.

However, even when using a shorter reaction time of 2 h, a mixture of the dibrominated, monobrominated and debrominated pentanones was observed. The reaction time was not shortened further. The quantity of side-products could be reduced *via* purification by column chromatography (Hex:EtOAc 1:1 to Hex:EtOAc 0:100), but not completely removed. The desired dibrominated pentanone was the major product from these reactions (Fig. 3.2), but this was still an inefficient method of preparation.

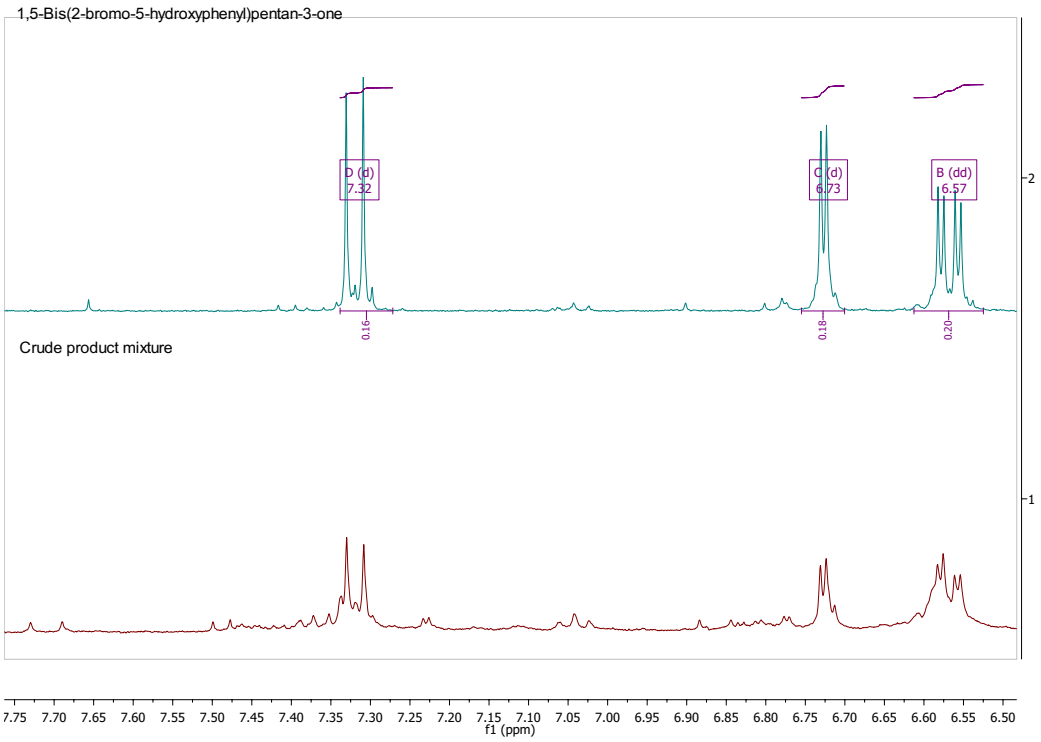

Fig. 3.2 ^{1}H NMR spectra of the desired dibrominated pentanone, compared with the crude product mixture.

We again hoped that more precise contact time using a packed catalyst bed flow reactor may lead to better chemoselectivity. Therefore 1,5-*bis*(2-bromo-5-hydroxyphenyl)penta-1,4-dien-3-one was dissolved in EtOH to create a stock solution of 0.050 mol dm^{-3}, and passed through a cartridge of 10% Pd/C catalyst using the H-Cube® reactor (Scheme 3.20).

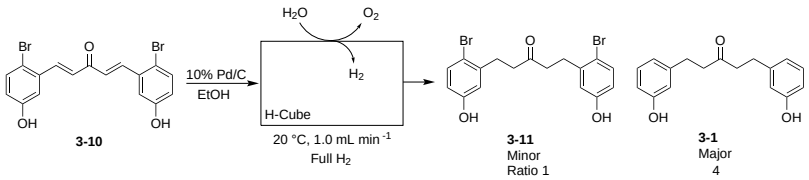

Scheme 3.20 Flow reduction of 1,5-*bis*(2-bromo-5-hydroxyphenyl)penta-1,4-dien-3-one using 10% Pd/C.

Unfortunately again, mixtures of dibrominated, monobrominated and furthermore the debrominated pentanones were obtained. The mixtures could not easily be separated but by ^{1}H NMR analysis, the major product was the debrominated pentanone.

In an attempt to regulate the catalyst activity, the addition of Ph_2S as a catalyst poison with the material being dissolved with the starting material in the EtOH stock solution was considered (Scheme 3.21).

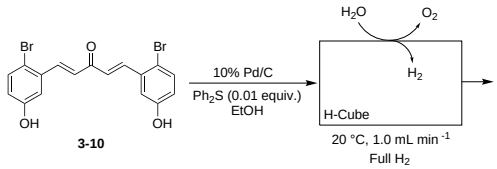

Scheme 3.21 Flow reduction of 1,5-*bis*(2-bromo-5-hydroxyphenyl)penta-1,4-dien-3-one using 10% Pd/C and Ph_2S.

This proved somewhat successful but generated a complicated mixture of di-brominated, monobrominated and debrominated pentadienones, pentanenones and pentanones which was not separated.

It was thought the Pd catalyst might be more prone to inserting into the C-Br bond than an alternative catalyst, and so the catalyst was changed to Raney Ni and a range of reaction temperatures were tested (Scheme 3.22).

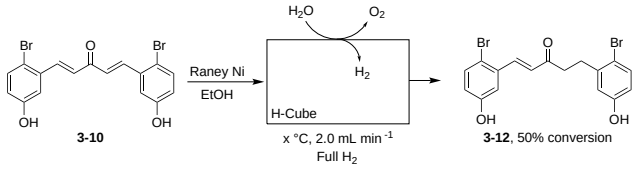

Scheme 3.22 Flow reduction of 1,5-*bis*(2-bromo-5-hydroxyphenyl)penta-1,4-dien-3-one using Raney Ni.

Even at the higher temperatures, approximately only 50% conversion of starting material to the mono-reduced pentaenone could be achieved, but as predicted, debromination was not observed. More forcing conditions may be required for full conversion to the di-reduced pentanone, or alternatively recycling the mixture, or employing a slower flow rate, which may increase the conversion.

Although temporarily put aside, this route was returned to after the publication in 2016 of an asymmetric synthesis of SPINOL by the Zhou group.[72]

In collaboration with Lauriane Peyrical, a bromination procedure using 1,5-*bis*(3-hydroxyphenyl)pentan-3-one as the starting material was developed (Scheme 3.23).

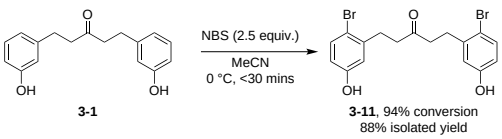

Scheme 3.23 Bromination of 1,5-*bis*(3-hydroxyphenyl)pentan-3-one using NBS.

Of particular note was that if the temperature and reaction time were not carefully controlled, dibromination on the aromatic rings was again observed.

However, maintaining the temperature below 0 °C and using 2.5 equivalents of NBS over a short reaction time allowed excellent conversions and good isolated yields of the desired product.

In their 2016 paper, Zhou *et al.* claimed to have used triflic acid to spirocyclise this brominated substrate. These conditions were thus examined and replicated (Scheme 3.24).

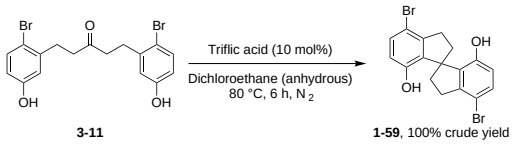

Scheme 3.24 Spirocyclisation of the brominated phenol using triflic acid.

However, although full conversion was achieved, the crude product obtained contained several side-products, and was of poor quality.

Instead, following previous examples, the 1,5-*bis*(2-bromo-5-hydroxyphenyl)pentan-3-one was spirocyclised using polyphosphoric acid (Scheme 3.25).

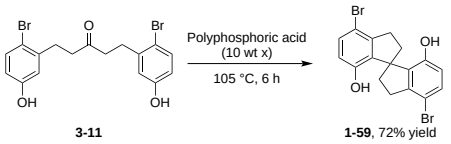

Scheme 3.25 Spirocyclisation of the brominated phenol using polyphosphoric acid.

The spirocyclised product was obtained in moderately high yield and high quality.

Debromination of this compound would give the desired *o*-SPINOL in 5 steps. Based upon our previous experiments using palladium catalysis and the ease of dehalogenation, a palladium-based debromination was attempted (Scheme 3.26).

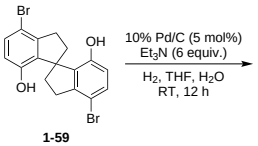

Scheme 3.26 Attempted palladium-based debromination of Br-SPINOL.

Unfortunately a complex mixture of products was obtained, along with a quantity of the starting material and the desired product, as determined by ^{1}H NMR spectroscopy. Indeed, despite several attempts to optimise this transformation, we were unable to improve the outcome. We speculate this may be a

consequence of the phenolic groups which coordinate to the palladium preventing dehalogenation.

Further work in this area should concentrate on achieving this step, ideally in flow. Preliminary experiments were attempted with the H-Cube® reactor, but equipment malfunctions meant that conversion was very low.

3.3 Conclusions on the 3-hydroxybenzaldehyde route

An aldol condensation using 3-hydroxybenzaldehyde and acetone was developed that gave high yields and purity. The flow reduction of the 1,5-*bis*(3-hydroxyphenyl)penta-1,4-dien-3-one was more efficient, safer, and gave higher yields than the corresponding batch reduction (Table 3.2).

Table 3.2 Comparison of the batch and flow reductions of 1,-*bis*(3-hydroxyphenyl)penta-1,4-dien-3-one.

Procedure	Batch	Flow
Isolated yield	91%	81-93%
Reaction time	24 h	2 min
Throughput	0.033 g h^{-1}	1.62 g h^{-1}

Spirocyclisation of the 1,5-*bis*(3-hydroxyphenyl)pentan-3-one with polyphosphoric acid was not successful. Alternatively, when run with Eaton's reagent, a spirobiindane was obtained but this was found to be a mesyl-protected *para*-spirobiindane rather than the desired *ortho* diphenol (Scheme 3.27).

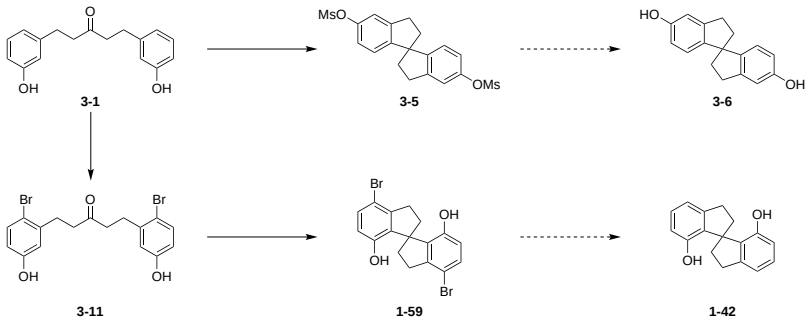

Scheme 3.27 Comparison between regioselectivity of spirocyclisation routes using hydroxybenzaldehydes.

An alternative sequence was also investigated. When proceeding *via* 2-bromo-5-hydroxybenzaldehyde, the batch bromination with Br_2/DCM gave superior yields to the flow set-up, as under flow conditions significant dibromination was

observed. The equivalent aldol reaction proceeded in lower yields but high purity to give 1,5-*bis*(2-bromo-5-hydroxyphenyl)penta-1,4-dien-3-one. With both the batch and flow reductions of the brominated pentadienone, a mixture of products was obtained, with some debromination observed as well as the desired reduction of the unsaturated ketone.

Performing the reduction of the pentadienone before bromination solved this problem. It has been possible to spirocyclise the brominated pentanone using polyphosphoric acid and phosphotungstic acid to give Br-SPINOL. The final step in this preparation of SPINOL would be debromination, which needs further optimisation.

These routes are summarised in the scheme below (Scheme 3.28).

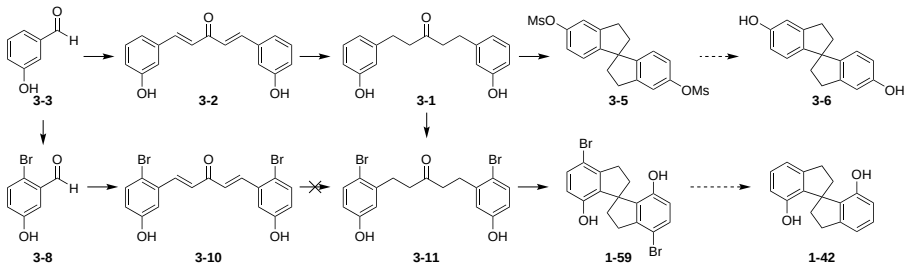

Scheme 3.28 Reactions from 3-hydroxybenzaldehyde to spirobiindanes.

Since it was discovered that the bromine atoms are indeed required as blocking groups during the spirocyclisation step in order to give the *ortho* product, the question arises as to whether bromination should be performed before or after the reduction of the unsaturated ketone. It was found to be markedly better to reduce first, and brominate the resulting ketone. It was later found to be possible to spirocyclise this brominated ketone in high yields and purity using rapid microwave heating (Section 4.5). The last remaining hurdle to the desired SPINOL is the debromination of Br-SPINOL to give the final product, believed to be possible after further experimentation. If successful, this would reduce the number of steps required to synthesise SPINOL from six to five, and eliminate the need to use boron tribromide to cleave the methyl protecting groups. At this point, the route starting from 3-methoxybenzaldehyde was investigated in order to attempt to improve the literature procedure.

Chapter 4

Synthesis of (±)-SPINOL from Methoxybenzaldehydes

One of the the literature syntheses of (±)-SPINOL starts from 3-methoxybenzaldehyde, and proceeds in 6 steps and 28% overall yield.[69] The first step is an aldol condensation of 3-methoxybenzaldehyde with acetone, followed by reduction with Raney Ni, then bromination with molecular bromine. The next step is a low-yielding spirocyclisation with polyphosphoric acid, followed by two deprotection steps to arrive at the desired product.

Two routes for bromination of the pentanone are described here: the first builds on work undertaken on 2-bromo-5-hydroxybenzaldehyde by synthesising 2-bromo-5-methoxybenzaldehyde and proceeding, and the other follows the literature procedure. Improvements to the literature procedure have been made to five of the six steps to SPINOL and are discussed below.

4.1 Reversing the literature reaction order

A potential route for the synthesis of 1,5-*bis*(2-bromo-5-methoxyphenyl)penta-1,4-dien-3-one follows the same pattern as for the synthesis of the diphenol pentadienone, that is, bromination followed by an aldol condensation, followed by reduction (Scheme 4.1). This differs in order of steps to the sequence found in the literature, which is an aldol condensation, followed by reduction then bromination.

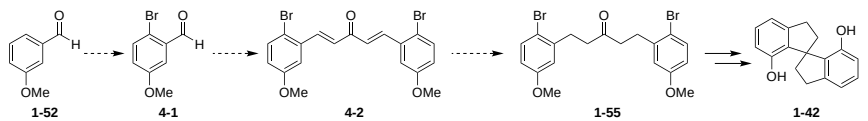

Scheme 4.1 Proposed synthetic route to 1,5-*bis*(2-bromo-5-methoxyphenyl)pentan-3-one.

Initial attempts at the bromination of 3-methoxybenzaldehyde used the same conditions as for the previous bromination of 3-hydroxybenzaldehyde (Br_2/DCM) (Scheme 4.2).

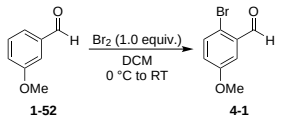

1-52 **4-1**

Scheme 4.2 Bromination of 3-methoxybenzaldehyde (Br_2/ DCM).

^{1}H NMR spectroscopy showed 70% conversion of the starting material after 4.5 h (63% monobromination product and 7% unknown), demonstrating the slower reaction of the protected methoxy substrate compared to the phenol.

A literature search was performed to identify a more efficient method, and conditions by Snyder *et al.* were found that used AcOH as the solvent (Scheme 4.3).[73]

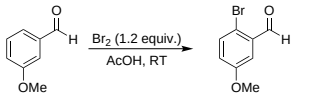

1-52 **4-1**, 56% isolated yield

Scheme 4.3 Bromination of 3-methoxybenzaldehyde (Br_2/ AcOH).

After 24 h, conversion was determined to be 90% by ^{1}H NMR spectroscopy. The crude yield was 95%, which after recrystallisation from EtOH:H_2O (9:1) gave the desired monobrominated product in 56% yield and >99% purity by ^{1}H NMR spectroscopy.

In contrast to the polybromination which was seen with 3-hydroxybenzaldehyde/ Br_2/ AcOH, this reaction did not yield any other product than the monobromination, and proceeded at a substantially slower rate. Again, the methyl 'protecting group' is responsible for this reduction in reactivity as it makes the oxygen lone pair less available for donation, and therefore lowers the activation of the aromatic ring.

The aldol condensation of 2-bromo-5-methoxybenzaldehyde with acetone was attempted in 10% NaOH and EtOH (Scheme 4.4). The starting material was found to be barely soluble in EtOH/ H_2O, but the reaction still proceeded very rapidly, and precipitation of the product was observed after 10 mins.

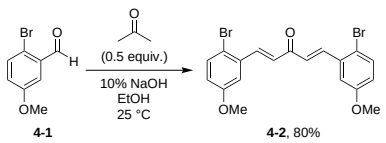

4-1 **4-2**, 80%

Scheme 4.4 Aldol condensation of 2-bromo-5-methoxybenzaldehyde (Dolliver-Ding conditions).

Large amounts of precipitation were observed from the solution to give a very high crude yield (96%). The composition of the crude was 87% product and 13% starting material as determined by ^{1}H NMR spectroscopy. After recrystallisation, the isolated yield was 80% (95% product).

The yellow 1,5-*bis*(2-bromo-5-methoxyphenyl)penta-1,4-dien-3-one (95% pure by ^{1}H NMR spectroscopy) was dissolved in EtOAc, and reduction conditions were screened using the H-Cube® reactor. The catalyst used throughout was Raney Ni, as it had been shown to target the pentadienone C=C rather than debrominating the aromatic rings.

The initial reduction attempt was performed at 20 °C, but after two passes through the H-Cube® reactor, TLC (Hex:EtOAc 1:1) showed that only starting material was present. The temperature was increased in stages through 50 °C, 60 °C, and 70 °C and each sample was passed through the H-Cube® reactor four times (Scheme 4.5).

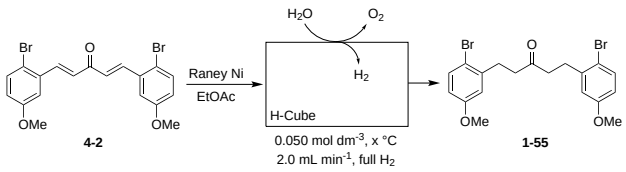

Scheme 4.5 Initial reduction of 1,5-*bis*(2-bromo-5-methoxyphenyl)penta-1,4-dien-3-one in the H-Cube® reactor.

Each sample was then dried over Na_2SO_4, filtered and concentrated *in vacuo* before being analysed by ^{1}H NMR spectroscopy to determine the approximate conversions (Table 4.1). In addition, LC-MS analysis indicated that neither bromine atom had been lost, as determined by the isotope ratios (Fig. 4.1).

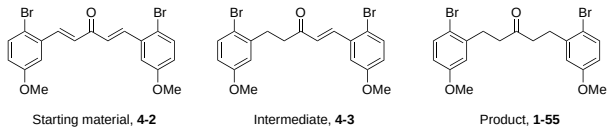

Fig. 4.1 Starting material, intermediate and product in the debromination reaction.

Table 4.1 Composition of product mixture after reduction in the H-Cube® reactor depending on reaction temperature.

Entry	Temperature /°C	% Starting material	% Intermediate	% Product
1	50 (4 passes)	20	13	68
2	60 (4 passes)	6	10	84
3	70 (4 passes)	2	10	88

Even at 70 °C after four passes through the H-Cube® reactor, the conversion to the product did not reach 100%. This reaction requires re-visiting with a new catalyst cartridge to verify the results. It may be that a higher reaction temperature increases the conversion, but the low concentrations and longer reaction times make this reaction inefficient for further development as a scaled-up procedure.

The route with the modified order of reactions is summarised below (Scheme 4.6).

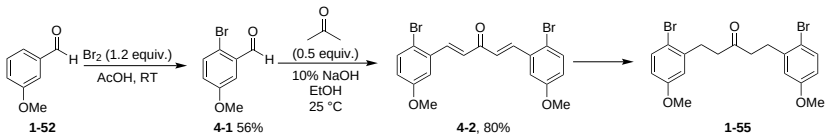

Scheme 4.6 Summary of alternative route to 1,5-*bis*(2-bromo-5-methoxyphenyl)pentan-3-one.

The first step required 24 h stirring at room temperature, and has only been tested on a 20 mmol scale. The yield of the crude product was 95% at 90% purity by ^{1}H NMR spectroscopy. The impurity was the starting material, which could be removed by recrystallisation from EtOH:H_2O 9:1 to give the product in 56% yield and >99% purity as fluffy white needle-like crystals. More material can also be recovered from the mother liquor. However, the aldol condensation is a rapid reaction requiring only 10 mins for product formation to be observed. Problematically, the product precipitation also dissolutions the starting material meaning the purity of the final material is not high, so that after recrystallisation the pentadienone was obtained in moderate to high yield. The final reduction step did not give complete conversion even when employing mildly forcing conditions. This route was set aside whilst work was performed on the conventional route.

4.2 Aldol condensation of methoxybenzaldehydes

The synthesis of the non-brominated pentadienone was attempted by two different methods. The first method followed the literature synthesis of (±)-SPINOL,[69] and the second method used the Dolliver-Ding conditions developed during the synthesis of 1,5-*bis*(3-hydroxyphenyl)penta-1,4-dien-3-one.

The conditions from Birman *et al.*[69] require 0.5 equivalents of acetone, 2.55 equivalents of sodium hydroxide and EtOH/ H_2O as the solvent mixture. The reaction was performed at room temperature with stirring for 4 h (73 mmol scale) (Scheme 4.7).

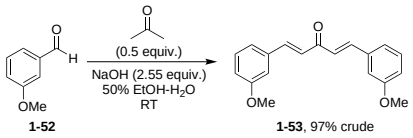

Scheme 4.7 Aldol condensation of 3-methoxybenzaldehyde (Birman conditions).

The crude product was obtained as a yellow-orange oil, which contained 93% pentadienone and 7% starting material as determined by ^{1}H NMR spectroscopy.

During the synthesis of 1,5-*bis*(3-hydroxyphenyl)penta-1,4-dien-3-one, a method was developed adapting conditions used for the synthesis of related compounds as described by Dolliver[67] and Ding.[68] This new method used 5 equivalents of 10% NaOH, and a solvent mixture of EtOH-H_2O. The starting material and acetone were added in two portions, and the mixture heated to 25 °C for 2-4 h, depending on the scale of the reaction. This maximised the conversion of 3-hydroxybenzaldehyde to the desired pentadienone product at 93%, from where it did not increase further.

This method was directly applied without alterations to the synthesis of 1,5-*bis*(3-methoxyphenyl)penta-1,4-dien-3-one (Scheme 4.8).

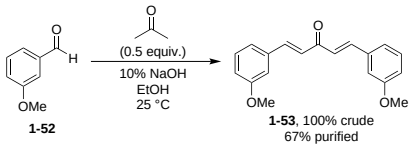

Scheme 4.8 Aldol condensation of 3-methoxybenzaldehyde (Dolliver-Ding conditions).

The crude product was a yellow oil, with a higher ratio of product to starting material (97:3) than was observed with the Birman method, and as a result the mixture proved much easier to purify. Purification was achieved by flash column chromatography (Hex:EtOAc 4:1) and gave the product as a yellow oil which solidified to a sticky yellow solid after several days in 67% yield.

Subsequent attempts at purification included recrystallisations. Attempts using IPA, H_2O, EtOAc, EtOH, MeOH, Et_2O, DCM and various combinations thereof were unsuccessful. However, purification using a solvent gradient of Hex:EtOAc 9:1 to 2:1 with column chromatography gave the highest isolated yield of 86%.

This reaction was also monitored by ^{1}H NMR spectroscopy, to give some additional insight into the rates of intermediate and product formation (Fig. 4.2 and Fig. 4.3).

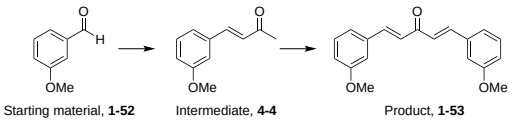

Fig. 4.2 Conversion of 3-methoxybenzaldehyde to 1,5-*bis*(3-methoxyphenyl)penta-1,4-dien-3-one *via* an intermediate

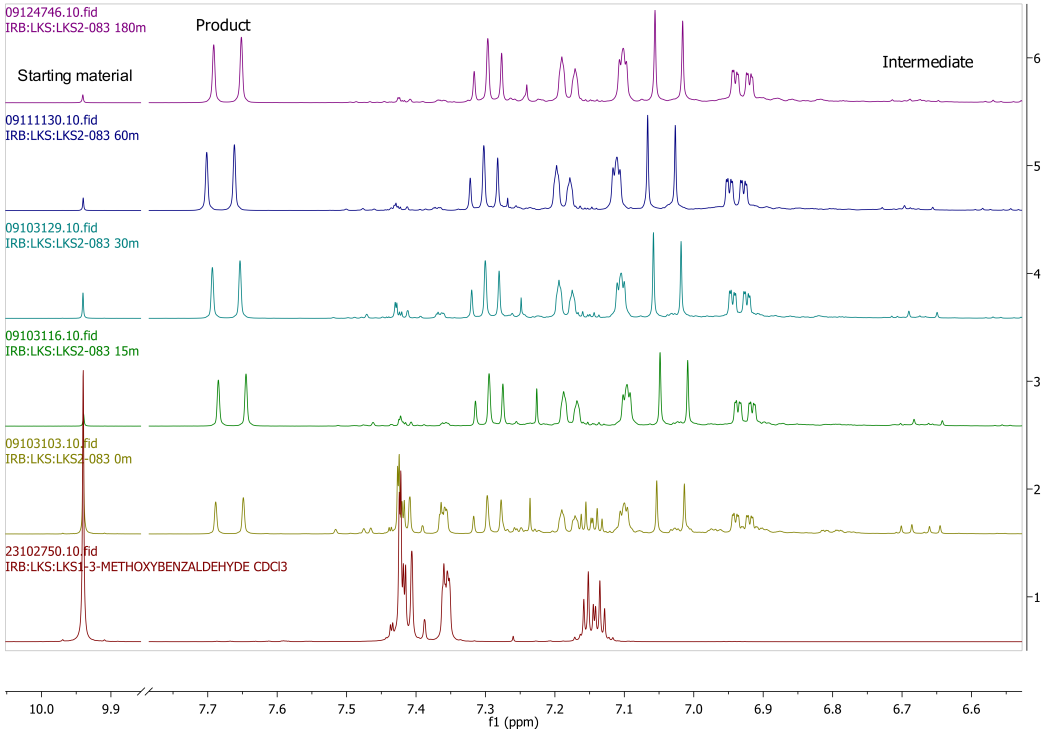

Fig. 4.3 Monitoring of the aldol condensation of 3-methoxybenzaldehyde with acetone by ^{1}H NMR spectroscopy.

The spectra show that even immediately after all components have been added, formation of product was observed. The reaction requires longer reaction times to ensure high conversion of the intermediate to the final product.

Therefore the Dolliver-Ding conditions gave a better quality product (97% product compared to 93% before purification) after a shorter reaction time (2 h compared to 4 h), thus demonstrating their superiority over the previous literature conditions.

For analytical purposes, the mono-condensation product 4-(3-methoxyphenyl)but-3-en-2-one was synthesised.

The Dolliver-Ding conditions that had previously been successful in the di-condensation were applied to the substrate, this time using one equivalent of acetone (Scheme 4.9).

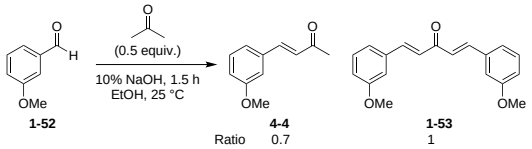

Scheme 4.9 Attempted synthesis of 4-(3-methoxyphenyl)but-3-en-2-one using the Dolliver-Ding conditions.

The mixture was stirred for 1.5 h at 25 °C, then neutralised with 6 M HCl. The same work-up as previously described was also utilised. ^{1}H NMR spectroscopy and LC-MS analysis indicated that the crude mixture contained both the mono- and di-condensed product, in a ratio of approximately 0.7:1. The two products were particularly difficult to separate, and column chromatography (Hex:EtOAc 2:1) was not very successful. Ideally, a synthetic method to form this product would deliver the mono-condensation product as the overwhelming major component.

To this end, a literature method by MacMillan *et al.*[74] was selected for a second attempt. This protocol used acetone in excess as both the reagent and solvent, with a 1 M NaOH solution added dropwise to a mixture of 3-methoxybenzaldehyde and acetone (Scheme 4.10).

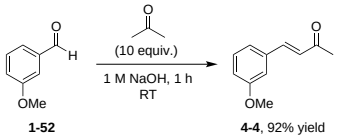

Scheme 4.10 Synthesis of 4-(3-methoxyphenyl)but-3-en-2-one using MacMillan protocol.

^{1}H NMR spectroscopic analysis indicated a single major product, which was the desired mono-condensation material. Thus no column chromatography or separation was required, and the product was obtained in 92% yield. The ^{1}H NMR spectrum was useful in assigning impurity peaks in the spectra of the di-condensation product.

4.3 Reduction of pentadienones

To obtain the desired pentanone, di-reduction of the conjugated dienone must occur.

The literature protocol for the reduction of 1,5-*bis*(3-methoxyphenyl)penta-1,4-dien-3-one requires stirring with Raney nickel under hydrogen for 24 h.[69] This reaction was attempted in acetone, and the reaction was monitored by TLC

(Hex:EtOAc 1:1) (Scheme 4.11). After 20 h, no starting material remained, and so the reaction was worked up.

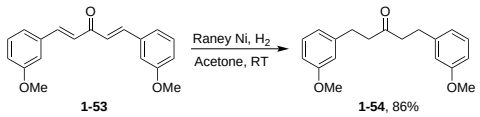

Scheme 4.11 Batch reduction of 1,5-*bis*(3-methoxyphenyl)penta-1,4-dien-3-one using Raney Ni.

^{1}H NMR spectroscopy of the crude product revealed 100% conversion of the pentadienone to the pentanone. The literature procedure had observed some over-reduced pentanol, but this was not present in our reaction mixture.

Raney Ni can be particularly challenging to work with, and poses several safety issues in regard to its handling and disposal. Thus the H-Cube® reactor offers an attractive alternative for the reduction of this pentadienone. Both Raney Ni and Pd catalyst cartridges were examined for efficacy, due to the lower cost of the palladium cartridges. Various solvents, temperatures, flow rates and concentrations were examined to find the optimal set-up for maximum conversion in minimum time.

Since reductions of the diphenol pentadienone had previously been successful successful with palladium on carbon, initial experiments with the methoxy pentadienone derivative were first performed with a 10% Pd/C catalyst cartridge (Scheme 4.12).

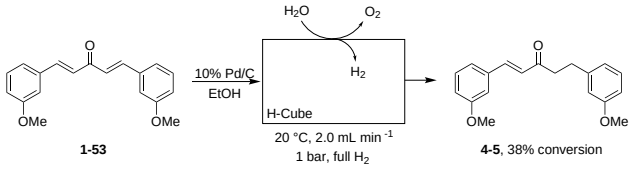

Scheme 4.12 Reduction of pentadienone in the H-Cube® reactor (10% Pd/C, EtOH).

By LC-MS spectroscopy, the crude product contained both starting material and the mono-reduced product. By ^{1}H NMR spectroscopy, conversion of starting material to the mono-reduced compound was 38%. Problematically, the starting material was not especially soluble in EtOH at room temperature.

Next, the use of Raney nickel catalyst cartridges were considered. The solvent was also changed to EtOAc because the starting material had a much higher solubility. The temperature was increased in 20 °C intervals and conversion was monitored by ^{1}H NMR spectroscopy (Scheme 4.13).

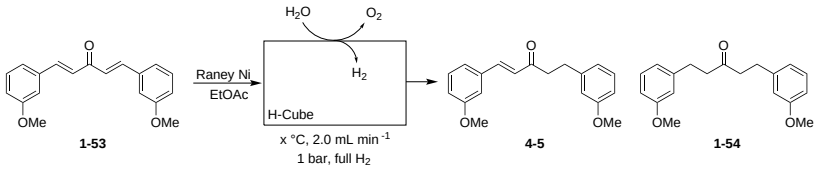

Scheme 4.13 Reduction of pentadienone in the H-Cube® reactor (Raney Ni, EtOAc).

The results obtained from this study were somewhat inconsistent, but exhibited a general trend of increasing product formation as the temperature was increased. Starting from a temperature of 60 °C, the flow rate was next reduced from 2.0 mL min^{-1} to 1.0 mL min^{-1} (Scheme 4.14).

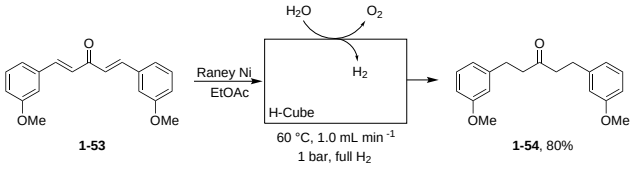

Scheme 4.14 Reduction of the pentadienone using Raney Ni/ EtOAc in the H-Cube® reactor.

^{1}H NMR spectroscopy of the crude product showed complete conversion of the starting material to the di-reduced pentanone and the product could be isolated as a pale yellow oil.

Subsequent attempts at replicating the success of this experiment were hampered by the intermittent hydrogen production of the H-Cube® reactor, leading to a mixture of starting material and product. These could be separated by column chromatography (Hex:EtOAc 2:1 to Hex:EtOAc 0:100). The problem was addressed by the addition of a sample collection robot set up to collect 15 mL samples. Any unreacted starting material present in the vials could be recycled back through the H-Cube® reactor. Further reduction of the pentanone to the alcohol or alkane was not observed.

Over a period of several months, the behaviour of the H-Cube® reactor became more erratic. Conditions which had previously given full conversion (60 °C/ 1.0 mL min^{-1}) were no longer sufficient and quantities of starting material were frequently observed in the crude product. It became necessary to begin multiple passes through the H-Cube® reactor to achieve >90% conversion. One such experiment was followed by ^{1}H NMR spectroscopy, and the spectra from this are shown below (Fig. 4.4).

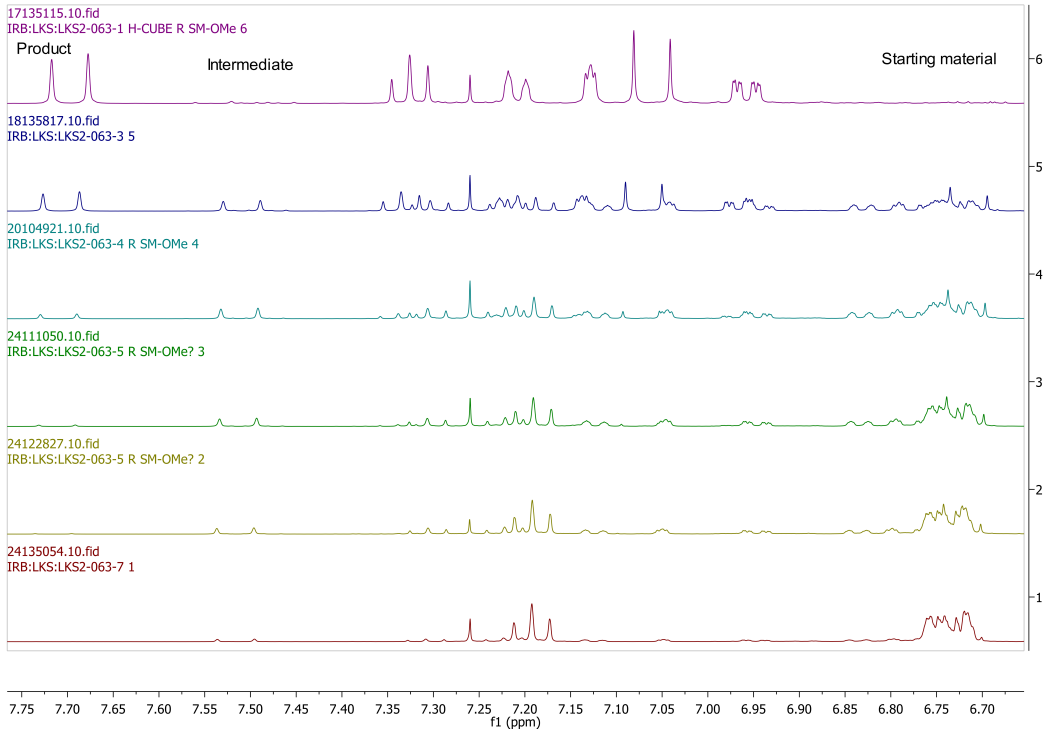

Fig. 4.4 Flow reduction of 1,5-*bis*(3-methoxyphenyl)penta-1,4-dien-3-one with multiple passes through the H-Cube® reactor (Raney Ni, EtOAc, 0.127 mol dm^{-3}, 60 °C, 1.0 mL min^{-1}, full H_2).

The conversion of starting material to intermediate required five passes through the H-Cube® reactor, and the final two passes through the machine furnished the product as the major component of the mixture.

To resolve these issues, various fixes were attempted, which included HPLC pump maintenance, changing catalyst cartridges, increasing temperatures and varying flow rates. Interestingly, water began to be observed in the product stream, which indicates a major issue with the membrane and electrolysis cell of the H-Cube® reactor. No single fix has yet solved these problems permanently.

When reviewing previous experimental data, the importance of concentration of the stock solution was considered. It was hypothesised that the concentration of 1,5-*bis*(3-methoxyphenyl)penta-1,4-dien-3-one may be the most important factor in determining the conversion.

To this end, an experiment was run with 21 stock solutions of varying concentrations. These were run through the H-Cube® reactor in a single pass (Raney Ni, EtOAc, 60 °C, full H_2), and the flow rate was altered. The data are summarised in the graph below (Fig. 4.5).

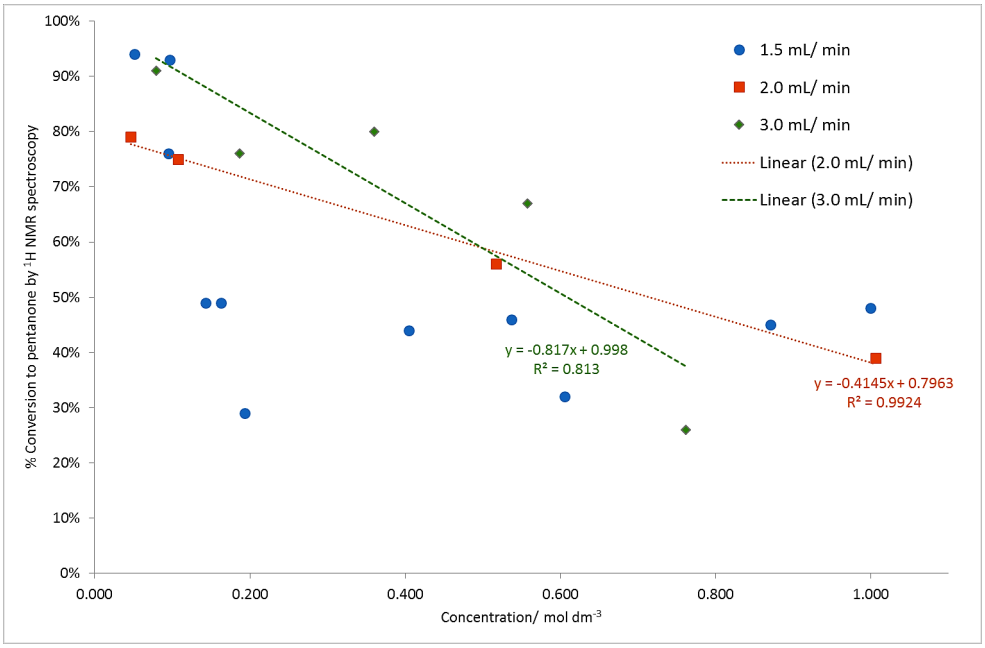

Fig. 4.5 Graph of concentration of stock solution versus % conversion to product at different flow rates.

When studying the results for the 1.5 mL min^{-1} flow rate, it becomes apparent that the results are much less predictable, giving less consistent conversions regardless of the solution concentration. Considering most earlier experiments were run at the even slower flow rate of 1.0 mL min^{-1}, this could help explain the erratic conversion results.

When flowing at 2.0 mL min^{-1}, the data becomes more predictable and it was possible to fit a line of least squares regression to the four data points, giving an R^2 value of 0.99.

It should be noted that to achieve conversions above 90%, it was found to be far more important to run the reaction at a concentration of 0.100 mol dm^{-3} or lower, rather than increasing the flow rate further. At this dilution, there was little difference in the conversions achieved across the range of flow rates.

Consequently a 0.100 mol dm^{-3} stock solution of 1,5-*bis*(3-methoxyphenyl)penta-1,4-dien-3-one was prepared and was run through the H-Cube® reactor at 3.0 mL min^{-1} (Scheme 4.15).

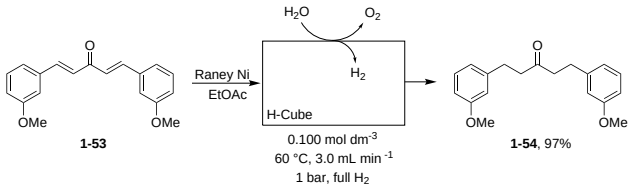

Scheme 4.15 Large-scale flow reduction of 1,5-*bis*(3-methoxyphenyl)penta-1,4-dien-3-one in the H-Cube® reactor.

After the first pass through the machine, analysis by ^{1}H NMR spectroscopy indicated that the mixture was composed of 9% starting material, 9% mono-reduced compound and 82% pentanone product. A second pass resulted in only 2% mono-reduced compound and 98% pentanone product which was deemed sufficient. This significantly faster flow rate allowed 12.048 g of material to be processed in 137 mins in a 97% yield (output = 5.17 g/ h) and is thus a far more efficient method for the reduction of 1,5-*bis*(3-methoxyphenyl)penta-1,4-dien-3-one than the literature batch reduction.

4.4 Brominations of pentanones

To block the *para* position relative to the mexthoxy group, and thus direct spirocyclisation to occur at the *ortho* positions, it was necessary to install two additional functional groups. Initially, these were two bromides as in the literature, but later work considered alternatives such as chlorides since they have a lower mass and thus reduce waste.

The Birman conditions using pyridine and bromine were applied to 1,5-*bis*(3-methoxyphenyl)pentan-3-one in the synthesis of 1,5-*bis*(2-bromo-5-methoxyphenyl)pentan-3-one (Scheme 4.16).

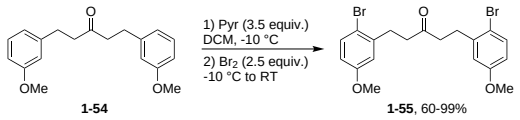

1-54 **1-55**, 60-99%

Scheme 4.16 Bromination of 1,5-*bis*(3-methoxyphenyl)pentan-3-one with pyridine/ Br_2.

Following the reaction, the mixture was quenched with 10% $Na_2S_2O_3$ and extracted with 1 M HCl and H_2O to give an orange oil in high yield (60-99%). ^{1}H NMR spectroscopy of the crude product matched the literature data, and showed that conversion was complete after 4 h. The largest scale the reaction was performed on was 18.7 mmol, and during bromine addition a significant exotherm was observed. The reaction time required also increased to 6 h.

This route to the brominated pentanone removes the need to attempt reduction of the brominated pentadienone in the H-Cube® reactor, as this method gives the product in high purity and the same number of steps. It has the additional benefit of making the route divergent, so that it was possible to use the non-brominated pentanone and the brominated pentanone to investigate spirocyclisations with different conditions. However, the reaction becomes difficult to perform on a larger scale, due to exotherms and the need for an extended reaction time.

Bromination with *N*-bromosuccinimide (NBS) was attempted, as it is safer and easier to handle than molecular bromine. The reaction was first attempted in MeCN (Scheme 4.17).

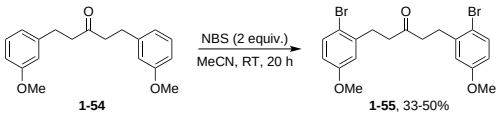

1-54 **1-55**, 33-50%

Scheme 4.17 Synthesis of 1,5-*bis*(2-bromo-5-methoxyphenyl)pentan-3-one with NBS.

The lowest yield of 33% was obtained with the shortest reaction time of 30 mins; a 50% yield was obtained after 3 h stirring at RT. Increasing the equivalents of NBS to 2.1 gave a similar yield of 51% (Scheme 4.18).

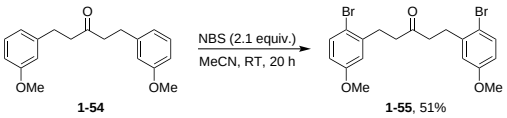

1-54 **1-55**, 51%

Scheme 4.18 Improved synthesis of 1,5-*bis*(2-bromo-5-methoxyphenyl)pentan-3-one with NBS.

This protocol has the advantage of being both safer and quicker, but the drawback of a significantly lower yield. The conversion of pentanone to brominated product was found to be 100% by ^{1}H NMR spectroscopy, but yields of 33-50% were observed, indicating the work-up was the source of the poor yields. In case it was the solvent that caused problems in the aqueous work-up, $CHCl_3$ was also considered (Scheme 4.19).

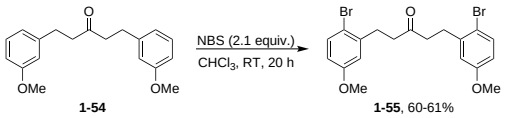

1-54 **1-55**, 60-61%

Scheme 4.19 Bromination of 1,5-*bis*(3-methoxyphenyl)pentan-3-one with NBS in chloroform.

Two reactions were performed at similar concentrations (0.25 mol dm^{-3}, 0.27 mol dm^{-3}) to the reactions in acetonitrile. After work-up, the yields obtained were consistent, at 60% and 61% respectively. It was noticed in the second reaction that after putting the starting material under high vacuum, approximately 22% of the mass was in fact solvent. This may have been a factor in reducing the yields of reactions, since less starting material was present than believed. However, this does not account for all of the 'missing' yield: for example, a predicted increase in yield from 51% to 68% for a reaction above (Scheme 4.18).

It was considered that potentially the low concentration of the reaction mixture may be a factor in the lower yields. To test this hypothesis, two reactions were performed in parallel at higher concentrations (0.5 mol dm^{-3} and 1.0 mol dm^{-3}) and gave much improved yields of 86% and 91% respectively.

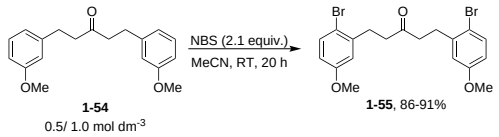

Scheme 4.20 Bromination of 1,5-*bis*(3-methoxyphenyl)pentan-3-one at higher concentrations in acetonitrile with NBS.

Therefore the problem of lower yields than the bromine/ pyridine reaction has been solved by running the bromination with NBS at higher concentrations. This has an added benefit of reducing the solvent volume, thus making the reaction less wasteful and the work-up easier.

The reaction was sequentially scaled up *via* 2 g of starting material to 10 g of starting material in preparation for a much larger-scale reaction. It was observed that the quenching step with 10% $Na_2S_2O_3$ was very exothermic at the larger scales.

In conclusion, an alternative bromination step using 2.1 equivalents of NBS in MeCN was found preferable to the literature reaction that uses bromine and pyridine in DCM. Temperature control of the initial addition was not critical. The required reaction time of the NBS reaction was not as heavily dependent on scale as the bromine reaction was.

Once the reaction was run at higher concentrations, the yield of the NBS reaction was consistently higher than with bromine. The product obtained was of higher purity by ^{1}H NMR spectroscopy, and was less highly coloured (pale yellow rather than dark orange). Importantly, NBS is a white solid that is easy to handle, whereas molecular bromine is a highly toxic volatile liquid. Acetonitrile is a more sustainable solvent than dichloromethane and also less harmful.[75]

Therefore the NBS reaction was considered preferable to the bromine reaction, representing an improvement in the synthesis of SPINOL.

4.5 Spirocyclisations of pentanones

The literature synthesis of (±)-SPINOL states that a blocking group *para* to the methoxy is required to prevent the *para* isomer of SPINOL forming preferentially over the desired *ortho* isomer, but does not investigate this claim further (Fig. 4.6).

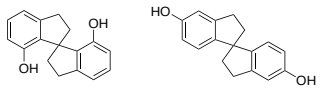

1-42, *o*-(±)-SPINOL **3-6**, *p*-(±)-SPINOL

Fig. 4.6 *ortho*- and *para*-(±)-SPINOL.

The need for this step has been examined in the previous chapter, but we will consider it in more depth here. To probe this wasteful step, we investigated spirocyclisations of the non-brominated pentanones, followed by replication of the literature procedure which uses brominated pentanones. Finally, we considered possible improvements to the procedure.

Spirocyclisation of the non-brominated pentanone 1,5-*bis*(3-methoxyphenyl)pentan-3-one was attempted with polyphosphoric acid and heating at 105 °C (Scheme 4.21).

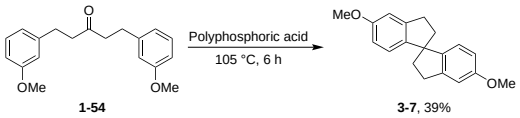

1-54 **3-7**, 39%

Scheme 4.21 Spirocyclisation of the non-brominated pentanone with polyphosphoric acid.

The reaction mixture was quenched with H_2O and extracted with Et_2O and DCM, then dry-loaded onto silica and washed through a short plug of silica (Hex:EtOAc 9:1) to give a yellow oil. The aromatic region of the ^{1}H NMR spectrum did not match that of the *ortho* spirobiindane. Instead, the peak splitting and COSY spectrum were more consistent with the isolated material being the *para* isomer as shown above.

Attempted spirocyclisations with Eaton's reagent gave a small amount of crude product, whose ^{1}H NMR spectrum also matched the *para* isomer. However, the yield was too low for this to be a viable preparative method (Scheme 4.22).

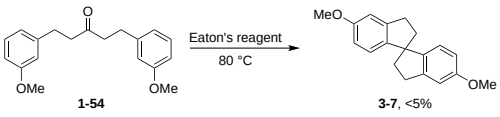

1-54 **3-7**, <5%

Scheme 4.22 Attempted spirocyclisation of 1,5-*bis*(3-methoxyphenyl)pentan-3-one with Eaton's reagent.

The first attempt at the spirocyclisation of the brominated pentanone followed the literature conditions using polyphosphoric acid with heating at 105 °C (Scheme 4.23).

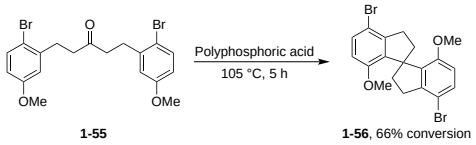

Scheme 4.23 Spirocyclisation of the brominated pentanone with polyphosphoric acid (5 h).

After 5 h, the reaction was quenched with H_2O and extracted sequentially with Et_2O then DCM. ^{1}H NMR spectroscopy of the crude product identified both starting material and the spirobiindane product, in the ratio 34:66. The reaction time was thus deemed insufficient for full conversion.

The reaction was repeated, and monitored by TLC (Hex:EtOAc 9:1) (Scheme 4.24).

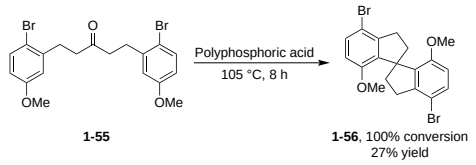

Scheme 4.24 Spirocyclisation of the brominated pentanone with polyphosphoric acid (8 h).

After 8 h, TLC showed no starting material remained. The crude purple product was dry-loaded onto silica and washed through a short plug of silica gel (Hex:EtOAc 9:1). ^{1}H and ^{13}C NMR spectra of the purified product matched the literature for the spirocyclic product.

Further attempted spirocyclisations with Eaton's reagent and subsequent aqueous/ organic work-up did not allow any organic material to be isolated (Scheme 4.25). This implies decomposition of the starting material or product, or the failure of the work-up to extract any organic material from the acidic aqueous layer, which seems unlikely based upon previous results.

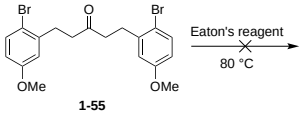

Scheme 4.25 Attempted spirocyclisation of 1,5-*bis*(2-bromo-5-methoxyphenyl)pentan-3-one using Eaton's reagent.

The only modification to the synthesis of SPINOL found in the literature is an improvement to the spirocyclisation step through the use of heteropoly acids instead of polyphosphoric acid. These heteropoly acids were considered with a series of pentanones and the findings are reported below.

A publication by Shan *et al.*[76] used heteropoly acids to synthesise spirobiindanes *via* *bis*-cyclisation. Both the brominated and non-brominated methoxyphenylpentanones were tested, with phosphotungstic, phosphomolybdic and silicotungstic acids. The optimal conditions were found to be phosphotungstic acid (0.15 equiv.) in toluene under Dean-Stark reflux conditions.

The first attempts to replicate these conditions used a hydrated form of phosphotungstic acid, $H_3PW_{12}O_{40} \cdot xH_2O$. Attempts at using this acid to spirocyclise the pentanone resulted in only the recovery of starting material. For the next attempt, the phosphotungstic acid hydrate was dehydrated by heating under vacuum to give the heteropoly acid as a fine white solid. It was now possible to use the literature conditions to synthesise 4,4'-dibromo-7,7'-dimethoxy-1,1'-spirobiindane (Scheme 4.26).

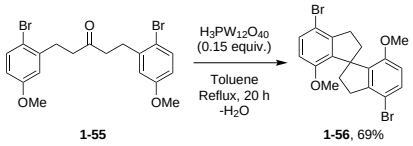

Scheme 4.26 Spirocyclisation of 1,5-*bis*(2-bromo-5-methoxyphenyl)pentan-3-one with phosphotungstic acid.

The NMR spectroscopic data matched the literature for 4,4'-dibromo-7,7'-dimethoxy-1,1'-spirobiindane, but the compound required further purification than had been specified in the literature, as the final product was purple in colour rather than colourless/ white.

Phosphomolybdic acid was dehydrated by heating under vacuum, then used in an attempt to replicate the literature conditions. However, only starting material was recovered from the reaction mixture.

In an effort to improve the ease of purification, it was postulated that immobilising the phosphotungstic acid on silica may make it simpler to remove the acid at the end of the reaction. To this end, phosphotungstic acid was immobilised on silica, and then used in an attempted spirocyclisation with 1,5-*bis*(2-bromo-5-methoxyphenyl)pentan-3-one. Again, only starting material was obtained at the end of the reaction. Therefore the most successful spirocyclisations used freshly-dehydrated phosphotungstic acid at a high reaction temperature of 110 °C.

The final improvement to the synthesis of Br-SPINOMe was to test the spirocyclisation in the microwave (Scheme 4.27).

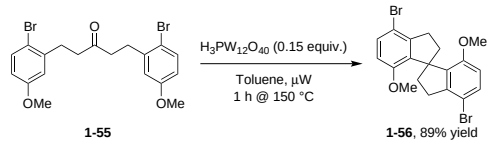

Scheme 4.27 Microwave spirocyclisation using phosphotungstic acid to give Br-SPINOMe.

There are several advantages to this protocol: the reduced reaction time leads to lower decomposition and a higher yield of product. The acid also undergoes less decomposition, so that most of it is still heterogeneous, making it easier to extract the product into solution. The catalyst could be recovered and recycled for the same reaction, with no significant loss of activity over five cycles.

Column chromatography (Hex:EtOAc 9:1) following spirocyclisation has been found to be the best purification step. Unfortunately, this only gave a 35% recovery of material, but in very high purity. This sample was recrystallised slowly from DCM to give a single crystal suitable for X-ray crystallography. The 3D structure of Br-SPINOMe is thus given below (Fig. 4.7).

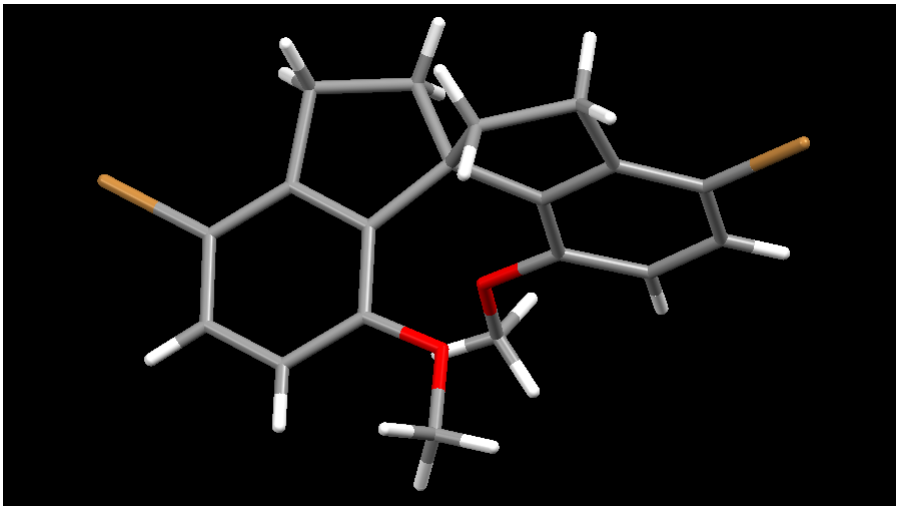

Fig. 4.7 Single crystal X-ray spectrum of 4,4'-dibromo-7,7'-dimethoxy-1,1'-spirobiindane after recrystallisation (DCM).

The X-ray crystal structure makes the environment around the methoxy groups clear, and they are closer in space than may be evident from diagrams representing their structure. The two spirobiindane rings are almost orthogonal to each other, with the twist at the quaternary spiro carbon.

With these vastly improved conditions, we returned to the original substrate for the spirocyclisation, 1,5-*bis*(2-bromo-5-hydroxyphenyl)pentan-3-one. This was performed with the heteropolyacid, using the same microwave conditions as above (Scheme 4.28).

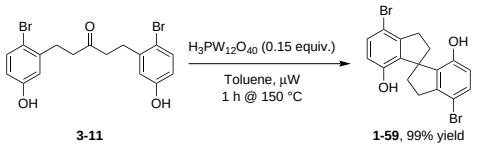

Scheme 4.28 Microwave spirocyclisation using phosphotungstic acid to give Br-SPINOL.

The spirocycle was obtained in an extremely high isolated yield of 99%.

4.6 Debromination of Br-SPINOMe

A double debromination of the spirobiindane was attempted first on a small scale (0.71 mmol), then later scaled up to 1.38 mmol. The reaction was performed under N_2 with dry solvent, and the starting material was stirred for 1 h at -78 °C with *n*-butyllithium (Scheme 4.29). A colour change was observed almost immediately after the addition of *n*-BuLi, from pale yellow to dark orange.

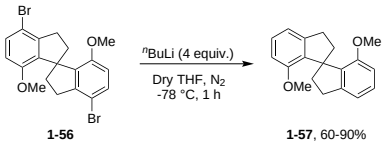

Scheme 4.29 Debromination of *o*-BrSPINOMe with BuLi.

The product obtained following work-up was a white solid, and ^{1}H and ^{13}C NMR spectroscopy showed that the data obtained matched the literature data. The product was fully assigned by ^{1}H and ^{13}C NMR spectroscopy.

Since it had previously been observed that it was possible to remove aromatic bromine atoms in the H-Cube® reactor with a 10% Pd/C catalyst, it was hypothesised that this might form the basis for a more straightforward deprotection method. The first attempt used a 10% Pd/C catalyst cartridge (Scheme 4.30).

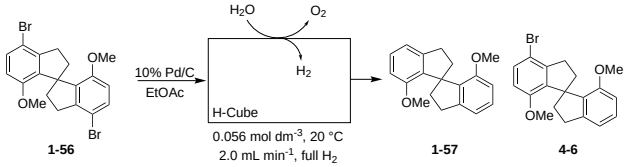

Scheme 4.30 Debromination of Br-SPINOMe using the H-Cube® reactor.

When analysed, 39% of the mixture obtained was determined to be starting material by ^{1}H NMR spectroscopy. The remaining 61% was made up of product (39%) and monobrominated intermediate (22%). Therefore more forcing conditions and/ or additional passes through the H-Cube® reactor were deemed necessary.

Later attempts considered a range of temperatures, and varied the number of passes through the H-Cube® reactor (Scheme 4.31).

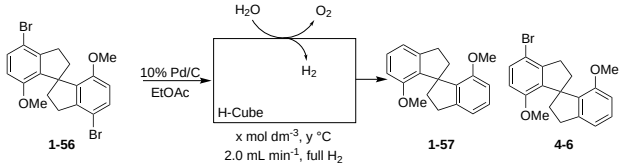

Scheme 4.31 Screening conditions for the debromination of Br-SPINOMe using the H-Cube® reactor.

The results are summarised in the table (Table 4.2) and graph below (Fig. 4.8).

Table 4.2 Removal of bromides from Br-SPINOMe in the H-Cube® reactor.

Entry	Concentration/ mol dm^{-3}	Temperature/ °C	Number of passes	% Starting material	% Intermediate	% Product
1	0.054	30	1	0	78	22
2	0.055	30	1	0	85	15
3	0.055	30	2	0	37	63
4	0.055	30	3	0	17	83
5	0.055	30	4	0	18	82
6	0.054	50	1	0	35	65
7	0.024	60	1	0	93	7
8	0.024	60	2	0	90	10

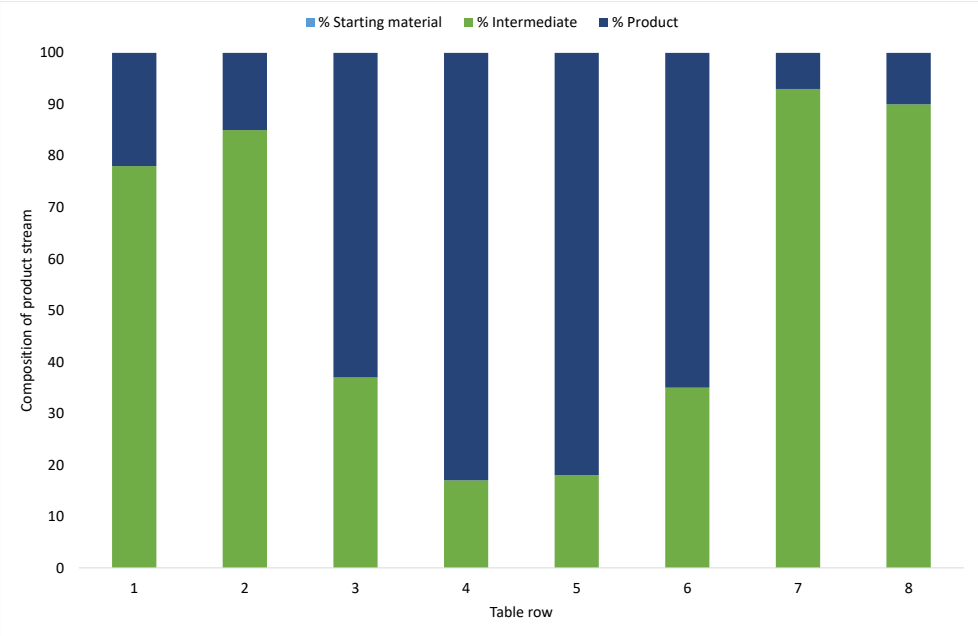

Fig. 4.8 Ratios between intermediate and product in the debromination of Br-SPINOMe. No starting material was observed in any of these reactions.

By increasing the temperature to $\geqslant$30 °C, it can be seen that no unreacted starting material was left. Further optimisation of concentration and temperature is required to maximise the conversion to product, but the above results are promising.

4.7 Deprotection of SPINOMe

The final step in the synthesis of *o*-(±)-SPINOL is the deprotection of the two methoxy groups.

Following the existing literature procedures, this reaction required the use of boron tribromide, which is a particularly unpleasant reagent to work with, due to the release of HBr fumes when exposed to air. The reaction was first attempted on a small scale (0.21 mmol), then later scaled up to 0.50 mmol (Scheme 4.32).

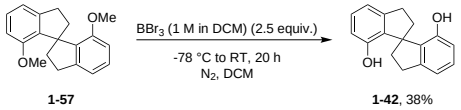

Scheme 4.32 Deprotection of SPINOMe with BBr_3 to give *o*-(±)-SPINOL.

Work-up was easier at the smaller scale, as the organic solution had to be washed with a large volume of water (approx. 500 mL for even the 0.21 mmol scale) to remove any acidic reagents. This led to a higher yield of 38% as opposed to around 20% for the larger scale reaction. The product was obtained as a pale yellow oil, which was fully assigned by ^{1}H and ^{13}C NMR spectroscopy and confirmed as *o*-(±)-SPINOL by comparison with literature data.

4.8 Conclusions on the 3-methoxybenzaldehyde route

Reversing the literature reaction order did not provide any significant benefits over the previous route but several successful reactions were identified.

The aldol reaction was improved on by using the Dolliver-Ding conditions developed during the synthetic route starting from 3-hydroxybenzaldehyde. It gave a better quality product after a shorter reaction time.

After optimisation of the reduction step using the H-Cube® reactor, conditions allowed 12.048 g of material to be processed in 137 mins in a 97% yield. This is therefore a far more efficient method for the reduction of 1,5-*bis*(3-methoxyphenyl)penta-1,4-dien-3-one than the literature batch reduction. It is also safer, as the Raney Ni was sealed in a catalyst cartridge and thus required no handling by the user.

A more successful bromination method was developed using NBS rather than molecular bromine as was used in the literature procedure. The time of the NBS reaction was not as heavily dependent on scale as the bromine reaction and once the reaction was run at higher concentrations, the yield of the NBS reaction was higher than with bromine. The product obtained was of higher purity by ^{1}H NMR spectroscopy. Finally, NBS and acetonitrile are safer to handle than bromine and DCM.

In agreement with the existing literature on the spirocyclisation of the pentanone, phosphotungstic acid was found to be more successful than polyphosphoric acid as the reagent. Eaton's reagent was not useful in this context. It was found that the bromine substitution on the aromatic rings was necessary to ensure the desired *ortho* regioselectivity during spirocyclisation.

Double debromination of the spirocycle was attempted in the H-Cube® reactor, and whilst further work is required to optimise the concentration and temperature to maximise the conversion to product, the initial results are promising. As yet, the only demethylation procedure attempted replicates the literature method which uses BBr_3. It would be highly desirable to substitute this reagent

for something milder, and so future work will be performed in this area.

The overall route is shown in the scheme below (Scheme 4.33).

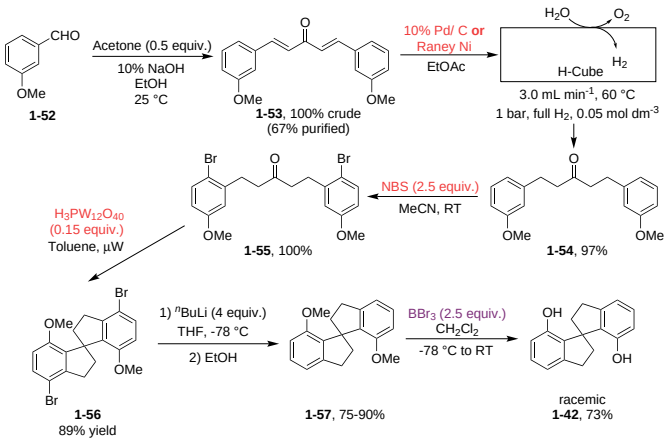

Scheme 4.33 Overall reaction scheme to *o*-(±)-SPINOL. Reagents shown in red are safer or more scalable than their equivalent in the literature procedure. Reagents in purple remain problematic.

The benefits of this route are that in proceeds in 6 steps and 32% overall yield (c.f. literature route: 6 steps, 28% overall yield). It incorporates flow technology and is safer, with improved yields, robustness and reproducibility. It is also more easily scaled.

Chapter 5

Synthesis of SPINOL using Chiral Diols as Auxiliaries

5.1 Introduction

Since the ketone functional group is the site of intramolecular Friedel-Crafts addition by two aromatic rings, it was suggested that modification of the ketone to create diastereoselectivity in the intermediate may lead to overall enantioselectivity during this spirocyclisation step. The two obvious derivatives are imines (formed by the reaction of the ketone with an amine) and acetals (formed by the reaction of the ketone with a diol).

The imine route was envisaged as shown below (Scheme 5.1).

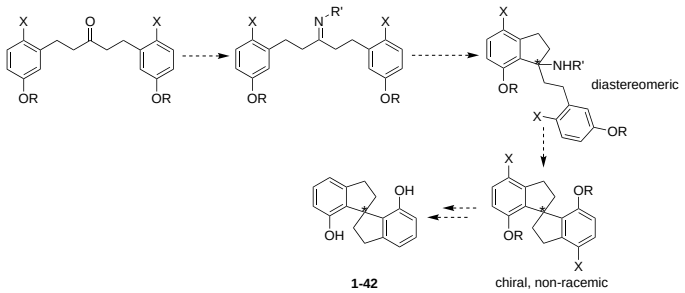

Scheme 5.1 Postulated imine-based spirocyclisation.

Early investigations into the feasibility of imine formation identified some issues. It was not possible to analyse the postulated imine product by ^{1}H NMR spectroscopy as the shift values of protons did not change sufficiently (Scheme 5.2). Instead, IR spectroscopy had to be used to confirm the identity of the product.

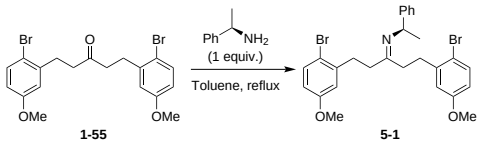

Scheme 5.2 Synthesis of the imine.

Subsequent attempts at spirocyclisation of the imine intermediate using *p*-TsOH were not successful, and in most cases simply led to regeneration of the ketone starting material.

Therefore instead of investing more time working on this reaction, acetal formation was considered as a more promising alternative. As a simple model process ethylene glycol was used as a test diol substrate (Scheme 5.3).

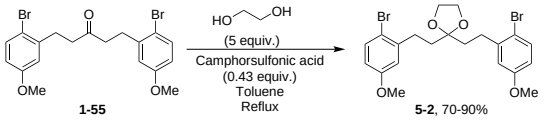

Scheme 5.3 Formation of an acetal using ethylene glycol.

Under typical acetal-forming conditions, the resulting acetal was synthesised in 70-90% yield without purification. It was also possible to perform the acetalisation in the microwave (Scheme 5.4), and the reaction was optimised by reducing the equivalents of ethylene glycol (Table 5.1).

Table 5.1 Reducing the equivalents of ethylene glycol during microwave acetalisation

Scheme 5.4 Microwave formation of an acetal using ethylene glycol.

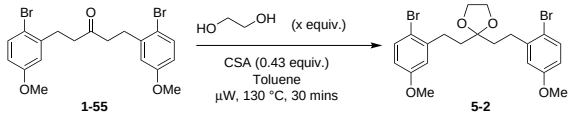

Entry	x equivalents of EG	Conversion by ^{1}H NMR spectroscopy (no internal standard)
1	5	58%
3	1.5	61%[a]
3	1.5	82%

[a]20 mins of heating instead of 30.

The acetal underwent spirocyclisation both in batch and the microwave to give Br-SPINOMe in moderate yields as shown below (Scheme 5.5).

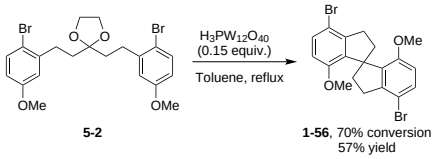

Scheme 5.5 Spirocyclisation of the acetal in batch.

The diols required for acetal formation must be chiral to impart chirality into the intermediate, which has previously been achiral. α-Amino acids (judiciously chosen) can be derivatised to give chiral diols (Fig. 5.1).

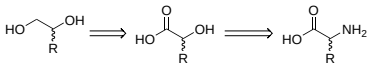

Fig. 5.1 Retrosynthesis of a chiral diol to identify an amino acid as a suitable substrate.

They have the advantage of the enantiopure L-amino acid being relatively cheap, and readily available. A variety of diols could be synthesised from a range of amino acids. Specific amino acids were selected by applying the following criteria:

1. Amino acid must be chiral
2. R-group must not contain -XH groups
3. R-group must be non-charged
4. R-group must be non-aromatic
5. R-group must be 'sufficiently' sterically bulky

The last of these is deliberately left somewhat open to interpretation. Of the twenty naturally-occurring α-amino acids, these criteria eliminate all but isoleucine, leucine, valine and phenylalanine. Isoleucine was unavailable in the laboratory at the time, and so the other three became the focus of investigation. Phenylalanine breaks the fourth criterion above, but was included for testing regardless, since it is thought to be unlikely that the aromatic C-H bonds will be correctly oriented to cause side-reactions during the Friedel-Crafts step (Fig. 5.2).

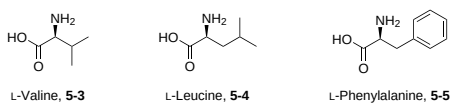

Fig. 5.2 Amino acids selected for diol synthesis.

Amino acids will be considered as both the racemic starting material and the enantiopure L-amino acid. The first step in derivatisation is the conversion of the amine group to an alcohol. There is literature precedent for the reaction of valine[77] with sodium nitrite to give the desired α-hydroxy acid (Scheme 5.6).

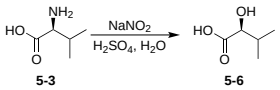

5-3 5-6

Scheme 5.6 Literature conversion of valine to the α-hydroxy acid.

The second step is the reduction of the carboxylic acid to the corresponding alcohol, which there is again literature precedent for when using $NaBH_4$ and I_2 (Scheme 5.7).[78]

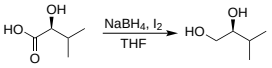

5-6 5-12

Scheme 5.7 Literature reduction of the α-hydroxy acid to the diol.

The different amino acids will be discussed below.

5.2 L-Amino acids

The mechanism of Step 1 proceeds *via* two inversion steps so that the overall stereochemistry is retained. However, racemisation may occur and so the product's enantiopurity was confirmed. The first approach was to use chiral amines to form a diastereomeric salt and assessment by ^{1}H NMR spectroscopy.

Further attempts were made to directly measure the enantiopurity of the amino acid derivatives by chiral HPLC but this was not successful. After a literature search, work by Ley *et al.* identified the possibility of derivatisation of the α-hydroxy acids as benzyl esters, followed by chiral HPLC as a method of determining the e.e.[79] Both the enantiopure and racemic derivatives were synthesised to enable comparison of the chiral HPLC results.

To determine the enantiopurity of the α-hydroxy acid, it was converted to the benzyl ester and submitted for chiral HPLC (Scheme 5.8).

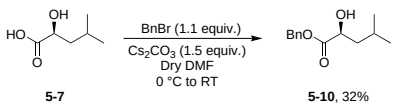

5-7 **5-10**, 32%

Scheme 5.8 Synthesis of the leucine-derived benzyl ester.

Salt formation was attempted with both (*R*)-(+)- and (*S*)-(–)-α-methylbenzylamines in parallel (Scheme 5.9).

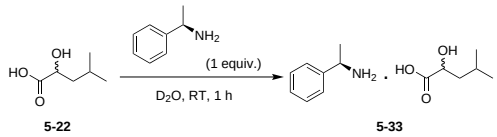

Scheme 5.9 Formation of a salt with (*R*)-(+)-α-methylbenzylamine.

Analysis of the ^{1}H NMR spectra of the two compounds confirmed salt formation due to the shifting of several important peaks, and only one diastereomer was observed. This was evidence that the original α-hydroxy acid was enantiomerically pure and had formed without scrambling of stereochemical information.

The first attempt at reduction of L-Val-ol used $NaBH_4$ and I_2, following a literature procedure;[80] however, no conversion was observed. The reduction was successfully completed by using lithium aluminium hydride. The yield was improved from around 20% to >40% by altering the work-up from an ethanol quench, evaporation and extraction with DCM/NaCl(aq). Feiser work-up conditions use a sodium hydroxide wash and magnesium sulfate to prevent contamination of the product with lithium salts.[81] The resulting diol was then reacted with the pentanone. After purification by column chromatography, the acetal was obtained in low yield but was fully characterised. The acetal-forming reaction was also performed in the microwave. Once formed, the acetal was reacted to undergo spirocyclisation in the microwave with the heteropoly acid $H_3PW_{12}O_{40}$.

The procedure was repeated, substituting L-valine for L-leucine, and subsequently for L-phenylalanine. The results are summarised in the scheme below (Scheme 5.10).

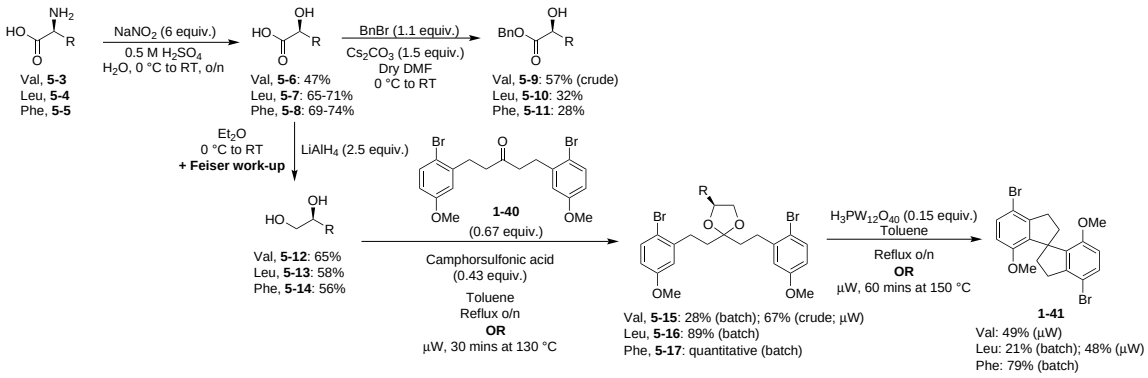

Scheme 5.10 Reactions involving L-amino acids discussed here.

5.3 Racemic Amino Acids

The synthetic protocol was repeated, using racemic valine, leucine and phenylalanine for comparison purposes. The results are summarised in the scheme below (Scheme 5.11).

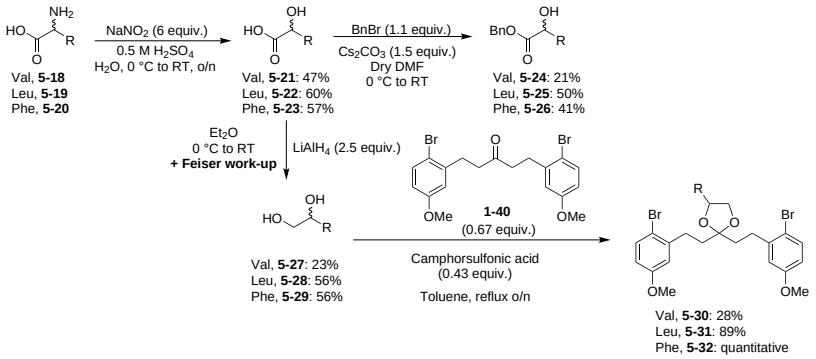

Scheme 5.11 Reactions involving racemic amino acids discussed here.

5.4 Chiral HPLC results

Chiral HPLC was performed on a number of samples of the benzyl hydroxy esters, varying the solvent conditions to obtain the optimum separation.

The benzyl ester amino acid derivatives were analysed by chiral chromatography (80% hexanes, 10% ethanol, 10% dichloromethane). The results did not allow meaningful conclusions to be drawn. Poor results were obtained from the chiral HPLC with the selected column. Other columns and solvent systems still require testing.

The enantiomers of Br-SPINOMe have previously been separated by analytical chiral HPLC. We were therefore able to use the same procedures to analyse our reaction products (Table 5.2).

Table 5.2 Outcomes of chiral HPLC of spirocycles

Starting material	Heating method	Outcome of chiral HPLC
Ketone	Batch and/ or microwave	ee = 1.7% (Hexane:dCM 99.25:0.75)
Phe-acetal	Batch	ee = -9.7% (Hexane:DCM 98:2) [a]
Leu-acetal	Batch	ee = -18.2% (Hexane:DCM 98:2)
Leu-acetal	Microwave	ee = -10.1% (Hexane:DCM 98:2), -7.1% (Hexane:DCM 99.25:0.75)
Val-acetal	Microwave	ee = -8.4% (Hexane:DCM 98:2)

[a]Poor quality

5.5 Conclusions

A variety of chiral diol derivatives were synthesised from the naturally-occurring L-amino acids, valine, leucine and phenylalanine. These derivatives were used in acetalisation reactions with 1,5-*bis*(2-bromo-5-methoxyphenyl)pentan-3-one. The acetal products were subjected to spirocyclisation reaction conditions using a heteropoly acid, with either microwave or standard hot-plate heating. Chiral HPLC data was not reliable enough to be able to determine whether enantioselectivity has been induced in the spirocycle product.

Since this work was performed, a report was published[6] which synthesised a wider range of acetals than was possible here. Some of these were used to induce enantioselectivity in the spirocyclisation reaction, proving that our concept was viable.

Chapter 6

Synthesis of SPINOL *via* an indanone intermediate

6.1 Introduction and rationale

Retrosynthetic analysis implies that an alkene intermediate could be synthesised from 3-methoxybenzaldehyde by the following route involving a key Wittig coupling reaction (Scheme 6.1).

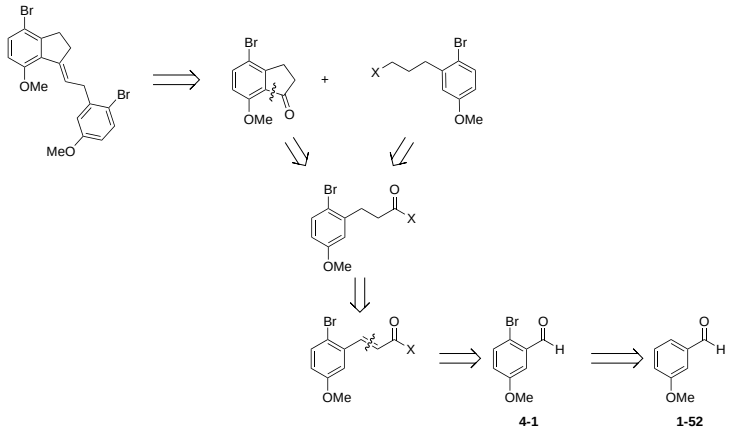

Scheme 6.1 Retrosynthesis of the alkene.

The corresponding forward synthetic route could proceed as shown below being divergent from the intermediate bromide (Scheme 6.2).

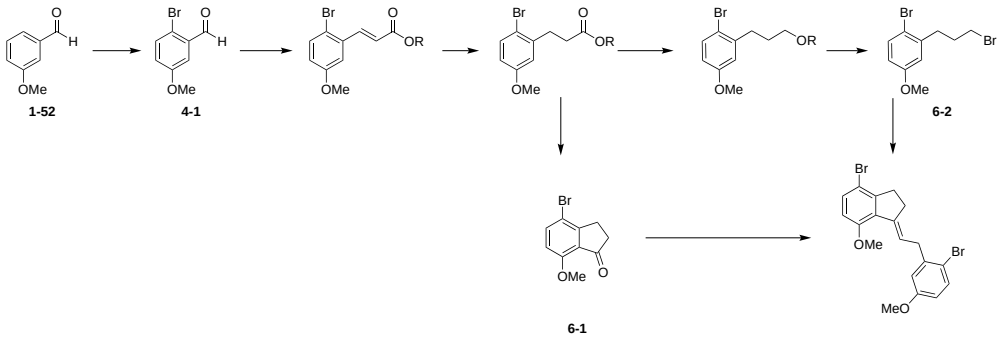

Scheme 6.2 Synthesis of the alkene, starting from 3-methoxybenzaldehyde.

The shared propanoic acid intermediate is an appealing feature of this synthetic route.

6.2 Horner-Wadsworth-Emmons reactions of 3-methoxybenzaldehyde

The first step in this second route is the bromination of 3-methoxybenzaldehyde (Scheme 6.3). This reaction had been attempted previously (Section 4.1), but a new method was attempted during this project which gave higher yields and a product of improved quality.[82]

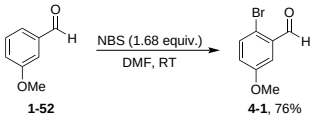

Scheme 6.3 Bromination of 3-methoxybenzaldehyde.

The crude product was recrystallised from IPA to give sparkly, needle-like white crystals. The same reaction was repeated on a larger scale to give a 94% yield of crude product which gave a 55% recovery following recrystallisation.

3-Methoxybenzaldehyde and 2-bromo-5-methoxybenzaldehyde were reacted with triethylphosphonoacetate using a Horner-Wadsworth-Emmons reaction to give the corresponding propenoates. The propenoates were then reduced using tosyl hydrazide in a biphasic reaction mixture (Scheme 6.4).

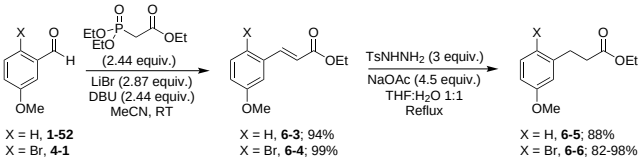

Scheme 6.4 Horner-Wadsworth-Emmons reaction with 3-methoxybenzaldehyde or 2-bromo-5-methoxybenzaldehyde, followed by reduction of the resulting propenoate.

After purification by column chromatography (pet. ether:EtOAc 4:1), the non-brominated propenoate was obtained as a pale yellow oil in excellent yield, whereas the brominated propenoate was obtained as a white solid with a melting point close to room temperature. After purification by column chromatography (hexanes:EtOAc 8:2), the non-brominated propanoate was obtained as a colourless oil in excellent yield whilst the brominated propanoate was found to exist as a waxy white solid.

Previous attempts at saponification of the propanate undertaken by an undergraduate student* had used 8 equivalents of NaOH, refluxing in EtOH to obtain the acid product. Milder conditions were also found to furnish the product in a similar yield and reaction time (Scheme 6.5).

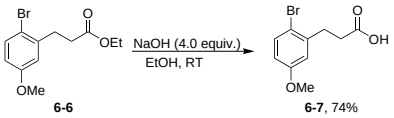

6-6 **6-7**, 74%

Scheme 6.5 Saponification of the ester to give the acid.

In addition, the product was of a higher quality than the material isolated under the previous harsher conditions, and after recrystallisation furnished a sparkly, needle-like white crystalline solid where it had previously been orange. However, it was discovered that the reaction required wet NaOH. Wet NaOH may have been the source of water in previously successful reactions, and thus reducing the amount of NaOH had inadvertently reduced the amount of water present. Various cyclisation reactions were attempted (Scheme 6.6), and the results are summarised in the table below (Table 6.1).

The reaction of the acid with Eaton's reagent gave a mixture of two products by ^{1}H NMR spectroscopy, in the ratio 56:44 (Fig. 6.1). The major product was identified as the desired indanone by comparison. The unknown product was thought to be due to a side-reaction between the acid starting material and methanesulfonic acid. It appears to contain three aromatic protons from the ^{1}H NMR spectrum, and thus has not cyclised. When repeated, heating for an additional hour gave a mixture of these same products in the ratio 72:28 (indanone:impurity). The impurity was removed *via* purification by column chromatography (Hex:EtOAc 1:1) to give the indanone product in 50% isolated yield.

*Joshua Goswell, Durham University, 2014-15

Table 6.1 Screening conditions for the synthesis of 1-indanone

Scheme 6.6 Cyclisation of the acid or ester to 1-indanone.

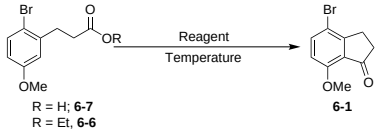

Entry	Starting material	Reagent	% Conversion to indanone
1	Acid	Polyphosphoric acid	100[a]
2	Acid	Eaton's reagent	See Fig. 6.1
3	Acid	H_2SO_4	100[b]
4	Acid	$H_3PW_{12}O_{40}$	0
5	Ester	Polyphosphoric acid	5
6	Ester	Eaton's reagent	6
7	Ester	$H_3PW_{12}O_{40}$	0

[a]32-47% isolated yield
[b]<10% isolated yield

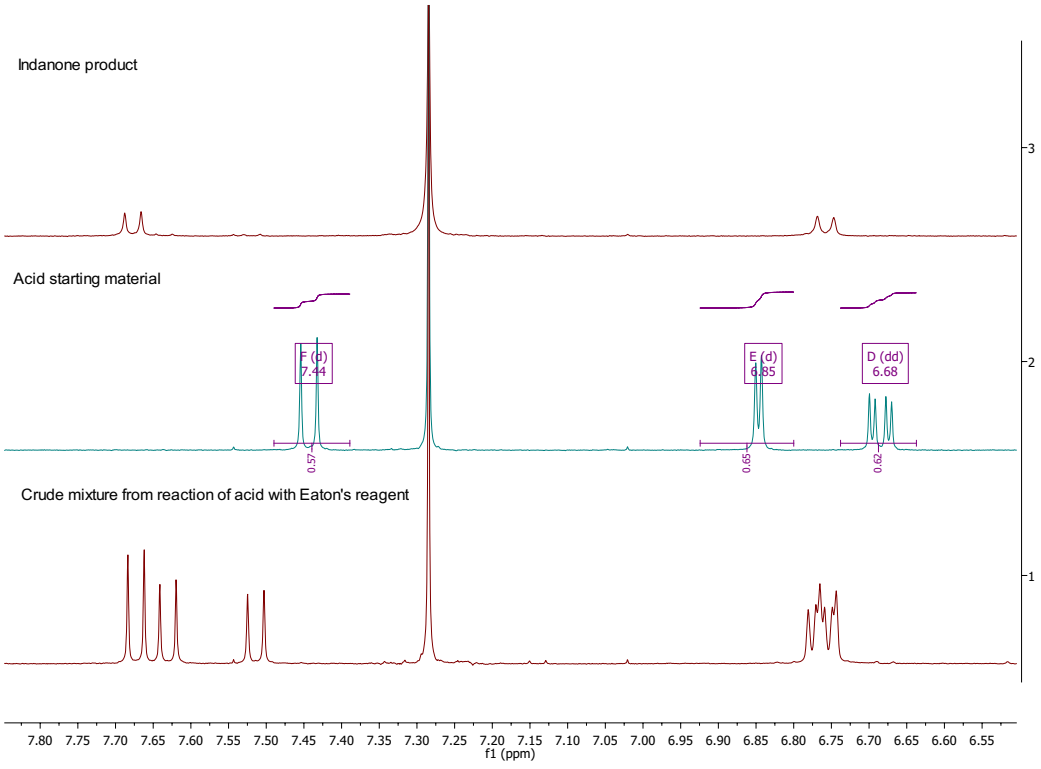

Fig. 6.1 Comparison between starting material, target compound and the crude mixture obtained from the reaction of the acid with Eaton's reagent.

The reduction of the ester to the corresponding alcohol has been attempted

several times, and gave the alcohol in high yields without the need for further purification. The Appel reaction was then utilised to convert the alcohol to the bromide as shown below (Scheme 6.7).

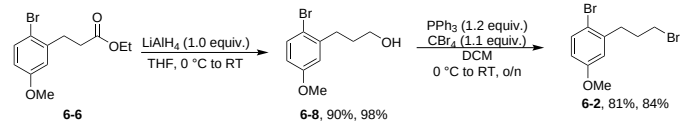

Scheme 6.7 Reduction of the ester followed by conversion of the alcohol to the corresponding bromide.

The reaction gave the corresponding bromide product in high yields after purification by column chromatography.

The subsequent transformation to the phosphonium bromide salt was readily realised and was performed several times by refluxing the bromide in toluene with PPh_3 (Scheme 6.8). Upon cooling the product precipitated from the organic solvent, and thus was easy to perform on a larger scale. The crude solid was purified by recrystallisation from H_2O to give an isolated yield of 51%.

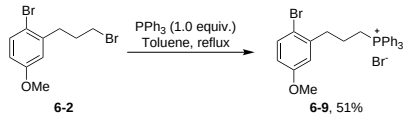

Scheme 6.8 Formation of the phosphonium bromide salt.

Having successfully prepared the phosphonium salt, we next screened reaction conditions for the formation of the ylid based upon literature conditions for related compounds.[83] Our first attempts were with BuLi.

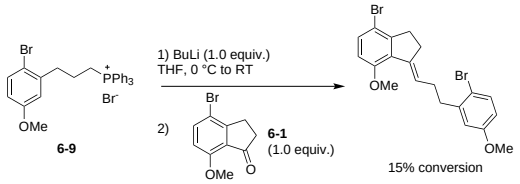

Scheme 6.9 First attempt at the Wittig reaction.

After 20 mins, ^{1}H NMR spectroscopy of the crude material (column, Hex:EtOAc 9:1) indicated the presence of an alkene but significant amounts of starting materials. The reaction was therefore attempted again with a longer running time. The starting materials were not very soluble in THF so a change of solvent could be more successful.

As a precaution, the BuLi was titrated against *N*−benzylbenzamide. The concentration was found to be 2.45 M, close to the quoted 2.5 M. This could

therefore not be the source of the low conversions. The equivalents of BuLi were increased to 1.2 from 1.0 and the reaction was repeated, giving the same result.

Next, to test whether ylid formation from the combination of the phosphonium bromide with BuLi was the issue, the reaction was attempted with a longer incubation time of these reagents. A model acceptor system was also employed, using benzaldehyde as a more reactive capture agent and varying the number of equivalents.

Assessment of the ^{1}H NMR spectrum indicated low conversion of the benzaldehyde to the alkene (<20%), as well as formation of additional side-products.

We considered that perhaps butyllithium as a base may be too strong and may be causing decomposition and side-reactions. It was therefore exchanged for potassium *tert*-butoxide, and the reaction repeated (Scheme 6.10).

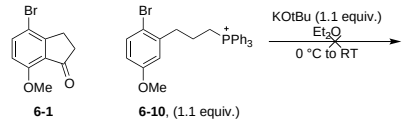

Scheme 6.10 Attempted Wittig reaction using potassium *tert*-butoxide.

However, analysis of the crude reaction mixture indicated only the indanone and the phosphonium starting materials.

It was hypothesised that the phosphonium bromide could be responsible for preventing the successful Wittig reaction. An alternative approach is the Horner-Wadsworth-Emmons reaction, a variant of the Wittig reaction that uses a phosphonate ester as a starting material.

The phosphonate ester was therefore synthesised from the bromide by the Arbuzov reaction (Scheme 6.11).

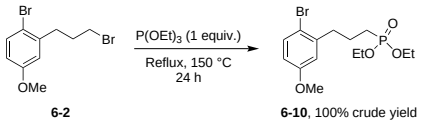

Scheme 6.11 Arbuzov reaction in the synthesis of the phosphonate ester derivative.

The phosphonate ester synthesised above was then reacted with cyclopentanone as a model substrate (Scheme 6.12).

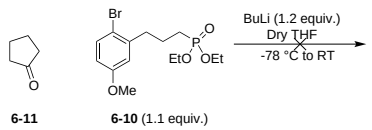

Scheme 6.12 Attempted Horner-Wadsworth-Emmons reaction using the phosphonate ester and cyclopentanone.

No conversion to the alkene was observed by ^{1}H NMR spectroscopy.

6.3 Alternative route to the propenoate

Whilst searching for an improved method to synthesise the unsaturated ester, it became apparent that the Knoevenagel condensation would provide a 'shortcut' to the unsaturated acid, giving the product in fewer steps and therefore potentially higher overall yield. The success of this route depended on whether it was still possible to reduce the unsaturated acid to the saturated acid, and whether it was easy to subsequently reduce the saturated acid to the necessary alcohol. If this were true, the saturated acid could act as the common intermediate in the overall reaction scheme. Furthermore, the saponification of the equivalent ester had been troublesome, and so this would also circumvent this reaction. The Knoevenagel condensation using the Doebner modification proceeded as shown below (Scheme 6.13).

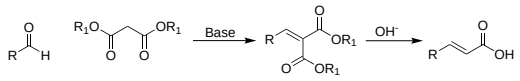

Scheme 6.13 Knoevenagel/Doebner reaction.

The mechanism applied to this reaction is illustrated below (Scheme 6.14).

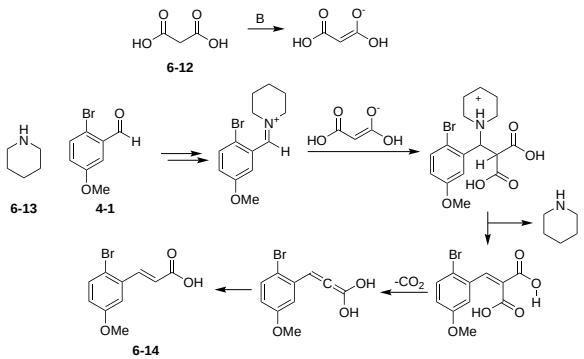

Scheme 6.14 Mechanism of the Knoevenagel/Doebner reaction.

This reaction was attempted several times and gave yields from 69-94% after purification by extraction with EtOAc to give the product as a fluffy white solid (Scheme 6.15).[84]

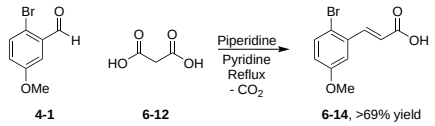

Scheme 6.15 Knoevenagel/Doebner reaction.

This protocol was also successfully employed with 2-bromo-5-hydroxybenzaldehyde as the starting material (Scheme 6.16).

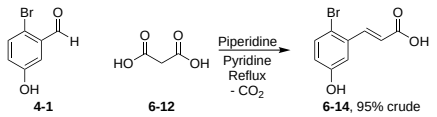

Scheme 6.16 Knoevenagel/Doebner reaction.

The product was obtained in 95% yield without purification.

The biphasic reduction conditions that use tosyl hydrazide were also successfully applied to the reduction of the unsaturated acid (Scheme 6.17).

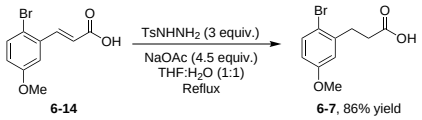

Scheme 6.17 Conjugate reduction.

Gratifyingly, the reaction was successful and thus repeated several times, on increasing scales. The product was obtained in high yields (86%, quantitative) after purification by column chromatography.

The initial attempt at the reduction of the saturated acid used 1.0 equivalents of $LiAlH_4$ as in the ester reduction (Scheme 6.18). The alcohol was obtained in 88% yield.

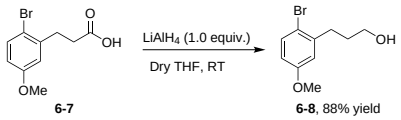

Scheme 6.18 Reduction.

When repeated with purification to remove lithium salts, the yield decreased to 49%. Increasing the equivalents of $LiAlH_4$ from 1.0 to 3.0 gave the alcohol and an undesired by-product (unidentified) and thus was significantly less successful.

6.4 Conclusions on Route 2

Several different approaches to the precursors to the Wittig reaction have been successfully completed. Several steps proceed in excellent yield, and have given access to previously undocumented compounds. Several common intermediates were identified: first, the ethyl ester, and later, the propanoic acid, from which the syntheses branched out (Scheme 6.19).

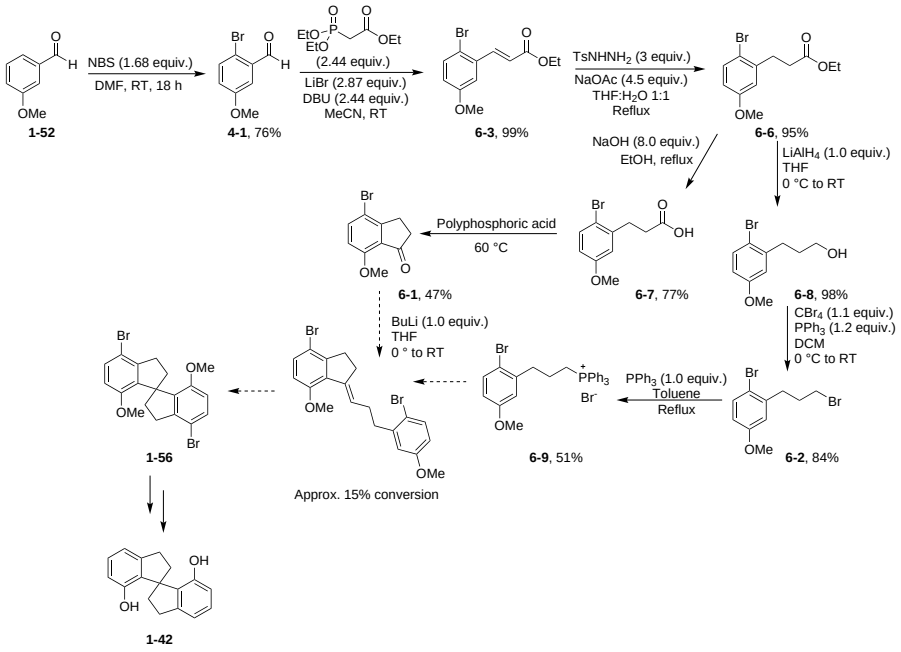

Scheme 6.19 Route 2 to SPINOL.

This project may yet yield the spirocyclic product. Work is required to develop the Wittig reaction into a successful procedure with higher conversions than observed here. Once this is complete, enantioselective cyclisations using metal catalysts with chiral ligands can be investigated.

Chapter 7

Conclusions

The synthesis of 1,1'-spirobiindane-7,7'-diol has been improved over the literature protocols. Key to this success is the use of continuous flow technologies: the H-Cube® has been used to great effect in this synthesis, removing the need for handling dangerous Raney nickel. Interconversions between related compounds have opened up new avenues of discovery. It is possible to synthesise SPINOL from a range of starting materials, proceeding *via* different routes. 3-Hydroxybenzaldehyde has been demonstrated to be a viable starting material for the synthesis of Br-SPINOL, from which it should be theoretically possible to reach SPINOL. These procedures have been thoroughly tested, and shown to be more reliable and reproducible than those already published.

These findings are summarised in the diagram below.

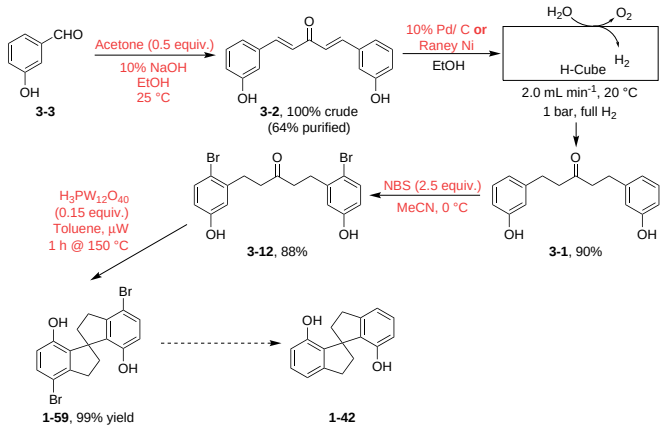

Scheme 7.1 Overall reaction scheme to *o*-(±)-Br-SPINOL. Reagents shown in red are safer or more scalable than their equivalent in the literature procedure.

The literature route to SPINOL has also been improved, and these are summarised in the scheme below.

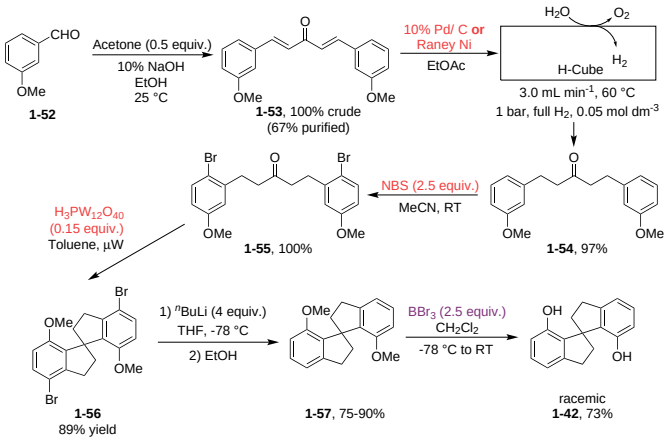

Scheme 7.2 Overall reaction scheme to *o*-(±)-SPINOL. Reagents shown in red are safer or more scalable than their equivalent in the literature procedure. Reagents in purple remain problematic.

This route proceeds in 6 steps and 32% overall yield (c.f. literature route: 6 steps, 28% overall yield).

When attempting to enantioselectively synthesise SPINOL, two approaches were considered: using amino acid-derived chiral diols in a chiral auxiliary-based strategy, and cyclisation of an alkene. Ultimately, neither were successful in selectively synthesising (+)- or (–)-SPINOL, but progress was made in both cases. In the chiral diol work, another group were later able to enantioselectively synthesise SPINOL using a very similar approach, demonstrating that our concept was sound. More work is required on the alkene-based indanone route, and it may still be possible to synthesise SPINOL by this approach.

Chapter 8

Future Work

If the debromination of Br-SPINOL were completed, it would be possible to access SPINOL from 3-hydroxybenzaldehyde in fewer steps than the equivalent synthesis from 3-methoxybenzaldehyde. Early attempts have been made, but an extensive testing of conditions has not been completed. If this were not possible, the most crucial step to improve would be the demethylation from SPINOMe to SPINOL, due to the hazardous nature of BBr_3 and the low-yielding procedure.

The 'chiral diols' approach held promise. The related results from the Zhou group[6] need to be verified and compared to this route. The 'indanone/alkene' approach requires successful synthesis of the alkene intermediate, followed by cyclisation.

Chapter 9

Experimental

9.1 1,1'-Spirobiindane-7,7'-diol (*o*-SPINOL), Compound 1-42

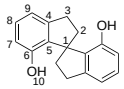

Chemical Formula: $C_{17}H_{16}O_2$
Exact Mass: 252.12

Procedure:[69]

7,7'-Dimethoxy-1,1'-spirobiindane (*o*-SPINOMe, **1-57**) (0.080 g, 0.29 mmol) was charged to an oven-dried 50 mL RBF, which was then fitted with a stirrer bar and septum. Dry DCM (2.0 mL) was charged to the RBF, which was then flushed with N_2. The solution was cooled to -78 °C and stirred for 10 mins. BBr_3 in DCM (1.0 mL) was charged to the RBF, which was allowed to warm to RT and stirred for 18 h. The solution was diluted with DCM (10 mL) and washed with H_2O until the washings were neutral (approximately 200 mL H_2O). The pale yellow organic solution was dried over Na_2SO_4, filtered and concentrated *in vacuo* to give a pale yellow film.

Isolated yield: 0.027 g (0.11 mmol, 38%)
^{1}H NMR (700 MHz, $CDCl_3$): δ/ppm 2.16-2.22 (2 H, m, H2), 2.29-2.32 (2 H, m, H2), 2.98-3.08 (4 H, m, H3), 4.63 (2 H, br s, H10), 6.68 (2 H, d, J = 8.0 Hz, H7), 6.89 (2 H, d, J = 8.1 Hz, H9), 7.17 (2 H, t, J = 7.7 Hz, H8);
^{13}C NMR (176 MHz, $CDCl_3$): δ/ppm 31.2 (C3), 37.4 (C2), 57.5 (C1), 114.3 (C7), 117.7 (C9), 129.9 (C8), 130.5 (C4), 145.8 (C5), 152.9 (C6).
IR (neat) ν = 3327.2 (OH, br), 1230.6 (C-O, s), 997.4 (m), 778.1 (s) cm^{-1}.

LC-MS: R_t = 3.16 min, m/z 253.2 $[MH]^+$; HR-MS calculated for $C_{17}H_{17}O_2$ at 253.1229, found 253.1227 (Δ = -0.8 ppm).

Reference[6,69,85]

9.2 1,5-*Bis*(3-methoxyphenyl)penta-1,4-dien-3-one, Compound 1-53

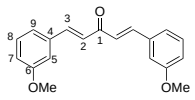

Chemical Formula: $C_{19}H_{18}O_3$
Exact Mass: 294.13

Procedure:[67–69]

NaOH (25.033 g, 625.8 mmol) was charged to a 1 L RBF fitted with a stirrer bar, followed by H_2O (250 mL) and the resulting solution was stirred until all the base had dissolved. EtOH (200 mL) was charged to the RBF, and the mixture was heated to 25 °C. Next 3-methoxybenzaldehyde (**1-52**, 15.23 mL, 125.0 mmol) followed by acetone (4.60 mL, 62.6 mmol) were charged to the RBF and the solution was stirred for 15 mins, after which time formation of a yellow oil was observed. A second aliquot of 3-methoxybenzaldehyde (**1-52**, 15.23 mL, 125.0 mmol) then acetone (4.60 mL, 62.6 mmol) were charged to the RBF and the solution was again stirred for 2.5 h. The solution was extracted with DCM (100 mL x 3), and the resulting organic layers were combined and washed with H_2O (100 mL x 3). The organic solution was dried over Na_2SO_4, filtered, and the solvent removed *in vacuo* to give a yellow oil which was 97% product by ^{1}H NMR spectroscopy. Purification by flash column chromatography (Hex:EtOAc 80:20 to 0:100) gave the product as a bright yellow oil.

Isolated yield: 31.702 g (107.8 mmol, 86%)
^{1}H NMR (700 MHz, $CDCl_3$): δ/ppm 3.85 (6 H, s, H10), 6.96 (2 H, dd, J = 2.5, 8.2 Hz, H8), 7.06 (2 H, d, J = 15.9 Hz, H2), 7.13 (2 H, m, H5), 7.21 (2 H, d, J = 7.6 Hz, H9), 7.32 (2 H, t, J = 7.9 Hz, H7), 7.70 (2 H, d, J = 15.9 Hz, H3);
^{13}C NMR (176 MHz, $CDCl_3$): δ/ppm 55.4 (C10), 113.3 (C5), 116.4 (C8), 121.1 (C9), 125.7 (C2), 130.0 (C7), 136.2 (C4), 143.3 (C3), 160.0 (C6), 188.9 (C1).
IR (neat) ν = 1620.7 (m, C=O), 1578.0 (s), 1593.0 (s), 1256.6 (s, C-O), 1043.3 (m, C-O), 985.0 (s), 859.8 (s), 763.8 (s), 705.8 (s), 665.6 (s) cm^{-1}.
LC-MS: R_t = 3.77 min, m/z 295.2 $[MH]^+$; HR-MS calculated for $C_{19}H_{19}O_3$ at 295.1334, found 295.1341 (Δ = +2.4 ppm).

Reference[69,86–89]

9.3 1,5-*Bis*(3-methoxyphenyl)pentan-3-one, Compound 1-54

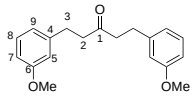

Chemical Formula: $C_{19}H_{22}O_3$
Exact Mass: 298.16

Flow procedure:

A stock solution was prepared from 1,5-*bis*(3-methoxyphenyl)penta-1,4-dien-3-one (**1-53**, 12.048 g, 40.96 mmol) was dissolved in EtOAc (410 mL, 0.100 mol dm^{-3}). The yellow solution was passed twice through the Thales Nano H-Cube® reactor (Raney Ni, 3.0 mL min^{-1}, 60 °C, full H_2) to give 100% conversion by ^{1}H NMR spectroscopy. The solvent was removed in vacuo to give the product as a pale yellow oil.

Isolated yield: 11.786 g (39.53 mmol, 97%)
Batch procedure:[69]

First, 1,5-*bis*(3-methoxyphenyl)penta-1,4-dien-3-one (**1-53**, 0.980g, 3.33 mmol) was charged to a 3-necked 100 mL RBF fitted with an overhead stirrer and two septa. Acetone (20 mL) was charged to the RBF, and the solution was degassed with N_2. Raney Ni was charged to the flask, which was then stirred for 20 mins at RT under N_2. An H_2 balloon was fitted to the flask, which was then stirred at RT for 20 h. The flask was flushed with N_2, then filtered through Celite over a scinter and rinsed with acetone. The solution was concentrated *in vacuo* to give a pale yellow oil, which was 100% pentanone by ^{1}H NMR spectroscopy, with no over-reduced alcohol present.

Isolated yield: 0.851 g (2.85 mmol, 86%).
^{1}H NMR (700 MHz, $CDCl_3$): δ/ppm 2.71 (4 H, t, J = 7.6 Hz, H2), 2.87 (4 H, t, J = 7.6 Hz, H3), 3.79 (6 H, s, H10), 6.75 (6 H, m, H7/8/9), 7.20 (2 H, t, J = 7.8 Hz, H5);
^{13}C NMR (176 MHz, $CDCl_3$): δ/ppm 29.8 (C3), 44.4 (C2), 55.1 (C10), 111.4 (C7/8/9), 114.1 (C7/8/9), 120.6 (C7/8/9), 129.5 (C5), 142.6 (C4), 159.7 (C6), 209.0 (C1).
IR (neat) ν = 1711.8 (C=O, m), 1583.9 (C=O, s), 1256.6 (C-O, s), 1152.5 (C-O, s), 1042.1 (m), 779.6 (m), 729.8 (m), 695.3 (s) cm^{-1}.
LC-MS: R_t = 3.73 min, m/z 321 $[M+Na]^+$; HR-MS calculated for $C_{19}H_{22}O_3{}^{23}Na$ at 321.1467, found 321.1477 (Δ = +3.1 ppm).
Reference[69,87]

9.4 1,5-*Bis*(2-bromo-5-methoxyphenyl)pentan-3-one, Compound 1-55

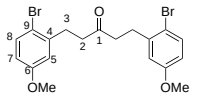

Chemical Formula: $C_{19}H_{20}Br_2O_3$
Exact Mass: 453.98

Batch procedure with Br_2:[69]

First, 1,5-*bis*(3-methoxyphenyl)pentan-3-one (**1-54**, 0.823 g, 2.76 mmol) then DCM (10 mL) were charged to a 100 mL RBF fitted with a stirrer bar. Pyridine (0.78 mL, 9.64 mmol) was charged to the RBF, which was cooled to -10 °C in an ice/ salt bath and stirred for 10 mins. A solution of Br_2 (0.36 mL, 6.99 mmol) in DCM (3 mL) was added dropwise to the RBF, and an exotherm was observed. The solution was warmed to RT, and stirred for 4 h. The reaction was quenched with 10% $Na_2S_2O_3$ (10 mL), then washed with 1 M HCl (15 mL x 3). The orange organic extract was washed with H_2O (20 mL x 2), dried over Na_2SO_4 and filtered. The solvent was removed *in vacuo* to give an orange oil which solidified to a pale yellow wax overnight.

Isolated yield: 1.007 g (2.22 mmol, 80%)
Batch procedure with NBS:

First, 1,5-*bis*(3-methoxyphenyl)pentan-3-one (**1-54**, 0.298 g, 0.99 mmol) was charged to a 50 mL RBF fitted with a stirrer bar. MeCN (4 mL) was charged to the RBF to give a pale yellow solution. NBS (0.360 g, 2.02 mmol) was charged to the RBF, which was stirred at RT for 30 mins. The reaction was quenched with 10% $Na_2S_2O_3$ (10 mL), then extracted with Et_2O (10 mL), 10% $Na_2S_2O_3$ (10 mL) followed by H_2O (10 mL). The organic extracts were combined and dried over Na_2SO_4, filtered and concentrated *in vacuo* to give a pale yellow oil.

Isolated yield: 0.228 g (0.50 mmol, 50%)
Flow procedure:

1,5-*Bis*(2-bromo-5-hydroxyphenyl)penta-1,4-dien-3-one (**3-10**, 0.0913 g, 0.203 mmol) was dissolved in EtOAc (6 mL, 0.034 mol dm^{-3}) and passed through the Thales Nano H-Cube® reactor (Raney Ni catalyst, 2.0 mL min^{-1}, 70 °C, 1 atm, full H_2 mode) six times. The solution was concentrated *in vacuo* to give the product.

Isolated yield: 0.030 g (0.066 mmol, 33%)
^{1}H NMR (700 MHz, $CDCl_3$): δ/ppm 2.73 (4 H, t, J = 7.7 Hz, H2), 2.96 (4 H, t, J = 7.7 Hz, H3), 3.76 (6 H, s, H10), 6.63 (2 H, dd, J = 8.7, 3.1 Hz, H7), 6.77 (2 H, d, J = 3.0 Hz, H5), 7.39 (2 H, t, J = 8.7 Hz, H8);
^{13}C NMR (176 MHz, $CDCl_3$): δ/ppm 30.6 (C3), 42.5 (C2), 55.4 (C10), 113.6 (C7), 114.6 (C9), 116.2 (C5), 133.4 (C8), 141.2 (C4), 159.0 (C6), 208.4 (C1).
IR (neat) ν = 1700.6 (C=O, m), 1571.9 (C=O, m), 1471.0 (s), 1240.1 (C-O, s), 1163.2 (C-O, s), 790.7 (s), 599.5 (s) cm^{-1}.
LC-MS: R_t = 4.18 min, m/z 477:479:481 (1:2:1) $[M+Na]^+$; HR-MS calculated for $C_{19}H_{20}O_3Br_2{}^{23}Na$ at 476.9677, found 476.9676 (Δ = -0.21 ppm).
Reference[69]

9.5 4,4'-Dibromo-7,7'-dimethoxy-1,1'-spirobiindane (Br-SPINOMe), Compound 1-56

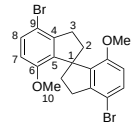

Chemical Formula: $C_{19}H_{18}Br_2O_2$
Exact Mass: 435.97

Polyphosphoric acid procedure:[69]

First, 1,5-*bis*(2-bromo-5-methoxyphenyl)pentan-3-one (**1-55**, 0.768 g, 1.69 mmol) was charged to a 50 mL RBF fitted with a stirrer bar. Polyphosphoric acid (4.250 g) was charged to the RBF, which was heated at 105 °C for 8 h. ^{1}H NMR spectroscopy after 6 h indicated 74% conversion. The dark brown solution was poured into H_2O (50 mL), then extracted with Et_2O (20 mL x 2), then DCM (20 mL x 2). The solution was decanted to remove brown solid, then the solvent removed *in vacuo*. The pale brown foam obtained was dry-loaded onto silica, then filtered through a 2 cm plug of silica (Hex:EtOAc 9:1). The solution was concentrated *in vacuo* to give a pale yellow solid.

Isolated yield: 0.199 g (0.46 mmol, 27%).
Heteropoly acid procedure:[76]

First, 1,5-*bis*(2-bromo-5-methoxyphenyl)pentan-3-one (**1-55**, 2.331 g, 5.13 mmol) was charged to a 100 mL RBF fitted with a stirrer bar. Toluene (20 mL) was charged to the flask, which was stirred until the solid dissolved to give an orange solution. $H_3PW_{12}O_{40}$ (2.123 g, 0.74 mmol) was charged to the flask, and the resulting mixture was stirred under Dean-Stark reflux conditions for 14 h. The dark-brown solution was allowed to cool to RT then filtered through a scinter and washed with $CHCl_3$ (20 mL). The solution was concentrated *in vacuo*, and the purple solid was purified by flash column chromatography (Hex:EtOAc 9:1) to give a white solid.

Isolated yield: 1.025 g (2.35 mmol, 46%).
^{1}H NMR (700 MHz, $CDCl_3$): δ/ppm 2.13-2.17 (2 H, m, H2), 2.28-2.33 (2 H, m, H2), 2.92-2.96 (2 H, m, H3), 3.03-3.07 (2 H, m, H3), 3.51 (6 H, s, H10), 6.51 (2 H, d, J = 8.6 Hz, H7), 7.25 (2 H, m, H8);
^{13}C NMR (176 MHz, $CDCl_3$): δ/ppm 33.1 (C3), 37.9 (C2), 55.4 (C10), 61.9 (C1), 110.5 (C9), 110.8 (C7), 130.3 (C8), 138.0 (C5), 144.8 (C4), 155.6 (C6).

IR (neat) ν = 1472.1 (m), 1260.9 (C-O, s), 1077.2 (m), 1054.2 (m), 795.8 (s) cm^{-1}.
LC-MS (ASAP): R_t = 0.72 min, m/z 437:439:441 (1:2:1) $[MH]^+$; HR-MS (AP^+) calculated for $C_{19}H_{18}Br_2O_2$ at 436.9752, found 436.9756 (Δ = +0.9 ppm).
GC-MS: 7.87 min, m/z 436:438:440 (1:2:1) $[M]^+$.
CHN analysis: calculated for $C_{19}H_{18}Br_2O_2$ at C 52.08%, H 4.14%, N 0.00%; found C 52.13%, H 4.12%, N -0.02%.
The structure and connectivity were confirmed by single crystal X-ray crystallography, performed by Dr Dmitry S. Yufit of the Durham University X-Ray Crystallography Service and has the unique identifier of '14srv270'.

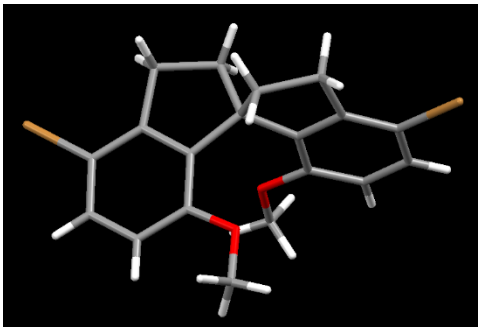

Space group	P-1
a/ Å	7.5094(4)
b/ Å	10.4475(6)
c/ Å	12.0959(6)
α/ °	107.731(5)
β/ °	106.488(5)
γ/ °	97.534(4)

Reference[69,76,90]

9.6 7,7'-Dimethoxy-1,1'-spirobiindane (*o*-SPINOMe), Compound 1-57

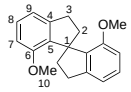

Chemical Formula: $C_{19}H_{20}O_2$
Exact Mass: 280.15

Batch procedure:[69]

First, 4,4'-dibromo-7,7'-dimethoxy-1,1'-spirobiindane (Br-SPINOMe, **1-56**) (0.205 g, 0.47 mmol) was charged to an oven-dried 100 mL RBF, which was then fitted with a stirrer bar and septum. The flask was flushed with N_2, and dry THF (8.0 mL) was charged to the RBF. The solution was cooled to -78 °C and stirred for 10 mins. *n*BuLi (3.0 mL, 3.30 mmol) was added dropwise to the RBF, and the solution changed colour from pale yellow to orange. After 1 h, the solution was quenched with EtOH (1.0 mL) and left to warm to RT. The solution was extracted with H_2O (15.0 mL x 3) and DCM (10.0 mL x 2). The pale yellow solution was dried over Na_2SO_4, filtered and concentrated *in vacuo* to give a white solid.

Isolated yield: 0.117 g (0.42 mmol, 89%)
Flow procedure:

First, 4,4'-dibromo-7,7'-dimethoxy-1,1'-spirobiindane (**1-56**, 0.098 g, 0.22 mmol) was dissolved in EtOAc (4 mL, 0.056 mol dm^{-3}) and passed through the Thales Nano H-Cube® reactor (10% Pd/C catalyst, 2.0 mL min^{-1}, 20 °C, 1 atm, full H_2 mode). The solution was concentrated *in vacuo* to give a mixture of products as a pale yellow oil.

^{1}H NMR (700 MHz, $CDCl_3$): δ/ppm 2.15-2.19 (2 H, m, H2), 2.32-2.36 (2 H, m, H2), 2.97-3.01 (2 H, m, H3), 3.04-3.08 (2 H, m, H3), 3.53 (6 H, s, H10), 6.62 (2 H, d, J = 8.0 Hz, H7), 6.86 (2 H, d, J = 7.4 Hz, H9), 7.13 (2 H, t, J = 7.7 Hz, H8);
^{13}C NMR (176 MHz, $CDCl_3$): δ/ppm 31.6 (C3), 38.8 (C2), 55.2 (C10), 59.2 (C1), 108.6 (C7), 116.8 (C9), 127.5 (C8), 136.9 (C5), 145.3 (C4), 156.5 (C6).
IR (neat) ν = 1585.3 (m), 1473.5 (m), 1261.8 (m), 1060.4 (m), 771.9 (s) cm^{-1}.
LC-MS: R_t = 3.71 min, m/z 281.2 $[MH]^+$; HR-MS calculated for $C_{19}H_{21}O_2$ at 281.1542, found 281.1548 (Δ = +2.1 ppm).
Reference[69]

9.7 4,4'-Dibromo-2,2',3,3'-tetrahydro-1,1'-spirobi[indene]-7,7'diol (Br-SPINOL), Compound 1-59

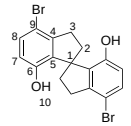

Chemical Formula: $C_{17}H_{14}Br_2O_2$
Exact Mass: 407.94

Procedure:

First, 1,5-*bis*(2-bromo-5-hydroxyphenyl)pentan-3-one (**3-11**, 0.100 g, 0.23 mmol) then $H_3PW_{12}O_{40}$ (0.105 g, 0.037 mmol) were charged to a 5 mL microwave vial, followed by toluene (3 mL) and a stirrer bar. The vial was capped and sealed, then heated in the micrwoave with 5 mins' pre-stirring at 150 °C for 60 mins. The vial was uncapped and the crude mixture filtered over a silica/ cotton wool plug, washing with $CHCl_3$ (5 mL). Concentration *in vacuo* gave the crude product as a pale yellow solid. Purification by column chromatography (Hex:EtOAc 9:1) gave the product as a white solid.

Isolated yield: 0.095 g (0.23 mmol, 99%)
^{1}H NMR (700 MHz, $CDCl_3$): δ/ppm 2.14-2.36 (4 H, m, H2), 2.91=3.10 (4 H, m, H3), 4.51 (2 H, s, H10), 6.58 (2 H, d, J = 8.5 Hz, H7), 7.29 (2 H, d, J = 8.5 Hz, H8);
^{13}C NMR (126 MHz, $CDCl_3$): δ/ppm 32.7 (C3), 36.7 (C2), 60.3 (C1), 111.0 (C9), 116.6 (C7), 132.1 (C5), 132.6 (C8), 145.4 (C4), 151.9 (C6).
IR (neat) ν = 3522.3 (O-H, br w), 1466.4 (s), 1274.8 (m), 804.7 (s), 655.0 (m) cm^{-1}.
LC-MS: R_t = 3.46 min, m/z 407.5:409.5:411.5 (1:2:1) $[M]^-$; HR-MS calculated for $C_{79}H_{13}O_2Br_2$ at 406.9282, found 406.9282 (Δ = 0.0 ppm).
Reference[6]

9.8 1,5-*Bis*(3-hydroxyphenyl)pentan-3-one, Compound 3-1

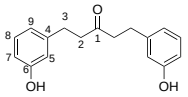

Chemical Formula: $C_{17}H_{18}O_3$
Exact Mass: 270.13

Procedure:[91]

First, 1,5-*bis*(3-hydroxyphenyl)penta-1,4-dien-3-one (**3-2**, 0.801 g, 3.01 mmol) and 10% Pd/C (0.0812 g, 10 wt%) were charged to a 50 mL RBF fitted with a stirrer bar which was flushed with N_2. EtOH (12 mL) then Ph_2S (5.0 L, 0.0299 mmol) were charged to the flask under N_2. The flask was put under vacuum then back-filled with H_2 twice, and stirred at room temperature under a H_2 balloon for 5 h. The flask was flushed with N_2 (15 mins), then the solution filtered through Celite and rinsed with EtOH (5 mL x 3). The solvent was removed *in vacuo* to give a pale yellow oil which solidified on standing.

Isolated yield: 0.737 g (2.73 mmol, 91%)
^{1}H NMR (700 MHz, d_6−DMSO): δ/ppm 2.69 (4 H, m, H2/3), 6.57 (3 H, m, H5/7/8/9), 7.04 (1 H, t, J = 8.0 Hz, H5/7/8/9), 9.28 (1 H, br s, Ar-OH);
^{13}C NMR (176 MHz, d_6−DMSO): δ/ppm 29.5 (C2/3), 43.8 (C2/3), 113.3 (CH), 115.6 (CH), 119.2 (CH), 129.7 (CH), 143.0 (C4), 157.7 (C6), 209.5 (C1).
IR (neat) ν = 3325.9 (OH, br), 1698.8 (C=O, s), 1585.6 (s), 1249.9 (C-O, m), 1231.1 (C-O, s), 769.8 (m), 690.0 (s), 644.1 (m) cm^{-1}.
LC-MS: R_t = 2.52 min, m/z 269 [M-H]$^-$; HR-MS calculated for $C_{17}H_{17}O_3$ at 269.1178, found 269.1189 (Δ = +4.1 ppm).
Reference[6]

9.9 1,5-*Bis*(3-hydroxyphenyl)penta-1,4-dien-3-one, Compound 3-2

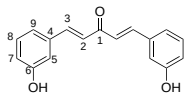

Chemical Formula: $C_{17}H_{14}O_3$
Exact Mass: 266.09

Procedure:[68,92]

10% NaOH (14.928 g, 373 mmol, 150 mL) was charged to a 500 mL RBF, followed by EtOH (120 mL) and the solution was heated at 25 °C with stirring. 3-Hydroxybenzaldehyde (**3-3**, 9.129 g, 74.8 mmol) was charged to the flask, followed by acetone (2.75 mL, 37.5 mmol), and the solution was stirred for a further 15 mins. The colour changed from yellow to red. A further portion of 3-hydroxybenzaldehyde (**3-3**, 9.123 g, 74.7 mmol) and acetone (2.80 mL, 38.1 mmol) were charged to the RBF. The resulting solution was stirred for 3.5 h at 25 °C. An aqueous solution of 6 M HCl was added until the solution was neutral, and a yellow precipitate had formed. The solution was filtered, dried *in vacuo*, then recrystallised from IPA to give a fine bright yellow powder.

Isolated yield: 11.902 g (44.7 mmol, 60%)
^{1}H NMR (700 MHz, d_4−MeOD): δ/ppm 6.85 (1 H, d, J = 8.0 Hz, H2), 7.10 (1 H, s), 7.15-7.18 (2 H, m), 7.24 (1 H, t, J = 7.8 Hz), 7.69 (1 H, d, J = 15.9 Hz, H3);
^{13}C NMR (176 MHz, d_4−MeOD): δ/ppm 114.3 (CH), 117.5 (C2), 119.8 (CH), 124.8 (CH), 129.6 (CH), 136.1 (C4), 143.9 (C3), 157.7 (C6), 190.1 (C1).
IR (neat) ν = 3229.8 (OH, br), 1618.2 (C=O, s), 1579.2 (s), 1561.1 (s), 1213.3 (s), 1105.0 (s), 982.0 (s), 863.5 (s), 782.2 (s) cm^{-1}.
LC-MS: R_t = 2.49 min, m/z 265.1 [M-H]$^-$; HR-MS (ES$^+$) calculated for $C_{17}H_{15}O_3$ at 267.1021, found 267.1029 (Δ = +3.0 ppm).
Melting point: decomposed to black solid by 202 °C (IPA).
Reference[93,94]

9.10 5,5'-Dimesylate-1,1'-spirobiindane (*p*-SPINOMs), Compound 3-5

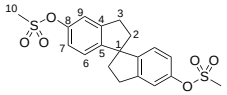

Procedure with Eaton's reagent:

1,5-*Bis*(3-hydroxyphenyl)pentan-3-one (**3-1**, 0.342 g, 1.27 mmol) was charged to a 50 mL RBF fitted with a stirrer bar. Eaton's reagent[70] (8.701 g, 25:1 by wt) was charged to the flask, which was heated at 60 °C for 2 h. The flask was transferred to an ice bath, and H_2O (40 mL) was charged to the flask slowly, followed by gradual addition of $NaHCO_3$ (100 mL) due to the exotherm. The solution was extracted twice with Et_2O (100 mL, then 50 mL), then the solvent removed *in vacuo* to give a colourless oil with some purple discolouration. The crude product was dissolved in DCM, then filtered through a 1 cm plug of silica, followed by solvent removal *in vacuo* to give the product as a solid foam.

Isolated yield: 0.198 g (0.785 mmol, 62%)
Procedure from *p*-SPINOL:[95]

1,1'-Spirobiindane-5,5'-diol (*p*-SPINOL, **3-6**) (0.050 g, 0.20 mmol) was charged to a 25 mL RBF fitted with a stirrer bar and a septum. The starting material was dissolved in dry DCM (0.4 mL) to give a pale yellow solution which was flushed with N_2. Dry pyridine (0.08 mL, 0.99 mmol) was charged to the RBF and the solution cooled to 0 °C and stirred for 10 mins. MsCl (0.10 mL, 1.29 mmol) was charged to the RBF and the solution was stirred in an ice bath for 3 h, then warmed to RT for 5 h. The solution was quenched with H_2O and the organic phase extracted. The aqueous layer was washed with DCM (3 x 2 mL). All the organic extracts were combined, washed with 1 M HCl (2 x 5 mL), then brine (2 x 4 mL), dried over Na_2SO_4, filtered and concentrated *in vacuo* to give a pale yellow oil.

Isolated yield: 0.054 g (0.13 mmol, 74%)
^{1}H NMR (400 MHz, $CDCl_3$): δ/ppm 2.15-2.23 (2 H, m, H2/3), 2.34-2.40 (2 H, m, H2/3), 3.02-3.06 (4 H, m, H2/3), 3.16 (3 H, s, H10), 6.93 (2 H, d, J = 8.2 Hz, H6), 7.05 (2 H, dd, J = 8.2, 2.3 Hz, H7), 7.21 (2 H, d, J = 2.1 Hz, H9);
^{13}C NMR (125 MHz, $CDCl_3$): δ/ppm 30.7 (C2/3), 37.8 (C10), 40.8 (C2/3), 59.7 (C1), 118.8 (Ar CH), 121.2 (Ar CH), 124.6 (Ar CH), 146.0 (Ar C), 148.7 (Ar

C), 149.2 (Ar C).
IR (neat) ν = 2939.5 (w), 1359.5m, 1175.5 (C-O, s), 1121.6 (C-O, m), 923.2 (s), 804.2 (m) cm^{-1}.
LC-MS: R_t = 3.31 min, m/z 409.6 $[MH]^+$; HR-MS calculated for $C_{19}H_{21}O_6S_2$ at 409.0780, found 409.0768 (Δ = -2.4 ppm).
No literature data available.

9.11 1,1'-Spirobiindane-5,5'-diol (*p*-SPINOL), Compound 3-6

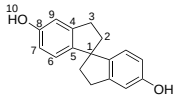

Chemical Formula: $C_{17}H_{16}O_2$
Exact Mass: 252.12

Procedure:

5,5'-Dimethoxy-1,1'-spirobiindane (*p*-SPINOMe, **3-7**) (0.538 g, 1.92 mmol) was dissolved in dry DCM (10 mL) and transferred to a dry 50 mL RBF fitted with a stirrer bar and septum. The RBF was flushed with N_2, and the solution cooled to -78 °C. BBr_3 in DCM (4.50 mL, 4.50 mmol) was transferred to the RBF, and the colour of the solution changed from pale yellow to dark red. The solution was then allowed to warm to RT and stirred for 20 h. The solution was diluted with DCM (10 mL) and vented to the atmosphere. The solution was washed with H_2O until the washings were neutral, and the organic layers were dried over Na_2SO_4 and then filtered and concentrated *in vacuo* to give a foam.

Isolated yield: 0.045 g (0.18 mmol, 9%)
^{1}H NMR (400 MHz, $CDCl_3$): δ/ppm 2.11-2.19 (2 H, m, H2), 2.26-2.37 (2 H, m, H2), 2.93-3.05 (4 H, m, H3), 4.92 (2 H, br s, H10), 6.63 (2 H, dd, J = 8.1, 2.5 Hz, Ar H), 6.77-6.81 (4 H, m, Ar H);
^{13}C NMR (101 MHz, $CDCl_3$): δ/ppm 30.8 (C2/C3), 40.1 (C2/C3), 59.2 (C1), 111.2 (CH), 113.7 (CH), 124.1 (CH), 143.0 (C4/5), 145.5 (C4/5), 154.7 (C8);
IR (neat) ν = 3278.1 (O-H, br m), 1609.8 (m), 1490.1 (m), 1450.6 9s), 1247.7 (s), 1215.5 (C-O, s), 1156.7 (s), 1095.7 (m), 722.5 (m), 857.0 (s), 592.9 (s) cm^{-1}.

Reference[6,96]

9.12 5,5'-Dimethoxy-1,1'-spirobiindane (*p*-SPINOMe), Compound 3-7

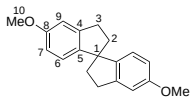

Chemical Formula: $C_{19}H_{20}O_2$
Exact Mass: 280.15

Procedure with polyphosphoric acid:

1,5-*Bis*(3-methoxyphenyl)pentan-3-one (**1-54**, 0.951 g, 3.19 mmol) was charged to a 100 mL RBF fitted with a stirrer bar. Polyphosphoric acid (8.174 g, 8.6 wt) was charged to the RBF, and the resulting viscous solution was heated to 105 °C for 6 h. The solution was quenched with H_2O (50 mL), then extracted with Et_2O (30 mL x 2), then extracted with DCM (20 mL x 2). The organic layers were concentrated *in vacuo*, and then dry-loaded onto silica. The crude product was purified by column chromatography (Hex:EtOAc 9:1) to give a yellow oil.

Isolated yield: 0.347 g (1.24 mmol, 39%)
Procedure with heteropoly acid:

1,5-*Bis*(3-methoxyphenyl)pentan-3-one (**1-54**, 1.075 g, 3.61 mmol) was charged to a 50 mL RBF fitted with a stirrer bar. Toluene (10 mL) was charged to the RBF and the mixture was stirred until all the solid dissolved to give an orange solution. $H_3PW_{12}O_{40}$ (1.552 g, 0.539 mmol) was charged to the RBF, which was heated under reflux with a Dean-Stark head for 20 h. The reaction was allowed to cool to RT, then filtered through a scinter and rinsed with $CHCl_3$. The solution was concentrated *in vacuo* to give an orange oil (0.833g, 2.97 mmol, 82% crude yield). The crude oil was purified by flash column chromatography (Hex:EtOAc 9:1) to give a white solid.

Isolated yield: 0.730 g (2.61 mmol, 72%).
^{1}H NMR (700 MHz, $CDCl_3$): δ/ppm 2.16 (2 H, m, H2), 2.29 (m, 2H, H2), 2.97 (m, 4H, H3), 3.80 (s, 6H, H10), 6.70 (dd, J = 8.5, 2.3 Hz, 2H, H6/7/9), 6.83 (m, 4H, H6/7/9);
^{13}C NMR (176 MHz, $CDCl_3$): δ/ppm 31.0 (C3), 41.1 (C2), 55.4 (C10), 59.3 (C1), 109.6 (C6/7/9), 112.6 (C6/7/9), 123.9 (C6/7/9), 142.9 (C4/5), 145.2 (C4/5), 158.9 (C8).
IR (neat) ν = 2934.9 (m), 1606.0 (m), 1492.1 (s), 1464.0 (m), 1247.2 (C-O, s), 1031.3 (C-O, m), 834.8 (s) cm^{-1}.
LC-MS: R_t = 3.66 min, m/z 281 $[MH]^+$.
Reference[76,96]

9.13 2-Bromo-5-hydroxybenzaldehyde, Compound 3-8

Chemical Formula: $C_7H_5BrO_2$
Exact Mass: 199.95

Procedure:

3-Hydroxybenzaldehyde (**3-3**, 2.465 g, 20.2 mmol) was charged to a 250 mL RBF fitted with a stirrer bar. DCM (80 mL) was charged to the flask and the resultant mixture was stirred in an ice bath (15 mins). A solution of Br_2 (1.1 mL, 21.4 mmol) in DCM (10 mL) was added dropwise over 5 mins. The solution was removed from the ice bath and allowed to warm to room temperature. After 30 mins, precipitation was observed and the heterogeneous solution changed colour from brown to orange. After 4 h stirring at room temperature, conversion to the product was 78% as determined by ^{1}H NMR spectroscopy and the flask was cooled in an ice bath for 30 mins. The solution was filtered and the solid left to air-dry. Recrystallisation from AcOH gave the product as fluffy white needles.

Isolated yield: 2.633 g (13.2 mmol, 65%)
^{1}H NMR (700 MHz, $CDCl_3$): δ/ppm 5.23 (1 H, br s, OH), 7.00 (1 H, dd, J = 8.6, 3.2 Hz), 7.38 (1 H, d, J = 3.2 Hz), 7.52 (1 H, d, J = 8.6 Hz), 10.29 (1 H, s, CHO);
^{13}C NMR (176 MHz, $CDCl_3$): δ/ppm 115.7 (CH), 117.8 (C), 123.3 (CH), 134.1 (C), 134.9 (CH), 155.5 (C), 191.9 (CHO).
IR (neat) ν = 3461.4 (OH, s), 1674.8 (C=O, s), 1590.9 (s), 1475.7 (m), 1428.1 (m), 1384.2 (m), 1298.0 (m), 1165.9 (s), 876.4 (m), 828.5 (m) cm^{-1}.
LC-MS: R_t = 2.35 min, m/z 198,8 [M-H]$^-$; HR-MS calculated for $C_7H_4BrO_2$ at 198.9395, found 198.9396 (Δ = +0.5 ppm).
CHN analysis: calculated for $C_7H_5BrO_2$ at C 41.82%, H 2.51%, N 0.00%; found C 41.93%, H 2.52%, N -0.02%.
Melting point: 133.7-134.5 °C (AcOH), literature[97] = 133 °C.
Reference[97]

9.14 1,5-*Bis*(2-bromo-5-hydroxyphenyl)penta-1,4-dien-3-one, Compound 3-10

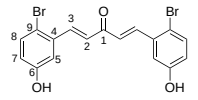

Chemical Formula: $C_{17}H_{12}Br_2O_3$
Exact Mass: 421.92

Procedure:[68,92]

10% NaOH (0.494 g, 12.4 mmol) was charged to a 100 mL RBF, followed by EtOH (4.0 mL). The solution was heated to 25 °C with stirring. 2-Bromo-5-hydroxybenzaldehyde (**3-8**, 0.509 g, 2.55 mmol) and acetone (0.092 mL, 1.25 mmol) were charged to the RBF, then the resulting solution was stirred for 15 mins. The colour changed from yellow to red. A second portion of 2-bromo-5-hydroxybenzaldehyde (**3-8**, 0.509 g, 2.55 mmol) was charged to the flask, followed by acetone (0.092 mL, 1.25 mmol). The solution was stirred for 3.5 h at 25 °C. An aqueous solution of 6 M HCl was added until the solution was neutral, with an orange precipitate. The solution was filtered, dried *in vacuo*, then recrystallised from IPA to give a fine bright yellow powder.

Isolated yield: 0.440 g (1.04 mmol, 41%)
^{1}H NMR (700 MHz, d_4−MeOD): δ/ppm 6.79 (1 H, dd, J = 8.7, 3.0 Hz, H4), 7.10 (1 H, d, J = 15.9 Hz, H8), 7.26 (1 H, d, J = 2.9 Hz, H6), 7.45 (1 H, d, J = 8.7 Hz, H3), 8.02 (1 H, d, J = 15.9 Hz, H7);
^{13}C NMR (176 MHz, d_4−MeOD): δ/ppm 113.9 (C5), 114.3 (C9), 119.5 (C7), 127.0 (C2), 133.7 (C8), 134.8 (C4), 142.0 (C3), 157.5 (C6), 189.1 (C1).
IR (neat) ν = 3301.9 (OH, br), 1615.0 (C=O, s), 1566.2 (s), 1464.4 (s), 1351.0 (s), 1311.8 (s), 1117.4 (s), 980.4 (s), 817.7 (s) cm^{-1}.
LC-MS: R_t = 3.62 min, m/z 420.8 [M-H]$^-$; HR-MS (ES$^+$) calculated for $C_{17}H_{13}O_3{}^{79}Br_2$ at 422.9231, found 422.9234 (Δ = +0.7 ppm).
Melting point: decomposed to black solid by 197 °C (IPA).
Reference[6]

9.15 1,5-*Bis*(2-bromo-5-hydroxyphenyl)pentan-3-one, Compound 3-11

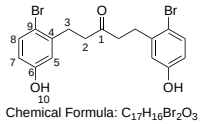

Procedure:

First, 1,5-*bis*(3-hydroxylphenyl)pentan-3-one (**3-1**, 1.00 g, 3.70 mmol) was dissolved in MeCN (15 mL) in a 50 mL RBF fitted with a stirrer bar. The RBF was then lowered into an ice bath. NBS (1.65 g, 9.25 mmol) was added slowly. The reaction was followed by TLC. After 30 mins, the reaction had reached 92% conversion. The reaction was quenched with 10% $Na_2S_2O_3$ (10 mL), then extracted with Et_2O (10 mL), 10% $Na_2S_2O_3$ (10 mL) followed by H_2O (10 mL). The organic extracts were combined and dried over Na_2SO_4, filtered and concentrated *in vacuo* to give the product as a white powder.

Isolated yield: 1.32 g (3.09 mmol, 91%)
^{1}H NMR (400 MHz, d_6−DMSO): δ/ppm 2.75 (8 H, h, J = 6.8, 6.4 Hz, H2/3), 6.57 (2 H, dd, J = 8.6 H, 3.0 Hz, H7), 6.73 (2 H, d, J = 2.9 Hz, H5), 7.32 (2 H, d, J = 8.6 Hz, H8), 9.62 (2 H, s, H10);
^{13}C NMR (101 MHz, d_6−DMSO): δ/ppm 30.1 (C3), 42.1 (C2), 112.5 (C9), 115.8 (C7), 133.4 (C8), 141.3 (C4), 157.4 (C6), 208.6 (C1).
IR (neat) ν = 3422.1 (O-H, br w), 1686.6 (C=O, s), 1591.5 (m), 1579.3 (m), 1471.7 (m), 1434.0 (s), 1222.3 (C-O, s), 1166.7 (s), 1030.3 (m), 858.9 (m), 797.2 (m), 706.9 (m), 601.2 (s) cm^{-1}.
LC-MS: R_t = 2.70 min, m/z 425:427:429 (1:2:1) $[M]^-$.
Reference[6]

9.16 2-Bromo-5-methoxybenzaldehyde, Compound 4-1

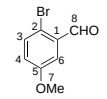

Chemical Formula: $C_8H_7BrO_2$
Exact Mass: 213.96

Procedure using Br_2:[98]

3-Methoxybenzaldehyde (**1-52**, 2.45 mL, 20.1 mmol) was charged to a 50 mL RBF fitted with a stirrer bar, followed by AcOH (5 mL). All the starting material dissolved to give a pale yellow solution. Neat Br_2 (1.25 mL, 24.4 mmol) was charged slowly to the RBF with stirring to give a dark orange solution. An exotherm was observed. After 24 h, substantial solid formation was observed and the reaction was stopped by the addition of 10% $Na_2S_2O_3$ (30 mL). The solution was poured into H_2O (30 mL) and extracted with Et_2O (30 mL x 4). The organic layers were combined and washed with H_2O (30 mL x 2) then sat. aqueous NaCl (30 mL), followed by drying over $MgSO_4$ and filtration. Removal of the solvent *in vacuo* gave the crude product as a pale yellow solid (4.076 g, 19.05 mmol, 95% crude yield) which was 90% product by ^{1}H NMR spectroscopy. Recrystallisation from EtOH:H_2O (9:1) followed by rinsing with cold EtOH gave the product as sparkly white fluffy needles.

Isolated yield: 2.683 g (12.5 mmol, 63%)
Procedure using NBS:[99]

3-Methoxybenzaldehyde (**1-52**, 10.0 mL, 81.9 mmol) was charged to a 500 mL RBF fitted with a stirrer, followed by DMF (65 mL). The RBF was lowered into an ice bath, and NBS (24.4 g, 133.3 mmol) was added slowly over 20 mins. The RBF was removed from the ice bath and allowed to warm to RT, turning an orange colour. After stirring overnight at RT, the solution was poured into a mixture of ice and water to quench the reaction, and stirred until the ice had melted. Formation of a yellow-white precipitate was observed immediately. The slurry was filtered and washed with H_2O (50 mL x 2). Recrystallisation from IPA gave the product as white, flaky crystals.

Isolated yield: 13.362 g (62.5 mmol, 76%)
^{1}H NMR (700 MHz, $CDCl_3$): δ/ppm 3.83 (1 H, s, H7), 7.03 (1 H, dd, J = 8.8, 3.2 Hz, H4), 7.41 (1 H, d, J = 3.2 Hz, H3), 7.52 (1 H, d, J = 8.8 Hz, H6), 10.30 (1 H, s, H8);

^{13}C NMR (176 MHz, $CDCl_3$): δ/ppm 55.7 (C7), 112.6 (C3), 118.0 (C2), 123.1 (C4), 134.0 (C1), 134.5 (C6), 159.2 (C5), 191.8 (C8).
IR (neat) ν = 1674.9 (m), 1569.5 (m), 1278.3 (m), 1197.8 (m), 931.9 (s), 865.0 (m), 819.7 (s), 647.1 (s), 597.5 (s) cm^{-1}.
LC-MS: R_t = 2.88 min, m/z 215 $[MH]^+$; HR-MS calculated for $C_8H_8{}^{79}BrO_2$ at 214.9708, found 214.9715 (Δ = +3.3 ppm).
CHN analysis: calculated for $C_8H_7BrO_2$ at C 44.68%, H 3.28%, N 0.00%; found C 44.61%, H 3.28%, N -0.03%.
Melting point: 74.5-75.5 °C (EtOH:H_2O 9:1), literature = 74.5-75.5 °C (EtOH). Reference[100]

9.17 4-(3-Methoxyphenyl)but-3-en-2-one, Compound 4-4

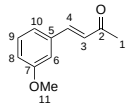

Chemical Formula: $C_{11}H_{12}O_2$
Exact Mass: 176.08

Procedure:[74]

3-Methoxybenzaldehyde (**1-52**, 2.44 mL, 20.0 mmol) was charged to a 100 mL RBF fitted with a stirrer bar. Acetone (14.70 mL, 200 mmol) was charged to the RBF, whereupon the starting material dissolved to give a pale yellow solution. NaOH (1.645 g, 41.1 mmol) was dissolved in H_2O (41 mL) to give a 1 M solution which was then charged dropwise to the RBF over 15 mins. An exotherm was observed, and the solution darkened to a yellow colour. The solution was stirred at RT for 2 h, and droplets of a yellow oil were observed to form during this time. The solution was neutralised with an aqeous solution of 6 M HCl, which forced the solution to separate into two phases. The solution was extracted with EtOAc (50 mL x 2), and the organic extracts were combined and washed with brine (50 mL), then dried over Na_2SO_4, filtered and concentrated *in vacuo* to give a yellow oil.

Isolated yield: 3.254 g (18.5 mmol, 92%)
^{1}H NMR (700 MHz, $CDCl_3$): δ/ppm 2.34 (3 H, s, H1), 3.79 (3 H, s, H11), 6.66 (1 H, d, J = 16.2, H3), 6.91 (1 H, d, J = 8.2, H8), 7.02 (1 H, s, H6), 7.09 (1 H, d, J = 7.2, H10), 7.27 (1 H, t, J = 7.9, H9), 7.44 (1 H, d, J = 16.3, H4);
^{13}C NMR (176 MHz, $CDCl_3$): δ/ppm 27.4 (C1), 55.3 (C11), 113.0 (C6), 116.4 (C8). 120.9 (C10), 127.4 (C3), 129.9 (C9), 137.8 (C5), 143.3 (C4), 159.9 (C7), 198.3 (C2).
IR (neat) ν = 1667.0 (m), 1608.2 (m), 1578.0 (m), 1256.3 (s), 1232.2 (s), 1158.9 (m), 1039.2 (m), 974.9 (m), 776.7 (m), 685.6 (m) cm^{-1}.
LC-MS: R_t = 3.11 min, m/z 177.1 $[MH]^+$.
Reference[101–103]

9.18 2,2-*Bis*[2-(2-bromo-5-methoxyphenyl)ethyl]-1,3-dioxolane, Compound 5-2

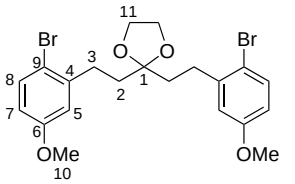

Chemical Formula: $C_{21}H_{24}Br_2O_4$
Exact Mass: 498.00

Procedure:

1,5-*Bis*(2-bromo-5-methoxyphenyl)pentan-3-one (**1-55**, 0.116 g, 0.26 mmol), ethylene glycol (40 μL, 0..75 mmol), camphorsulfonic acid (0.026 g, 0.11 mmol) and toluene (3 mL) were charged to a microwave vial fitted with a stirrer bar. The solution underwent microwave heating at 130 °C for 30 mins with 5 mins pre-stirring. The solution was allowed to cool to RT, then filtered through a mini column (silica/ cotton wool) and rinsed through with $CHCl_3$. The yellow solution was concentrated *in vacuo* to give a yellow oil (0.092 g). Purification by column chromatography (Hex:EtOAc 8:2) gave the product as a colourless oil.

Isolated yield: 0.061 g (0.12 mmol, 48%)
^{1}H NMR (700 MHz, $CDCl_3$): δ/ppm 1.95-2.00 (2 H, m, H11), 2.72 (2 H, t, J = 7.7 Hz, H2), 2.84-2.88 (2 H, m, H11), 2.95 (2 H, t, J = 7.7 Hz, H3), 3.76 (6 H, d, J = 7.5 Hz, H10), 6.62 (2 H, dt, J = 8.7, 2.5 Hz, H7), 6.78 (2 H, dd, J = 16.7, 3.0 Hz, H5), 7.38 (2 H, dd, J = 8.7, 6.9 Hz, H8);
^{13}C NMR (126 MHz, $CDCl_3$): δ/ppm 30.6 (C11), 31.05 (C3), 37.1 (C11), 42.4 (C2), 55.4 (C10), 65.1 (C1), 113.3/113.6 (C7 - d), 114.6/114.8 (C9 - d), 115.9/116.1 (C5 - d), 133.26/133.33 (C8 - d), 141.2/142.4 (C4 - d), 159.0 (C6).
IR (neat) ν = 2936.3 (w), 1714.0 (w), 1594.0 (w), 1571.3 (m), 1470.3 (s), 1414.9 (w), 1277.4 (m), 1239.2 (s), 1162.2 (m), 1137.7 (m), 1049.9 (s), 1013.8 (s), 853.6 (w), 800.3 (m), 599.6 (s) cm^{-1}.
LC-MS: R_t = 0.941 min, m/z 499.01 $[MH]^+$.
No literature data available.

9.19 (2*S*)-2-Hydroxy-3-methylbutanoic acid, 2-hydroxy-3-methylbutanoic acid, Compounds 5-6 and 5-21

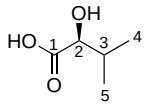

Chemical Formula: $C_5H_{10}O_3$
Exact Mass: 118.06

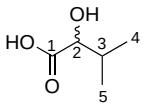

Chemical Formula: $C_5H_{10}O_3$
Exact Mass: 118.06

Procedure with L-valine, adapted from literature:[104]

L-Valine (7.034 g, 60 mmol) was charged to a 500 mL RBF fitted with a stirrer bar. An aqueous solution of 0.5 M H_2SO_4 (240 mL) was charged to the RBF and stirred for 15 mins at 0 °C until all the solid dissolved. $NaNO_2$ (24.8 g, 360 mmol) was dissolved in H_2O (90 mL) and the resulting solution was charged dropwise over 2 h. The RBF was removed from the ice bath and allowed to warm to RT, stirring overnight. The solution was extracted with Et_2O (3 x 50 mL), and the combined organic layers were washed with a saturated solution of NaCl(aq) (2 x 50 mL), dried over Na_2SO_4, filtered and concentrated *in vacuo* to give the crude product as a pale yellow oil.

Isolated yield: 3.310 g (28.0 mmol, 47%)
Procedure with rac-valine:

DL-Valine (0.584 g, 4.99 mmol) was charged to a 100 mL RBF fitted with a stirrer bar. An aqueous solution of 0.5 M H_2SO_4 (20 mL) was charged to the RBF and stirred for 15 mins at 0 °C until all the solid dissolved. $NaNO_2$ (2.1 g, 30 mmol) was dissolved in H_2O (7.5 mL) and the resulting solution was charged dropwise over 2 h. The RBF was removed from the ice bath and allowed to warm to RT, stirring overnight. The solution was extracted with Et_2O (3 x 5 mL), and the combined organic layers were washed with a saturated solution of NaCl(aq) (2 x 5 mL), dried over Na_2SO_4, filtered and concentrated *in vacuo* to give the crude product as a pale yellow oil. Purification from toluene/Et_2O gave the product as colourless, needle-like crystals.

Isolated yield: 0.279 g (2.36 mmol, 47 %)
^{1}H NMR (700 MHz, D_2O): δ/ppm 0.76 (3 H, d, J = 6.9 Hz, H4/5), 0.85 (3 H, d, J = 7.0 Hz, H4/5), 1.95 (1 H, pd, J = 6.9, 4.2 Hz, H3), 3.98 (1 H, d, J = 4.2 Hz, H2);
^{13}C NMR (126 MHz, D_2O): δ/ppm 15.7 (C4/5), 17.9 (C4/5), 31.4 (C3), 75.1

(C2), 177.6 (C1).
IR (neat) ν = 3419.1 (w), 2966.5 (w), 1704.0 (C=O, s), 1258.0 (m), 1213.1 (m), 1135.0 (m), 1027.4 (s), 891.3 (m) cm^{-1}.
LC-MS: R_t = 1.06 min, m/z 117.5 $[M]^-$; HR-MS calculated for $C_5H_9O_3$ at 117.0552, found 117.0553 (Δ = +0.9 ppm).
Reference[105]

9.20 (2*S*)-2-Hydroxy-4-methylpentanoic acid, 2-hydroxy-4-methylpentanoic acid, Compounds 5-7 and 5-22

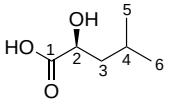

Chemical Formula: $C_6H_{12}O_3$
Exact Mass: 132.08

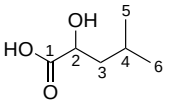

Chemical Formula: $C_6H_{12}O_3$
Exact Mass: 132.08

Procedure with L-leucine:[104]

L-Leucine (7.864 g, 60 mmol) was charged to a 500 mL RBF fitted with a stirrer bar. An aqueous solution of 0.5 M H_2SO_4 (240 mL) was charged to the RBF and stirred for 15 mins at 0 °C until all the solid dissolved. $NaNO_2$ (24.9 g, 360 mmol) was dissolved in H_2O (90 mL) and the resulting solution was charged dropwise over 2 h. The RBF was removed from the ice bath and allowed to warm to RT, stirring overnight. The solution was extracted with Et_2O (3 x 50 mL), and the combined organic layers were washed with a saturated solution of NaCl(aq) (2 x 50 mL), dried over Na_2SO_4, filtered and concentrated *in vacuo* to give the crude product as a pale yellow oil.

Isolated yield: 5.168 g (39.1 mmol, 65%)
Procedure with rac-leucine:[104]

DL-Leucine (0.660 g, 5.04 mmol) was charged to a 100 mL RBF fitted with a stirrer bar. An aqueous solution of 0.5 M H_2SO_4 (20 mL) was charged to the RBF and stirred for 15 mins at 0 °C until all the solid dissolved. $NaNO_2$ (2.1 g, xx mmol) was dissolved in H_2O (90 mL) and the resulting solution was charged dropwise over 2 h. The RBF was removed from the ice bath and allowed to warm to RT, stirring overnight. The solution was extracted with Et_2O (3 x 5 mL), and the combined organic layers were washed with a saturated solution of NaCl(aq) (2 x 5 mL), dried over Na_2SO_4, filtered and concentrated *in vacuo* to give the crude product as a white solid (0.462 g). Recrystallisation (toluene/Et_2O) gave the product as white needle-like crystals.

Isolated yield: 0.397 g (3.01 mmol, 60%)
^{1}H NMR (700 MHz, D_2O): δ/ppm 0.79 (6 H, dd, J = 6.7, 2.9 Hz, H5+6), 1.43-1.51 (2 H, m, H3) 1.62-1.66 (1 H, m, H4), 4.17 (1 H, dd, J = 9.2, 4.4 Hz, H2);

^{13}C NMR (126 MHz, D_2O): δ/ppm 20.6 (C5/6), 22.4 (C5/6), 23.8 (C4), 42.3 (C3), 68.8 (C2), 178.8 (C1).
IR (neat) ν = 3418.2 (m), 2958.2 (m), 1699.9 (C=O, s), 1266.3 (s), 1226.7 (m), 1136.4 (m), 1075.7 (s), 895.9 (s), 688.4 (m), 521.0 (m) cm^{-1}.
LC-MS: R_t = 1.67 min, m/z 131 $[M]^-$; HR-MS calculated for $C_6H_{11}O_3$ at 131.0708, found 131.0704 (Δ = -3.1 ppm).
Reference[79]

9.21 (2*S*)-2-Hydroxy-3-phenylpropanoic acid, 2-hydroxy-3-phenylpropanoic acid, Compounds 5-8 and 5-23

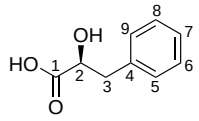

Chemical Formula: $C_9H_{10}O_3$
Exact Mass: 166.06

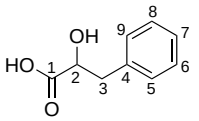

Chemical Formula: $C_9H_{10}O_3$
Exact Mass: 166.06

Procedure with L-phenylalanine adapted from literature:[104]

L-Phenylalanine (9.9 g, 60 mmol) was charged to a 500 mL RBF fitted with a stirrer bar. An aqueous solution of 0.5 M H_2SO_4 (240 mL) was charged to the RBF and stirred for 15 mins at 0 °C until all the solid dissolved. $NaNO_2$ (25.0 g, 360 mmol) was dissolved in H_2O (90 mL) and the resulting solution was charged dropwise over 2 h. The RBF was removed from the ice bath and allowed to warm to RT, stirring overnight. The solution was extracted with Et_2O (3 x 50 mL), and the combined organic layers were washed with a saturated solution of NaCl(aq) (2 x 50 mL), dried over Na_2SO_4, filtered and concentrated *in vacuo* to give the crude product as a white solid which could be recrystallised from toluene:Et_2O (1:1) to give the product as sparkly white fluffy crystals.

Isolated yield: 6.841 g (41.2 mmol, 69%)
Procedure with rac-phenylalanine:[104]

DL-Phenylalanine (0.826 g, 5.01 mmol) was charged to a 100 mL RBF fitted with a stirrer bar. An aqueous solution of 0.5 M H_2SO_4 (20 mL) was charged to the RBF and stirred for 15 mins at 0 °C until all the solid dissolved. $NaNO_2$ (2.1 g, 30 mmol) was dissolved in H_2O (90 mL) and the resulting solution was charged dropwise over 2 h. The RBF was removed from the ice bath and allowed to warm to RT, stirring overnight. The solution was extracted with Et_2O (3 x 20 mL), and the combined organic layers were washed with a saturated solution of NaCl(aq) (2 x 20 mL), dried over Na_2SO_4, filtered and concentrated *in vacuo* to give the crude product as a yellow oil (0.672 g). Purification by recrystallisation (toluene/Et_2O) gavethe product as a fluffy, sparkly white solid.

Isolated yield: 0.478 g (2.88 mmol, 57%)
^{1}H NMR (700 MHz, D_2O): δ/ppm 2.86 (2 H, dd, J = 14.1, 4.8 Hz, H3), 4.40 (1 H, dd, J = 7.7, 4.8 Hz, H2), 7.17-7.26 (5 H, m, H5-9);

^{13}C NMR (126 MHz, D_2O): δ/ppm 39.5 (C3), 71.2 (C2), 126.9 (C5/6/7/8/9), 128.5 (C5/6/7/8/9), 129.0 (C5/6/7/8/9), 129.4 (C5/6/7/8/9), 136.7 (C4), 177.1 (C1).
IR (neat) ν = 3441.7 (m), 1723.3 (C=O, m), 1240.6 (m), 1191.5 (m), 1090.3 (s), 1066.6 (m), 794.3 (m), 739.2 (m), 699.5 (s), 621.9 (m), 488.1 (m) cm^{-1}.
LC-MS: R_t = 1.31 min, m/z 165 $[M]^-$; HR-MS calculated for $C_9H_9O_3$ at 165.0552, found 165.0547 (Δ = -3.0 ppm).
Melting point: 122.0-123.3 °C (toluene:Et_2O 1:1).
Reference[79]

9.22 Benzyl (2*S*)-2-hydroxy-3-methylbutanoate, benzyl 2-hydroxy-3-methoylbutanoate, Compounds 5-9 and 5-24

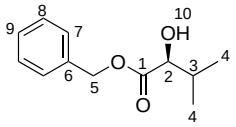

Chemical Formula: $C_{12}H_{16}O_3$
Exact Mass: 208.11

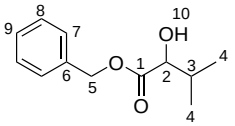

Chemical Formula: $C_{12}H_{16}O_3$
Exact Mass: 208.11

Procedure for benzyl (2*S*)-2-hydroxy-3-methylbutanoate (**5-9**):[79]

(2*S*)-2-Hydroxy-3-methylbutanoic acid (**5-6**, 0.120 g, 1.0 mmol) was charged to an oven-dried 25 mL RBF fitted with a stirrer bar and septum. Dry DMF (0.7 mL), was charged to the RBF at 0 °C. Cs_2CO_3 (0.500 g, 1.5 mmol) was charged to the RBF in two portions, and the resulting slurry was stirred at 0 °C for 20 mins. BnBr (0.13 mL, 1.1 mmol) was added dropwise to the RBF, which was allowed to warm to RT overnight. A white precipitate was observed, which was removed by filtration and washed with Hex:EtOAc (8:2), and then discarded. The filtrate was extracted with half-saturated NH_4Cl (3 x 5 mL) then half-saturated $NaHCO_3$ (10 mL). The organic layers were combined, dried over Na_2SO_4, filtered and concentrated *in vacuo* to give a pale yellow oil (0.121 g). The crude material was purified by column chromatography (Hex:EtOAc 8:2) to give the product as a colourless oil.

Isolated yield: 0.039 g (0.187 mmol, 19%)
Procedure for benzyl 2-hydroxy-3-methylbutanoate (**5-24**):[79]

2-Hydroxy-3-methylbutanoic acid (**5-21**, 0.120 g, 1.0 mmol) was charged to an oven-dried 25 mL RBF fitted with a stirrer bar and septum. Dry DMF (0.7 mL), was charged to the RBF at 0 °C. Cs_2CO_3 (0.499 g, 1.5 mmol) was charged to the RBF in two portions, and the resulting slurry was stirred at 0 °C for 20 mins. BnBr (0.13 mL, 1.1 mmol) was added dropwise to the RBF, which was allowed to warm to RT overnight. A white precipitate was observed, which was removed by filtration and washed with Hex:EtOAc (8:2), and then discarded. The filtrate was extracted with half-saturated NH_4Cl (3 x 5 mL) then half-saturated $NaHCO_3$ (10 mL). The organic layers were combined, dried over Na_2SO_4, filtered and concentrated *in vacuo* to give a colourless oil (0.176 g). The crude material

was purified by column chromatography (Hex:EtOAc 8:2) to give the product as a colourless oil.

Isolated yield: 0.043 g (0.207 mmol, 21%)
^{1}H NMR (700 MHz, $CDCl_3$): δ/ppm 0.82 (3 H, d, J = 6.9 Hz, H4), 1.00 (3 H, d, J = 7.0 Hz, H4), 2.08 (1 H, ddt, J = 10.3, 6.9, 3.4 Hz, H3), 2.71 (1 H, d, J = 6.1 Hz, H10), 4.07-4.08 (1 H, m, H2), 5.18-5.24 (2 H, m, H5), 7.33-7.37 (5 H, m, H7-9);
^{13}C NMR (126 MHz, $CDCl_3$): δ/ppm 15.9 (C4), 18.8 (C4), 32.2 (C3), 67.3 (C5), 75.0 (C2), 128.4 (C7/8/9), 128.5 (C7/8/9), 128.6 (C7/8/9), 135.2 (C6), 174.8 (C1).
LC-MS: R_t = 2.93 min, m/z 231.4 $[M+Na]^+$; HR-MS calculated for $C_{12}H_{17}O_3$ at 209.1178, found 209.1185 (Δ = +3.3 ppm).
Reference[79]

9.23 Benzyl (2*S*)-2-hydroxy-4-methylpentanoate, benzyl 2-hydroxy-4-methylpentanoate, Compounds 5-10 and 5-25

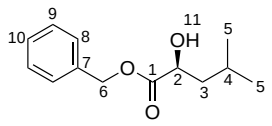

Chemical Formula: $C_{13}H_{18}O_3$
Exact Mass: 222.13

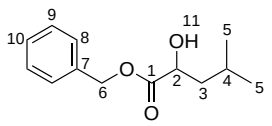

Chemical Formula: $C_{13}H_{18}O_3$
Exact Mass: 222.13

Procedure for benzyl (2*S*)-2-hydroxy-4-methylpentanoate (**5-10**):[79]

(2*S*)-2-Hydroxy-4-methylpentanoic acid (**5-7**, 0.133 g, 1.0 mmol) was charged to an oven-dried 25 mL RBF fitted with a stirrer bar and septum. Dry DMF (0.7 mL), was charged to the RBF at 0 °C. Cs_2CO_3 (0.487 g, 1.5 mmol) was charged to the RBF in two portions, and the resulting slurry was stirred at 0 °C for 20 mins. BnBr (0.13 mL, 1.1 mmol) was added dropwise to the RBF, which was allowed to warm to RT overnight. A white precipitate was observed, which was removed by filtration and washed with Hex:EtOAc (8:2), and then discarded. The filtrate was extracted with half-saturated NH_4Cl (3 x 5 mL) then half-saturated $NaHCO_3$ (10 mL). The organic layers were combined, dried over Na_2SO_4, filtered and concentrated *in vacuo* to give a pale yellow oil (0.208 g). The crude material was purified by column chromatography (Hex:EtOAc 8:2) to give the product as a colourless oil.

Isolated yield: 0.071 g (0.320 mmol, 32%)
Procedure for benzyl (2-hydroxy-4-methylpentanoate (**5-25**):[79]

2-Hydroxy-4-methylpentanoic acid (**5-22**, 0.129 g, 1.0 mmol) was charged to an oven-dried 25 mL RBF fitted with a stirrer bar and septum. Dry DMF (0.7 mL), was charged to the RBF at 0 °C. Cs_2CO_3 (0.487 g, 1.5 mmol) was charged to the RBF in two portions, and the resulting slurry was stirred at 0 °C for 20 mins. BnBr (0.13 mL, 1.1 mmol) was added dropwise to the RBF, which was allowed to warm to RT overnight. A white precipitate was observed, which was removed by filtration and washed with Hex:EtOAc (8:2), and then discarded. The filtrate was extracted with half-saturated NH_4Cl (3 x 5 mL) then half-saturated $NaHCO_3$ (10 mL). The organic layers were combined, dried over Na_2SO_4, filtered and concentrated *in vacuo* to give a colourless oil.

Crude yield: 0.110 g (0.495 mmol, 50%)
^{1}H NMR (700 MHz, $CDCl_3$): δ/ppm 0.93 (6 H, t, J = 7.6 Hz, H5), 1.55-1.58 (2 H, m, H3), 1.86-1.90 (1 H, m, H4), 2.66 (1 H, d, J = 6.0 Hz, H11), 4.24 (1 H, dt, J = 10.1, 5.3 Hz, H2), 5.20 (2 H, d, J = 3.4 Hz, H6), 7.30-7.38 (5 H, m, H8-10);
^{13}C NMR (126 MHz, $CDCl_3$): δ/ppm 21.5 (C5), 23.2 (C5), 24.4 (C4), 43.4 (C3), 67.3 (C6), 69.2 (C2), 128.3 (C8/9/10), 128.5 (C8/9/10), 128.6 (C8/9/10), 135.2 (C7), 175.7 (C1).
IR (neat) ν = 2957.3 (w), 1733.0 (s), 1456.0 (w), 1368.6 (w), 1266.3 (m), 1192.5 (m), 1138.1 (s), 1082.9 (m), 1003.0 (m), 745.3 (m), 695.8 (s), 602.8 (w) cm^{-1}.
LC-MS: R_t = 3.16 min, m/z 245.4 $[M+Na]^+$; HR-MS calculated for $C_{13}H_{19}O_3$ at 223.1334, found 223.1340 (Δ = +2.7 ppm).
Reference[79]

9.24 Benzyl (2*S*)-2-hydroxy-3-phenylpropanoate, benzyl 2-hydroxy-3-phenylpropanoate, Compounds 5-11 and 5-26

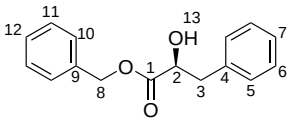

Chemical Formula: $C_{16}H_{16}O_3$
Exact Mass: 256.11

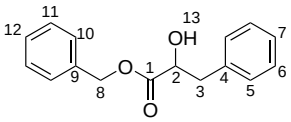

Chemical Formula: $C_{16}H_{16}O_3$
Exact Mass: 256.11

Procedure for benzyl (2*S*)-2-hydroxy-3-phenylpropanoate (**5-11**):[79]

Recrystallised (2*S*)-2-hydroxy-3-phenylpropanoic acid (**5-8**, 0.165 g, 1.0 mmol) was charged to an oven-dried 25 mL RBF fitted with a stirrer bar and septum. Dry DMF (1.0 mL), was charged to the RBF at 0 °C. Cs_2CO_3 (0.489 g, 1.5 mmol) was charged to the RBF in two portions, and the resulting slurry was stirred at 0 °C for 30 mins. BnBr (0.13 mL, 1.1 mmol) was added dropwise to the RBF, which was allowed to warm to RT overnight. A white precipitate was observed, which was removed by filtration and washed with Hex:EtOAc (8:2), and then discarded. The filtrate was extracted with half-saturated NH_4Cl (3 x 5 mL) then half-saturated $NaHCO_3$ (10 mL). The organic layers were combined, dried over Na_2SO_4, filtered and concentrated *in vacuo* to give a pale yellow oil (0.164 g). The crude material was purified by column chromatography (Hex:EtOAc 8:2) to give the product as a pale yellow oil.

Isolated yield: 0.072 g (0.281 mmol, 28%)
Procedure for benzyl 2-hydroxy-3-phenypropanoate (**5-26**):[79]

Recrystallised 2-hydroxy-3-phenylpropanoic acid (**5-23**, 0.167 g, 1.0 mmol) was charged to an oven-dried 25 mL RBF fitted with a stirrer bar and septum. Dry DMF (1.0 mL), was charged to the RBF at 0 °C. Cs_2CO_3 (0.489 g, 1.5 mmol) was charged to the RBF in two portions, and the resulting slurry was stirred at 0 °C for 30 mins. BnBr (0.13 mL, 1.1 mmol) was added dropwise to the RBF, which was allowed to warm to RT overnight. A white precipitate was observed, which was removed by filtration and washed with Hex:EtOAc (8:2), and then discarded. The filtrate was extracted with half-saturated NH_4Cl (3 x 5 mL) then half-saturated $NaHCO_3$ (10 mL). The organic layers were combined, dried over Na_2SO_4, filtered and concentrated *in vacuo* to give a colourless oil (0.199 g). The

crude material was purified by column chromatography (Hex:EtOAc 8:2) to give the product as a colourless oil.

Isolated yield: 0.105 g (0.410 mmol, 41%)
^{1}H NMR (700 MHz, $CDCl_3$): δ/ppm 2.70 (1 H, br s, H13), 2.97 (1 H, dd, J = 140., 6.5 Hz, H3), 3.12 (1 H, dd, J = 13.9, 4.7 Hz, H3), 4.49 (1 H, d, J = 5.3 Hz, H2), 5.17 (2 H, d, J = 3.1 Hz, H8), 7.13-7.15 (2 H, m, H5+6+7), 7.21-7.25 (3 H, m, H5+6+7), 7.31-7.38 (5 H, m, H10+11+12);
^{13}C NMR (126 MHz, $CDCl_3$): δ/ppm 40.5 (C3), 67.4 (C8), 71.2 (C2), 126.8 (C5/6/7), 128.4 (C5/6/7), 128.59 (C10/11/12), 128.62 (C10/11/12), 128.64 (C10/11/12), 129.5 (C5/6/7), 135.0 (C), 136.1 (C4), 174.0 (C1).
IR (neat) ν = 3474.4 (br, w), 3031.2 (w), 1733.0 (C=O, m), 1497.1 (w), 1454.7 (w), 1262.7 (w), 1187.2 (m), 1090.9 (m), 1029.8 (w), 909.8 (w), 742.9 (m), 695.4 (s), 60.1 (w), 487.7 (m) cm^{-1}.
LC-MS: R_t = 3.14 min, m/z 279.4 $[M+Na]^+$; HR-MS calculated for $C_{16}H_{16}O_3$ at 257.1178, found 257.1173 (Δ = -1.9 ppm).
Reference[79]

9.25 (2*S*)-3-Methylbutane-1,2-diol, 3-Methylbutane-1,2-diol, Compounds 5-12 and 5-27

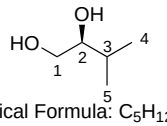

Chemical Formula: $C_5H_{12}O_2$
Exact Mass: 104.08

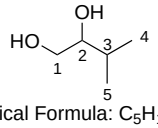

Chemical Formula: $C_5H_{12}O_2$
Exact Mass: 104.08

Procedure for (2*S*)-3-methylbutane-1,2-diol (**5-12**):

$LiAlH_4$ (0.974 g, 25 mmol) was charged under N_2 to an oven-dried 250 mL RBF fitted with a stirrer bar and septum at 0 °C. Dry Et_2O (10 mL) was charged to the RBF. (2*S*)-2-Hydroxy-3-methylbutanoic acid (**5-6**, 1.188 g, 10 mmol) was dissolved in dry Et_2O (10 mL), then charged dropwise to the $LiAlH_4$ solution at 0 °C. The RBF was allowed to warm to RT overnight with stirring. The solution was diluted with Et_2O (5 mL) and cooled to 0 °C, then quenched with H_2O (1 mL). The subsequent work-up followed a procedure by Fieser[81] which begins with the addition of 15% NaOH (1 mL). The solution is further diluted with H_2O (3 mL), then warmed to RT and stirred for 15 mins. $MgSO_4$ (approx. 1 g) was added, followed by further Et_2O (5 mL), and the resulting slurry was stirred for 15 mins. The slurry was filtered over Celite and rinsed through with Et_2O. The filtrate was concentrated *in vacuo* to give the product as a pale yellow oil.

Isolated yield: 0.677 g (6.50 mmol, 65%)
Procedure for 3-methylbutane-1,2-diol (**5-27**):

$LiAlH_4$ (0.096 g, 2.5 mmol) was charged under N_2 to an oven-dried 25 mL RBF fitted with a stirrer bar and septum at 0 °C. Dry THF (1.0 mL) was charged to the RBF. 2-Hydroxy-3-methylbutanoic acid (**5-21**, 0.114 g, 1.0 mmol) was dissolved in dry THF (1.0 mL), then charged dropwise to the $LiAlH_4$ solution at 0 °C. The RBF was allowed to warm to RT overnight with stirring. The solution was diluted with THF (1 mL) and cooled to 0 °C, then quenched with H_2O (1 mL). The subsequent work-up followed a procedure by Fieser[81] which begins with the addition of 15% NaOH (1 mL). The solution is further diluted with H_2O (3 mL), then warmed to RT and stirred for 15 mins. $MgSO_4$ (approx. 0.5 g) was added, followed by further Et_2O (5 mL), and the resulting slurry was stirred for 15 mins. The slurry was filtered over Celite and rinsed through with THF. The filtrate was concentrated *in vacuo* to give the product as a pale yellow oil.

Isolated yield: 0.024 g (0.231 mmol, 23%)
^{1}H NMR (700 MHz, D_2O): δ/ppm 0.76 (3 H, d, J = 3.8 Hz, H4/5), 0.77 (3 H, d, J = 3.8 Hz, H4/5), 1.58 (1 H, dq, J = 13.6, 6.8 Hz, H3), 3.29 (1 H, ddd, J = 7.4, 6.2, 3.5 Hz, H2), 3.38 (1 H, dd, J = 11.7, 7.5 Hz, H1), 3.53 (1 H, dd, J = 11.7, 3.5 Hz, H1);
^{13}C NMR (126 MHz, D_2O): δ/ppm 16.9 (C4/5), 18.1 (C4/5), 29.9 (C3), 63.7 (C1), 76.9 (C2).
IR (neat) ν = 3344.1 (br, m), 2960.2 (m), 1467.8 (w), 1386.6 (w), 1061.8 (s), 1008.1 (s), 867.2 (m) cm^{-1}.
Reference[106]

9.26 (2*S*)-4-Methylpentane-1,2-diol, 4-methylpentane-1,2-diol, Compounds 5-13 and 5-28

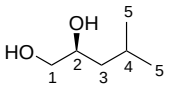

Chemical Formula: $C_6H_{14}O_2$
Exact Mass: 118.10

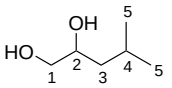

Chemical Formula: $C_6H_{14}O_2$
Exact Mass: 118.10

Procedure for (2*S*)-4-methylpentane-1,2-diol (**5-13**):

$LiAlH_4$ (0.964 g, 24 mmol) was charged under N_2 to an oven-dried 250 mL RBF fitted with a stirrer bar and septum at 0 °C. Dry Et_2O (10 mL) was charged to the RBF. (2*S*)-2-Hydroxy-4-methylpentanoic acid (**5-7**, 1.320 g, 10 mmol) was dissolved in dry Et_2O (10 mL), then charged dropwise to the $LiAlH_4$ solution at 0 °C. The RBF was allowed to warm to RT overnight with stirring. The solution was diluted with Et_2O (5 mL) and cooled to 0 °C, then quenched with H_2O (1 mL). The subsequent work-up followed a procedure by Fieser[81] which begins with the addition of 15% NaOH (1 mL). The solution is further diluted with H_2O (3 mL), then warmed to RT and stirred for 15 mins. $MgSO_4$ (approx. 1 g) was added, followed by further Et_2O (5 mL), and the resulting slurry was stirred for 15 mins. The slurry was filtered over Celite and rinsed through with Et_2O. The filtrate was concentrated *in vacuo* to give the product as a colourless oil.

Isolated yield: 0.681 g (5.77 mmol, 58%)
Procedure for 4-methylpentane-1,2-diol (**5-28**):

$LiAlH_4$ (0.097 g, 2.5 mmol) was charged under N_2 to an oven-dried 25 mL RBF fitted with a stirrer bar and septum at 0 °C. Dry THF (1.0 mL) was charged to the RBF. 2-Hydroxy-4-methylpentanoic acid (**5-22**, 0.135 g, 1.0 mmol) was dissolved in dry THF (1.0 mL), then charged dropwise to the $LiAlH_4$ solution at 0 °C. The RBF was allowed to warm to RT overnight with stirring. The solution was diluted with THF (0.5 mL) and cooled to 0 °C, then quenched with H_2O (1 mL). The subsequent work-up followed a procedure by Fieser[81] which begins with the addition of 15% NaOH (1 mL). The solution is further diluted with H_2O (3 mL), then warmed to RT and stirred for 15 mins. $MgSO_4$ (approx. 0.5 g) was added, followed by further Et_2O (5 mL), and the resulting slurry was stirred for 15 mins. The slurry was filtered over Celite and rinsed through with THF. The filtrate was concentrated *in vacuo* to give the product as a colourless oil.

Isolated yield: 0.087 g (0.572 mmol, 56%)
^{1}H NMR (700 MHz, D_2O): δ/ppm 0.77 (6 H, dd, J = 11.5, 6.6 Hz, H5+6), 1.10-1.14 (1 H, ddd, J = 4.5, 9.0, 18.4 Hz, H3), 1.18-1.20 (1 H, ddd, J = 5.5, 9.2, 14.4 Hz, H3), 1.53-1.60 (1 H, m, H4), 3.29-3.32 (1 H, dd, J = 11.6, 3.9 Hz, H1), 3.41-3.44 (1 H, dd, J = 11.7, 6.9 Hz, H1), 3.62-3.66 (1 H, ddt, J = 8.7, 6.9, 4.2 Hz, H2);
^{13}C NMR (126 MHz, D_2O): δ/ppm 21.1 (C5/6), 22.6 (C5/6), 23.7 (C4), 41.3 (C3), 65.8 (C1), 70.0 (C2).
IR (neat) ν = 3339.6 (O-H, br), 2954.9 (s), 2927.6 (m), 2870.6 (m), 1468.5 (m), 1367.5 (m), 1065.7 (C-O, s), 1025.7 (C-O, s), 881.1 (m) cm^{-1}.
LC-MS: R_t = 1.59 min, m/z 141 $[M+Na]^+$.
Reference[107]

9.27 (2*S*)-3-Phenylpropane-1,2-diol, 3-phenylpropane-1,2-diol, Compounds 5-14 and 5-29

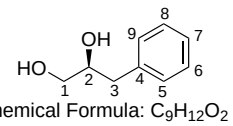

Chemical Formula: $C_9H_{12}O_2$
Exact Mass: 152.08

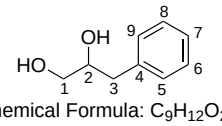

Chemical Formula: $C_9H_{12}O_2$
Exact Mass: 152.08

Procedure for (2*S*)-3-phenylpropane-1,2-diol (**5-14**):

$LiAlH_4$ (0.974 g, 25 mmol) was charged under N_2 to an oven-dried 250 mL RBF fitted with a stirrer bar and septum at 0 °C. Dry Et_2O (10 mL) was charged to the RBF. (2*S*)-2-Hydroxy-3-phenylpropanoic acid (**5-8**, 1.654 g, 10 mmol) was dissolved in dry Et_2O (10 mL), then charged dropwise to the $LiAlH_4$ solution at 0 °C. The RBF was allowed to warm to RT overnight with stirring. The solution was diluted with Et_2O (5 mL) and cooled to 0 °C, then quenched with H_2O (1 mL). The subsequent work-up followed a procedure by Fieser[81] which begins with the addition of 15% NaOH (1 mL). The solution is further diluted with H_2O (3 mL), then warmed to RT and stirred for 15 mins. $MgSO_4$ (approx. 1 g) was added, followed by further Et_2O (5 mL), and the resulting slurry was stirred for 15 mins. The slurry was filtered over Celite and rinsed through with Et_2O. The filtrate was concentrated *in vacuo* to give the product as a colourless oil.

Isolated yield: 0.846 g (5.56 mmol, 56%)
Procedure for 3-phenylpropane-1,2-diol (**5-29**):

$LiAlH_4$ (0.110 g, 2.5 mmol) was charged under N_2 to an oven-dried 250 mL RBF fitted with a stirrer bar and septum at 0 °C. Dry THF (1.0 mL) was charged to the RBF. 2-Hydroxy-3-phenylpropanoic acid (**5-23**, 0.170 g, 1.0 mmol) was dissolved in dry THF (1.0 mL), then charged dropwise to the $LiAlH_4$ solution at 0 °C. The RBF was allowed to warm to RT overnight with stirring. The solution was diluted with THF (0.5 mL) and cooled to 0 °C, then quenched with H_2O (1 mL). The subsequent work-up followed a procedure by Fieser[81] which begins with the addition of 15% NaOH (1 mL). The solution is further diluted with H_2O (3 mL), then warmed to RT and stirred for 15 mins. $MgSO_4$ (approx. 0.5 g) was added, followed by further Et_2O (5 mL), and the resulting slurry was stirred for 15 mins. The slurry was filtered over Celite and rinsed through with THF. The filtrate was concentrated *in vacuo* to give the product as a colourless oil.

Isolated yield: 0.846 g (5.56 mmol, 56%)
^{1}H NMR (700 MHz, D_2O): δ/ppm 2.55 (1 H, dd, J = 13.9, 8.4 Hz, H3), 2.74 (1 H, dd, J = 13.9, 5.1 Hz, H3), 3.37 (1 H, dd, J = 11.7, 6.7 Hz, H1), 3.49 (1 H, dd, J = 11.7, 3.9 Hz, H1) 3.82-3.84 (1 H, m, H2), 7.15-7.18 (3 H, m, H5/6/7/8/9), 7.23-7.26 (2 H, m, H5/6/7/8/9);
^{13}C NMR (126 MHz, D_2O): δ/ppm 38.7 (C3), 64.9 (C1), 72.8 (C2), 126.4 (C5/6/7/8/9), 128.5 (C5/6/7/8/9), 129.3 (C5/6/7/8/9), 138.3 (C4).
IR (neat) ν = 3234.6 (O-H, br), 2923.8 (w), 1494.9 (w), 1455.2 (w), 1092.0 (m), 1071.8 (m), 1040.9 (s), 898.2 (m), 748.0 (m), 695.7 (s), 549.3 (s) cm^{-1}.
LC-MS: R_t = 1.70 min, m/z 175.3 $[M+Na]^+$; HR-MS calculated for $C_9H_{12}O_2{}^{23}Na$ at 175.0735, found 175.0742 (Δ = +4.0 ppm).
Reference[108]

9.28 2,2-*Bis*[2-(2-bromo-5-methoxyphenyl)ethyl]-4-(propan-2-yl)-1,3-dioxolane, Compound 5-15/5-30

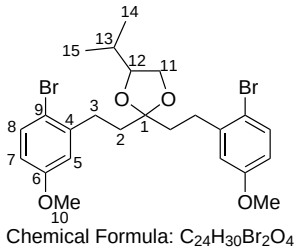

Chemical Formula: $C_{24}H_{30}Br_2O_4$
Exact Mass: 540.05

Procedure:

1,5-*Bis*(2-bromo-5-methoxyphenyl)pentan-3-one (**1-55**, 0.225 g, 0.5 mmol), (2*S*)-3-methylbutane-1,2-diol (**5-12**, 0.079 g, 0.8 mmol), camphorsulfonic acid (0.050 g, 0.2 mmol) and toluene (3 mL) were charged to a microwave vial fitted with a stirrer bar. The solution underwent microwave heating at 130 °C for 45 mins with 5 mins pre-stirring. The solution was extracted with $NaHCO_3$ (3 x 5 mL) and washed with a saturated solution of NaCl(aq) (5 mL), then dried over Na_2SO_4 and filtered. The solution was concentrated *in vacuo* to give the crude product as an orange oil.

Isolated yield: 0.122 g (0.2 mmol, 46%)
^{1}H NMR (700 MHz, $CDCl_3$): δ/ppm 0.89 (3 H, d, J = 6.8 Hz, H14/15), 1.05 (3 H, d, J = 6.7 Hz, H14/15), 1.80 (1 H, dq, J = 13.5, 6.8 Hz, H13), 1.89-2.03 (4 H, m, H2), 2.74-2.90 (4 H, m, H3), 3.65 (1 H, t, J = 8.0 Hz, H11), 3.77 (6 H, d, J = 2.6 Hz, H10), 3.86 (1 H, q, J = 7.9 Hz, H12), 4.10 (1 H, dd, J = 7.8, 6.3 Hz, H11), 6.62 (2 H, dt, J = 8.7, 3.0 Hz, H7), 6.79 (2 H, dd, J = 9.6, 3.0 Hz, H5), 7.39 (2 H, dd, J = 8.7, 3.8 Hz, H8);
^{13}C NMR (126 MHz, $CDCl_3$): δ/ppm 18.2 (C14/15), 19.3 (C14/15), 30.9 (C3), 31.3 (C3), 31.8 (C13), 37.5d (C2), 55.4 (C10), 68.6 (C11), 81.9 (C12), 110.8 (C1), 113.2d (C7), 114.9d (C9), 115.9 (C5), 133.2 (C8), 142.6d (C4), 159.0 (C6).

IR (neat) ν = 2959.7 (w), 1571.5 (w), 1471.1 (s), 1368.0 (w), 1283.0 (m), 1239.6 (s), 1162.4 (s), 1162.4 (m), 1129.6 (m), 1052.7 (s), 1013.8 (s), 799.4 (m), 601.1 (m) cm^{-1}.
No literature data available.

9.29 2,2-*Bis*[2-(2-bromo-5-methoxyphenyl)ethyl]-4-(2-methylpropyl)-1,3-dioxolane, Compound 5-16/5-31

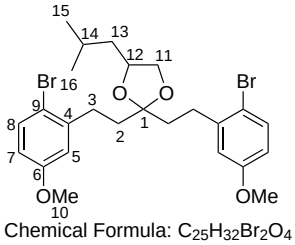

Chemical Formula: $C_{25}H_{32}Br_2O_4$
Exact Mass: 554.07

Procedure:

1,5-*Bis*(2-bromo-5-methoxyphenyl)pentan-3-one (**1-55**, 0.912 g, 2.0 mmol), (2*S*)-4-methylpentane-1,2-diol (**5-13**, 0.354 g, 3.0 mmol), camphorsulfonic acid (0.201 g, 0.86 mmol) and toluene (10 mL) were charged to a 50 mL RBF fitted with a stirrer bar. The solution was heated under Dean-Stark reflux conditions with stirring overnight. The solution was allowed to cool to RT, then extracted with $NaHCO_3$ (3 x 10 mL) and washed with a saturated solution of NaCl(aq) (10 mL), then dried over Na_2SO_4 and filtered. The solution was concentrated *in vacuo* to give the crude product as an orange oil (0.784 g). Purification by column chromatography (Hex:EtOAc 1:1) gave the product as a yellow oil.

Isolated yield: 0.596 g (1.08 mmol, 54%)
^{1}H NMR (700 MHz, $CDCl_3$): δ/ppm 0.95 (6 H, dd, J = 11.3, 6.7 Hz, H15+16), 1.38 (2 H, m, H13), 1.77 (1 H, m, H14), 1.98 (4 H, m, H2), 2.81 (4 H, m, H3), 3.53 (1 H, t, J = 8.0 Hz, H11), 3.77 (6 H, d, J = 3.3 Hz, H10), 4.15-4.25 (2 H, m, H11+12), 6.61 (2 H, dt, J = 8.8, 3.1 Hz, H7), 6.79 (2 H, dd, J = 10.6, 3.0 Hz, H5), 7.39 (2 H, dd, J = 8.8, 3.9 Hz, H8);
^{13}C NMR (126 MHz, $CDCl_3$): δ/ppm 22.6 (C15/16), 23.2 (C15/16), 25.6 (C14), 30.9 (C3), 31.3 (C3), 37.7 (C2), 37.8 (C2), 42.6 (C13), 55.4 (C10), 70.7 (C11), 75.2 (C12), 110.6 (C1), 113.2 (C7), 114.6 (C9), 115.9 (C5), 132.2 (C8), 141.2 (C4), 159.0 (C6).
IR (neat) ν = 2955.0 (w), 1593.8 (w), 1571.6 (m), 1468.6 (s), 1239.1 (s), 1162.4 (m), 1135.0 (m), 1049.5 (s), 1013.5 (s), 906.2 (w), 851.9 (w), 798.6 (m), 600.3 (s) cm^{-1}.
No literature data available.

9.30 4-Benzyl-2,2-*bis*[2-(2-bromo-5-methoxyphenyl)ethyl]-1,3-dioxolane, Compound 5-17/5-32

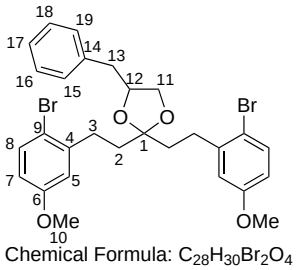

Chemical Formula: $C_{28}H_{30}Br_2O_4$
Exact Mass: 588.05

Procedure:

1,5-*Bis*(2-bromo-5-methoxyphenyl)pentan-3-one (**1-55**, 0.115 g, 0.3 mmol), (2*S*)-3-phenylpropane-1,2-diol (**5-14**, 0.087 g, 0.6 mmol), camphorsulfonic acid (0.029 g, 0.1 mmol) and toluene (2 mL) were charged to a microwave vial fitted with a stirrer bar. The solution underwent microwave heating at 130 °C for 30 mins with 5 mins pre-stirring. The solution was extracted with $NaHCO_3$ (3 x 5 mL) and washed with a saturated solution of NaCl(aq) (5 mL), then dried over Na_2SO_4 and filtered. The solution was concentrated *in vacuo* to give the crude product as an orange oil.

Isolated yield: 0.142 g (0.2 mmol, 95%)
^{1}H NMR (700 MHz, $CDCl_3$): δ/ppm 1.94-2.03 (4 H, m, H2), 2.77-2.84 (6 H, m, H3+H13), 3.10 (1 H, dd, J = 13.8, 6.2 Hz, H13), 3.71 (1 H, t, J = 7.9 Hz, H11), 3.76 (6 H, d, J = 15.7 Hz, H10), 4.09 (1 H, dd, J = 8.0, 6.0 Hz, H11), 4.43 (1 H, dt, J = 13.2, 6.3 Hz, H12), 6.62 (2 H, ddd, J = 15.0, 8.8, 3.1 Hz, H7), 6.78 (2 H, dd, J = 26.2, 3.1 Hz, H5), 7.21-7.31 (5 H, m, H15-19), 7.39 (2 H, dd, J = 19.0, 8.7 Hz, H8);
^{13}C NMR (126 MHz, $CDCl_3$): δ/ppm 30.9 (C2), 31.3 (C2), 37.5 (C3), 37.7 (C3), 40.0 (C13), 55.4 (C10), 69.8 (C11), 77.1 (C12), 111.2 (C1), 113.2 (C7 - d), 114.9 (C9 - d), 115.9 (C5 - d), 126.6 (C15/16/17/18/19), 128.5 (C15/16/17/18/19), 129.2 (C15/16/17/18/19), 133.3 (C8), 137.4 (C14), 142.4 (C4 - d), 159.0 (C6).
IR (neat) ν = 2935.0 (w), 1574.5 (w), 1470.2 (s), 1436.4 (m), 1261.8 (s), 1172.6 (m), 1080.6 (m), 1056.3 (m), 797.3 (s) cm^{-1}.
No literature data available.

9.31 4-Bromo-7-methoxy-2,3-dihydro-1H-inden-1-one, Compound 6-1

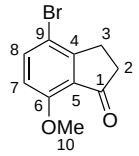

Chemical Formula: $C_{10}H_9BrO_2$
Exact Mass: 239.98

Procedure:

3-(2-Bromo-5-methoxyphenyl)propanoic acid (**6-7**, 0.641 g, 2.48 mmol) and polyphosphoric acid (10.652 g, 16.6 wt/wt) were charged to a 50 mL RBF fitted with a stirrer bar. The resulting viscous solution was heated to 60 °C for 1 h, after which it was removed from the heat and allowed to cool to RT. The dark red solution was quenched with H_2O (10 mL) then diluted with DCM (10 mL) and extracted with DCM (15 mL x 2). The combined organic extracts were washed with H_2O (15 mL), $NaHCO_3$ (15 mL) and a saturated solution of NaCl(aq) (15 mL), dried over Na_2SO_4, filtered and concentrated *in vacuo* to give a yellow solid (0.398 g, 1.66 mmol). The crude material was purified by column chromatography (hexanes:EtOAc 1:1) to give the product as a yellow solid.

Isolated yield: 0.283 g (1.18 mmol, 47%)
^{1}H NMR (700 MHz, $CDCl_3$): δ/ppm 2.68-2.70 (2 H, m, H2), 2.99-3.01 (2 H, m, H3), 3.93 (3 H, s, H10), 6.72 (1 H, d, J = 8.7 Hz, H7), 7.64 (1 H, d, J = 8.6 Hz, H8);
^{13}C NMR (126 MHz, $CDCl_3$): δ/ppm 26.9 (C3), 36.6 (C2), 56.1 (C10), 111.2 (C7), 111.8 (C9), 127.0 (C5), 138.6 (C8), 156.7 (C4), 157.4 (C6), 204.0 (C1).
IR (neat) ν = 1695.4 (C=O, m), 1582.9 (m), 1473.3 (s), 1281.3 (m), 1271.1 (m), 1195.0 (m), 1125.3 (m), 1074.5 (s), 1018.9 (s), 804.6 (s) cm^{-1}.
LC-MS: R_t = 2.18 min, m/z 240.84 $[M]^+$; HR-MS calculated for $C_{10}H_{10}O_2Br$ at 240.9864, found 240.9863 (Δ = -0.4 ppm).
Reference[109]

9.32 1-Bromo-2-(3-bromopropyl)-4-methoxybenzene, Compound 6-2

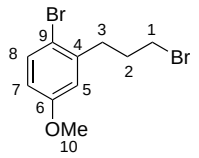

Chemical Formula: $C_{10}H_{12}Br_2O$
Exact Mass: 305.93

Procedure:

3-(2-Bromo-5-methoxyphenyl)propan-1-ol (**6-8**, 0.837 g, 3.43 mmol) was charged to a 100 mL RBF fitted with a stirrer bar and dissolved in DCM (10.0 mL). The solution was cooled to 0 °C, and PPh_3 (1.082 g, 4.13 mmol) and CBr_4 (1.256 g, 3.79 mmol) were charged to the RBF, which was allowed to warm to RT and stirred overnight. The solvent was removed *in vacuo* and the crude material purified by column chromatography (hexanes:EtOAc 1:1) and fractions containing the product were combined and the solvent removed *in vacuo* to give the product as a colourless oil.

Isolated yield: 0.118 g (3.86 mmol, 84%)
^{1}H NMR (700 MHz, $CDCl_3$): δ/ppm 2.17 (2 H, dt, J = 13.8, 6.7 Hz, H2), 2.85 (2 H, t, J = 7.5 Hz, H3), 3.42 (2 H, t, J = 6.6 Hz, H1), 3.77 (3 H, s, H10), 6.64 (1 H, dd, J = 8.8, 3.0 Hz, H7), 6.80 (1 H, d, J = 3.0 Hz, H5), 7.40 (1 H, d, J = 8.7 Hz, H8);
^{13}C NMR (126 MHz, $CDCl_3$): δ/ppm 32.4 (C2), 33.0 (C1), 34.7 (C3), 55.4 (C10), 113.5 (C7), 114.8 (C9), 116.3 (C5), 133.4 (C8), 140.8 (C4), 158.9 (C6).
IR (neat) ν = 1571.6 (m), 1471.5 (s), 1276.4 (m), 1255.6 (s), 1239.5 (s), 1162.2 (m), 1017.4 (m), 800.50 (m) cm^{-1}.
LC-MS: R_t = 0.426 min, m/z 308.9 $[MH]^+$ (ASAP, AS^+); HR-MS calculated for $C_{10}H_{12}Br_2O$ at 305.9255, found 305.9258 (Δ = +1.0 ppm).
Reference[110]

9.33 Ethyl 3-(3-methoxyphenyl)prop-2-enoate, Compound 6-3

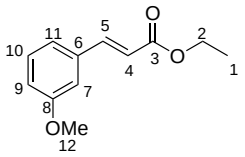

Chemical Formula: $C_{12}H_{14}O_3$
Exact Mass: 206.09

Procedure:

Triethylphosphonoacetate (4.85, 24.5 mmol) and MeCN (30 mL) were charged to a 100 mL RBF fitted with a stirrer bar. DBU (3.65 mL, 24.4 mmol) was charged to the solution which turned a pale yellow colour. LiBr (2.507 g, 28.9 mmol) was charged to the solution and an exotherm was observed. The RBF was fitted with a dropping funnel, lowered into an ice bath and stirred at 0 °C for 10 mins. 3-Methoxybenzaldehyde (**1-52**, 1.25 mL, 10.2 mmol) was added dropwise to the RBF over 15 mins. The solution was removed from the ice bath and stirred at RT overnight. The solution was poured into a saturated aqueous solution of NH_4Cl (100 mL) and stirred for 20 mins. The biphasic solution was transferred to a RBF and concentrated *in vacuo*. The solution was extracted with Et_2O (3 x 20 mL), then the organic extracts were combined and washed with H_2O (2 x 20 mL) then a saturated solution of NaCl(aq) (20 mL), dried over Na_2SO_4, filtered and concentrated *in vacuo* to give a pale yellow oil. The oil was dry-loaded onto silica *via* DCM and purified by column chromatography (EtOAc:petroleum ether 1:4) to give the product as a pale yellow oil.

Isolated yield: 1.904 g (9.42 mmol, 94%)
^{1}H NMR (700 MHz, $CDCl_3$): δ/ppm 1.31 (3 H, t, J = 7.2 Hz, H1), 3.78 (3 H, s, H12), 4.24 (2 H, q, J = 7.1 Hz, H2), 6.40 (1 H, d, J = 16.0 Hz, H5), 6.89 (1 H, dd, J = 8.6, 2.1 Hz, H9/10/11), 7.01 (1 H, s, H7), 7.08 (1 H, d, J = 7.6 Hz, H9/10/11), 7.26 (1 H, t, J = 7.9 Hz, H9/10/11), 7.62 (1 H, d, J = 16.0 Hz, H4);
^{13}C NMR (176 MHz, $CDCl_3$): δ/ppm 14.3 (C1), 55.2 (C12), 60.4 (C2), 112.9 (C7), 116.0 (C9/10/11), 118.5 (C5), 120.7 (C9/10/11), 129.8 (C9/10/11), 135.8 (C6), 144.4 (C4), 159.9 (C8), 166.8 (C3).
IR (neat) ν = 1705.9 (C=O, s), 1637.1 (m), 1579.5 (m), 1292.0 (m), 1247.2 (C-O, s), 1230.3 (C-O, s), 1160.1 (C-O, s), 979.8 (m), 781.1 (m), 697.1 (m) cm^{-1}.
LC-MS: R_t = 2.61 min, m/z 207.2 $[MH]^+$; HR-MS calculated for $C_{12}H_{15}O_3$ at

207.1021, found 207.1032 (Δ = +5.3 ppm).
Reference[111]

9.34 3-(2-Bromo-5-methoxyphenyl)prop-2-enoate, Compound 6-4

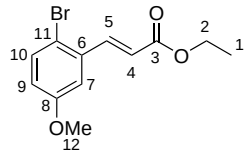

Chemical Formula: $C_{12}H_{13}BrO_3$
Exact Mass: 284.00

Procedure:

Triethylphosphonoacetate (19 mL, 75.0 mmol) and MeCN (80 mL) were charged to a 500 mL RBF fitted with a stirrer bar. DBU (19.0 mL, 127.0 mmol) was charged to the solution which turned a pale yellow colour. LiBr (12.9 g, 148.5 mmol) was charged to the solution and an exotherm was observed. The RBF was fitted with a dropping funnel, lowered into an ice bath and stirred at 0 °C for 10 mins. 2-Bromo-5-methoxybenzaldehyde (**4-1**, 11.097 g, 51.9 mmol) was dissolved in MeCN (70 mL) before being added dropwise to the RBF over 15 mins. The solution was removed from the ice bath and stirred at RT overnight. The solution was poured into a saturated aqueous solution of NH_4Cl (450 mL) and stirred for 20 mins. The biphasic solution was transferred to a RBF and concentrated *in vacuo*. The solution was extracted with Et_2O (3 x 75 mL), then the organic extracts were combined and washed with H_2O (2 x 100 mL) then a saturated solution of NaCl(aq) (150 mL), dried over Na_2SO_4, filtered and concentrated *in vacuo* to give a yellow oil (15.6 g). The oil was dry-loaded onto silica *via* DCM and purified by column chromatography (Et_2O:petroleum ether 1:4) to give the product as a white solid.

Isolated yield: 12.3 g (43.4 mmol, 84%)
^{1}H NMR (700 MHz, $CDCl_3$): δ/ppm 1.34 (3 H, t, J = 7.1 Hz, H1), 3.80 (3 H, s, H12), 4.28 (2 H, q, J = 7.1 Hz, H2), 6.36 (1 H, d, J = 15.9 Hz, H4), 6.80 (1 H, dd, J = 8.8, 3.0 Hz, H9), 7.10 (1 H, d, J = 3.0 Hz, H7), 7.48 (1 H, d, J = 8.8 Hz, H10), 7.99 (1 H, d, J = 15.9 Hz, H5);
^{13}C NMR (126 MHz, $CDCl_3$): δ/ppm 14.3 (C1), 55.5 (C12), 60.7 (C2), 112.5 (C7), 115.9 (C11), 117.6 (C9), 121.2 (C4), 133.9 (C10), 135.1 (C6), 143.0 (C5), 159.0 (C8), 166.3 (C3).
IR (neat) ν = 1675.8 (C=O, s), 1570.1 (m), 1457.2 (s), 1278.2 (C-O, s), 928.0 (s), 864.3 (s), 819.0 (s), 646.5 (s), 597.3 (s) cm^{-1}.

LC-MS: R_t = 3.18 min, m/z 285 $[MH]^+$; HR-MS calculated for $C_{12}H_{14}O_3Br$ at 285.0126, found 285.0126 (Δ = 0.0 ppm).
Melting point: 31.7-33.3 °C (EtOAc).
Reference[112]

9.35 Ethyl 3-(3-methoxyphenyl)propanoate, Compound 6-5

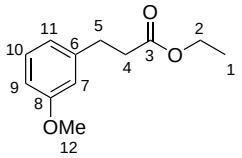

Chemical Formula: $C_{12}H_{16}O_3$
Exact Mass: 208.11

Procedure:

3-(3-Methoxyphenyl)prop-2-enoate (1.010 g, 4.90 mmol) was dissolved in THF (15 mL) and stirred until all of the solid had dissolved to give a colourless solution. H_2O (15 mL) was charged to the RBF to give a cloudy biphasic solution. $TsNHNH_2$ (2.662 g, 14.3 mmol) was gradually added to the solution, followed by $NaOAc \cdot 3\,H_2O$ (3.1 g, 22.8 mmol). The biphasic solution was heated to reflux overnight, then removed from the heat and allowed to cool to RT. The solution was diluted with H_2O (30 mL) then extracted with EtOAc (30 mL x 3), washed with a saturated solution of NaCl(aq) (30 mL), dried over Na_2SO_4 and filtered. The solution was concentrated *in vacuo* to give a colourless oil (1.310 g). The oil was purified by column chromatography (hexanes:EtOAc 8:2), and the fractions containing the product were combined and concentrated *in vacuo* to give a colourless oil.

Isolated yield: 0.900 g (4.33 mmol, 88%)
^{1}H NMR (700 MHz, $CDCl_3$): δ/ppm 1.21-1.25 (3 H, m, H1), 2.60 (2 H, t, J = 7.8 Hz, H4), 2.91 (2 H, t, J = 7.8 Hz, H5), 3.78 (3 H, s, H12), 4.09-4.13 (2 H, m, H2), 6.73-6.78 (3 H, m, H9+10+11), 7.18 (1 H, dd, J = 8.9, 7.6 Hz, H7);
^{13}C NMR (126 MHz, $CDCl_3$): δ/ppm 14.1 (C1), 31.0 (C5), 35.8 (C4), 55.1 (C12), 60.4 (C2), 111.6 (C9/10/11), 114.0 (C9/10/11), 120.6 (C9/10/11), 129.4 (C7), 142.1 (C6), 159.6 (C8), 173.0 (C3).
IR (neat) ν = 1730.5 (C=O, s), 1257.6 (C-O, s), 1151.9 (C-O, s), 1040.5 (C-O, s), 779.3 (m), 695.0 (m) cm^{-1}.
LC-MS: R_t = 3.00 min, m/z 209.44 $[MH]^+$.
Reference[113]

9.36 Ethyl 3-(2-bromo-5-methoxyphenyl)propanoate, Compound 6-6

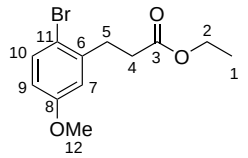

Chemical Formula: $C_{12}H_{15}BrO_3$
Exact Mass: 286.02

Procedure:

3-(2-Bromo-5-methoxyphenyl)prop-2-enoate (**6-4**, 4.0 g, 14.1 mmol) was dissolved in THF (100 mL) and stirred until all of the solid had dissolved to give a colourless solution. H_2O (100 mL) was charged to the RBF to give a cloudy biphasic solution. $TsNHNH_2$ (7.859 g, 42.2 mmol) was gradually added to the solution, followed by $NaOAc \cdot 3\,H_2O$ (8.519 g, 62.6 mmol). The biphasic solution was heated to reflux overnight, then removed from the heat and allowed to cool to RT. The solution was diluted with H_2O (50 mL) then extracted with EtOAc (30 mL x 3), washed with a saturated solution of NaCl(aq) (50 mL), dried over Na_2SO_4 and filtered. The solution was concentrated *in vacuo* to give a pale yellow oil (5.240 g, 18.3 mmol). The oil was purified by column chromatography (hexanes:EtOAc 8:2), and the fractions containing the product were combined and concentrated *in vacuo* to give a colourless oil.

Isolated yield: 3.957 g (13.8 mmol, 98%)
^{1}H NMR (700 MHz, $CDCl_3$): δ/ppm 1.23 (3 H, t, J = 7.2 Hz, H1), 2.61 (2 H, t, J = 7.7 Hz, H4), 3.00 (2 H, t, J = 7.7 Hz, H5), 3.74 (3 H, s, H12), 4.12 (2 H, q, J = 7.1 Hz, H2), 6.62 (1 H, dd, J = 8.7, 3.1 Hz, H9), 6.79 (1 H, d, J = 3.1 Hz, H7), 7.38 (1 H, d, J = 8.7 Hz, H10);
^{13}C NMR (126 MHz, $CDCl_3$): δ/ppm 14.2 (C1), 31.6 (C5), 34.1 (C4), 55.4 (C12), 60.5 (C2), 113.6 (C9), 114.7 (C11), 116.0 (C7), 133.3 (C10), 140.7 (C6), 159.0 (C8), 172.6 (C3).
IR (neat) ν = 1729.5 (C=O, s), 1471.7 (m), 1240.3 (C-O, w), 1160.2 (C-O, s), 1020.1 (C-O, m), 802.5 (m) cm^{-1}.
LC-MS: R_t = 3.09 min, m/z 286.91 $[MH]^+$; HR-MS calculated for $C_{12}H_{16}O_3Br$ at 287.0283, found 287.0278 (Δ = -1.7 ppm).
Reference[114]

9.37 3-(2-Bromo-5-methoxyphenyl)propanoic acid, Compound 6-7

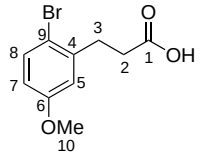

Chemical Formula: $C_{10}H_{11}BrO_3$
Exact Mass: 257.99

Procedure:

Ethyl 3-(2-bromo-5-methoxyphenyl)propanoate (**6-6**, 0.966 g, 3.38 mmol) was dissolved in EtOH (12.0 mL). NaOH (0.540 g, 13.5 mmol) was charged to the RBF and the resulting pale yellow solution was stirred at RT for 30 mins. The solution was then heated to 30 °C for 30 mins. The reaction was quenched with 1M HCl (20 mL) until acidic, then extracted with Et_2O (20 mL), H_2O (20 mL x 2) and a saturated solution of NaCl(aq) (20 mL). The solution was dried over Na_2SO_4, filtered and concentrated *in vacuo* to give a white solid (0.821 g, 3.18 mmol). The solid was recrystallised from hexanes to give the product as sparkly white needle-like crystals.

Isolated yield: 0.641 g (2.48 mmol, 74%)
^{1}H NMR (700 MHz, $CDCl_3$): δ/ppm 2.69 (2 H, t, J = 7.8 Hz, H2), 3.02 (2 H, t, J = 7.8 Hz, H3), 3.76 (3 H, s, H10), 6.65 (1 H, dd, J = 8.7, 3.0 Hz, H7), 6.81 (1 H, d, J = 3.0 Hz, H5), 7.41 (1 H, d, J = 8.7 Hz, H8);
^{13}C NMR (126 MHz, $CDCl_3$): δ/ppm 31.3 (C3), 33.5 (C2), 55.4 (C10), 113.8 (C7), 114.6 (C9), 116.1 (C5), 133.4 (C8), 140.3 (C4), 159.0 (C6), 177.1 (C1).
IR (neat) ν = 2838.2 (O-H, br w), 1709.7 (m), 1426.2 (m), 1203.2 (s), 1051.1 (m), 866.9 (s), 814.0 (m), 603.3 (m) cm^{-1}.
LC-MS: R_t = 2.32 min, m/z 241.30 [M-H_2O]$^-$; HR-MS calculated for $C_{10}H_{10}O_3Br$ at 256.9813, found 256.9811 (Δ = -0.8 ppm).
CHN analysis: calculated for $C_{10}H_{11}BrO_3$ at C 46.36%, H 4.28%, N 0.00%; found C 46.15%, H 4.29%, N -0.02%.
Melting point: 83.1-84.0 °C (hexanes), literature = 81-83 °C.
Reference[109]

9.38 3-(2-Bromo-5-methoxyphenyl)propan-1-ol, Compound 6-8

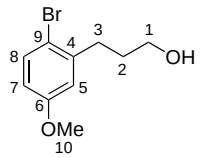

Chemical Formula: $C_{10}H_{13}BrO_2$
Exact Mass: 244.01

Procedure:

Ethyl 3-(2-bromo-5-methoxyphenyl)propanoate (**6-6**, 0.997 g, 3.49 mmol) was dissolved in dry THF (4.0 mL). In a separate RBF, $LiAlH_4$ (0.136 g, 3.58 mmol) was charged to an oven-dry RBF fitted with a stirrer bar and flushed with N_2. Dry THF (4.0 mL) was charged to this flask which was cooled in an ice bath. The ester/ THF solution was charged to the first RBF and the resulting solution was allowed to warm to RT and stirred for 30 mins under N_2. The solution was quenched with EtOH (10 mL), flushed with N_2, filtered through silica on a scinter and rinsed through with EtOH. The solution was concentrated *in vacuo* to give a colourless oil.

Isolated yield: 0.837 g (3.43 mmol, 98%)
^{1}H NMR (700 MHz, $CDCl_3$): δ/ppm 1.85-1.90 (2 H, m, H2), 2.76-2.79 (2 H, m, H3), 3.68-3.71 (2 H, m, H1), 3.76 (3 H, s, H10), 6.62 (1 H, dd, J = 8.7, 3.1 Hz, H7), 6.78 (1 H, d, J = 3.0 Hz, H5), 7.39 (1 H, d, J = 8.7 Hz, H8);
^{13}C NMR (126 MHz, $CDCl_3$): δ/ppm 32.6 (C3), 32.7 (C2), 55.4 (C10), 62.1 (C1), 113.2 (C7), 114.9 (C9), 116.1 (C5), 133.3 (C8), 142.1 (C4), 158.9 (C6)..
IR (neat) ν = 3326.7 (O-H, br w), 1571.3 (m), 1371.5 (s), 1276.0 (m), 1239.4 (s), 1160.9 (m), 1053.6 (m), 1011.6 (s), 799.8 (m) cm^{-1}.
LC-MS: R_t = 2.86 min, m/z 245 $[MH]^+$; HR-MS calculated for $C_{10}H_{12}BrO$ (M-H_2O) at 227.0072, found 227.0062 (Δ = -4.5 ppm).
Reference[115]

9.39 [3-(2-Bromo-5-methoxyphenyl)propyl]triphenylphosphonium bromide, Compound 6-9

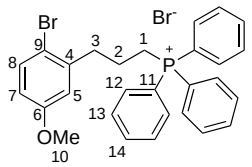

Chemical Formula: $C_{28}H_{27}Br_2OP$
Exact Mass: 568.02

Procedure:

1-Bromo-2-(3-bromopropyl)4-methoxybenzene (0.884 g, 2.89 mmol) was charged to a 50 mL RBF fitted with a stirrer bar. PPh_3 (0.748 g, 2.85 mmol) and toluene (3.0 mL) were charged to the RBF and the resulting solution was refluxed for 6 h. A white precipitate formed when the solution was allowed to cool to RT. Filtration afforded a white solid (0.839 g, 1.48 mmol) which was recrystallised from H_2O to give the product as white sparkly needle-like crystals.

Isolated yield: 0.826 g (1.45 mmol, 51%)
^{1}H NMR (700 MHz, $CDCl_3$): δ/ppm 1.98 (2 H, h, J = 8.4 Hz, H1), 3.13 (2 H, t, J = 7.5 Hz, H3), 3.80 (3 H, s, H10), 3.94 (2 H, dd, J = 16.3, 12.9 Hz, H2), 6.61 (1 H, dd, J = 8.7, 3.0 Hz, H7), 7.19 (1 H, d, J = 3.0 Hz, H5), 7.29 (1 H, d, J = 8.7 Hz, H8), 7.64-7.67 (6 H, m, H12/13/14), 7.75-7.80 (9 H, m, H12/13/14);
^{13}C NMR (126 MHz, solvent): δ/ppm 21.9d (C2), 22.4d (C1), 36.5d (C3), 56.1 (C10), 114.1 (C9), 115.2 (C7), 116.7 (C5), 118.3d (C11/12/13/14), 130.4d (C11/12/13/14), 133.1 (C8), 133.7d (C11/12/13/14), 134.9 (C11/12/13/14), 140.5 (C4), 159.2 (C6).
IR (neat) ν = 1436.5 (P-Ph, m), 1243.1 (m), 1112.4 (m), 1105.0 (m), 740.7 (m), 731.9 (s), 723.9 (s), 690.0 (s) cm^{-1}.
LC-MS: R_t = 0.62 min, m/z 489.1 [M-Br$^-$]$^+$ (ASAP$^+$); HR-MS calculated for $C_{28}H_{27}BrOP$ at 489.0983, found 489.0977 (Δ = -1.2 ppm).
Melting point: 173.8-174.7 °C (H_2O), literature = 174-175 °C.
Reference[110]

9.40 3-(2-Bromo-5-methoxyphenyl)prop-2-enoic acid, Compound 6-14

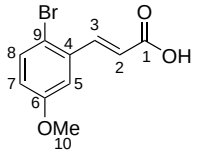

Chemical Formula: $C_{10}H_9BrO_3$
Exact Mass: 255.97

Procedure:

2-Bromo-5-methoxybenzaldehyde (**4-1**, 20.906 g, 98 mmol) was dissolved in pyridine (126 mL) in a 500 mL RBF fitted with a stirrer bar. Malonic acid (40.6 g, 391 mmol) 6.272 g, 60.27 mmol) then piperidine (6.5 mL) were charged to the solution, which was heated at reflux for 4 h. The solution was quenched by pouring into an aqueous 1 M solution of HCl (600 mL). Immediate formation of a white precipitate was observed. The slurry was filtered and the solid washed with HCl (20 mL x 2) then H_2O. The white solid was transferred to a RBF, dissolved in EtOAc and extracted with H_2O (20 mL) before being dried over Na_2SO_4, filtered and concentrated *in vacuo* to give a fluffy white solid.

Isolated yield: 18.014 g (70.4 mmol, 72%) ^{1}H NMR (700 MHz, $CDCl_3$): δ/ppm 3.78 (3 H, s, H10), 6.62 (1 H, d, J = 15.8 Hz, H2), 6.93 (1 H, dd, J = 8.8, 3.1 Hz, H7), 7.40 (1 H, d, J = 3.1 Hz, H5), 7.56 (1 H, d, J = 8.8 Hz, H8), 7.75 (1 H, d, J = 15.9 Hz, H3), 12.6 (1 H, br s, H11);
^{13}C NMR (126 MHz, $CDCl_3$): δ/ppm 56.1 (C10), 113.2 (C5), 115.5 (C9), 119.0 (C7), 123.2 (C2), 134.3 (C8), 134.7 (C4), 141.8 (C3), 159.4 (C6), 167.6 (C1).
IR (neat) ν = 2837.4 (br), 1675.2 (s), 1626.5 (m), 1567.1 (m), 1471.4 (m), 1417.1 (m), 1304.1 (m), 1286.9 (s), 1220.7 (s), 1201.9 (s), 1059.6 (s), 977.9 (s), 947.7 (m), 855.1 (s), 808.6 (s), 685.5 (m), 596.6 (s) cm^{-1}.
LC-MS: R_t = 3.09 min, m/z 257.3 $[MH]^+$; HR-MS calculated for $C_{10}H_{10}O_3Br$ at 256.9813, found 256.9809 (Δ = -1.6 ppm).
CHN analysis: calculated for $C_{10}H_9BrO_3$ at C 46.72%, H 3.53%, N 0.00%; found C 46.73%, H 3.54%, N -0.02%.
Melting point: 190.5-191.0 °C, literature = 189 °C.
Reference[116]

9.41 4-(3-Hydroxyphenyl)but-3-en-2-one

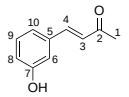

Chemical Formula: $C_{10}H_{10}O_2$
Exact Mass: 162.07

Procedure:[117]

3-Hydroxybenzaldehyde (**3-3**, 4.90 g, 40.1 mmol) and EtOH (30 mL) were charged to a 100 mL RBF with stirring. Acetone (15.5 mL, 211 mmol) was charged to the flask and the reaction was stirred in an ice bath. 10% NaOH (2.99 g, 74.8 mmol, 30 mL) was charged to the flask and the solution turned yellow then orange. The solution was stirred at RT for 2 h and monitored by TLC (Hex:EtOAc 1:1). The solution was extracted with EtOAc (50 mL x 2), then the organic layers were washed with a saturated aqueous solution of NaCl (30 mL), dried over $MgSO_4$ and filtered. The solvent was removed *in vacuo* to give a pale yellow solid which was recrystallised from Et_2O to give the product as a fine yellow solid which was 91% pure by ^{1}H NMR spectroscopy.

Isolated yield: 3.718 g (22.9 mmol, 57%)
^{1}H NMR (400 MHz, d_4−MeOD): δ/ppm 2.39 (3 H, s), 6.73 (1 H, d, J = 16.3 Hz), 6.87 (1 H, ddd, J = 8.2, 2.5, 1.0 Hz), 7.06 (1 H, t, J = 2.5 Hz), 7.11 (1 H, m), 7.25 (1 H, t, J = 7.9 Hz), 7.58 (1 H, d, J = 16.3 Hz);
^{13}C NMR (101 MHz, d_4−MeOD): δ/ppm 25.9 (CH_3), 114.1 (CH), 117.5 (CH), 119.7 (CH), 126.3 (CH), 129.7 (CH), 133.8 (C), 133.5 (CH), 157.7 (C), 200.0 (C=O).
IR (neat) ν = 3072.6 (OH, br), 1621.4 (C=O, s), 1576.4 (s), 1253.9 (s), 961.6 (s), 775.5 (s), 683.8 (s) cm^{-1}.
LC-MS: R_t = 2.12 min, m/z 160.9 [M-H]$^-$.
Melting point: 88.1-93.4 °C (Et_2O), literature = 94-95 °C.
Reference[117,118]

9.42 3-[3-Hydroxy-5-(3-hydroxyphenyl)pentyl]phenol

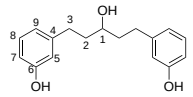

Chemical Formula: $C_{17}H_{20}O_3$
Exact Mass: 272.14

Procedure:[119]

1,5-*Bis*(3-hydroxyphenyl)penta-1,4-dien-3-one (**3-2**, 0.269 g, 1.01 mmol) and IPA (5.60 mL) were charged to a 25 mL RBF fitted with a stirrer bar. The RBF was flushed with N_2, and 10% Pd/C (0.031 g, 10 wt%) was charged to the RBF. AcOH (0.114 mL, 2.00 mmol) was charged in one portion to the RBF with stirring. $NaBH_4$ (0.160 g, 4.23 mmol) was charged gradually to the flask with stirring due to the rapid evolution of gas. The solution was stirred at RT for 1 h. An aqueous solution of 1 M HCl (2 mL) was added dropwise to the solution until no more bubbled were observed. $NaHCO_3$ was added dropwise to the solution until it was basic (pH 8). The solution was extracted with Et_2O (25 mL x 2) and H_2O (10 mL x 2). The organic layer was dried over $MgSO_4$, filtered through Celite and concentrated *in vacuo* to give the product as a pale yellow oil.

Isolated yield: 0.215 g (0.790 mmol, 78%)
^{1}H NMR (700 MHz, d_6−DMSO): δ/ppm 1.53-1.66 (4 H, m, H2), 2.47-2.63 (4 H, m, H3), 3.38-3.45 (1 H, m, H1), 6.52-6.60 (6 H, m, H5/8/9), 7.03 (2 H, t, J = 7.7, H7), 9.18 (2 H, s, OH);
^{13}C NMR (176 MHz, d_6−DMSO): δ/ppm 32.0 (C3), 39.5 (C2), 69.1 (C1), 112.9 (C5/8/9), 115.6 (C5/8/9), 119.4 (C5/8/9), 129.6 (C7), 144.4 (C4), 157.7 (C6).
LC-MS: R_t = 2.87 min, m/z 271 $[M\text{-}H]^-$.

No literature data available.

9.43 2,4,6-Tribromo-3-hydroxybenzaldehyde

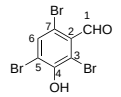

Chemical Formula: $C_7H_3Br_3O_2$
Exact Mass: 355.77

Procedure:[120]

3-Hydroxybenzaldehyde (**3-3**, 1.275 g, 10.4 mmol) was charged to a 500 mL RBF fitted with a stirrer bar. MeCN (200 mL) was charged to the flask and the resulting solution was stirred for 10 mins. NBS (5.362 g, 30.1 mmol) was charged to the flask and the solution turned pale yellow. The reaction was stirred at room temperature for 24 h, then quenched with 10% $Na_2S_2O_3$ (100 mL) and extracted with Et_2O (100 mL). The crude was washed with 10% $Na_2S_2O_3$ (20 mL x 2), then H_2O (20 mL x 3). The solution was dried over $MgSO_4$, filtered and the solvent removed *in vacuo* to give the product as cream needle-like crystals.

Isolated yield: 2.954 g (8.30 mmol, 79%)
^{1}H NMR (400 MHz, $CDCl_3$): δ/ppm 6.37 (1 H, s, ArOH), 7.85 (1 H, s, H5), 10.17 (1 H, s, H1);
^{13}C NMR (101 MHz, $CDCl_3$): δ/ppm 111.6, 115.0, 115.8, 131.7, 136.6, 150.1 (C4), 190.2 (C1).
IR (neat) ν = 3348.2 (OH, br w), 1633.8 (C=O, s), 1437.0 (C-O, s), 1160.5 (C-O, s), 790.0 (s), 760.0 (m), 670.5 (s) cm^{-1}.
LC-MS: R_t = 2.85 min, m/z 354.7 $[M\text{-}H]^-$; HR-MS calculated for $C_7H_2O_2Br_3$ at 354.7605, found 354.7605 (Δ = +0.0 ppm).
Melting point: 117.3-118.8 °C (AcOH), literature = 115-116 °C (AcOH).
Reference[121]

9.44 7,7'-Dimesylate-1,1'-spirobiindane (*o*-SPINOMs)

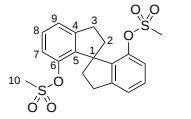

Procedure from *o*-SPINOL:[95]

1,1'-Spirobiindane-7,7'-diol (*o*-SPINOL, **1-42**) (0.030 g, 0.12 mmol) was dissolved in dry DCM (0.150 mL) and transferred to a 5 mL RBF fitted with a stirrer bar and septum. Dry pyridine (0.05 mL, 0.62 mmol) was charged to the RBF and the mixture cooled to 0 °C. MsCl (0.05 mL, 0.64 mmol) was charged to the RBF and the solution changed colour from dark yellow to pale yellow. The solution was stirred in the ice bath for 4 h, then allowed to warm to RT and stirred for 30 mins. The solution was quenched with H_2O (0.5 mL) and the organic phase extracted with DCM (3 x 2 mL). The organic extracts were washed with an aqueous solution of 1 M HCl (2 x 4 mL) and then a saturated aqueous solution of NaCl (3 x 2 mL). The solution was dried over $MgSO_4$, filtered and concentrated *in vacuo* to give a yellow oil. Conversion to the product was 80% by ^{1}H NMR spectroscopy.

^{1}H NMR (700 MHz, d_6−DMSO): δ/ppm 2.08-2.21 (2 H, m, H2), 2.31-2.41 (2 H, m, H2), 3.04 (4 H, t, J = 7.4 Hz, H3), 6.97 (2 H, d, J = 8.3 Hz, H7), 7.12 (2 H, d, J = 8.3 Hz, H9), 7.29 (2 H, s, H8);
^{13}C NMR (176 MHz, d_6−DMSO): δ/ppm 30.6 (CH2), 37.6 (CH), 40.8 (CH2), 59.6 (C), 118.8 (CH), 121.0 (CH), 124.5 (CH), 146.2 (C), 149.4 (C).
IR (neat) ν = 2939.5 (w), 1359.5 (m), 1175.5 (C-O, s), 1121.6 (m), 932.2 (s), 904.2 (m) cm^{-1}.
LC-MS (ASAP): R_t = 0.76 min, m/z 409.1 $[M+H]^+$.
No literature data available.

9.45 1,5-*Bis*(2-chloro-5-nitrophenyl)penta-1,4-dien-3-one

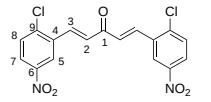

Chemical Formula: $C_{17}H_{10}Cl_2N_2O_5$
Exact Mass: 392.00

Procedure:

NaOH (1.015 g, 25.38 mmol) was charged to a 100 mL RBF fitted with a stirrer bar. H_2O (10 mL) was charged to the RBF, followed by EtOH (10 mL). 2-Chloro-5-nitrobenzaldehyde (1.828 g, 9.85 mmol) was charged to the RBF, then stirred for 5 mins until all the solid had dissolved to give an orange solution. Acetone (0.38 mL, 5.18 mmol) was charged to the RBF. After 15 mins stirring at RT, the solution was brown and viscous. After 2 h, 1 M HCl was added dropwise until the solution was neutral. The coffee-coloured suspension was filtered over a scinter, rinsed with H_2O, and left to air-dry overnight. The crude solid was dried *in vacuo* to give a pale-brown solid.

Isolated yield: 1.888 g (4.80 mmol, 96%)
^{1}H NMR (700 MHz, $CDCl_3$): δ/ppm 7.20 (2 H, d, J = 15.9, H2), 7.65 (2 H, d, J = 8.8, H8), 8.12 (2 H, d, J = 15.9, H3), 8.20 (2 H, dd, J = 8.8, 2.6, H7), 8.59 (2 H, d, J = 2.6, H5);
^{13}C NMR (176 MHz, $CDCl_3$): δ/ppm 112.6 (C5), 125.4 (C7), 129.5 (C2), 131.4 (C8), 134.3 (C4), 137.7 (C3), 141.7 (C9), 146.8 (C6), 187.0 (C1).
IR (neat) ν = 1516.4 (m), 1346.1 (s), 1051.0 (w), 819.4 (w), 739.2 (m) cm^{-1}.
LC-MS: R_t = 0.61 min, m/z 393.0 $[MH]^+$.
No literature data available.

References

[1] L. K. Smith and I. R. Baxendale, *Organic and Biomolecular Chemistry*, 2015, **13**, 9907–9933.

[2] K. W. Quasdorf and L. E. Overman, *Nature*, 2014, **516**, 181–191.

[3] M. Sannigrahi, *Tetrahedron*, 1999, **55**, 9007–9071.

[4] E. Corey and A. Guzman-Perez, *Angewandte Chemie International Edition*, 1998, **37**, 388–401.

[5] K. Fuji, *Chemical Reviews*, 1993, **93**, 2037–2066.

[6] S. Li, J.-W. Zhang, X.-L. Li, D.-J. Cheng and B. Tan, *Journal of the American Chemical Society*, 2016, **138**, 16561–16566.

[7] V. Birman, A. Rheingold and K. Lam, *Tetrahedron: Asymmetry*, 1999, **10**, 125–131.

[8] K. Lan, Z. Shan and S. Fan, *Tetrahedron Letters*, 2006, **47**, 4343–4345.

[9] J.-H. Zhang, J. Liao, X. Cui, K.-B. Yu, J. Zhu, J.-G. Deng and S.-F. Zhu, *Tetrahedron: Asymmetry*, 2002, **13**, 1363–1366.

[10] Z. Li, X. Liang, F. Wu and B. Wan, *Tetrahedron: Asymmetry*, 2004, **15**, 665–669.

[11] D. T. McQuade and P. H. Seeberger, *Journal of Organic Chemistry*, 2013, **78**, 6384–6389.

[12] J. Wegner, S. Ceylan and A. Kirschning, *Chemical Communications*, 2011, **47**, 4583–4592.

[13] J. C. Pastre, D. L. Browne and S. V. Ley, *Chemical Society Reviews*, 2013, **42**, 8849–8869.

[14] M. Baumann, I. R. Baxendale, S. V. Ley, N. Nikbin, C. Smith and J. P. Tierney, *Organic and Biomolecular Chemistry*, 2008, **6**, 1577–1586.

[15] M. Baumann, I. R. Baxendale, S. V. Ley, N. Nikbin and C. D. Smith, *Organic and Biomolecular Chemistry*, 2008, **6**, 1587–1593.

[16] C. J. Smith, C. D. Smith, N. Nikbin, S. V. Ley and I. R. Baxendale, *Organic and Biomolecular Chemistry*, 2011, **9**, 1927–1937.

[17] C. J. Smith, N. Nikbin, S. V. Ley, H. Lange and I. R. Baxendale, *Organic and Biomolecular Chemistry*, 2011, **9**, 1938–1947.

[18] L. J. Martin, A. L. Marzinzik, S. V. Ley and I. R. Baxendale, *Organic Letters*, 2011, **13**, 320–323.

[19] P. Löb, H. Löwe and V. Hessel, *Journal of Fluorine Chemistry*, 2004, **125**, 1677–1694.

[20] M. Eissen and D. Lenoir, *Chemistry*, 2008, **14**, 9830–9841.

[21] A. Palmieri, S. V. Ley, K. Hammond, A. Polyzos and I. R. Baxendale, *Tetrahedron Letters*, 2009, **50**, 3287–3289.

[22] V. Hessel, *Chemical Engineering and Technology*, 2009, **32**, 1655–1681.

[23] T. Illg, P. Löb and V. Hessel, *Bioorganic and Medicinal Chemistry*, 2010, **18**, 3707–3719.

[24] C. F. Carter, H. Lange, S. V. Ley, I. R. Baxendale, B. Wittkamp, J. G. Goode and N. L. Gaunt, *Organic Process and Research Development*, 2010, **14**, 393–404.

[25] D. L. Browne, S. Wright, B. J. Deadman, S. Dunnage, I. R. Baxendale, R. M. Turner and S. V. Ley, *Rapid Communications in Mass Spectrometry*, 2012, **26**, 1999–2010.

[26] Y. Tomida, A. Nagaki and J.-I. Yoshida, *Journal of the American Chemical Society*, 2011, **133**, 3744–3747.

[27] S. Newton, S. V. Ley, E. C. Arcé and D. M. Grainger, *Advanced Synthesis and Catalysis*, 2012, **354**, 1805–1812.

[28] A. Odedra and P. H. Seeberger, *Angewandte Chemie International Edition*, 2009, **48**, 2699–2702.

[29] P. Lozano, E. Garcia-Verdugo, S. V. Luis, M. Pucheault and M. Vaultier, *Current Organic Synthesis*, 2011, **8**, 810–823.

[30] M. I. Burguete, E. García-Verdugo and S. V. Luis, *Beilstein Journal of Organic Chemistry*, 2011, **7**, 1347–1359.

[31] X. C. Cambeiro, R. Martín-Rapún, P. O. Miranda, S. Sayalero, E. Alza, P. Llanes and M. A. Pericàs, *Beilstein Journal of Organic Chemistry*, 2011, **7**, 1486–1493.

[32] L. Shi, X. Wang, C. A. Sandoval, Z. Wang, H. Li, J. Wu, L. Yu and K. Ding, *Chemistry*, 2009, **15**, 9855–9867.

[33] R. Augustine, S. Tanielyan, N. Mahata, Y. Gao, A. Zsigmond and H. Yang, *Applied Catalysis, A*, 2003, **256**, 69–76.

[34] D. Zhao and K. Ding, *ACS Catalysis*, 2013, **3**, 928–944.

[35] F. Shibahara, K. Nozaki and T. Hiyama, *Journal of the American Chemical Society*, 2003, **125**, 8555–8560.

[36] G. Moss, *Pure Applied Chemistry*, 1999, **71**, 531–558.

[37] A. G. Myers, B. H. Yang, H. Chen, L. McKinstry, D. J. Kopecky and J. L. Gleason, *Journal of the American Chemical Society*, 1997, **119**, 6496–6511.

[38] L. A. Paquette, *Handbook of Reagents for Organic Synthesis: Chiral Reagents for Asymmetric Synthesis*, John Wiley & Sons, 2003, pp. 42–44.

[39] D. Seebach, J. Aebi and D. Wasmuth, in *Diastereoselective alpha-Alkylation of beta-Hydroxycarboxylic Esters through Alkoxide Enolates: Diethyl (2S, 3R)-(+)-3-Allyl-2-Hydroxysuccinate from Diethyl (S)-()-Malate*, John Wiley Sons, Inc., 2003.

[40] E. J. Corey, S. Shibata and R. K. Bakshi, *Journal of Organic Chemistry*, 1988, **53**, 2861–2863.

[41] D. L. Hughes, *Organic Synthesis*, 2014, **91**, 1–11.

[42] J. M. Brunel, *Chemical Reviews*, 2005, **105**, 857–897.

[43] D. Parmar, E. Sugiono, S. Raja and M. Rueping, *Chemical Reviews*, 2014, **114**, 9047–9153.

[44] M. Rueping, E. Sugiono and C. Azap, *Angewandte Chemie International Edition*, 2006, **45**, 2617–2619.

[45] L. Simón and J. Goodman, *Journal of Organic Chemistry*, 2011, **76**, 1775–1788.

[46] R. Noyori and H. Takaya, *Accounts of Chemical Research*, 1990, **23**, 345–350.

[47] Z. Zhang, H. Qian, J. Longmire and X. Zhang, *Journal of Organic Chemistry*, 2000, **65**, 6223–6226.

[48] K. Mori, Y. Masuda and S. Kashino, *Acta Crystallographica Section C*, 1993, **49**, 1224–1227.

[49] X. H. Huo, J. H. Xie, Q. S. Wang and Q. L. Zhou, *Advanced Synthesis and Catalysis*, 2007, **349**, 2477–2484.

[50] M.-N. Birkholz, Z. Freixa and P. W. N. M. van Leeuwen, *Chemical Society Reviews*, 2009, **38**, 1099–118.

[51] S. Zhu, J. Xie, Y. Zhang, S. Li and Q. Zhou, *Journal of the American Chemical Society*, 2006, **128**, 12886–12891.

[52] M. Grayson, S. Pellegrinet and J. Goodman, *Journal of the American Chemical Society*, 2012, **134**, 2716–2722.

[53] P. Christ, A. G. Lindsay, S. S. Vormittag, J. M. Neudörfl, A. Berkessel and A. C. O'Donoghue, *Chemistry, a European Journal*, 2011, **17**, 8524–8528.

[54] L. Hong and R. Wang, *Advanced Synthesis and Catalysis*, 2013, **355**, 1023–1052.

[55] G. Singh and Z. Desta, *Chemical Reviews*, 2012, **112**, 6104–6155.

[56] Y. Zheng, C. M. Tice and S. B. Singh, *Bioorganic and Medicinal Chemistry Letters*, 2014, **24**, 3673–3682.

[57] R. Phipps, G. Hamilton and F. Toste, *Nature Chemistry*, 2012, **4**, 603–614.

[58] K. Ishihara, S. Nakamura and H. Yamamoto, *Journal of the American Chemical Society*, 1999, **121**, 4906–4907.

[59] S. Nakamura, K. Ishihara and H. Yamamoto, *Journal of the American Chemical Society*, 2000, **122**, 8131–8140.

[60] K. Ishihara, H. Ishibashi and H. Yamamoto, *Journal of the American Chemical Society*, 2001, **123**, 1505–1506.

[61] K. Ishihara, H. Ishibashi and H. Yamamoto, *Journal of the American Chemical Society*, 2002, **124**, 3647–3655.

[62] H. Yamamoto and K. Futatsugi, *Angewandte Chemie International Edition*, 2005, **44**, 1924–1942.

[63] O. Kanno, W. Kuriyama, Z. Wang and F. Toste, *Angewandte Chemie International Edition*, 2011, **50**, 9919–9922.

[64] R. LaLonde, W. Brenzovich, Jr., D. Benitez, E. Tkatchouk, K. Kelley, W. Goddard, III and F. Toste, *Chemical Science*, 2010, **1**, 226–233.

[65] B. Cochran and F. Michael, *Journal of the American Chemical Society*, 2008, **130**, 2786–2792.

[66] D. Cristina Silva Costa, *Arabian Journal of Chemistry*, 2017.

[67] M. A. Dolliver and C. R. Conrad, *Organic Synthesis, Collection Volume 2*, 1943, **12**, 167.

[68] X. Wang, Z. Han, Z. Wang and K. Ding, *Angewandte Chemie International Edition*, 2012, **51**, 936–940.

[69] V. Birman, A. Rheingold and K. Lam, *Tetrahedron: Asymmetry*, 1999, **10**, 125–131.

[70] E. Eaton, *Journal of Organic Chemistry*, 1973, **38**, 4071–4073.

[71] V. L. Heasley, T. J. Louie, D. K. Luttrull, M. D. Millar, H. B. Moore, D. F. Nogales, A. M. Sauerbrey, A. B. Shevel, T. Y. Shibuya, M. S. Stanley, D. F. Shellhamer and G. E. Heasley, *Journal of Organic Chemistry*, 1988, **53**, 2199–2204.

[72] S. Li, J.-W. Zhang, X.-L. Li, D.-J. Cheng and B. Tan, *Journal of the American Chemical Society*, 2016, **138**, 16561–16566.

[73] S. Snyder, T. Sherwood, A. Ross, H. Oh and S. Ghosh, WO2011103442 A2, 2011.

[74] J. C. Conrad, J. Kong, B. N. Laforteza and D. W. C. Macmillan, *Journal of the American Chemical Society*, 2009, **131**, 11640–11641.

[75] R. K. Henderson, C. Jiménez-González, D. J. C. Constable, S. R. Alston, G. G. a. Inglis, G. Fisher, J. Sherwood, S. P. Binks and A. D. Curzons, *Green Chemistry*, 2011, **13**, 854.

[76] K. Lan, Z. Shan and S. Fan, *Tetrahedron Letters*, 2006, **47**, 4343–4345.

[77] A. Zubia, L. Mendoza, S. Vivanco, E. Aldaba, T. Carrascal, B. Lecea, A. Arrieta, T. Zimmerman, F. Vidal-Vanaclocha and F. P. Cossío, *Angewandte Chemie International Edition*, 2005, **44**, 2903–2907.

[78] K. Burgess and W. Li, *Tetrahedron Letters*, 1995, **36**, 2725–2728.

[79] D. X. Hu, M. O'Brien and S. V. Ley, *Organic Letters*, 2012, **14**, 4246–4249.

[80] A. S. Bhanu Prasad, J. V. Bhaskar Kanth and M. Periasamy, *Tetrahedron*, 1992, **48**, 4623–4628.

[81] M. C. Pirrung, *The Synthetic Organic Chemist's Companion*, John Wiley & Sons, 2007, pp. 115–116.

[82] B. F. Molino, S. Liu, A. Sambandam, P. R. Guzzo, M. Hu, C. Zha, K. Nacro, D. D. Manning, M. L. Isherwood, K. N. Fleming, W. Cui and R. E. Olson, *WO2007011820A2*, 2007.

[83] M. H. Shaw, R. A. Croft, W. G. Whittingham and J. F. Bower, *Journal of the American Chemical Society*, 2015, **137**, 8054–8057.

[84] S. W. Leong, S. M. Mohd Faudzi, F. Abas, M. F. F. Mohd Aluwi, K. Rullah, L. K. Wai, M. N. Abdul Bahari, S. Ahmad, C. L. Tham, K. Shaari and N. H. Lajis, *Molecules*, 2014, **19**, 16058–16081.

[85] J.-H. Zhang, J. Liao, X. Cui, K.-B. Yu, J. Zhu, J.-G. Deng and S.-F. Zhu, *Tetrahedron: Asymmetry*, 2002, **13**, 1363–1366.

[86] P.-C. Leow, P. Bahety, C. P. Boon, C. Y. Lee, K. L. Tan, T. Yang and P.-L. R. Ee, *European Journal of Medicinal Chemistry*, 2014, **71**, 67–80.

[87] D. Vonlanthen, J. Rotzler, M. Neuburger and M. Mayor, *European Journal of Organic Chemistry*, 2010, 120–133.

[88] K. D. Ashtekar, X. Ding, E. Toma, W. Sheng, H. Gholami, C. Rahn, P. Reed and B. Borhan, *Organic Letters*, 2016, **18**, 3976–3979.

[89] H. Yamakoshi, H. Ohori, C. Kudo, A. Sato, N. Kanoh, C. Ishioka, H. Shibata and Y. Iwabuchi, *Bioorganic and Medicinal Chemistry*, 2010, **18**, 1083–1092.

[90] S. Zhu, Y. Fu, J. Xie, B. Liu, L. Xing and Q. Zhou, *Tetrahedron: Asymmetry*, 2003, **14**, 3219–3224.

[91] A. Mori, Y. Miyakawa, E. Ohashi, T. Haga, T. Maegawa and H. Sajiki, *Organic Letters*, 2006, **8**, 3279–3281.

[92] M. A. Dolliver and C. R. Conrad, *Organic Synthesis, Collection Volume 2*, 1943, **12**, 167.

[93] B. K. Adams, E. M. Ferstl, M. C. Davis, M. Herold, S. Kurtkaya, R. F. Camalier, M. G. Hollingshead, G. Kaur, E. A. Sausville, F. R. Rickles, J. P. Snyder, D. C. Liotta and M. Shoji, *Bioorganic and Medicinal Chemistry*, 2004, **12**, 3871–3883.

[94] T. Hosoya, A. Nakata, F. Yamasaki, F. Abas, K. Shaari, N. H. Lajis and H. Morita, *Journal of Natural Medicine*, 2012, **66**, 166–176.

[95] D. A. Wilson, C. J. Wilson, C. Moldoveanu, A. M. Resmerita, P. Corcoran, L. M. Hoang, B. M. Rosen and V. Percec, *Journal of the American Chemical Society*, 2010, **132**, 1800–1801.

[96] S. Hagishita and K. Kuriyama, *Bulletin of the Chemical Society of Japan*, 1971, **44**, 496–505.

[97] L. F. Tietze, G. Brasche, A. Grube, N. Böhnke and C. Stadler, *Chemistry, a European Journal*, 2007, **13**, 8543–8563.

[98] S. A. Snyder, T. C. Sherwood, A. G. Ross, H. Oh and S. Ghosh, *WO2011103442A2*, 2011.

[99] B. F. Molino, S. Liu, P. R. Guzzo and J. P. Beck, *US2015274713A1*, 2015.

[100] M. Barbasiewicz, K. Błocki, M. Malińska and R. Pawłowski, *Dalton Transactions*, 2013, **42**, 355–358.

[101] Y. F. Wang, Y. R. Gao, S. Mao, Y. L. Zhang, D. D. Guo, Z. L. Yan, S. H. Guo and Y. Q. Wang, *Organic Letters*, 2014, **16**, 1610–1613.

[102] X.-W. Feng, C. Li, N. Wang, K. Li, W.-W. Zhang, Z. Wang and X.-Q. Yu, *Green Chemistry*, 2009, **11**, 1933–1936.

[103] W. J. Kerr, R. J. Mudd, L. C. Paterson and J. A. Brown, *Chemistry, a European Journal*, 2014, **20**, 14604–14607.

[104] N. Franz, L. Menin and H. A. Klok, *European Journal of Organic Chemistry*, 2009, 5390–5405.

[105] G. Van Der Heijden, J. A. W. Jong, E. Ruijter and R. V. A. Orru, *Organic Letters*, 2016, **18**, 984–987.

[106] C. Aciro, S. G. Davies, A. C. Garner, Y. Ishii, M. S. Key, K. B. Ling, R. Shyam Prasad, P. M. Roberts, H. Rodriguez-Solla, C. O'Leary-Steele, A. J. Russell, H. J. Sanganee, E. D. Savory, A. D. Smith and J. E. Thomson, *Tetrahedron*, 2008, **64**, 9320–9344.

[107] C. N. Barry and S. A. Evans, *Journal of Organic Chemistry*, 1983, **48**, 2825–2828.

[108] A. D. Worthy, X. Sun and K. L. Tan, *Journal of the American Chemical Society*, 2012, **134**, 7321–7324.

[109] M. D. Meyer, J. J. DeBernardis and A. A. Hancock, *Journal of Medicinal Chemistry*, 1994, **37**, 105–112.

[110] H. Hazimeh, J.-M. Mattalia, C. Marchi-Delapierre, F. Kanoufi, C. Combellas and M. Chanon, *European Journal of Organic Chemistry*, 2009, 2775–2787.

[111] D. F. Taber and C. G. Nelson, *Journal of Organic Chemistry*, 2006, **71**, 8973–8974.

[112] E. D. D. Calder, F. I. McGonagle, A. H. Harkiss, G. A. McGonagle and A. Sutherland, *Journal of Organic Chemistry*, 2014, **79**, 7633–7648.

[113] M. Amatore, C. Gosmini and J. Périchon, *Journal of Organic Chemistry*, 2006, **71**, 6130–6134.

[114] J. M. Wurst, G. Liu and D. S. Tan, *Journal of the American Chemical Society*, 2011, **133**, 7916–7925.

[115] M. P. Collins, M. G. B. Drew, J. Mann and H. Finch, *Journal of the Chemical Society, Perkin Transactions 1*, 1992, 3211–3217.

[116] J. Idris Jones and T. Campbell James, *Journal of the Chemical Society*, 1935, 1600–1604.

[117] D. Fattori, C. Rossi, C. I. Fincham, M. Berettoni, F. Calvani, F. Catrambone, P. Felicetti, M. Gensini, R. Terracciano, M. Altamura, A. Bressan, S. Giuliani, C. A. Maggi, S. Meini, C. Valenti and L. Quartara, *Journal of Medicinal Chemistry*, 2006, **49**, 3602–3613.

[118] T. Chuprajob, C. Changtam, R. Chokchaisiri, W. Chunglok, N. Sornkaew and A. Suksamrarn, *Bioorganic and Medicinal Chemistry Letters*, 2014, **24**, 2839–2844.

[119] A. T. Russo, K. L. Amezcua, V. A. Huynh, Z. M. Rousslang and D. B. Cordes, *Tetrahedron Letters*, 2011, **52**, 6823–6826.

[120] P. Bovonsombat, R. Ali, C. Khan, J. Leykajarakul, K. Pla-on, S. Aphimanchindakul, N. Pungcharoenpong, N. Timsuea, A. Arunrat and N. Punpongjareorn, *Tetrahedron*, 2010, **66**, 6928–6935.

[121] M. Ramrez Osuna, G. Aguirre, R. Somanathan and E. Molins, *Tetrahedron: Asymmetry*, 2002, **13**, 2261–2266.

Part II

Continuous Flow Synthesis of Coumalic Acid and Derivatives

Chapter 10

Literature Review

10.1 Introduction

Coumalic acid is a valuable platform compound which can be prepared from malic acid, a biorenewable feedstock derived from glucose. Current batch procedures to synthesise this compound have several drawbacks, which we address here with two flow syntheses and a new type of heated rotating flow reactor. Coumalate derivatives can be used in inverse electron demand Diels-Alder reactions to synthesise compounds with applications in molecular electronics, with the added advantage of a metal-free preparation.

10.2 Green chemistry

Green chemistry can be defined by 'a set of principles that reduce or eliminate the use or generation of hazardous substances in the design, manufacture and application of chemical products'.[1]

The 12 principles of green chemistry are summarised below:

1. Prevent waste
2. Atom economy
3. Less hazardous synthesis
4. Design benign chemicals
5. Benign solvents and auxiliaries
6. Design for energy efficiency
7. Use of renewable feedstocks

8. Reduce derivatives
9. Catalysis (vs. stoichiometric)
10. Design for degradation
11. Real-time analysis for pollution prevention
12. Inherently benign chemistry for accident prevention

This project had a particular focus on Principle 7: the use of renewable feedstocks. The environmental and health impacts of a process and the efficacy of the synthetic pathway must be considered when switching to an alternate feedstock or starting material. Petroleum has historically been the most important source of chemicals, but tends to require polluting oxidation steps to transform the hydrocarbons into useful starting materials. An alternative source is agricultural and biological feedstocks. These species tend to already be highly oxygenated.

When evaluating feedstocks and starting materials, one must consider their origin, for example, mining, refinery, synthesis, distillation, etc. and whether the resource is renewable or depleting. The downstream implications of the choice of feedstock must also be taken into account.

10.3 Biomass as a source of useful compounds

Biomass can be used as a source of energy (e.g. biofuels), but the more valuable components can be used to make fine chemicals with greater added value, leading to useful chemical building blocks.[2] Biomass includes terpenes, carbohydrates, proteins and triglycerides. Biomass carbohydrates are the most abundant renewable resources available, and contain lignin, cellulose and hemicellulose.[3] There are two types of sugars present in biomass: hexoses and pentoses. The two main methods for transforming sugars into bioproducts are fermentation and chemical processes. The conversion of biomass to commodity chemicals can proceed *via* complete deoxygenation to petroleum hydrocarbons or direct conversion to oxygenates as platform chemicals. The products of enzymatic glucose fermentation include lactic acid, succinic acid, 3-hydroxypropionic acid, itaconic acid, glutamic acid and malic acid.

10.4 Malic acid as a platform molecule

In 2004, the U.S. Department of Energy published a report on 'The Top Ten Value Added Chemicals from Biomass'.[4] This list included malic acid as a 1,4-diacid

building block derived from sugar, along with succinic and fumaric acids. The pathway to these building blocks from sugars is fermentation to over-produce C4 diacids from the Krebs cycle. Technical barriers to overcome include improving the microbial biocatalyst to reduce acetic acid co-products and increase yield and productivities, lowering the costs of the recovery process to reduce unwanted diols and scale-up and system integration issues. The report identified three groups of useful derivatisations, which will be described below.

1. Reductions to THF, butanediol and γ-butyrolactone families. The potential uses of these derivatives include solvents and fibres such as Lycra®.

2. Reductive aminations to the pyrrolidinone family *via* γ-butyrolactone. The potential uses of these derivatives include green solvents and water-soluble polymers, with applications in water treatment.

3. Direct polymerisation to straight- and branched-chain polymers. The potential uses of these derivatives include fibres such as Lycra®, among others.

Other uses of malic acid as a platform compound include the production of substituted THF derivatives, as well as the synthesis of 3-hydroxybutyrolactone. One possible route would proceed *via* cyclic reduction to malic acid to hydroxysuccinic anhydride, followed by reduction to 3-hydroxybutyrolactone.

10.5 Methyl coumalate as a valuable intermediate

Methyl coumalate is a doubly functional α,β-unsaturated compound. It has been extensively used in Diels-Alder reactions,[5–12] but also in pyridine synthesis and photochemical reactions.[13,14] Its utility in Diels-Alder reactions encompass both normal and inverse electron demand as well as hetero-Diels-Alder reactions. Additionally, it has been used in the total synthesis of natural products.[11–14] A literature survey of these reactions will be summarised below.

Coumalic acid is a common precursor to methyl coumalate, and several synthetic procedures have been used to synthesise this compound from aliphatic starting materials.

The earliest procedure for the synthesis of coumalic acid was published by von Pechmann in 1891 and started from malic acid.[15] A mixture of concentrated sulfuric acid (97-98%) and fuming sulfuric acid were used at 70 °C to effect conversion to coumalic acid. No isolated yield is given for this procedure.

In 1963, Wiley *et al.* performed this reaction on a 100 g scale, using the von Pechmann conditions allowing isolation of the product in 65-70% yield (Scheme 10.1).[16]

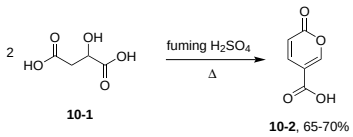

Scheme 10.1 Synthesis of coumalic acid from malic acid.

More recently, the mechanism of this reaction was investigated by Ashworth *et al.* in 2003.[17] They found it proceeded *via* an acid-catalysed dehydration/ decarbonylation of malic acid to give an aldehyde acid enol which condenses by Michael addition of the enol to the enone, followed by lactonisation and dehydration to give coumalic acid (Scheme 10.2). The major gaseous by-product was not CO_2, but instead was CO.

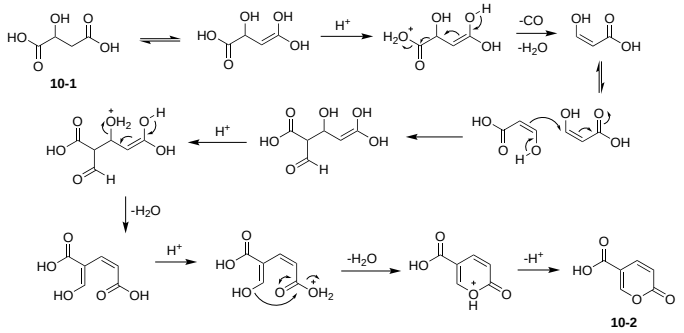

Scheme 10.2 Mechanism of the synthesis of coumalic acid from malic acid.

Kaminski and Kirch used a more concentrated solution of sulfuric acid with malic acid in 2008 (Scheme 10.3).[18]

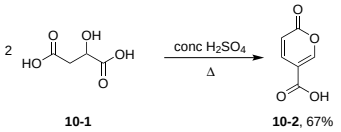

Scheme 10.3 Synthesis of coumalic acid from malic acid.

Since then, Kraus *et al.* have investigated various different reaction conditions to synthesise coumalic acid from malic acid.[19] They have varied the acid, reaction temperature, solvent and additive, and found that the relative amounts of malic and fumaric acid produced depends very specifically on the reaction conditions. Fumaric acid was a by-product observed in varying amounts; the most successful conditions are shown below (Scheme 10.4). The ratio of products shown is an NMR yield.

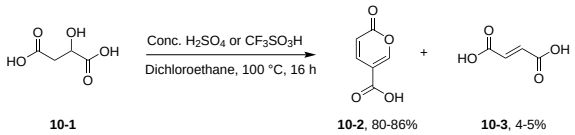

Scheme 10.4 Synthesis of coumalic acid from malic acid.

Synthesis of methyl coumalate

The two main synthetic routes to methyl coumalate proceed from either aliphatic starting materials, or more commonly, coumalic acid.

Kraus *et al.* synthesised methyl coumalate from methyl 3-oxo-propionate.[19] They had success with either concentrated H_2SO_4 or trifluoromethanesulfonic acid (Scheme 10.5).

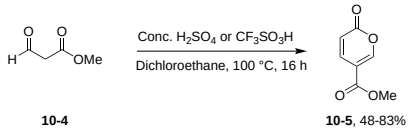

Scheme 10.5 Synthesis of methyl coumalate from methyl 3-oxo-propionate.

A related synthesis is that of ethyl coumalate. Starting from ethyl 3,3-diethylpropionate Maeda *et al.* were able to synthesise ethyl coumalate and screened a variety of Lewis acids.[59] The most successful was $FeCl_3 \cdot 6\,H_2O$ (Scheme 10.6). Interestingly, they observed triethyl 1,3,5-benzenetricarboxylate as a side-product in some of these reactions.

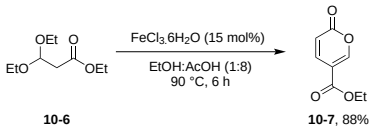

Scheme 10.6 Synthesis of ethyl coumalate from ethyl 3,3-diethoxypropionate.

Coumalic acid can be methylated by esterification to give methyl coumalate, and several groups have performed this transformation.

The first was Boyer *et al.* in 1956.[20] They used MeOH in concentrated H_2SO_4 and reported a 32-45% yield of methyl coumalate (Scheme 10.7).

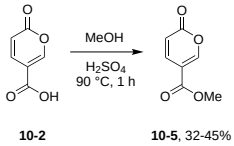

Scheme 10.7 Synthesis of methyl coumalate from coumalic acid.

Ashworth *et al.* experienced difficulties with this procedure, and instead attempted acid chloride formation followed by reaction with MeOH, as well as mixed anhydride formation followed by reaction with MeOH. However, once formed, methyl coumalate decomposition was observed (Scheme 10.8).

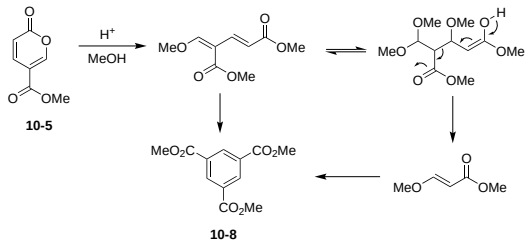

Scheme 10.8 Transformation of methyl coumalate to trimethyl 1,3,5-benzenetricarboxylate.

A milder esterification procedure gave them methyl coumalate in good yield, by first deprotonating coumalic acid using the non-nucleophilic *N,N*-diisopropylethylamine and then reacting the coumalate anion formed with dimethyl sulfate (Scheme 10.9).

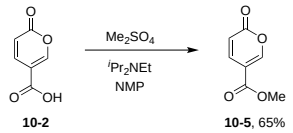

Scheme 10.9 Synthesis of methyl coumalate from coumalic acid.

Methyl coumalate in Diels-Alder reactions

The [4+2] cycloaddition known as the Diels-Alder reaction is a powerful tool in synthetic chemistry and natural product synthesis.[21] It requires a diene and dienophile component. Methyl coumalate can be described as an electron-poor diene because it contains two α,β-unsaturated ester units (Fig. 10.1).

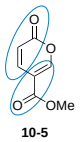

Fig. 10.1 The α,β-unsaturated esters in methyl coumalate.

This is a reversal of the normal electronic demand. With a suitable dienophile partner (typically electron-rich), inverse electronic demand Diels-Alder reactions are possible. In frontier molecular orbital theory, electron-withdrawing groups (EWG) on dienes and dienophiles lower the energies of both the highest-occupied

molecular orbital (HOMO) and lowest-unoccupied molecular orbital (LUMO). Electron-donating groups (EDG) raise the energies of both the HOMO and LUMO. For a better orbital overlap, the energy gap between the HOMO and LUMO must be minimised. In normal electronic demand reactions, it is the HOMO of the diene and the LUMO of the dienophile that react together. To decrease the size of the HOMO-LUMO gap, there should be an EDG on the diene and an EWG on the dienophile. It is the reverse for the inverse electronic demand reaction, which requires the LUMO of the diene and the HOMO of the dienophile to react. Therefore an EWG on the diene and an EDG on the dienophile will decrease the size of the HOMO-LUMO gap (Fig. 10.2).

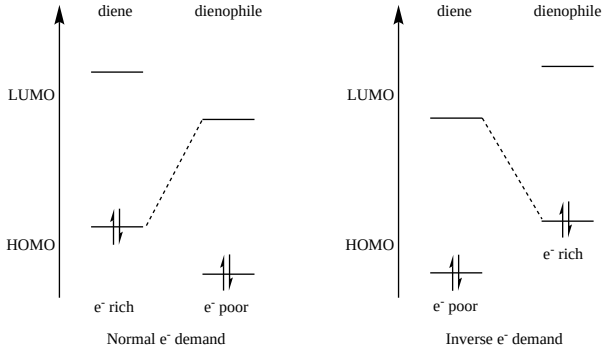

Fig. 10.2 Frontier molecular orbital theory in normal and inverse electron demand Diels-Alder reactions.

Thus the most favourable inverse electron demand Diels-Alder reactions with methyl coumalate will have an electron-donating group(s) such as alkoxy groups and amines on the dienophile.

Several research groups have used methyl coumalate as the diene in Diels-Alder reactions, with a variety of dienophile partners.

The Harrity group has used a variety of alkynylboronates in a series of papers over the last ten years (Scheme 10.10).[22–24]

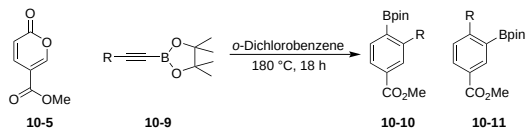

Scheme 10.10 Diels-Alder reactions of methyl coumalate with alkynyl boronates. The ratio of products depends on the nature of the R-group.

They found that cycloaddition was more efficient for 2-pyrones if they had an EWG at the 5-position rather than the 4-position. Aromatic boronic esters are valuable intermediates in organic synthesis due to their stability and versatility.

Methyl coumalate has been used in Diels-Alder reactions by the Kraus group, using a wider range of dienophiles. The procedure is a one-pot Diels-Alder/ decar-

boxylation/ aromatisation sequence. Products formed include dimethyl terephthalate and terephthalic acid, a polymerisation co-polymer.[25,26] A range of ketals, orthoesters and vinyl ethers were used as electron-rich olefinic dienophiles to give substituted benzoate products (for example, Scheme 10.11).[27]

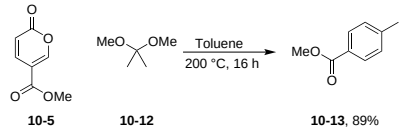

Scheme 10.11 Diels-Alder reaction of methyl coumalate with 2,2-dimethoxypropane.

The procedure is regioselective and high-yielding.

A Diels-Alder reaction with methyl coumalate has been used by the Snyder group as the first step in the synthesis of (+)-scholarisine A. The target compound is a polycylic alkaloid which is isolated from the traditional Chinese medicinal plant *Alstonia scholaris* (Scheme 10.12).[28]

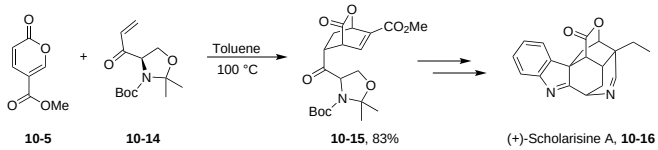

Scheme 10.12 Diels-Alder reaction of methyl coumalate used in the synthesis of (+)-scholarisine A.

They acknowledge that this cycloaddition would appear to be unfavourable on paper, due to the presence of electron-withdrawing groups on both components, but that it proceeds with efficiency. Two minor components were found: one was a separable diastereomer of the product, and the other was unknown.

Epidithiodiketopiperazines are metabolites with a range of biological activities including antiviral, antibacterial, antiallergic, antimalarial and cytotoxic properties.[29] A diastereoselective inverse electron demand Diels-Alder reaction has been used to form a hydroindole precursor of these natural products (Scheme 10.13).

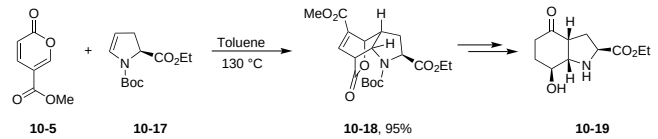

Scheme 10.13 Diels-Alder reaction of methyl coumalate used in the synthesis of a precursor to epidithiodiketopiperazines.

The electron-rich dienophile allowed the reaction to proceed in excellent yields with a good level of diastereoselectivity over 10:1.

Methyl coumalate in photochemical reactions

The Baran group has used a photochemical reaction of methyl coumalate to synthesise some members of the piperarborenine family. These compounds were isolated from *Piper arborescens*, and have shown *in vitro* toxicity against several cancer cell lines. They share an unsymmetrical cyclobutane core with pendant groups that have different side chains and stereochemistry, thus presenting a challenging target. Compounds synthesised so far include piperarborenines B,[30] D (proposed structure[30]) and pipercyclobutanamide A (proposed structure[31]). These syntheses share a common photochemical first step, and the amine in the subsequent amide formation is varied. The example shown below is the synthesis of piperarborenine B (Scheme 10.14).

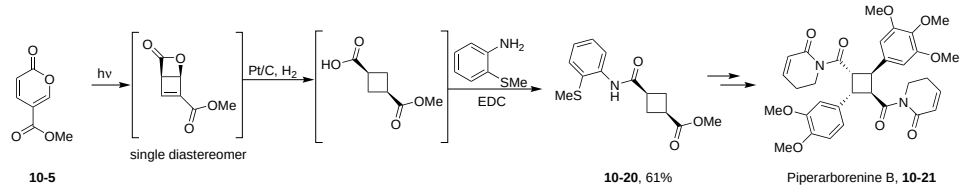

Scheme 10.14 Photochemical reaction of methyl coumalate as used in the synthesis of several piperarborenines, including piperarborenine B.

10.6 Diels-Alder derivatives and molecular electronics

Molecular electronics is a branch of nanotechnology that uses single molecules as components in electronic circuits, and numerous reviews have been written on the subject.[32] These molecular materials include conductive polymers and molecular salts. One important family of molecules with wide ranging applications as molecular electronic components including in the area of organic light-emitting diodes (OLEDs) are the terphenyls.[33]

A critical consideration in the syntheses of such molecules is their purity, as even low levels of contamination (ppb) can have a significant impact on their properties. This is particularly true of residual heavy metal contamination. However, traditional syntheses of such compounds inevitably rely on reactions such as nickel or palladium-catalysed coupling reactions.[32] An alternative metal free approach would be *via* the inverse electron demand Diels-Alder reaction, with coumalic acid derivatives as the electron-poor diene, partnered with a suitable electron-rich dienophile.[5–14]

10.7 Heteropoly acids

Heteropoly acids (HPA) are a class of acids containing acidic hydrogen atoms, oxygen, and specific metals M (e.g. W, Mo, V) and p-block non-metals X (e.g. Si, P, As). They are strong Brønsted acid catalysts and oxidants, and have been used in a variety of homogeneous and heterogeneous reactions.

The Keggin structure makes up the majority of heteropoly acids, with the general formula $H_nXM_{12}O_{40}$, and so will be discussed in more detail here. The Dawson structure applies to compounds with the general formula $H_nX_2M_{18}O_{62}$ and is much rarer.

The Keggin structure has tetrahedral symmetry by X-ray crystallography, and comprises a central XO_4 tetrahedron surrounded by 12 MO_6 octahedra.[34] These octahedra share edges and corners, and are arranged in four groups of MO_{13}. The Keggin structure is retained in a concentrated solution, but in other cases, the structure depends on pH, the solvent, the composition of the HPA and its concentration.

The crystal structure of an HPA depends on the quantity of waters of crystallisation, and many hydrates are possible. The strength of the acid increases on dehydration.

There are three potential protonation sites, as there are three types of outer oxygen atoms. These are the terminal oxygens of the M=O bonds, and the edge- and corner-sharing bridging oxygen atoms of the M-O-M bonds.

The acid strength of an HPA depends on its composition: tungsten-containing acids are stronger than molybdenum-containing acids, for example. Dissociation constants and Hammett acidity functions have been investigated for HPAs in solution. They are highly soluble in polar solvents such as water and methanol, but are insoluble in non-polar solvents such as hexane. HPAs are strong, fully dissociated acids in aqueous solution. Equimolar solutions of H_2SO_4 are less strong than HPAs: for example, the pK values of $H_3PW_{12}O_{40}$ are $pK_1 = 1.6$, $pK_2 = 3.0$ and $pK_3 = 4.0$ whilst for H_2SO_4 they are $pK_1 = 6.6$.

Homogeneous catalysis performed with HPAs has several advantages over conventional mineral acids. HPAs are stronger acids, leading to higher catalytic activity and thus requiring lower catalyst loading or temperatures. They avoid side-reactions that can occur with mineral acids, such as sulfonation (H_2SO_4), chlorination (HCl) and nitration (HNO_3). They are less toxic, crystalline solids and so are safer and easier to handle. However, the challenge of catalyst recovery and recycling is a serious issue.

Reactions that have used HPAs as homogeneous catalysts include olefin hydration (Scheme 10.15),[35] esterification and condensation (Scheme 10.16).[36]

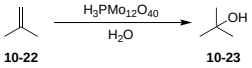

Scheme 10.15 One-step industrial hydration of isobutene to synthesise *t*-butyl alcohol, catalysed by $H_3PW_{12}O_{40}$.

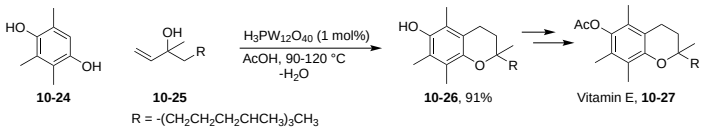

Scheme 10.16 Synthesis of vitamin E by the HPA-catalysed condensation of isophytol with 2,3,5-trimethylhydroquinone.

Biphasic reactions with two immiscible liquid phases have also been used, for example in the polymerisation of THF,[37,38] and in esterification (Scheme 10.17).[39]

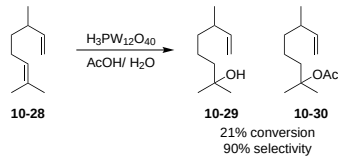

Scheme 10.17 Biphasic hydration and acetoxylation of dihydromyrcene catalysed by $H_3PW_{12}O_{40}$.

Heterogeneous catalysis avoids the major problem in homogeneous catalysis, which is the separation of catalyst and product at the end of a reaction. However, a new problem arises: the coking (formation of carbonaceous deposits) on the surface of the catalyst, which leads to deactivation.

Reactions that have used HPAs as heterogeneous catalysts include alkylation of paraffins, Friedel-Crafts reactions (Scheme 10.18),[40] esterification[41] and hydrolysis.

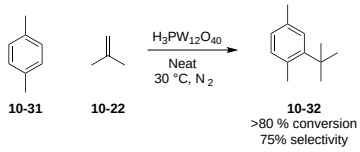

Scheme 10.18 Heterogeneous Friedel-Crafts reaction of *p*-xylene with 2-methylpropene, catalysed by solid $H_3PW_{12}O_{40}$.

HPAs have been immobilised on a variety of materials, including silica, mesoporous molecular sieves, and carbon, among others.[42]

10.8 Polyoxometalates

The conjugate anion of a heteropoly acid is known as a polyoxometalate (POM). In liquid phase oxidation, a variety of metal-substituted heteropoly anions are found. These include the Keggin-type vanadium-doped series of HPAs with the general formula $PMo_{12}V_nO_{40}{}^{(3+n)-}$, where n = 2 to 6 (HPA-n). These are reversibly-acting oxidants which require only mild conditions, and have a stepwise redox mechanism. A series of pH-dependent equilibria determine their state in solution which are largely unknown, and so their mechanisms of action are not well-understood.

The HPA-n series of anions is the most efficient and versatile POM for oxidation using O_2. The catalytic activity of POMs is solvent-dependent. Homogeneous oxidation can be performed using a one-component HPA-n system. Examples include oxidation of hydrocarbons, of aldehyes to carboxylic acids, of alkylphenols, of sulfur compounds, of 2-methylnaphthalene to quinone and in the presence of an aldehyde to effect epoxidation of olefins.[43–47] Others are the dehydrogenation of α-terpinene to p-cymene, oxidative bromination of aromatics, and Baeyer-Villiger oxidation of cyclic ketones to lactones.[48,49]

Two-component HPA-n systems can be formed by the addition of other metals, for example Pd^{II}. This system has had success in the oxidation of olefins, alcohols, arenes, and other compounds. HPA-n acts as the co-catalyst, and O_2 as the oxidant. It can be considered as being analogous to Wacker-type oxidation with $CuCl_2/PdCl_2$. Biphasic oxidation is possible, and avoids the difficult separation with homogeneous systems.

There is limited information about the mechanism of redox reactions catalysed by HPA-n. Solutions of HPA-n increase in structural complexity as n increases. ^{31}P NMR spectroscopy illustrates this, and the large number of observed peaks correspond to the great number of polyanionic species present in solution, as well as their positional isomers.[42]

Oxidation has also been performed with hydrogen peroxide as the oxidant rather than O_2, in particular by the groups of Venturello[50] and Ishii.[51–58]

Chapter 11

Project Aims

The batch synthesis of coumalic acid was first verified, before beginning efforts to transfer the reaction into flow. Factors affecting the reaction were investigated systematically to determine critical parameters for development of the most appropriate flow process. A large-scale flow process would be highly beneficial in making coumalic acid and derivatives more accessible.

Methylation and other esterifications of coumalic acid were also investigated in batch and then flow. The coumalate derivatives prepared were used in Diels-Alder reactions to give terphenyls with applications in molecular electronics.

Chapter 12

Batch Syntheses of Coumalic Acid and Derivatives

12.1 Preliminary batch experiments

Before moving the reaction into a flow format, the reaction was first investigated in batch. There were several literature procedures to test, which will be described below.

Following a literature procedure by Kaminski *et al.*, the first attempt at synthesising coumalic acid in batch was on a large scale, using 200 g of malic acid (Scheme 12.1).[18]

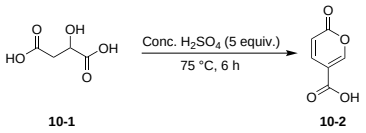

10-1 10-2

Scheme 12.1 Synthesis of coumalic acid from malic acid.

The reaction was heated for 6 h, and significant foaming of the mixture was observed. After quenching with ice and stirring overnight, the solid isolated after filtration was a pale brown wet paste. After air-drying, purification by recrystallisation from MeOH in the presence of activated carbon was attempted, but only gave a recovery of 22%.

Kraus *et al.* claim in a patent that the reaction of malic acid with concentrated sulfuric acid or triflic acid in DCE generates an 80-86% yield of coumalic acid, and observe 4- 5% of fumaric acid side-product formation (Scheme 12.2).[19]

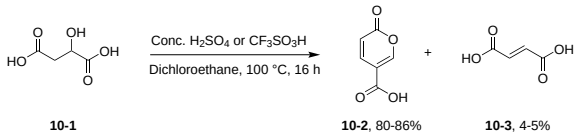

Scheme 12.2 Synthesis of coumalic acid from malic acid.

The reaction with sulfuric acid gave a lower yield of coumalic acid, and a higher composition of fumaric acid in the crude reaction mixture (Scheme 12.3).

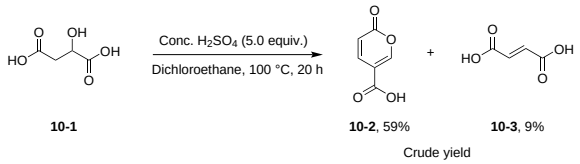

Scheme 12.3 Synthesis of coumalic acid from malic acid.

The reaction with triflic acid gave coumalic acid in good yield but poor quality (Scheme 12.4).

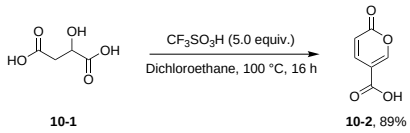

Scheme 12.4 Synthesis of coumalic acid from malic acid.

In this latter reaction, no fumaric acid was observed by ^{1}H NMR spectroscopy.

A one-pot, one step batch synthesis of methyl coumalate gave the ester product in low yield (Scheme 12.5).

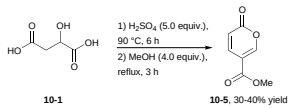

Scheme 12.5 Synthesis of methyl coumalate from malic acid in a one-pot process.

A one-pot, two step synthesis of methyl coumalate from malic acid was performed (Scheme 12.6).[12]

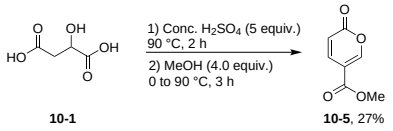

Scheme 12.6 Synthesis of methyl coumalate from malic acid in a one-pot process.

The total isolated yield of methyl coumalate after recrystallisation from EtOAc was 27%.

Methyl coumalate was synthesised from methyl-3,3-dimethoxypropionate using sulfuric acid (Scheme 12.7).

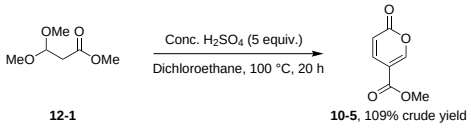

12-1 **10-5**, 109% crude yield

Scheme 12.7 Synthesis of methyl coumalate from methyl-3,3-dimethoxypropionate.

Significant impurities were observed in the ^{1}H NMR spectrum, and the mixture was not purified.

Methyl coumalate was also synthesised from methyl-3,3-dimethoxypropionate using triflic acid (Scheme 12.8).

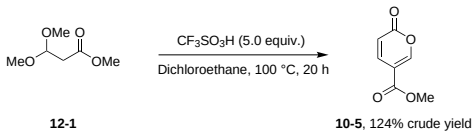

12-1 **10-5**, 124% crude yield

Scheme 12.8 Synthesis of methyl coumalate from methyl-3,3-dimethoxypropionate.

Analysis by ^{1}H NMR spectroscopy revealed the presence of significant levels of impurities, and the mixture was not purified.

Hydrates of iron trichloride were used in the synthesis of methyl coumalate, working from a literature procedure (Scheme 12.9).[59]

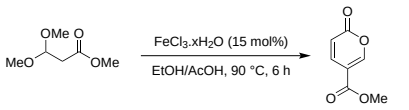

12-1 **10-5**
When x = 0; 14%
x = 6; 47%

Scheme 12.9 Synthesis of methyl coumalate from methyl-3,3-dimethoxypropionate.

Methyl coumalate was isolated in low yield after purification by column chromatography. To try and improve the yield, anhydrous iron trichloride was used instead. In this case, a low yield of white crystalline methyl coumalate was isolated after purification by column chromatography. Finally, the hexahydrate of iron trichloride gave white crystalline methyl coumalate in a moderate yield.

An alternative to these acid catalysts is a class of compounds known as heteropoly acids. A vanadium-doped molybdenum-based heteropoly acid was considered as an acid catalyst in the synthesis of methyl coumalate. First, the

heteropoly acid [$H_5PMo_{10}V_2O_{40} \cdot xH_2O$] (HPMoV) was synthesised according to a literature procedure (Scheme 12.10).[60]

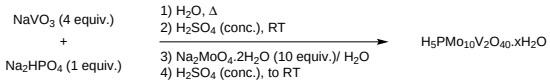

Scheme 12.10 Synthesis of the heteropoly acid HPMoV.

Confirmation of the product was made by comparison with literature data, including ^{31}P NMR spectroscopy and IR spectroscopy. The solid was dehydrated by heating under vacuum to give the acid as an orange-green powder.

The dehydrated acid was subsequently tested in experiments with methyl-3,3-dimethoxypropionate (MDMP) in DCE (Scheme 12.11).

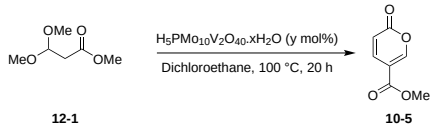

Scheme 12.11 Reaction of MDMP with heteropoly acid.

The mol % catalyst loading was increased from 1% where no methyl coumalate was observed, through 10 mol% to 20 mol% which gave methyl coumalate in low yield (<20%) after purification by column chromatography.

The same heteropoly acid reaction was attempted with malic acid (Scheme 12.12).

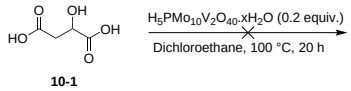

Scheme 12.12 Reaction of malic acid with heteropoly acid.

Only starting material was observed by ^1H NMR spectroscopy.

12.2 Conclusions on batch reactions

Malic acid is the most promising starting material, even though it was possible to access methyl coumalate in only one step from methyl-3,3-dimethoxypropionate. Malic acid is a much cheaper and readily available feedstock.

The best choice of acid catalyst for the process is concentrated sulfuric acid. The homogeneous process should be possible to translate into flow.

The synthesis of methyl coumalate from coumalic acid could be telescoped so that a two-step, one-pot procedure is adapted into continuous flow.

Chapter 13

First Flow Synthesis of Coumalic Acid and Derivatives

13.1 Developing a flow synthesis of coumalic acid

Moving from batch to flow, there are several factors that need to be investigated before designing the experimental set-up.

As malic acid is not readily soluble in concentrated sulfuric acid at RT, several solubility experiments were performed at different temperatures. Malic acid (25 g) and conc. sulfuric acid (50 mL) were combined and stirred at 360 rpm, holding for 10 mins at each interval. The results are summarised below (Table 13.1).

Table 13.1 Solubility experiments of malic acid in conc. H_2SO_4 at different temperatures.

Entry	Internal temperature/ °C	Appearance
1	20	White solid and pale yellow liquid.
2	25	White slurry.
3	32	Pale yellow slurry, frothing.
4	38	Yellow solution, with substantial foaming which dissipates when stirring is stopped. No product formation is observed by ^{1}H NMR spectroscopy.

The higher temperatures approaching 40 °C were required to ensure dissolution of the solid malic acid. Therefore the stock solutions were prepared by stirring malic acid and conc. sulfuric acid at 40 °C for 10–30 mins, depending on scale.

An experiment was also performed to find the solubility limit of malic acid in conc. sulfuric acid at approx. 40 °C. As before, malic acid (25 g) was charged to conc. sulfuric acid (50 mL), and the mixture was heated to an external set temperature of 45 °C (internal temperature = 38 °C) and held for 10 mins, until all the solid had dissolved. Further portions of malic acid was added in 5 g increments. An additional 20 g of malic acid was below the solubility limit, whereas 25 g was above the limit. Thus the solubility limit of malic acid in conc. sulfuric acid lies between 45–50 g per L at 38 °C.

The Lambda Doser® powder feeder is a powder rotary dispenser for continuous addition of free-flowing solids (powders, powdery and crystalline substances). It requires calibration with each solid to determine which settings correspond to which addition rates. Malic acid is a free-flowing powdery white solid, and thus is suitable for continuous addition.

The results of the calibration dosing are summarised in two graphs below, one reporting speed *versus* time taken to dose 100 g of malic acid (Fig. 13.1), and the other for speed *versus* the average mass dose in 1 minute (Fig. 13.2). Both were useful when experimenting with connecting the powder doser in series with the flow machine.

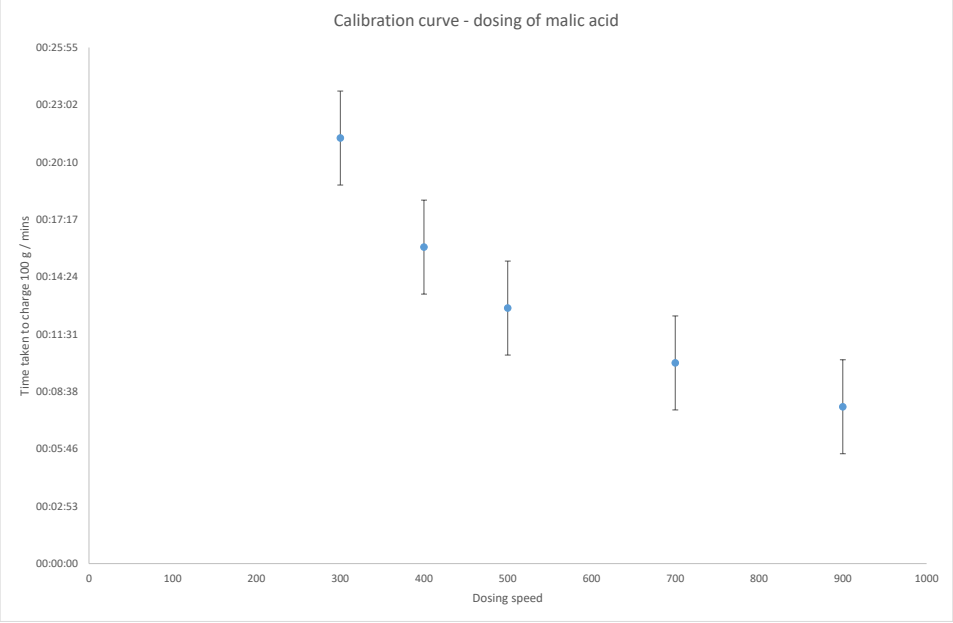

Fig. 13.1 Calibrating the powder doser with malic acid.

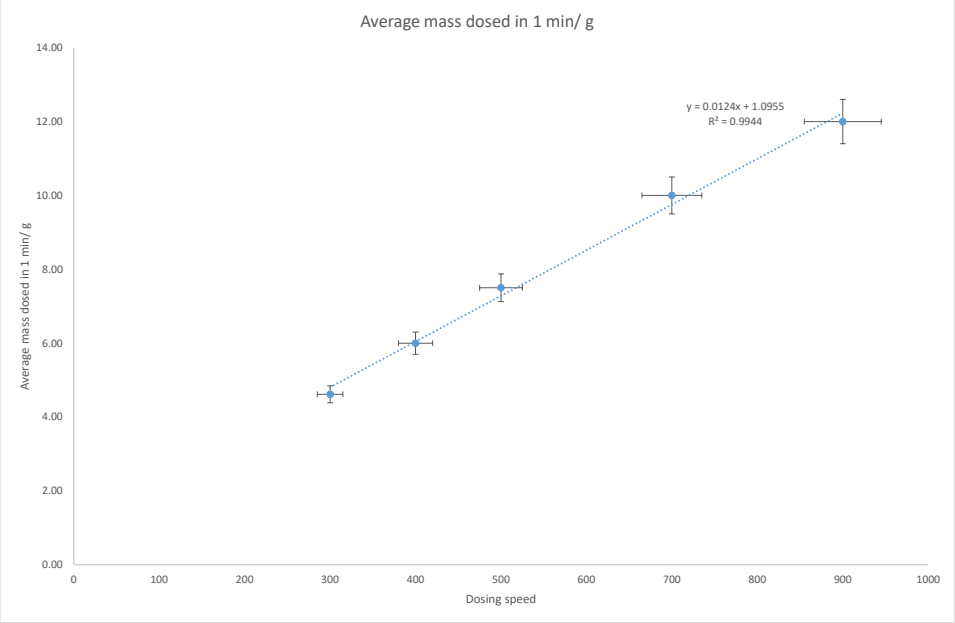

Fig. 13.2 Calibrating the powder doser speed with mass of malic acid.

Batches of malic acid in conc. sulfuric acid (100 g in 200 mL) were pre-prepared by stirring at 40 °C, and were sometimes allowed to cool to RT before use. Whether or not the stock solution was at RT or 40 °C when pumping did not seem to have a significant effect on the conversion but was not specifically investigated.

Initial scoping experiments were performed with a 10 mL heated FEP reactor coil, starting at the relatively low temperature of 40 °C and increasing to 90 °C whilst using the Polar Bear Plus® reactor. A colour change was observed which was indicative of the reaction progress. At higher temperatures, the solution turns a dark yellow/ orange. As the mixture progresses through the reactor, the solution can change colour from almost-colourless, to yellow through to dark orange and eventually dark brown. The dark brown colour is a sign of 'over-cooking' the reaction mixture at higher temperatures, and leads to a poorer quality product of darker colour which is isolated in lower yields from the crude mixture. It rapidly became apparent that the conversion was highly dependent on the temperature. This relationship can be seen in the graph below (Fig. 13.3).

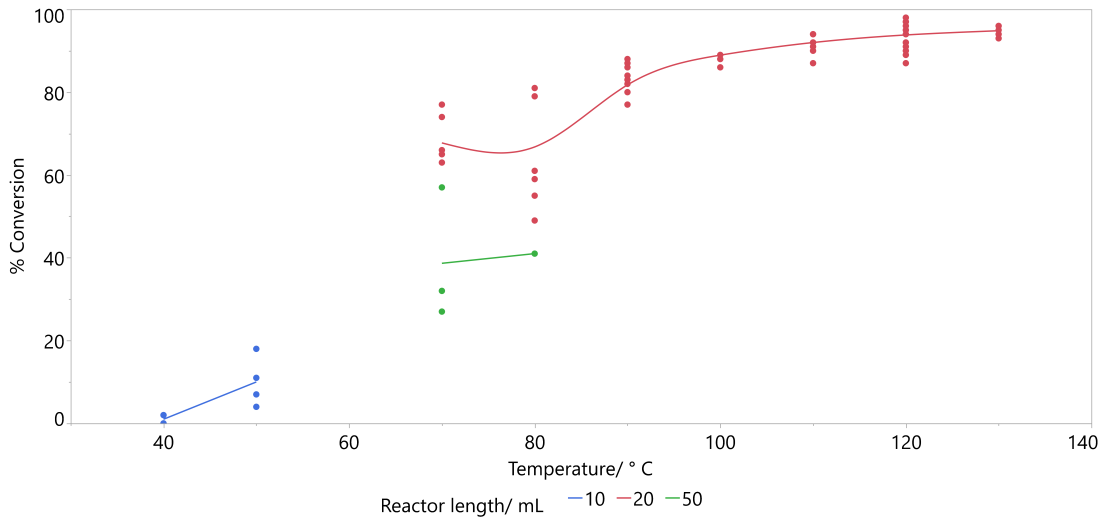

Fig. 13.3 Temperature *versus* conversion in the Vapourtec® system.

Regardless of reactor length, there is a positive correlation between temperature and conversion.

However, there is a trade-off to be made as temperatures above 120 °C lead to a substantially darker solution of product, and a much lower isolated yield. These higher temperatures 'over-cook' the sugar-derived reaction components. This means the temperature is effectively capped at 120 °C.

The initial 10 mL heated reactor coil was doubled by the addition of a second 10 mL reactor placed in series to increase the residence time. Conversions to coumalic acid began to increase from 19% to 71% with precipitation of coumalic acid observed, and so these coils were exchanged for a 50 mL Polar Bear Plus® reactor (Scheme 13.1).

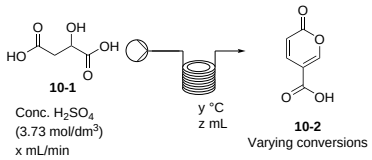

Scheme 13.1 Experiment 1: 10 mL; Experiment 2: 2 x 10 mL; Experiment 3: 50 mL

A graph of reactor size *versus* conversion is shown below (Fig. 13.4).

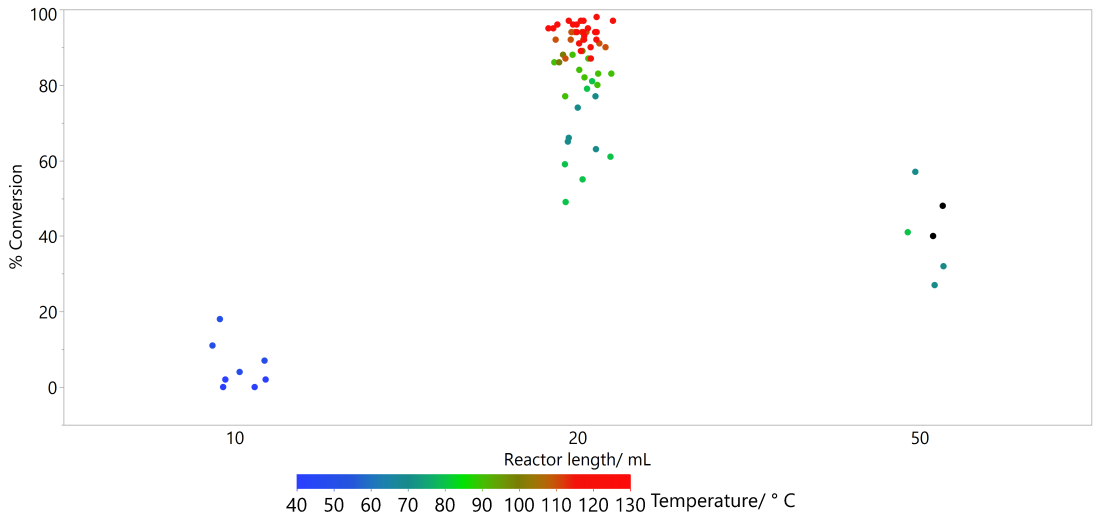

Fig. 13.4 Reactor length *versus* conversion, colour-coded by temperature. The x-axis is discrete: for example, all values clustered around the 10 mL reactor length were collected using a 10 mL reactor.

Both the shorter and longer reactors were essentially used with lower temperatures (shown by colour-coding), so it is possible that these may be capable of giving higher conversions than observed. There is a balance to be struck between the high desired conversions, and shorter residence times, which result in greater throughputs. Two 10 mL reactors presented a good compromise.

It should be noted that the nominal flow rate does not reflect the **actual** flow rate of malic acid in conc. H_2SO_4 due to the high viscosity of sulfuric acid. The viscosity of sulfuric acid depends on the temperature, and so the actual flow rate will also depend on the temperature used (Fig. 13.5).

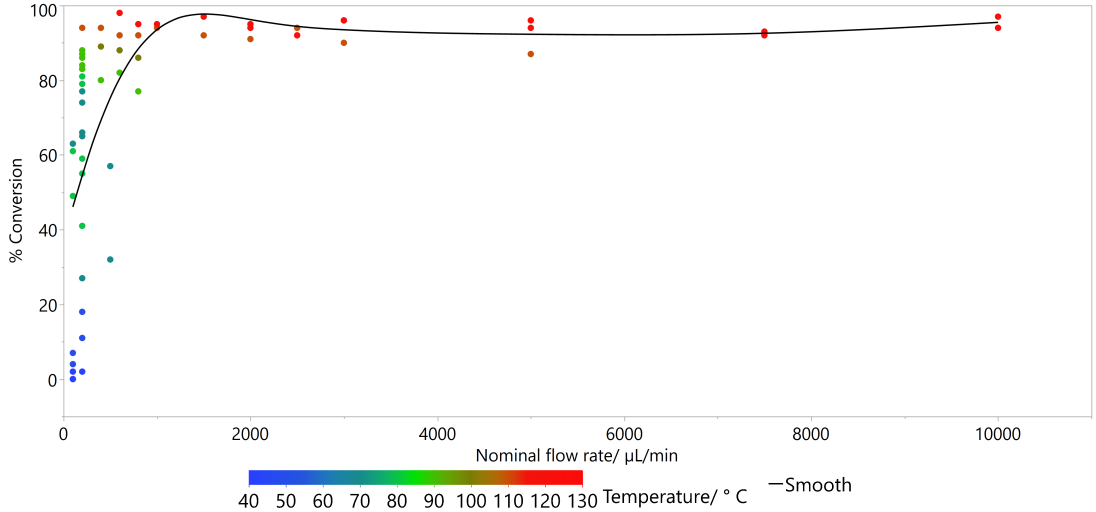

Fig. 13.5 Nominal flow rate *versus* concentration, colour-coded by temperature.

Faster flow rates are preferred since they generate greater throughput of material. The relationship between nominal (as specified by the Vapourtec® pump) and actual (based on the volume of material pumped through in a fixed time period) flow rates is not linear.

Gas production during the reaction leads to significant segmentation of the flow stream, with 'slugs' of material separated by gases proceeding through the reactor. The pressure was monitored and found to be around 4 bar, but was not controlled by the use of a back-pressure regulator, which is more common in a flow process (Fig. 13.6).

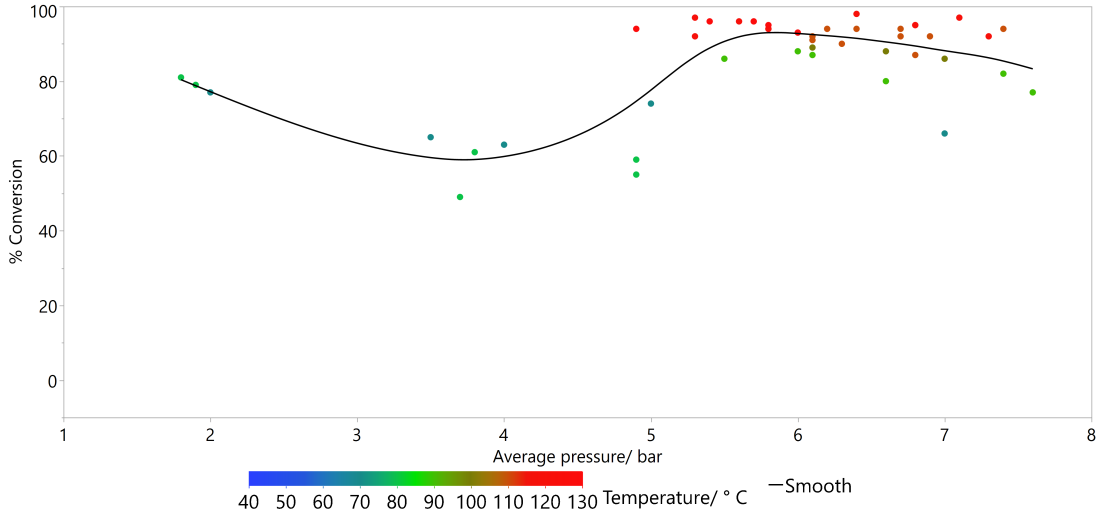

Fig. 13.6 Pressure *versus* concentration, colour-coded by temperature.

There is no obvious relationship between the observed pressure and conversion.

It would be desirable to be able to perform the reaction at higher concentrations, as this would allow a greater amount of material to be processed in a fixed time, giving the flow process a significant advantage over the equivalent batch reaction. Initial flow experiments indicate that the viscosity of the solution is greatly increased, and so only a 10 mL reactor coil is required (Scheme 13.2). A longer residence time results in an 'over-cooked' solution, even when operating at the maximum nominal flow rate ('10000' μL min^{-1}; actual flow rate: around 0.7 mL min^{-1}). A stock solution was prepared using 200 g of malic acid and 200 mL of conc. sulfuric acid. The pre-heating period required was longer, as the malic acid took 90 mins to dissolve in the sulfuric acid at 40 °C at this scale.

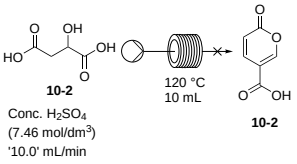

Scheme 13.2 Increasing the concentration of malic acid in conc. H_2SO_4.

The high temperature somewhat decreased the viscosity of the solution, but the residence time was greatly increased compared to the lower concentration reaction, at over 6 mins for the single 10 mL reactor. The actual flow rate was less than 0.1 mL min^{-1}, even though the peristaltic pumps were operating at their maximum nominal flow rate of 10.0 mL min^{-1}. The material was in fact so viscous and the residence time so extended that 'over-cooking' was observed to the point where it was not possible to isolate any coumalic acid from the crude solution. Pump failure occurred multiple times during one run.

The in-built peristaltic pumps of the Vapourtec® system are able to pump at a nominal maximum flow rate of 10.0 mL min^{-1}, but in reality this is significantly reduced for the highly viscous malic acid/ sulfuric acid solution. This places an inherent limitation on the throughput of the process. As an alternative, an external peristaltic Masterflex® L/S pump was connected to the heated coil reactors of the Vapourtec® system.

Two chemically-compatible tubing sizes were considered, the Masterflex® C-Flex tubing sizes 13 and 14, with internal diameters of 0.8 and 1.6 mm respectively. The internal diameter of the previously-used FEP tubing was approx. 0.5 mm.

The Masterflex® L/S pump speeds must be calibrated for the starting material, and so the first step was to perform the standardisation using water, sulfuric acid as a blank and the malic acid/ sulfuric acid solution (Fig. 13.7).

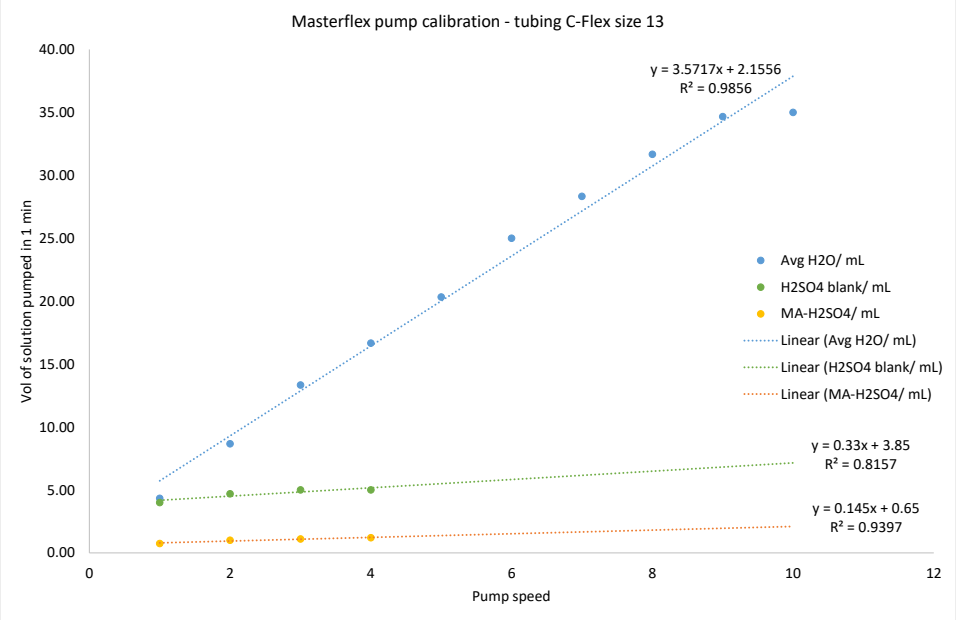

Fig. 13.7 Calibrating the Masterflex® peristaltic pump with size 13 tubing, with three different solutions.

The nominal pump speeds correspond linearly to actual flow rates for all three. Unsurprisingly, the pumping of water is much easier compared to the blank of sulfuric acid. There is an increase in viscosity on adding malic acid to sulfuric acid. The pump was unable to handle speeds above '4'. A similar experiment was performed with the size 14 tubing, but the tubing repeatedly failed and was deemed unsafe to use in this process.

The Masterflex® pump was connected in series to the heated coiled reactors, and three experiments were performed at each pump speed. The average flow rate for each pump speed was calculated, and is plotted on the graph below (Fig. 13.8).

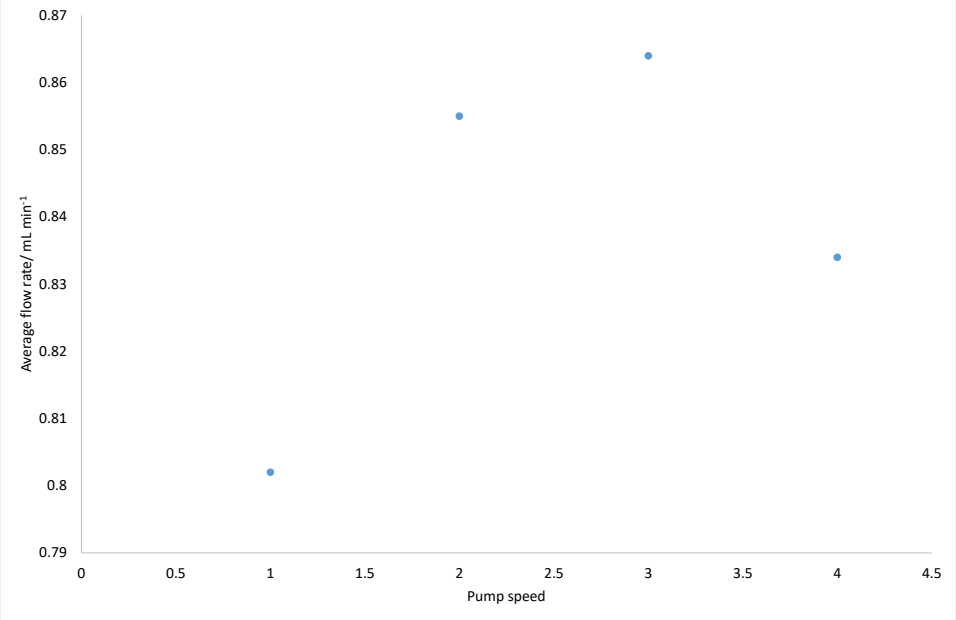

Fig. 13.8 Masterflex® pump speed *versus* actual flow rate.

A pump speed of '2' was used in future reactions, which gave a typical flow rate of around 0.8 mL min^{-1}.

13.2 Semi-optimised flow synthesis of coumalic acid

Two set-ups were semi-optimised to produce coumalic acid in flow. They differed in the peristaltic pumping systems used: either the in-built Vapourtec® pump, or an external Masterflex® pump. They were both used on larger scale syntheses, and the results are presented below.

Malic acid (25 g) was dissolved in sulfuric acid (50 mL), and processed at 120 °C and a nominal flow rate of '10' mL min^{-1} (actual flow rate = 0.71 mL min^{-1}) using the in-built Vapourtec® pump (Scheme 13.3).

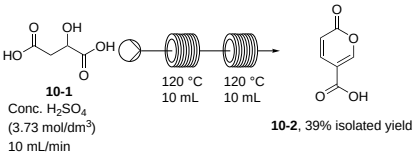

Scheme 13.3 Processing malic acid using the in-built Vapourtec® peristaltic pumps.

After 70 mins, the total volume collected was 50 mL, which was quenched with H_2O (200 mL) and allowed to cool and precipitate in the freezer overnight. After filtration and drying *in vacuo*, 5.1 g of crude coumalic acid (39% yield) was isolated. This gives a throughput of 4.4 g h^{-1}.

An attempt was made to use the powder doser (see above) to deliver the malic acid into a flask which was receiving sulfuric acid *via* a dropping funnel. The two would be mixed at 40 °C with the solution then pumped through the Vapourtec® flow reactor. Some difficulties were observed: significant foaming of the mixture made it very difficult to withdraw only solution, and not a gas/foam mixture. Matching the addition rates of the calibrated powder doser with the uncalibrated dropping funnel was not precise enough, meaning that the concentration of the solution was never known exactly. This method was abandoned in favour of pre-mixing the two reagents and allowing the foam to dissipate before reacting.

Changing to an external Masterflex® peristaltic pump enabled a higher pumping speed. A run using 50 mL of starting solution took 52 mins to process, giving 37 mL of product (a decrease of 13 mL from the starting volume) and an average flow rate of 0.712 mL min^{-1} (Scheme 13.4).

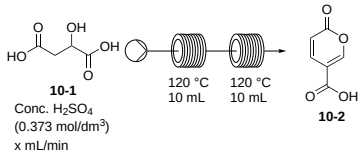

Scheme 13.4 Processing malic acid using the separate Masterflex® peristaltic pumping system.

13.3 Modelling the Vapourtec® process

The Vapourtec® flow process was modelled using the temperature, nominal flow rate and % conversion estimated by ^{1}H NMR spectroscopy in JMP.* A Design of Experiments approach was not used here, and instead the collected data was analysed after scoping and optimisation. Inputs such as temperature, nominal flow rate and % conversion were used to construct model effects, by looking at the effects of these factors, but also whether there are any interactions between these factors. A 'standard least squares, fit y by x' model was used, which creates a formula that includes these effects. The graphs shown below are leverage plots for each effect, which show the unique effect of a term in the model. The solid red line represents the unconstrained model with the term, and the horizontal blue line shows the constrained model without the term. The p-value is also shown on

*Software: JMP Pro 12.2

the x-axis, where if p <0.05, there is strong evidence that the factor affects the model. These details apply to all model analyses in the following chapter.

There was a strong positive correlation between temperature and % conversion (Fig. 13.9).

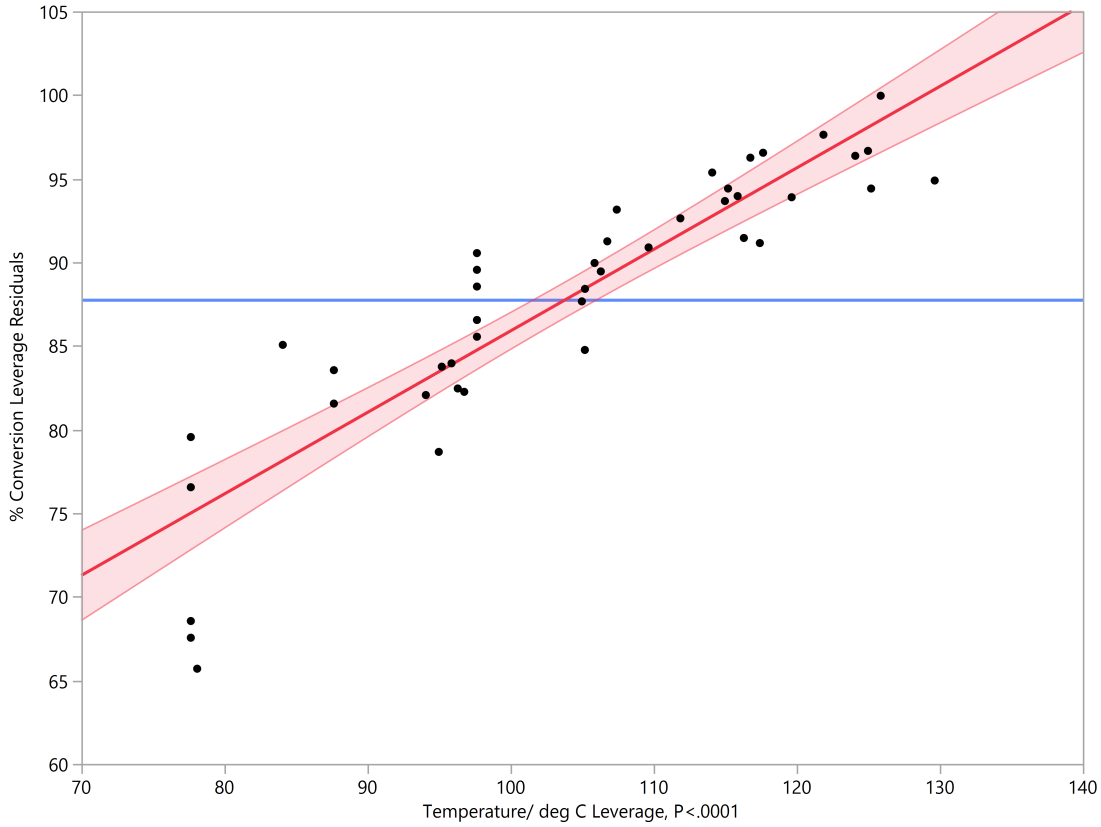

Fig. 13.9 Temperature *versus* conversion in the Vapourtec® model.

There was very little correlation between the nominal flow rate and the % conversion when using the in-built Vapourtec® peristaltic pumps (Fig. 13.10).

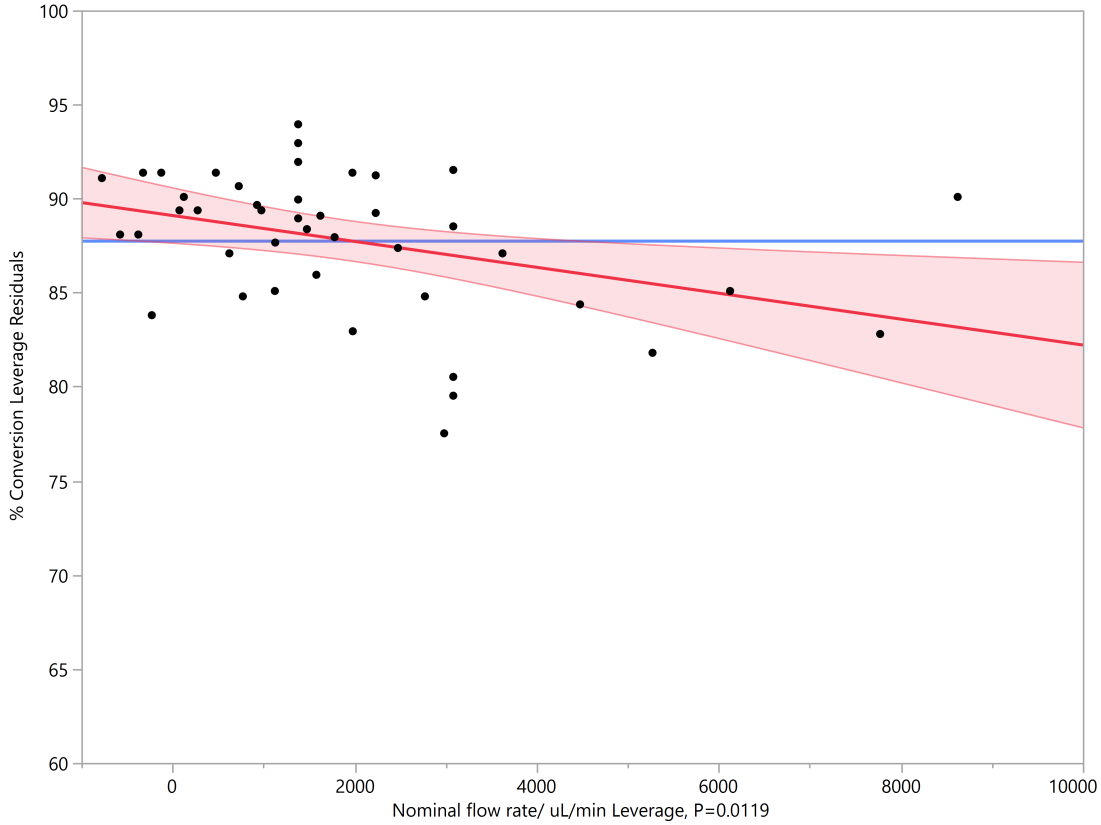

Fig. 13.10 Nominal flow rate *versus* conversion in the Vapourtec® model.

The accuracy of the model can be examined using the root-mean-square error and R^2 ('RMSE' and 'RSq' respectively on the x-axis). The RMSE is used as a measure of the differences between values predicted by a model and the values actually observed. RSq is a statistical measure of how close the data are to the fitted regression line on a scale of 0 to 1, where a value of 1 is the maximum and represents a perfect fit. The model was able to predict the conversion based on the temperature and nominal flow rate with fairly high accuracy (Fig. 13.11).

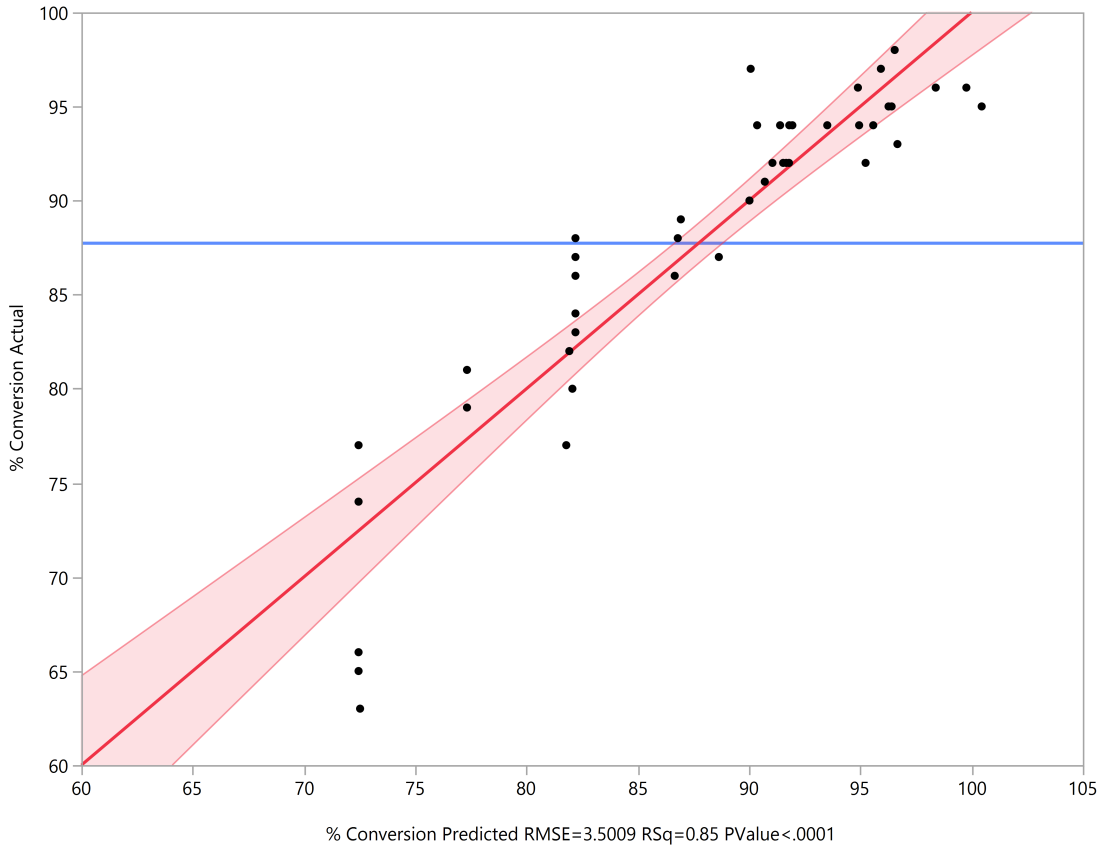

Fig. 13.11 Accuracy of the Vapourtec model predictions.

13.4 Developing a flow methylation of coumalic acid

With a successful small-scale flow procedure for the synthesis of coumalic acid, our attention turned to the second step in the synthesis of methyl coumalate: the methylation.

Once the crude product solution is mixed with methanol, the viscosity was expected to decrease. To test this hypothesis the nominal flow rate was calibrated against the actual flow rate, and the results are plotted in the graph below (Fig. 13.12).

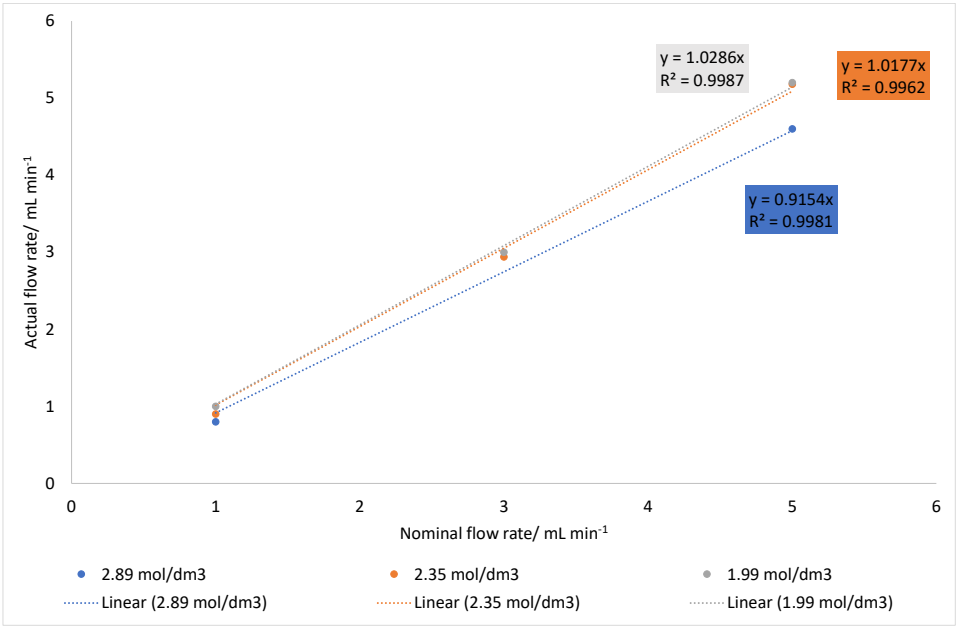

Fig. 13.12 Nominal *versus* actual flow rate for the three different concentrations.

As more methanol was added and the product solutions became more dilute, the actual flow rates became more similar to the nominal flow rates. The gradients for all three concentrations are close to 1.00, implying that for all of these concentrations, their nominal and actual flow rates are very similar. This makes it much easier to determine the necessary flow rate of methanol to combine with the product stream as it is generated.

The combination of a stream of methanol with the exiting product stream was simulated by simply mixing the two together in a flask, then passing this methanol/product mixture through a heated reactor coil to effect the methylation step. The first attempt used a short coil (2.75 mL) in the Polar Bear Plus® reactor (Scheme 13.5). Three experiments were performed, with concentrations of 1.99, 2.35 and 2.89 mol dm^{-3} as in Fig. 13.12 above. This was to determine the volume of methanol and thus the flow rate of the methanol stream required.

The outcomes were analysed by ^{1}H NMR spectroscopy, using the peak around δ 8.30 ppm as a marker for methyl coumalate compared to a quartet at δ 4.25 ppm for coumalic acid, as all other aromatic peaks overlap. The results are summarised below (Table 13.2).

Table 13.2 Screening methanol quantities in the flow methylation of coumalic acid.

Scheme 13.5 Initial screening of concentration using the Polar Bear reactor.

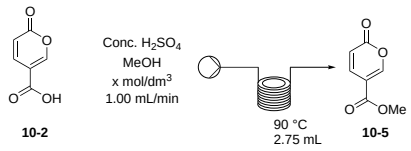

10-2 10-5

Entry	Concentration/ mol dm^{-3}	% coumalic acid	% methyl coumalate[a]
1	2.89	65%	35%
2	2.35	37%	63%
3	1.99	33%	67%

[a]Both % conversions estimated by ^{1}H NMR spectroscopy

The concentration of 2.35 mol dm^{-3} (row 2) represents an addition rate of 0.500 mL min^{-1} of methanol. This value was chosen to conduct further optimisation.

Coumalic acid was dissolved in conc. H_2SO_4, and methanol was added to the viscous solution in an exothermic mixing process. Six experiments were performed, varying the residence time of the reaction by altering the reactor coils and the flow rate (Scheme 13.6). The crude solution was extracted with toluene/H_2O and dried *in vacuo* to give the solid product. No coumalic acid or methyl coumalate were observed in the aqueous layer by ^{1}H NMR spectroscopy. The results are summarised below (Table 13.3).

Table 13.3 Conditions used to optimise the flow synthesis of methyl coumalate.

Scheme 13.6 Optimising the flow synthesis of methyl coumalate from coumalic acid.

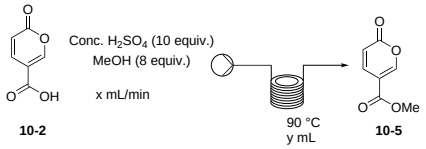

Entry	Flow rate/ mL min^{-1}	Reactor volume/ mL	Residence time/ min	Outcome[a]
1	1.00	2.75	2.75	94%
2	0.500	2.75	5.50	96%
3	1.00	8.25	8.25	99%
4	1.00	11.00	11.00	99%
5	0.500	8.25	16.50	99%
6	0.500	11.00	22.00	99%

[a] % conversion estimated by ^{1}H NMR spectroscopy

It can be seen in the graph below that a residence time of 8.25 mins is sufficient to give 99% conversion of coumalic acid to methyl coumalate. The residence time and % conversion have been plotted on the graph below (Fig. 13.13 - please note that the graph does not begin at the origin).

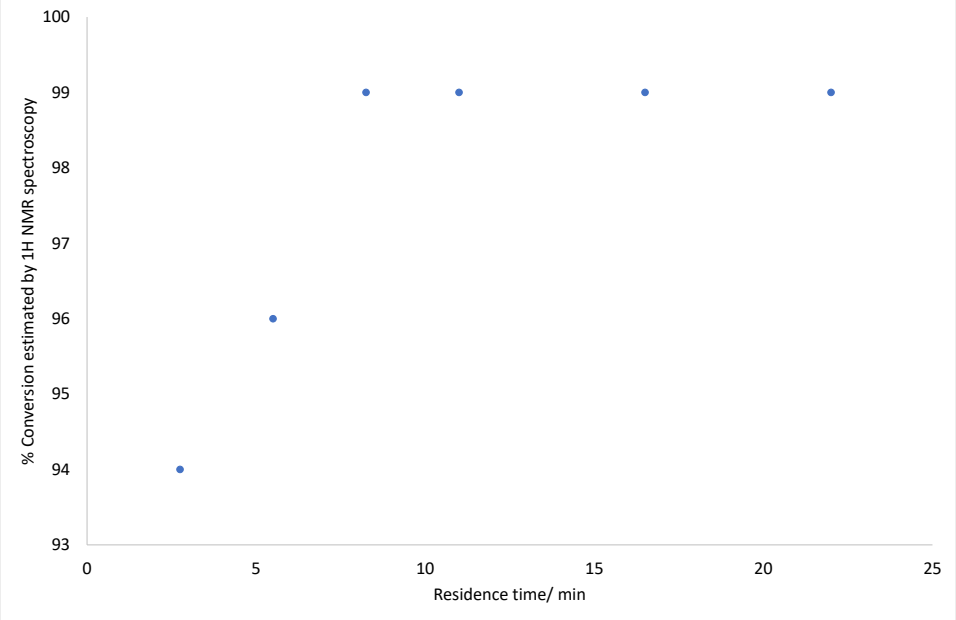

Fig. 13.13 Residence time *versus* conversion of coumalic acid to methyl coumalate.

A residence time of 8.25 mins is achievable using a reactor coil which is 8.25 mL in volume, in combination with a flow rate of 1.00 mL min^{-1}. This process can be telescoped with the flow synthesis of coumalic acid to give a flow synthesis of methyl coumalate from malic acid without isolating the coumalic acid intermediate.

13.5 Telescoping the flow synthesis of methyl coumalate

As established above, it is possible to perform both the synthesis of coumalic acid from malic acid and the methylation of coumalic acid in flow. We therefore wished to evaluate the potential telescoped process combining these two steps.

To increase the temperature, a Polar Bear Plus® reactor with a 2.75 mL FEP reactor maintained at 70 °C was used after T-piece mixing (Scheme 13.7).

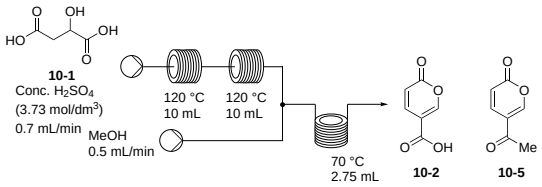

Scheme 13.7 T-piece mixing followed by heating in the Polar Bear reactor.

A mixture of malic acid, coumalic acid and methyl coumalate was obtained, in the ratio 14:68:17 (estimated from ^{1}H NMR spectrum). Heating has enabled the methylation process to occur, but higher temperatures were evidently required to increase conversion. The gases produced in the first step remain in the reactor. Some issues were observed with reactor blocking.

Degassing after the first step would be preferable, and could be achieved using an open vessel to collect the intermediate, to which the methanol could be added. The mixture could be stirred and then pumped through the Polar Bear reactor at an increased temperature.

An experiment was performed with 5.00 g of malic acid and conc. sulfuric acid (10 mL), running through to the methyl coumalate without isolating the coumalic acid intermediate (Scheme 13.8).

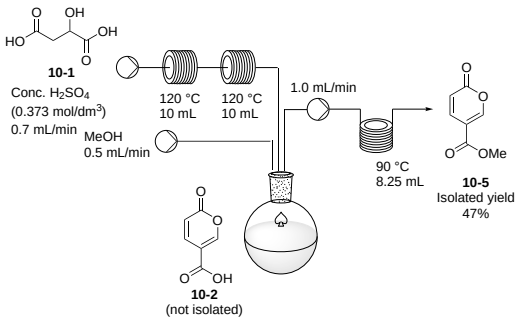

Scheme 13.8 Telescoping the flow synthesis of methyl coumalate from malic acid.

After extraction with toluene/H_2O, and drying *in vacuo*, crude methyl coumalate was isolated (1.345 g) in 47 % yield.

A flow chart is shown below, detailing the times at which various reaction steps were performed (Fig. 13.14).

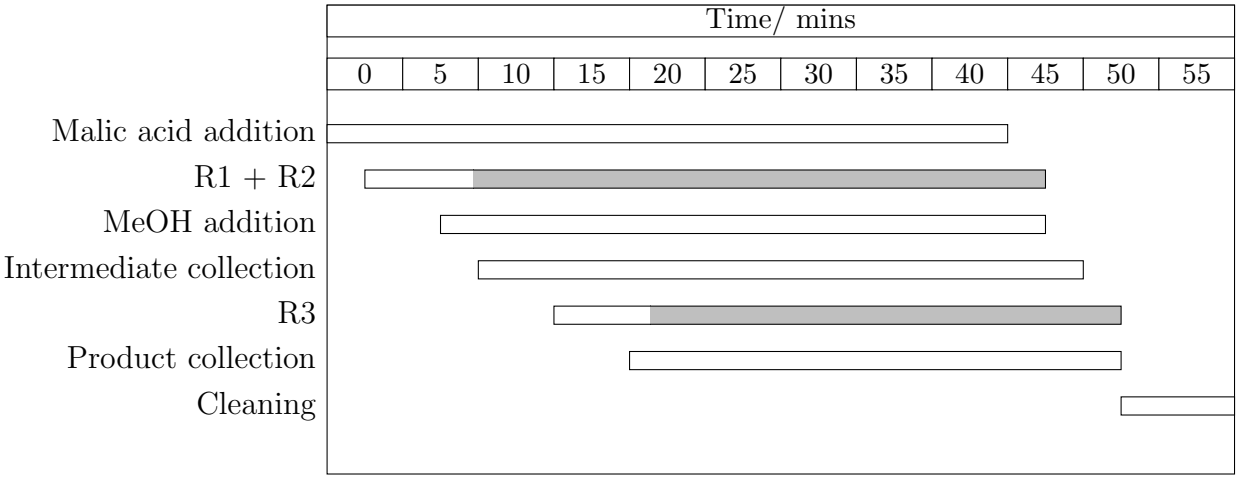

Fig. 13.14 Example timeline of the telescoped flow process, where RX refers to Reactor X. White shading of incomplete bars indicates the residence time in Reactor X.

From start (defined as beginning to pump the malic acid solution) to finish (defined as the point when all of the crude product solution had left Reactor 3), the process took 51 mins. It took 42.5 mins to pump 12.5 mL of starting material, an effective flow rate of 0.294 mL min^{-1} which is slower than previously observed. Taking this into account, the throughput of methyl coumalate is 1.58 g h^{-1}.

13.6 Comparison between the flow and existing batch processes

Two measures of efficiency and productivity were used to compare these processes with the established literature protocols. Where possible, the space-time yield has been calculated from experimental data provided in the literature.

The first of these was the throughput – the mass of coumalic acid produced in a given time (13.1).

$$Throughput = \frac{mass\ (g)}{time\ (h)} \tag{13.1}$$

The second is the space-time yield, or the amount of material processed in a given time for a given reactor volume (13.2).

$$Space - time\ yield = \frac{mass\ (kg)}{reactor\ volume\ (m^3)\ .\ time\ (h)} \tag{13.2}$$

The results are summarised below (Table 13.4).

Table 13.4 Comparing throughputs and space-time yields of syntheses of coumalic acid.

Reference	Throughput/ g h^{-1}	Space-time yield/ kg m^{-3} h^{-1}
Wiley *et al.*[16]	17.6	55.1
Ashworth *et al.*[17]	11.8	37.1
Kraus *et al.*[19]	0.13	1.5
Batch (based on Kaminski *et al.*[18])	6.7	6.7
Vapourtec-pumped flow process	4.4	
Masterflex-pumped Vapourtec® flow process	11.2	560

13.7 Conclusions on the Vapourtec® flow process

By changing from batch to flow, the gas production and foaming is no longer an issue, and the viscosity of sulfuric acid is reduced at these higher temperatures. However, the pumping depends on the viscosity of the solvent which limits the speed material can be processed, therefore restricting the throughput of material.

Chapter 14

Development, Construction and Testing of a Heated Rotating Reactor to Synthesise Coumalic Acid

14.1 Concept

Motivated by the desire to avoid the dependence on need for pumping such a viscous solution, we considered using a gravity feed in a new design of reactor.

There are inherent limitations in the small-scale flow set-up: crucially, the pumping efficiency depends on the viscosity of the solvent. Even when changing to a Masterflex® pump with tubing with a larger diameter and greater pumping capability, the high viscosity of the concentrated sulfuric acid solution slows the process down. We therefore considered designing a rotating heated reactor which relied on gravity to deliver the starting material rather than a peristaltic pump.

A Kugelrohr is apparatus typically used for short-path distillation. It was modified in this case to test the idea of a rotating heated reactor without vacuum, and whether this would give conversion to coumalic acid (Fig. 14.1).

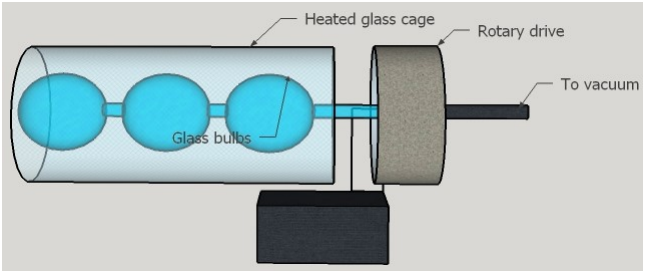

Fig. 14.1 Schematic of Kugelrohr apparatus adapted as a reactor.

The solution of malic acid in concentrated sulfuric acid (3.43 mol dm^{-3}) was added to the left-most bulb, and a range of conditions were screened. Temperature, rotation speed and concentration of the solution were considered, and the results are summarised below (Table 14.1).

Table 14.1 Screening conditions for the Kugelrohr proof of concept.

Entry	Temperature/ °C	Time/ mins	Rotation speed/ rpm	% Conversion[a]
1	120	20	10	47, 55
2	120	20	25	62, 70, 80
3	120	30	25	90
4	120	20	50	49, 52
5	130	20	25	79[b]
6	140	20	25	93[b]

[a]Estimated by ^{1}H NMR spectroscopy
[b]Over-cooked

Higher temperatures led to 'over-cooking' of the reaction mixture to give a viscous brown liquid from which no precipitation occurred when water was added as a quench. There seems to be a trade-off between time and rotation speed. It is possible that temperature equilibration was still occurring with the shorter runs, since the glass bulbs are not in direct contact with the heating element. Faster rotation speeds and longer reaction times seem to give higher conversions. Several mixtures were prepared with high concentrations of malic acid in sulfuric acid. Those which were more concentrated had a lower volume and thus created a thinner reactive film on the inside of the glass bulb. This may give more efficient heating even though the viscosity is increased. The film thickness could be a confounding factor which is difficult to investigate. Regardless, the Kugelrohr experiments act as a good proof of concept: it is possible to synthesis coumalic acid from malic acid by heating in a rotating glass vessel.

14.2 Aims

The aims of this project were to design and build a heated rotating reactor system that was compatible with concentrated sulfuric acid and temperatures up to 150 °C. The reactor was to be tested and easily adapted based on progressive experimental findings. Factors affecting the conversion of malic acid would be investigated systematically. Where possible, modelling using software such as JMP allowed us to gain further understanding of the process. High conversions of malic

acid to coumalic acid are required to call this process successful. Additionally, high throughputs of material are necessary as part of this process intensification.

14.3 Planning and design of the reactor

There were several components to source:

1. furnace
2. rotary drive
3. work-tube
4. delivery mechanism
5. connecting tubing
6. collection vessels
7. supports and height adjustment devices

A standard laboratory glass drying oven had three holes drilled through the sides. The hole on the left-hand side is the entrance hole; the two holes on the right-hand side are exit holes with angles of 2 ° and 11 ° below the plane (Fig. 14.2). The hole diameter was constrained by the dimensions of the cutting device available, and was therefore fixed at 50.8 mm (2 in).

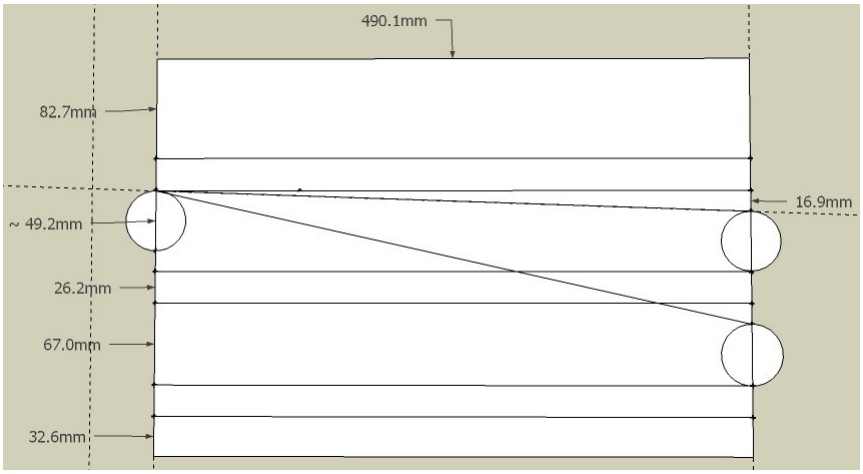

Fig. 14.2 Cross-section of oven, showing the placement of holes to be drilled.

The angles below the plane were calculated using the following diagram Fig. 14.3.

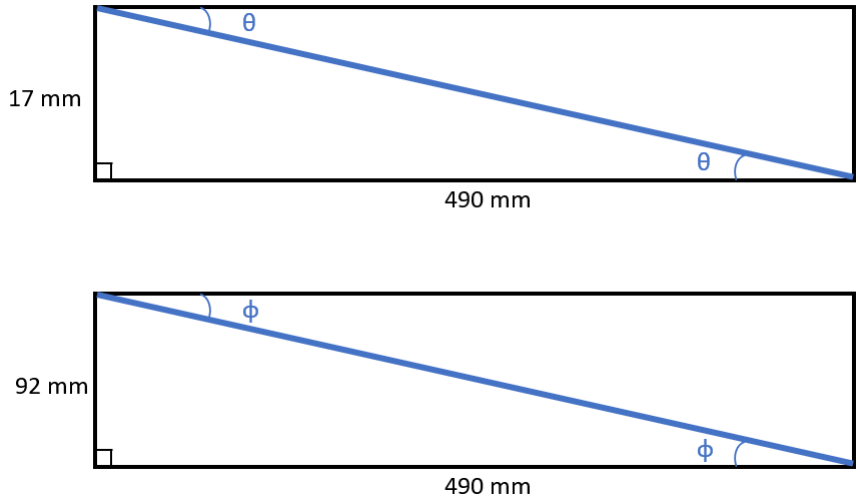

Fig. 14.3 Schematics of the two angles possible in the oven.

Trigonometric identities were used to calculate the angles as shown:

$$\tan\theta = \frac{17}{490} \therefore \theta = 2^\circ \tag{14.1}$$

$$\tan\phi = \frac{92}{490} \therefore \theta = 11^\circ \tag{14.2}$$

A rotary evaporator (Büchi Rotavapor R-124) was used as the rotary drive. Initially, the entire evaporator (minus the water bath, chilled condenser, tension nut for chilled condenser, collection vessel and evaporation flask) was considered (see below).

The work-tube was custom-made by the glass-blowers in the department. The initial specifications were that it was to be 600 mm in length, with a diameter of 44 mm, with a B29 cone and B34 socket (Fig. 14.4).

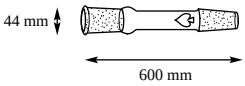

Fig. 14.4 The first work-tube with dimensions.

A dropping funnel was to be used as the tank for delivering material to the work-tube. This was not automated, and was operated manually. The inner diameter of the connecting tubing depended on the size of the dropping funnel used. Initially, a 1 L funnel was used. This required tubing with an inner diameter of 0.5 in which was compatible with concentrated sulfuric acid, which was ordered from Masterflex®. Round-bottomed flasks and adapters were made by the departmental glass-blowers to be used as collection vessels. Initially, measuring cylinders were used instead to allow for easy calculation of production rate (volume/ time). This equipment resulted in the anticipated configuration shown

below as a simplified schematic, showing the relationships between apparatus (Fig. 14.5).

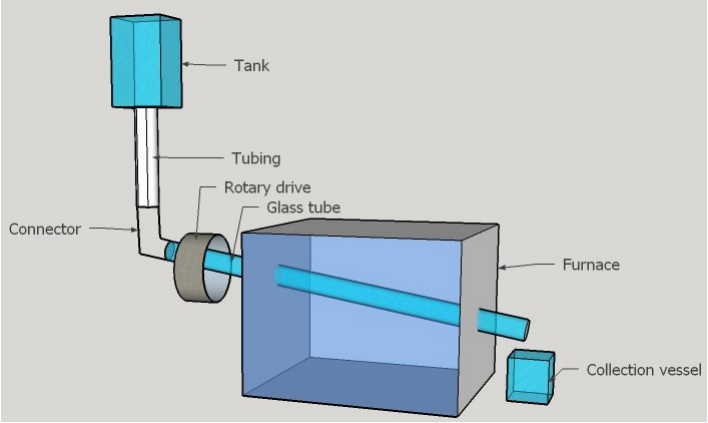

Fig. 14.5 Schematic of the planned reactor, showing components.

Several challenges became immediately apparent: the oven had to be raised on three lab jacks to reach the required height of the rotary drive. When manoeuvring the oven, the base of the rotary evaporator caused problems. Eventually the rotary drive was separated from the base, and raised on a custom-built shelving system, with a lab jack for fine-tuning.

The fit of the work-tube through the oven was tighter than anticipated. It was not possible to use the top hole drilled in the oven (2.1 °) because the rotary drive did not align to allow for such a shallow angle. This hole was therefore sealed. This left only the lower hole available for experimentation. The aligning of the rotary drive and work-tube with the holes had to be exact: a fraction of a millimetre difference could (and did) cause breakages.

The next issue to overcome was the dropping funnel/ connecting tubing positioning. Initially a combination of 1 L dropping funnel with the Masterflex® 0.5 in tubing was tested. Ensuring a suitable union was found to be difficult. A connect made from PTFE tubing heat-stretched to fit the tap of a 100 mL dropping funnel was used. This arrangement was less convenient for running on larger scale, but provided a temporary fix until a more permanent solution could be found.

The reactor is shown below (Fig. 14.6 and Fig. 14.7). Some minor modifications were later made to the design, but the reactor design did not change substantially from this point.

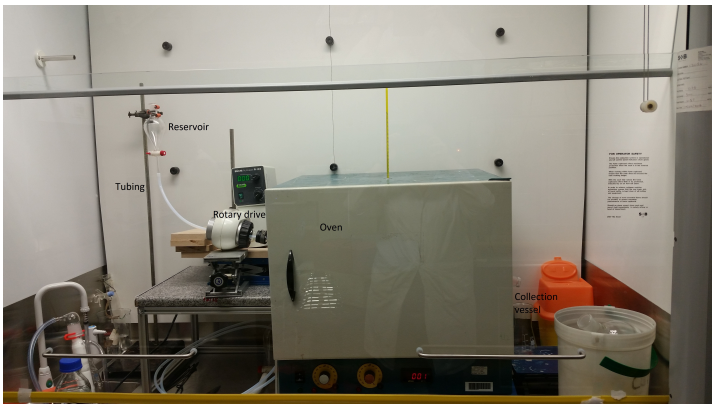

Fig. 14.6 Photograph of the reactor *in situ*.

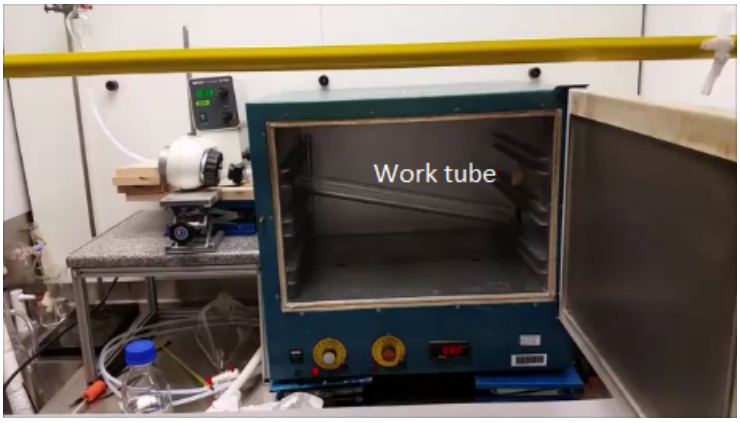

Fig. 14.7 Photograph of the reactor with the oven door opened to allow the work-tube to be seen.

14.4 Statistical analysis

Conversion of malic acid to coumalic was estimated by ^{1}H NMR spectroscopy, using the peaks as shown on the scheme below (Scheme 14.1).

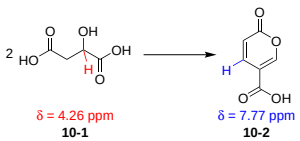

Scheme 14.1 Synthesis of coumalic acid from malic acid.

The stoichiometry of the reaction gives the following equation which was used to calculate the % conversion, where CA = the integral of the peak at $\delta = 7.77$ ppm, and MA = the integral of the peak at $\delta = 4.26$ ppm (14.3).

$$\%\ Conversion = \frac{2CA}{MA + 2CA} \tag{14.3}$$

An example spectrum is given below (Fig. 14.8).

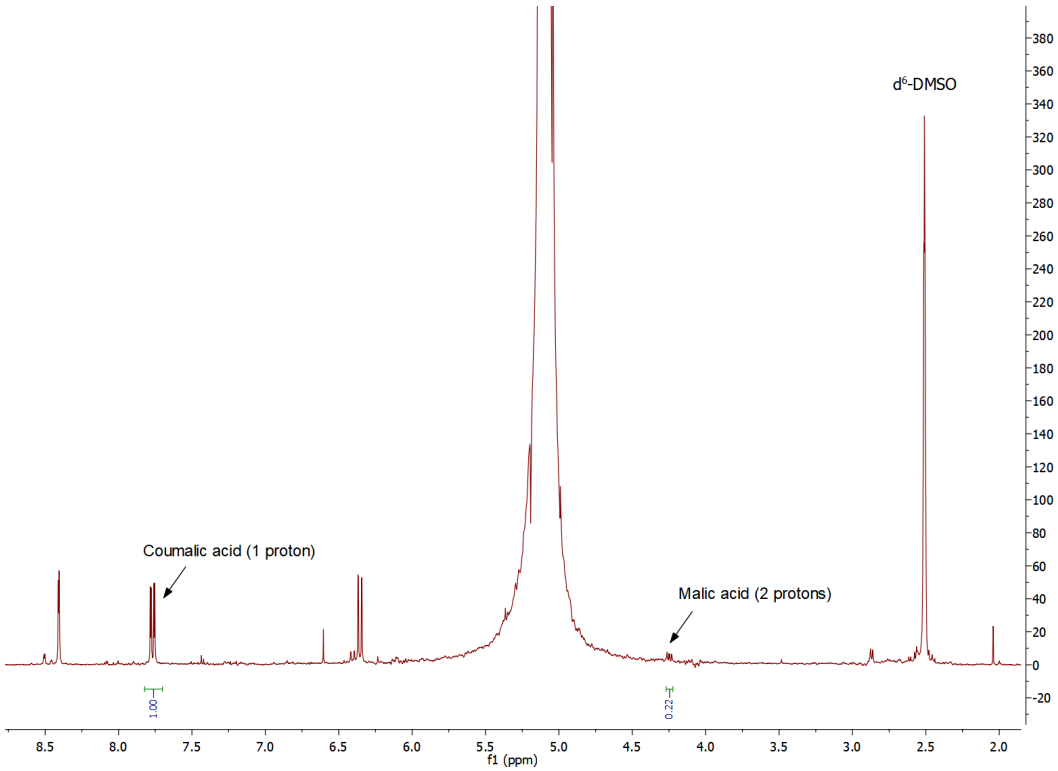

Fig. 14.8 Example ^{1}H NMR spectrum showing coumalic acid, malic acid, solvent and acid.

14.5 Reactor development

Early experiments scoped suitable temperature ranges, rotation speeds and addition rates. Several factors were held constant: the diameter of the work tube (44 mm), the angle of the work-tube, and the concentration of the stock solution (3.76 mol dm^{-3}). Raw data from all experiments can be found in the Appendices.

Over 30 samples were collected, and each sample was quenched with H_2O, and then allowed to cool. Precipitate formation on cooling is an indicator of coumalic acid formation, and was observed in approx. half of samples. This heterogeneous solution was analysed by ^{1}H NMR spectroscopy, and the results are summarised below (Fig. 14.9).

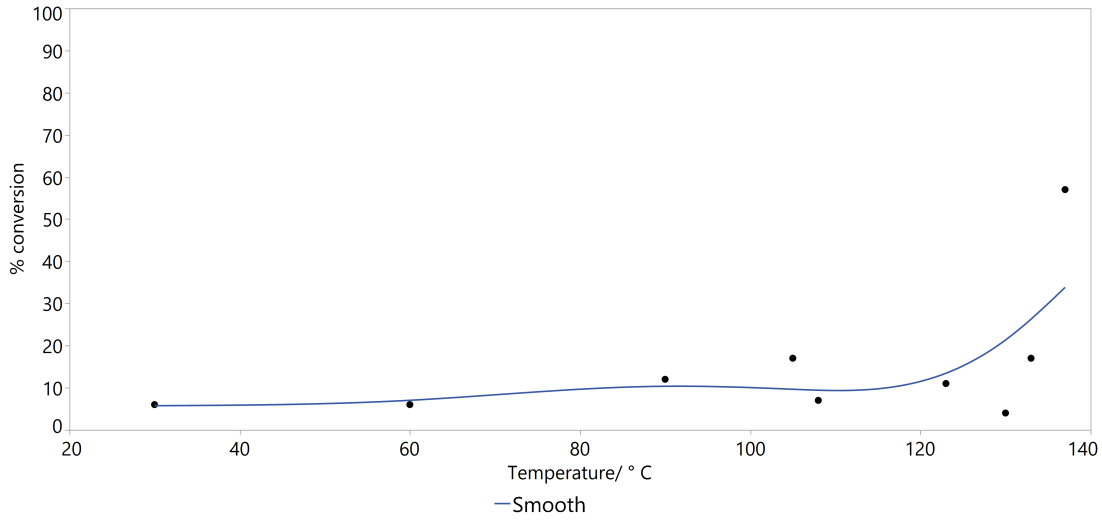

Fig. 14.9 Temperature *versus* % conversion for rotation speed = 7 rpm and a very slow addition rate.

It was apparent that a 'critical' temperature was reached 110-120 °C, at which point the reaction began to occur. Conversions below this critical temperature were very low.

The effects of rotation speed and addition rate were also investigated. Increasing the rotation speed seemed to increase the % conversion, but relatively unreliably. It was not possible to safely rotate the work-tube faster than 28 rpm. The addition rate did not seem to affect the percentage conversion, and so at this point until further notice, it was recorded but not held constant.

At the end of the initial testing phase, several modifications were made to the reactor. The weight of the work-tube as a self-supporting unit became a problem over time, so a support bar was introduced. As the rotation speed was increased (>14 rpm), the work-tube began to catch on the metal edges of the holes, causing etching of the glass. Several attempts were made to re-configure the system by moving the equipment around by increments, but it was not possible to adjust it enough. A more radical solution was sought: new work-tubes were prepared with smaller diameters (32 and 36 mm), which would have a looser fit with the oven holes (Smith Scientific R/38, outer diameter = 38.0 ± 0.8 mm, inner diameter = 36 mm). They also had the added benefit of weighing slightly less, which reduced the load on the rotary drive.

14.6 Studying the helical reactant path

During the early testing phase, it was observed that the viscous stock solution followed a helical path, depending on reaction conditions (Fig. 14.10).

Fig. 14.10 Photograph of a helix formed by the reactants travelling down the work-tube as it rotates.

This helix can be described by the parameters shown in the following diagram (Fig. 14.11).

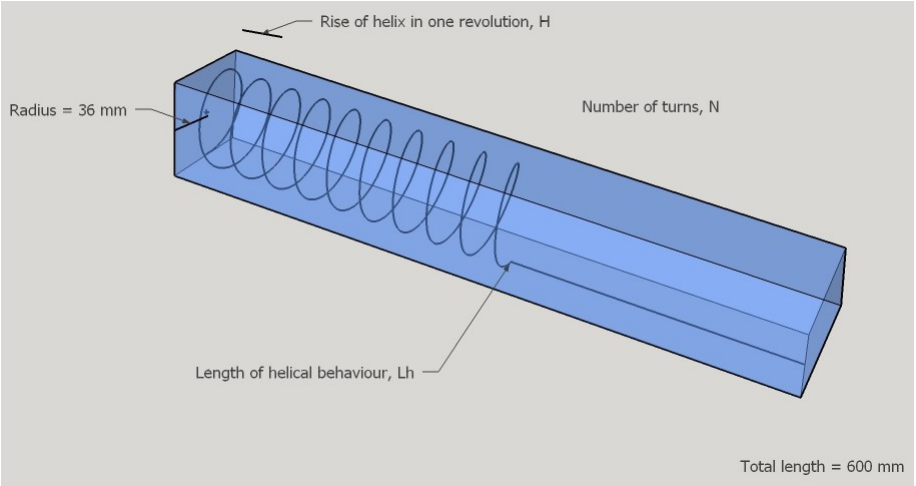

Fig. 14.11 Model of an idealised helix, with parameters.

This helical behaviour dramatically increases the path length of the reactants, and thus also increases the residence time of the materials within the reactor. Several experiments were performed to ascertain at what point the helix formed, as well as its appearance and the effect this has on the path length.

The effects of the rotation speed on the length of the helical behaviour were examined at an addition rate of 1.0 drop/ s, and a temperature of 110 °C. At rotation speeds below 7 rpm, no helix was observed. The length of the helix was found by opening the oven door, and rapidaly measured using a tape measure. The results of these experiments are summarised below (Fig. 14.12).

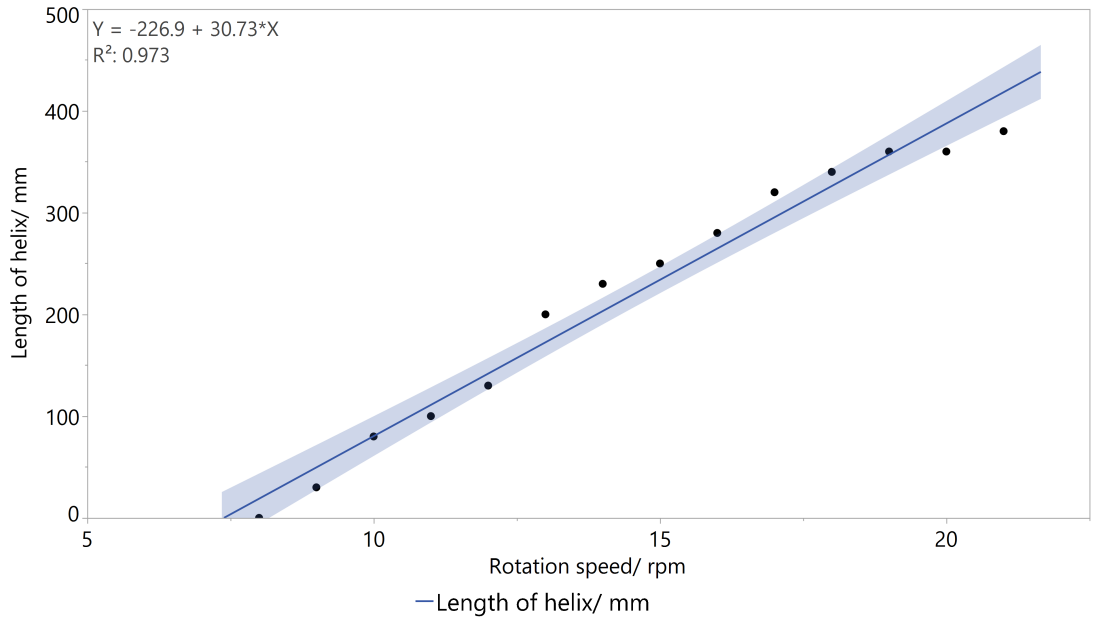

Fig. 14.12 The effect of increasing rotation speed on the length of the helix.

As the rotation speed increases, the length of the helix increases approximately linearly. The maximum would be 600 mm, since this is the full length of the work-tube.

The effect of the rotation speed on the rise of the helix in one revolution was examined for different addition rates, and the results are summarised below (Fig. 14.13).

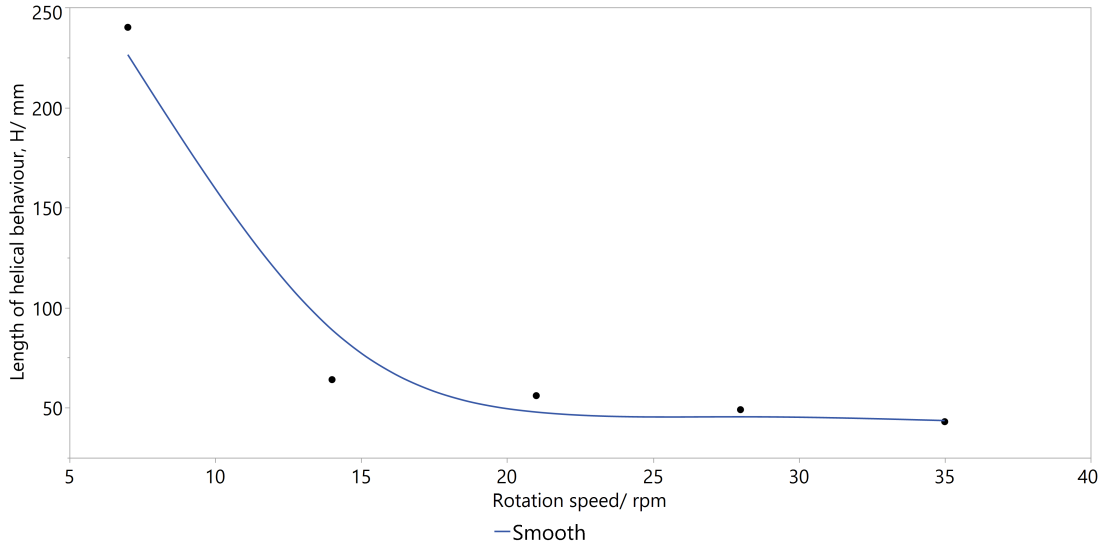

Fig. 14.13 The effect of changing the rotation speed on the length of each helix revolution.

As the rotation speed increases, the helix becomes 'tighter', and the rise of each helix in one revolution decreases.

The equation to calculate the path length is as follows, where N = number of turns; H = rise of helix in one revolution (mm); r = radius (36 mm); L_h = length of helical behaviour (Eqn. 14.4).

$$Pathlength, D = N\sqrt{H^2 + (2\pi r)^2} + (600 - L_h) \tag{14.4}$$

A series of manipulated helices which exhibited full helical behaviour (L_h = 600 mm) were created by changing the rotation speed and addition rate, and are shown below (Table 14.2).

Table 14.2 Helix dimensions and path lengths.

Entry	Number of turns, N	Rise of helix in one revolution, H/ mm	Path length, D/ mm	D/ 600
1	10	60	1171	1.95
2	13	46	1438	2.40
3	14	43	1531	2.55
4	60	10	6063	10.11
5	120	5	12082	20.14

For the most extreme example (Entry 5, Table 14.2), it was possible to increase the path length by more than 20 times, so that the material will have travelled more than 12 metres as opposed to the actual path length of the tube of 0.6 m with no rotation.

The reduced radius of the new work-tube (36 mm compared to 44 mm) will decrease the path length, and explains why % conversions are lower for the narrower tube when other conditions are held constant. For example, if Entry 5 in Table 14.2 had been performed with an increased radius of 44 mm and assuming all other factors were constant, the effect can be seen in Eqn. 14.5:

$$Pathlength, D = 120\sqrt{(5^2 + (2\pi.44)^2)} = 33180 \text{ mm} \tag{14.5}$$

This is an increase by 2.75 times in path length.

14.7 Data analysis – Diameter and concentration

Changing to a narrower work-tube affected the % conversions negatively, but ultimately allowed the tube to be rotated at much greater speeds, more than compensating for any loss of conversion or throughput (Fig. 14.14).

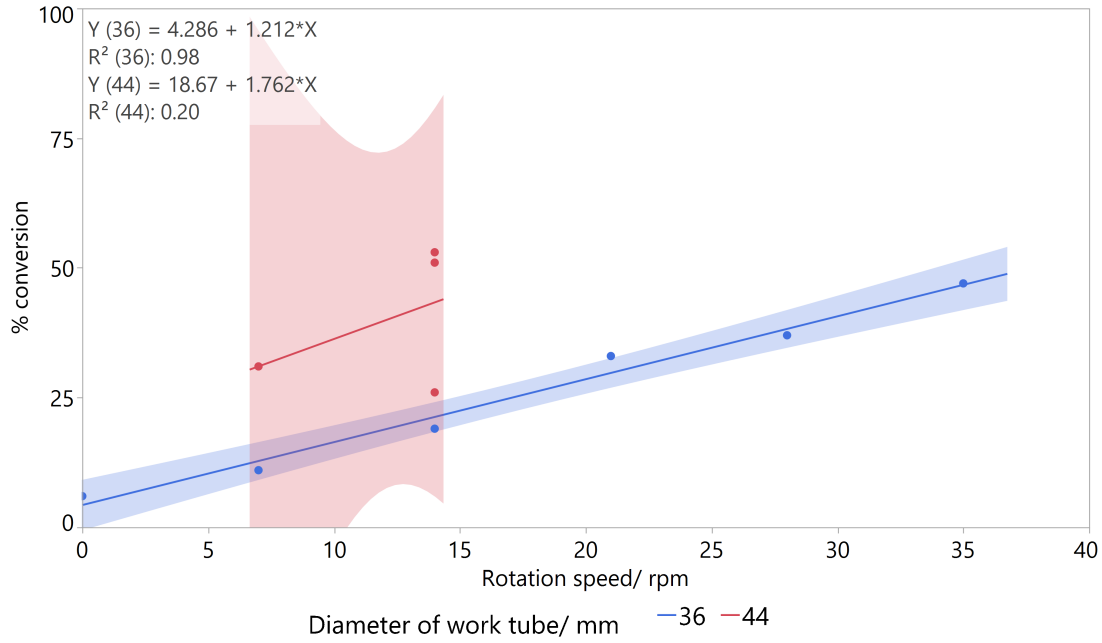

Fig. 14.14 The effect of changing the work-tube on the % conversion. Temperature = 120 °C, addition rate = medium, concentration = 3.73 mol dm^{-3}, rotation speed = variable.

Whilst the data for the wider work-tube was less reliable, it shows a general trend of higher conversions than the narrower work-tube. This tallies with the helical path length depending on the radius of the tube; the wider tube will give a longer path length, and so a longer residence time which is likely to give a greater conversion. However, the 44 mm diameter work-tube was discarded in favour of the 36 mm work-tube, which was able to rotate freely and was less prone to breakages.

Running the reaction at a higher concentration would increase the throughput of material and thus make the process much more efficient. Since this gravity-driven system no longer depends on the pumping of a highly viscous solution, a solution of malic acid in conc. sulfuric acid (7.46 mol dm^{-3}) was prepared, run and compared to the 'standard' 3.73 mol dm^{-3} solution (Fig. 14.15).

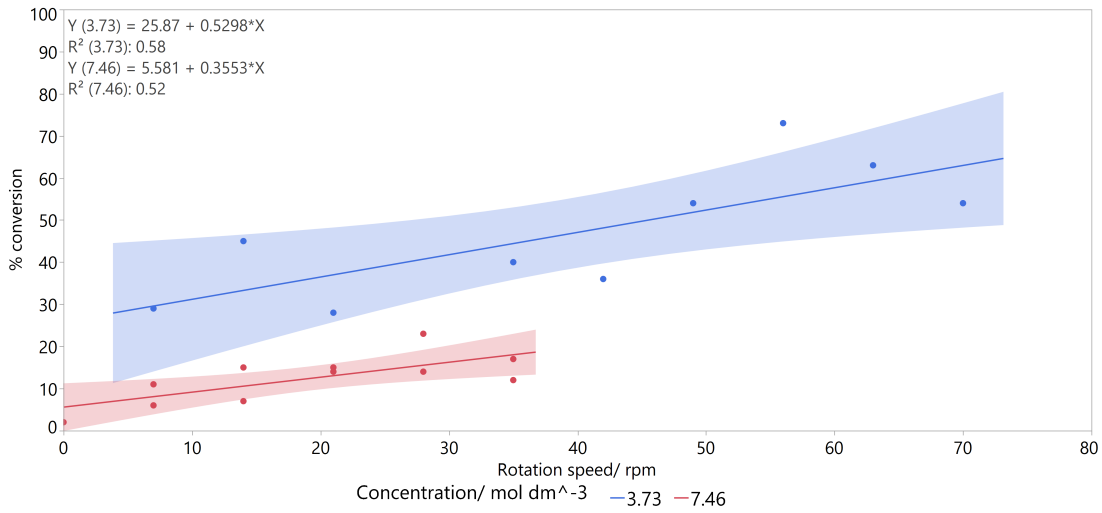

Fig. 14.15 The effect of doubling the concentration of the solution on % conversion.

Conversions to the product are significantly lower for the higher-concentration solution. Subsequent experiments were all performed at a concentration of 3.73 mol dm^{-3}.

14.8 Data analysis – Rotation speed, temperature and addition rate

At first, it was thought that the restricted rotation speed (maximum = 28 rpm for diameter = 44 mm) was the main factor in limiting the conversions. Several experiments that varied both rotation speed and temperature were performed, and are shown below (Fig. 14.16).

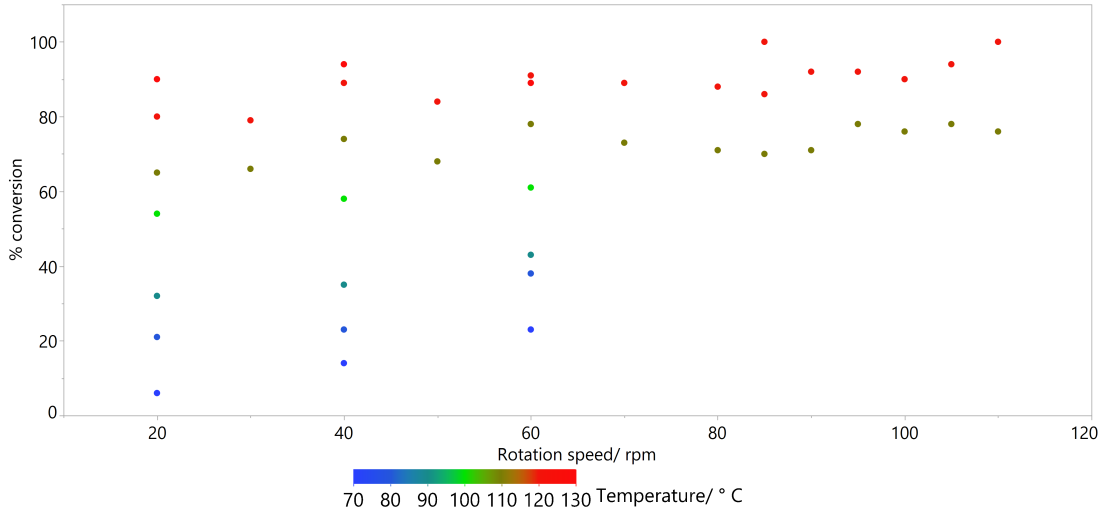

Fig. 14.16 The effect of changing rotation speed on conversion, colour-coded by temperature.

It can be seen that even at low rotation speeds of 20 rpm, high conversions are possible if the temperature is sufficient. By examining a series at fixed temperature (for example, the blue data points on the graph for 70 °C), there is an approximately linear trend relating rotation speed and conversion. This fails somewhat at higher temperatures.

It would appear that the temperature of the reaction is more important than the rotation speed in determining the conversion (Fig. 14.17).

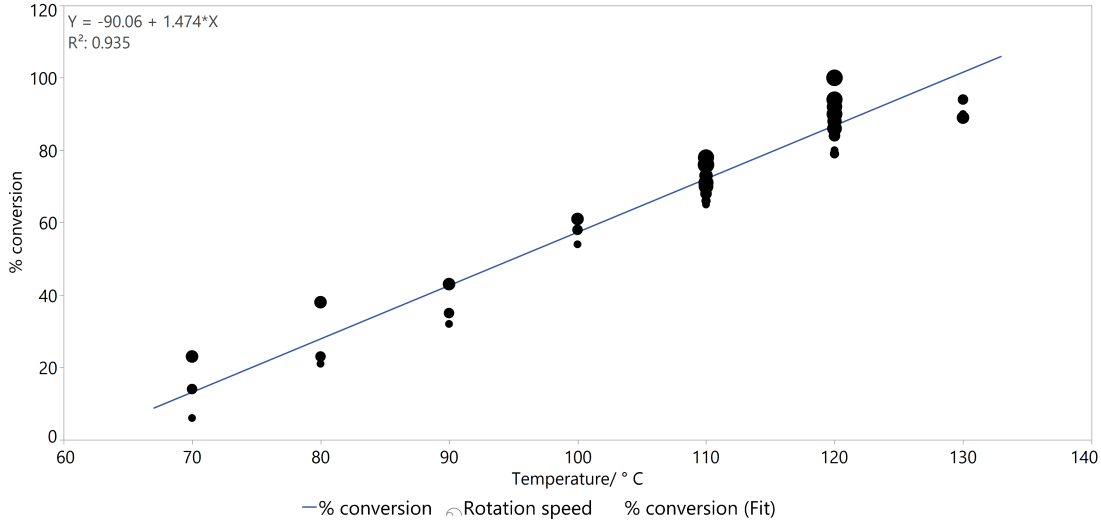

Fig. 14.17 The effect of changing temperature on conversion, with dot size depending on rotation speed where the smallest dot is 20 rpm and the largest is 110 rpm.

Even though the rotation speeds vary substantially, the graph of temperature *versus* conversion has a strong linear relationship. This can be described by the

line of best fit, shown in Eqn. 14.6 and 14.7:

$$y = -90.1 + 1.47x \tag{14.6}$$

$$R^2 = 0.935 \tag{14.7}$$

The appearance of the water-quenched solutions are striking when compared next to each other (Fig. 14.18). It is possible to qualitatively identify which experiments have given low and high conversions by visual inspection, based on both colour of the solution and the degree of precipitation of the solid product. It is worth noting in the image below that the experiments conducted at 130 °C exhibit 'over-cooking', with a dark brown solution and only a small amount of precipitation. It would seem that there is a narrow window of opportunity for high conversions and high isolations, which lies between 110-130 °C.

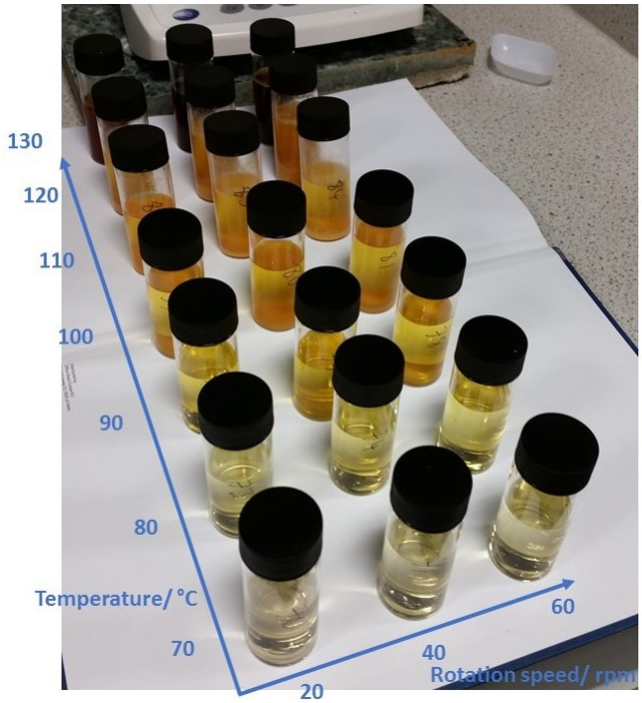

Fig. 14.18 Quenched crude solutions from experiments performed at a range of rotation speeds and temperatures.

The temperatures and rotation speeds of these experiments as well as some additional reactions between 110-130 °C can be seen in the graph below, with colour-coding indicating the conversion (Fig. 14.19).

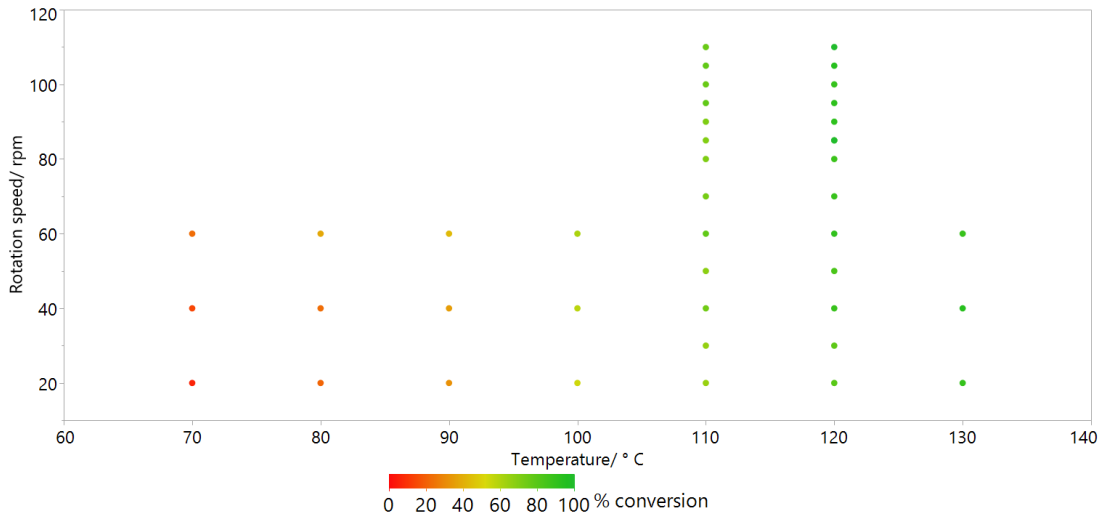

Fig. 14.19 Temperature *versus* rotation speed, colour-coded for conversion.

The trend from left to right of red to green as the conversion increases as temperature is raised is obvious. A more subtle trend is the increase in conversion with rotation within a temperature, as conversion now begins to exceed 80%.

An early model was developed using results from experiments at 70 °C to 130 °C increasing in 10 °C increments, considering the effects of temperature and rotation speed on percentage conversion. The diameter of the work-tube, the concentration of the stock solution, and the addition rate were all held constant.

At this point, both rotation speed and temperature were found to correlate with conversion with statistical significance. The leverage plots can be seen below. There was a strong positive correlation between temperature and percentage conversion (Fig. 14.20).

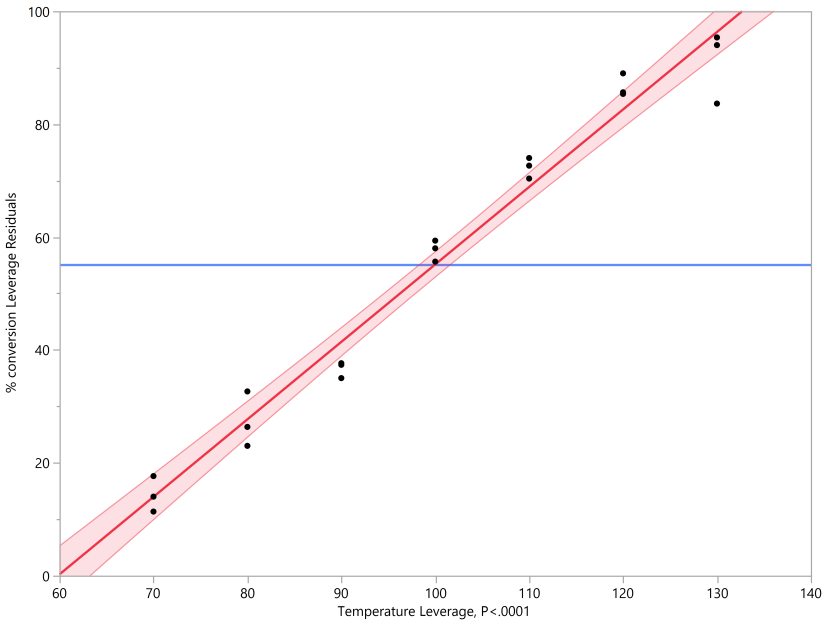

Fig. 14.20 Temperature *versus* conversion in model 1.0.

The link between rotation speed and percentage conversion was weaker, but still positive, as can be seen in the graph below (Fig. 14.21).

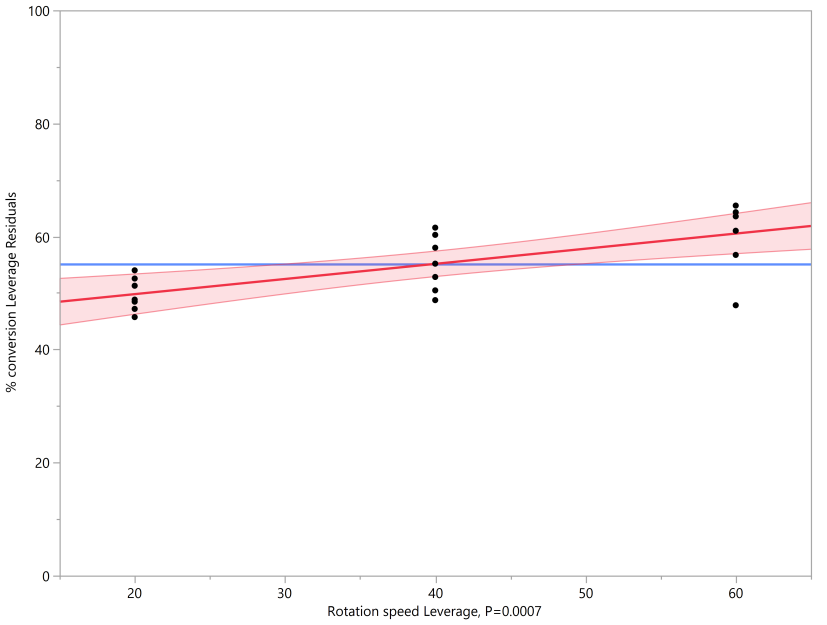

Fig. 14.21 Rotation speed and conversion in model 1.0.

The predicted *versus* actual conversion plot can be seen below, indicating an excellent correlation (Fig. 14.22).

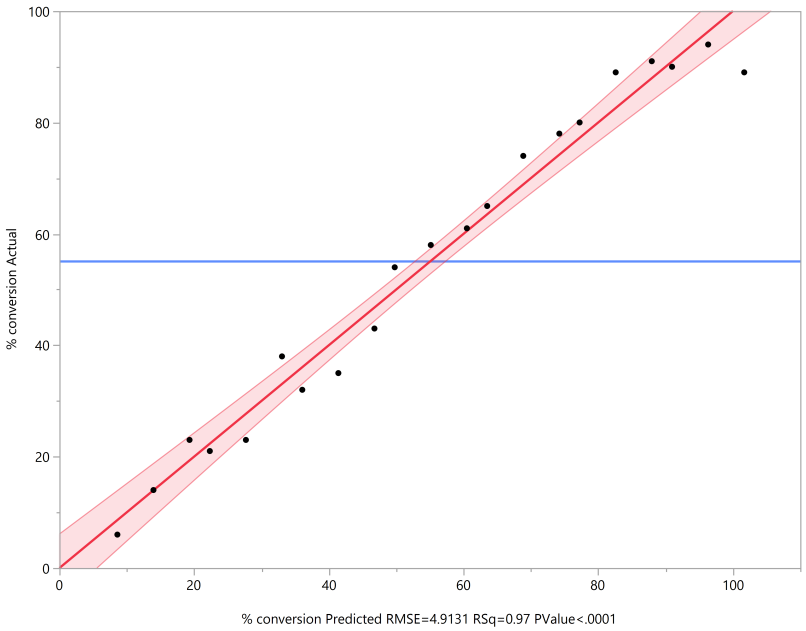

Fig. 14.22 Accuracy of model 1.0.

The prediction expression for HeRo 1.0 was found to be described by Eqn. 14.8:

$$\%\,Conversion = -92.83 + (1.373.\text{Temperature } (^{\circ}\text{C})) + (0.268.\text{Rotation speed (rpm)}) \tag{14.8}$$

14.9 Data collection and HeRo model 2.0

A wider range of temperatures and rotation speeds were examined to cover a larger chemical space. These experiments were built into a second refined model, HeRo 2.0. As the model became more populated, the aim was to increase its reliability. The strong positive correlation between temperature and conversion remains - and is reinforced by the additional experiments which also fit the line of best fit (Fig. 14.23).

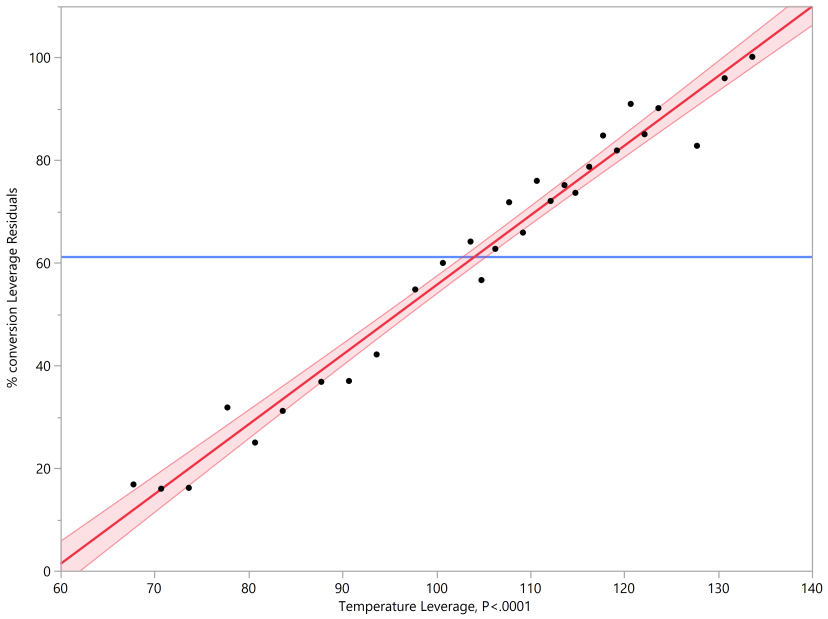

Fig. 14.23 Temperature *versus* conversion in model 2.0.

The connection between rotation speed and conversion remains weakly positive (Fig. 14.24).

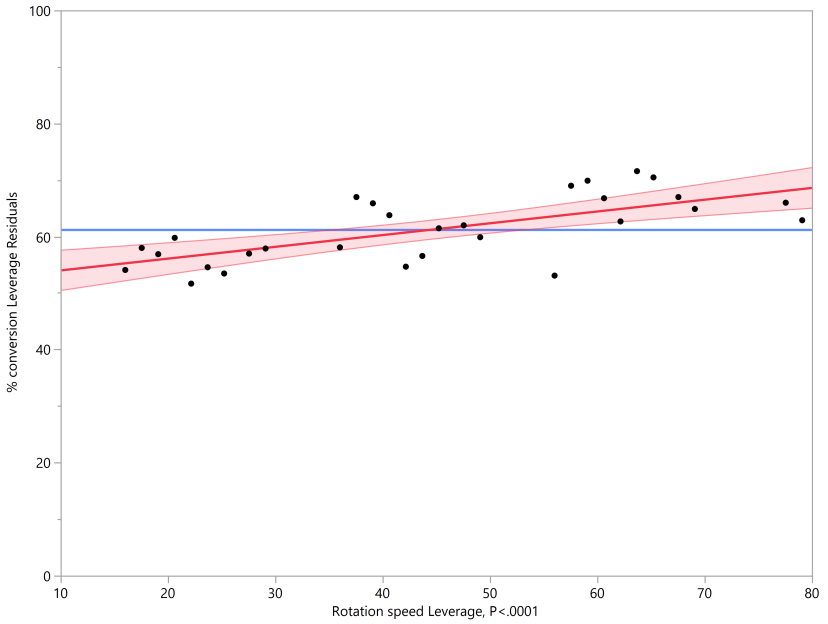

Fig. 14.24 Rotation speed *versus* conversion in model 2.0.

The fit of this model is shown below, and appears to be excellent (Fig. 14.25).

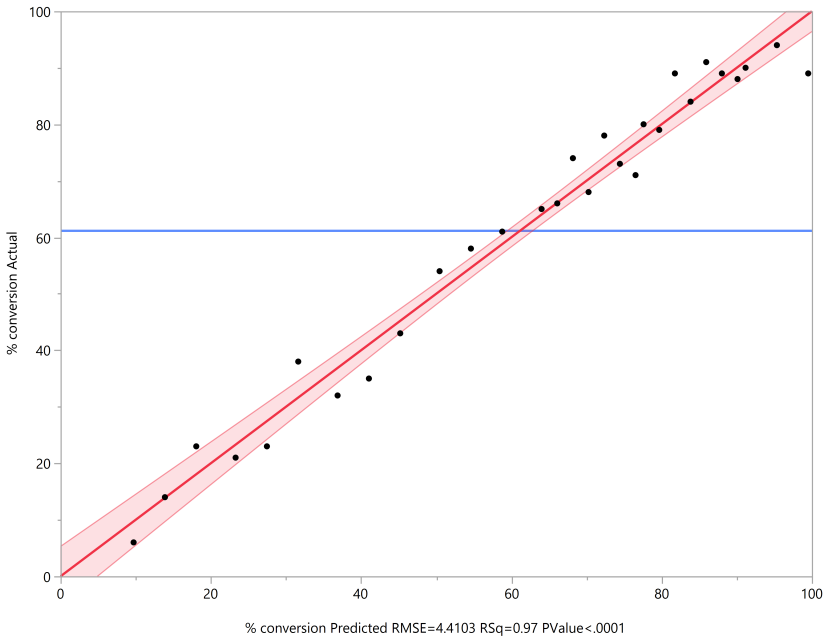

Fig. 14.25 Accuracy of model 2.0.

The prediction expression for HeRo 2.0 has changed only slightly from HeRo 1.0, decreasing the importance of the rotation speed coefficient, increasing the importance of the temperature and slightly altering the intercept as shown in Eqn. 14.9:

$$\%\,Conversion = -89.47 + (1.358.\text{Temperature } (^{\circ}\text{C})) + (0.208.\text{Rotation speed (rpm)}) \tag{14.9}$$

14.10 Data collection and HeRo model 3.0

At this point, a further modification was made to the reactor to prevent the rotary drive shifting around at higher rotation speeds (60 rpm and above). It was stabilised using wedges and a curved rest. It was now possible to safely run the reactor at speeds above 80 rpm, up to 110 rpm. The maximum speed the rotary drive is capable of is 240 rpm.

A series of experiments run at rotary speeds above 80 rpm were performed, and the data collected was used to build a third iteration of the model, HeRo 3.0. The temperature was also varied.

The relationship between temperature and conversion remains strong. A slightly wider scatter around the line of best fit is now observed (Fig. 14.26).

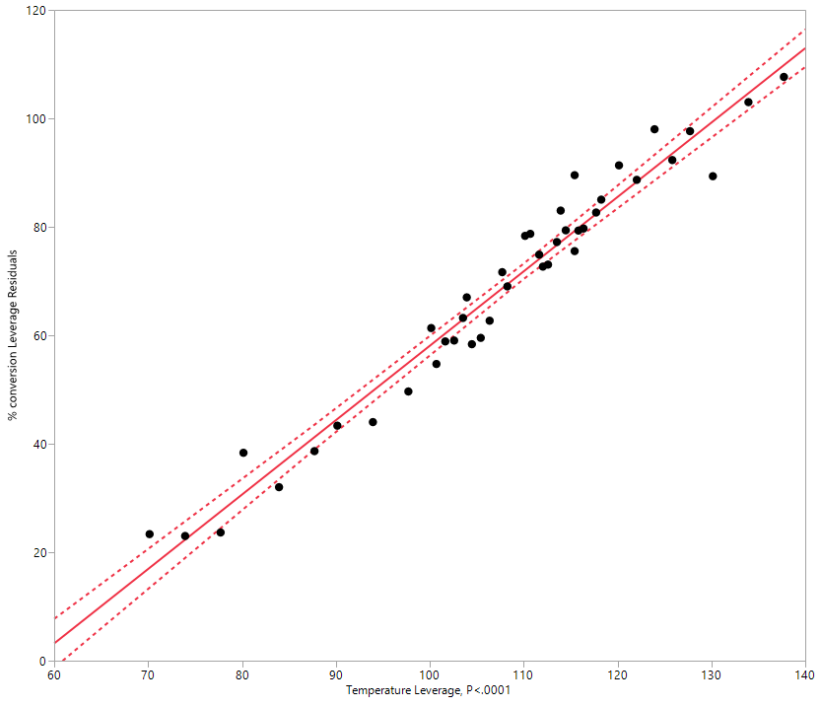

Fig. 14.26 Temperature *versus* concentration in model 3.0.

The link between rotation speed and temperature continues to weaken (Fig. 14.27).

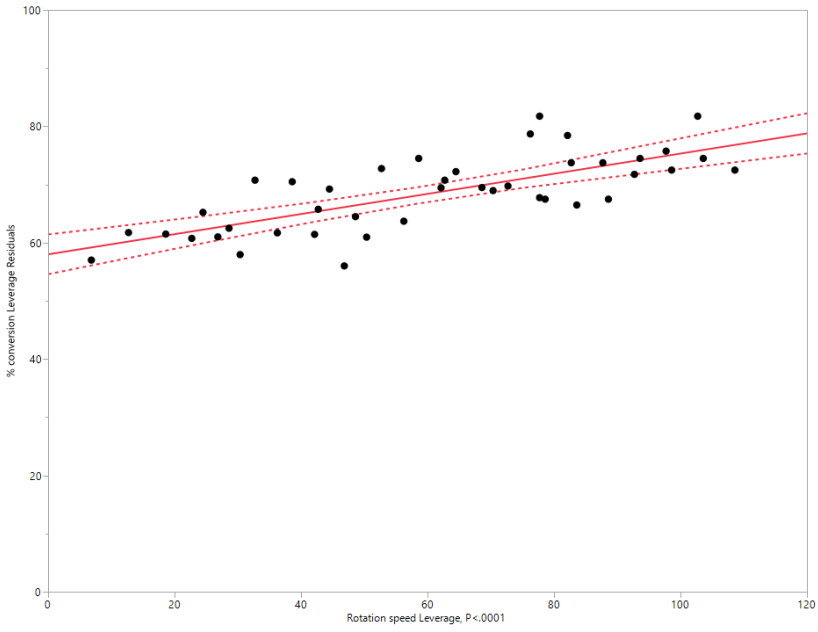

Fig. 14.27 Rotation *versus* conversion in model 3.0.

However, the accuracy of the predictive model remains very high, with an excellent fit (Fig. 14.28).

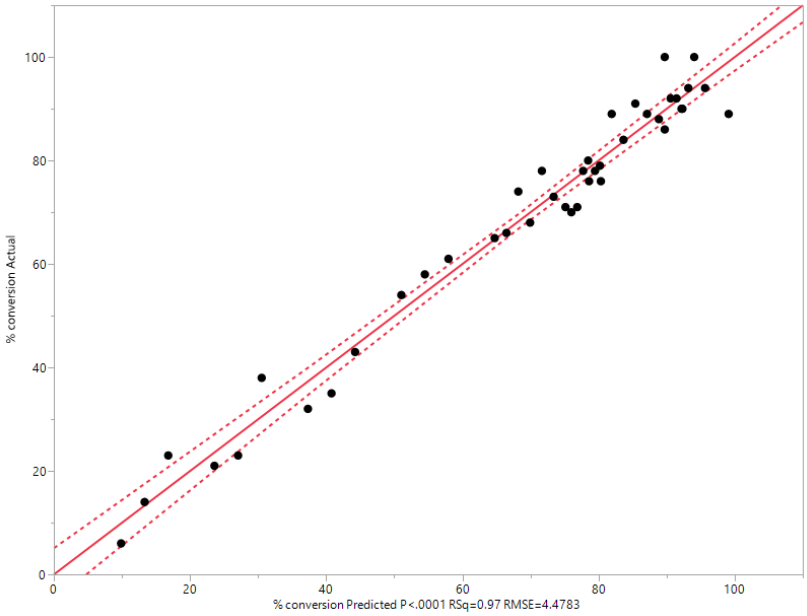

Fig. 14.28 Accuracy of model 3.0.

The equation describing HeRo 3.0 is given below. The intercept has barely changed from HeRo 2.0. The importance of the temperature variable has increased, whereas the rotational speed importance has decreased substantially (Eqn. 14.10).

$$\%\,Conversion = -89.63 + (1.371.\text{Temperature } (^{\circ}\text{C})) + (0.173.\text{Rotation speed (rpm)}) \tag{14.10}$$

14.11 Data collection and HeRo model 4.0

The reproducibility of the data was a concern. A factorial Design of Experiments (DOE) approach was taken to identify the experiments needed to test the reproducibility of the conversion data. Temperatures from 80-120 °C and rotational speeds from 40-100 rpm were taken as the boundaries. Three repeats of each set of conditions were performed, and the results are summarised below (Fig. 14.29).

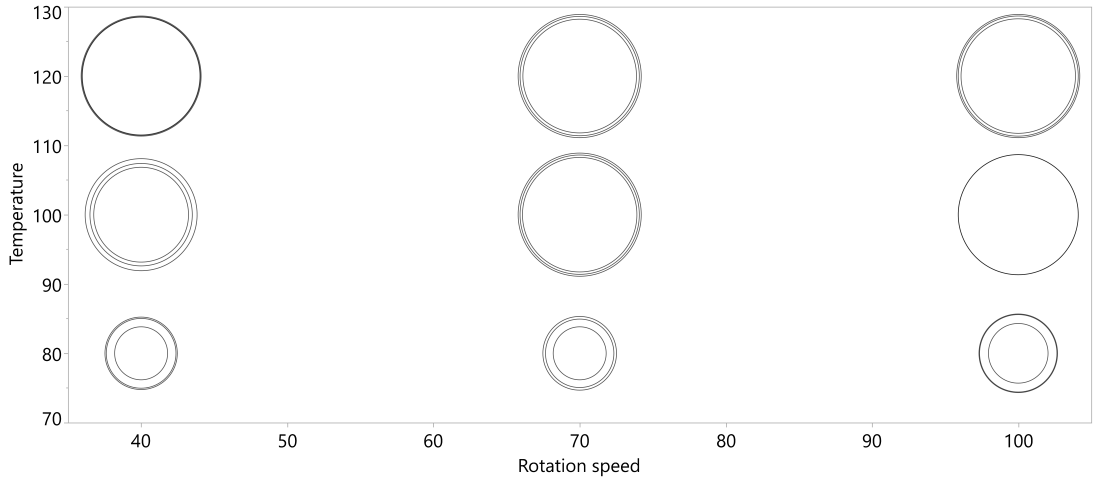

Fig. 14.29 Reproducibility of a data sample. The closer the rings, the more similar the results are. The size of the rings is proportional to the % conversion. The biggest diameter difference represents a conversion difference of around ±5%.

The size of the circle is proportional to the conversion for those conditions. It can be seen that the experiments run at lower temperatures are less reproducible, as the circle sizes vary more. They can be seen to become more similar as the temperature increases. There is no obvious trend in conversion when changing the rotation speed.

In addition, the data from several previous experiments using the same conditions was combined, the % conversions averaged, and plotted against rotation speed, colour-coded by temperature. An error of ±5% can be expected from integration data from ^{1}H NMR spectroscopy. The results can be seen below (Fig. 14.30).

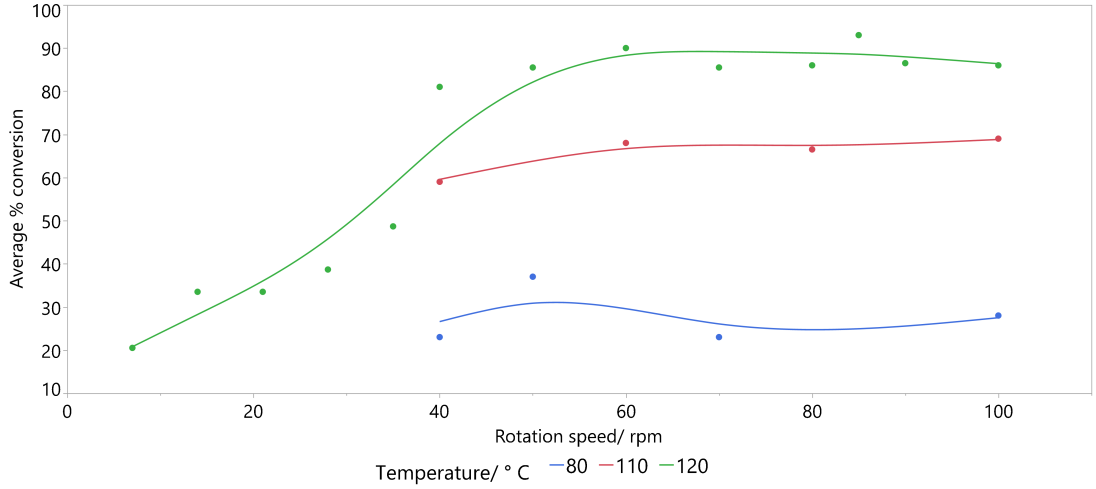

Fig. 14.30 Rotation speed *versus* average conversion, colour-coded by temperature.

One trend is immediately apparent: as the temperature is increased, the aver-

age percentage conversion increases. Once a rotation speed of approx. 60 rpm has been reached, there was little change in average percentage conversion; this held true for all three temperatures considered here. Prior to this point, the rotation speed was critical in determining the average percentage conversion.

It may be that the effects of rotation speed are more important than temperature at lower rotation speeds, and once a 'critical' speed has been achieved, temperature takes over as the dominant factor in determining percentage conversion.

To investigate how the percentage conversion varied with time, a series of experiments were designed to determine the time at which 'steady-state' operation was reached for three different temperatures (Fig. 14.31). Here, 'steady-state' was defined as the point at which conversion remained approximately constant.

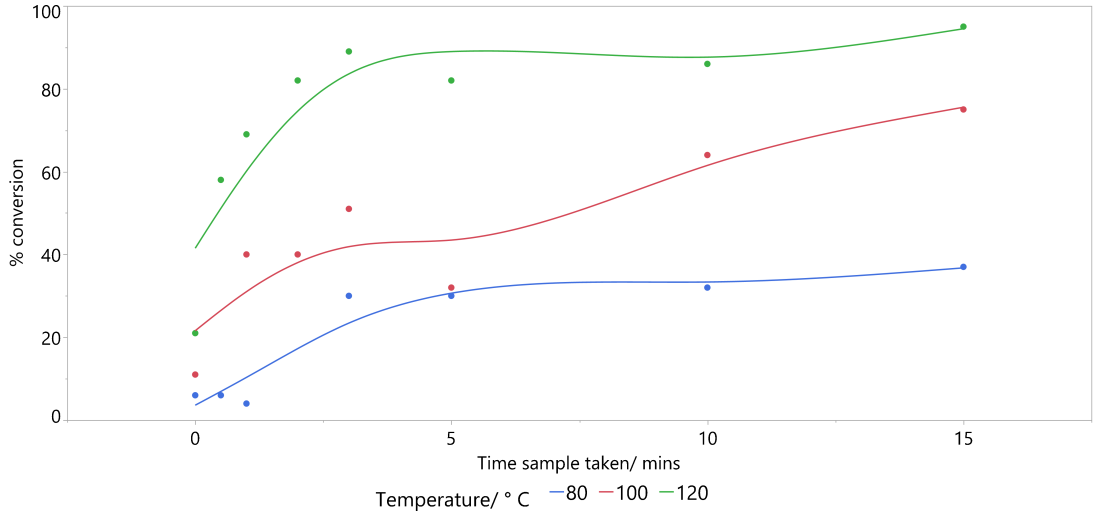

Fig. 14.31 Conversions over the first 15 mins of product collection.

For 80 °C, 'steady-state' operation is reached after 7 mins. 100 °C presents an interesting fluctuation, and the % conversion has not settled even after 15 mins. At 120 °C, the 'steady-state' point was reached after 4 mins. The trend of increasing conversion with increasing temperature is evident here. The conversion becomes more consistent more quickly at higher temperatures.

Up until this point, the addition rate has been disregarded from the data analysis, although it was recorded for all experiments. Several experiments were performed to calculate the volume of one drop of stock solution, as the number of drops per second has been used as the measure of addition rate. The number of drops in 10 s had previously been counted and divided by 10 to give the number of drops/ s.

To calculate the volume of each drop, the number of drops in 10 s was varied by changing the position of the dropping funnel tap, and the volume of stock

solution collected in a set time which was recorded. This gave an addition rate in mL/min, which was plotted against the number of drops (Fig. 14.32).

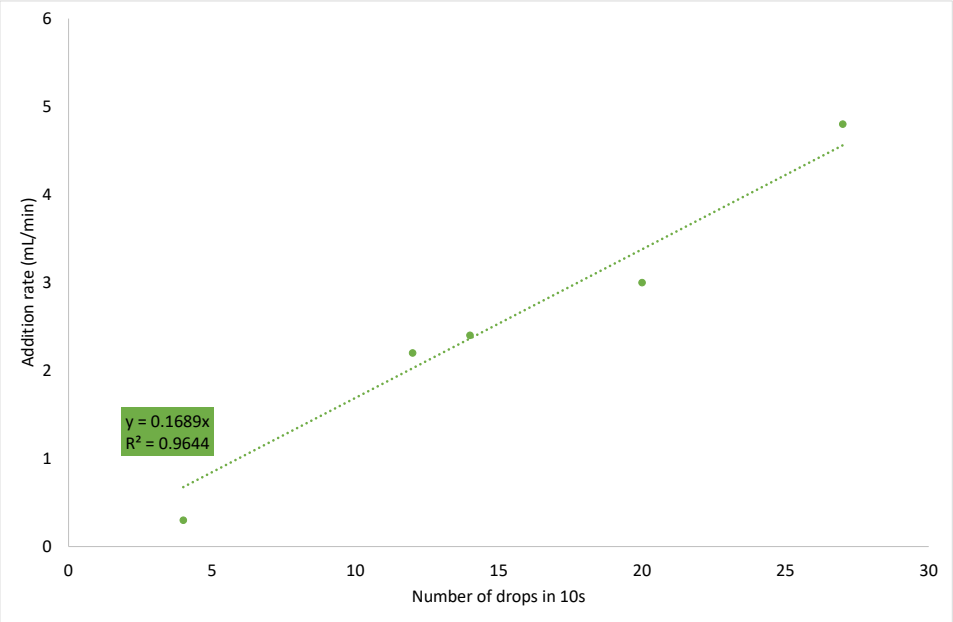

Fig. 14.32 Calibration of the number of drops by addition rate.

The intercept of the line of best fit was set as zero, and the data exhibits a linear trend. The gradient of the graph gives the average drop size in mL, and is therefore 0.169 mL.

To examine whether the addition rate varied over time according to the height of the stock solution in the dropping funnel, a graph of time *versus* volume was plotted (Fig. 14.33).

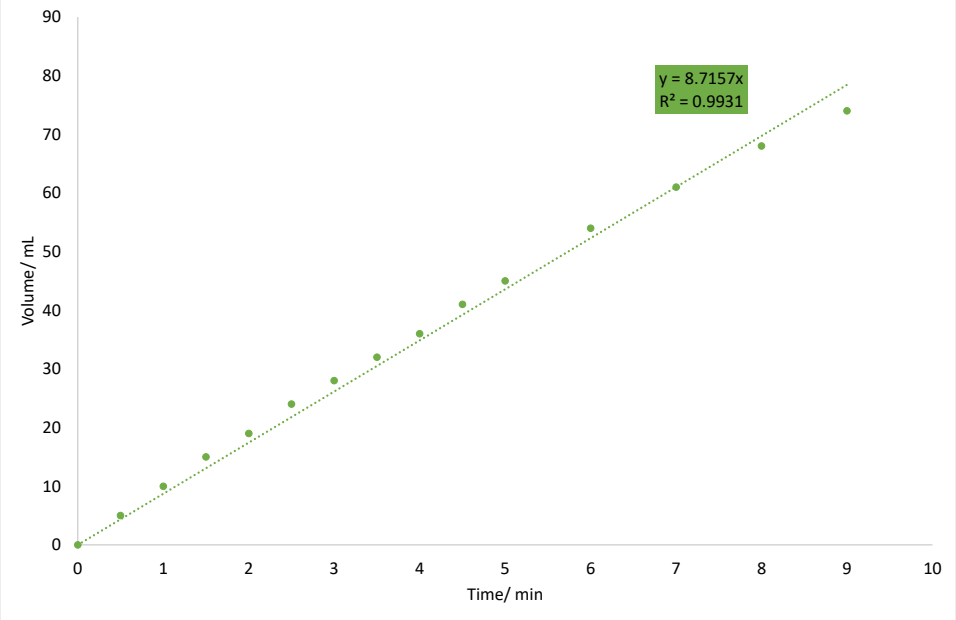

Fig. 14.33 Time *versus* volume in the dropping funnel.

The intercept of the line of best fit was again set as zero, and the data exhibits a linear trend. This implies that the addition rate does not significantly vary with the volume/ height of stock solution in the dropping funnel. The steady-state behaviour persists for a large proportion of the dropping funnel's capacity. There did not seem to be a meaningful correlation between conversion and addition rate in the range evaluated (1.25-3.00 mL min^{-1}).

The observed addition rates (drops/ s) were retroactively converted into mL/min, and overlayed onto a temperature-conversion plot to look for a pattern (Fig. 14.34).

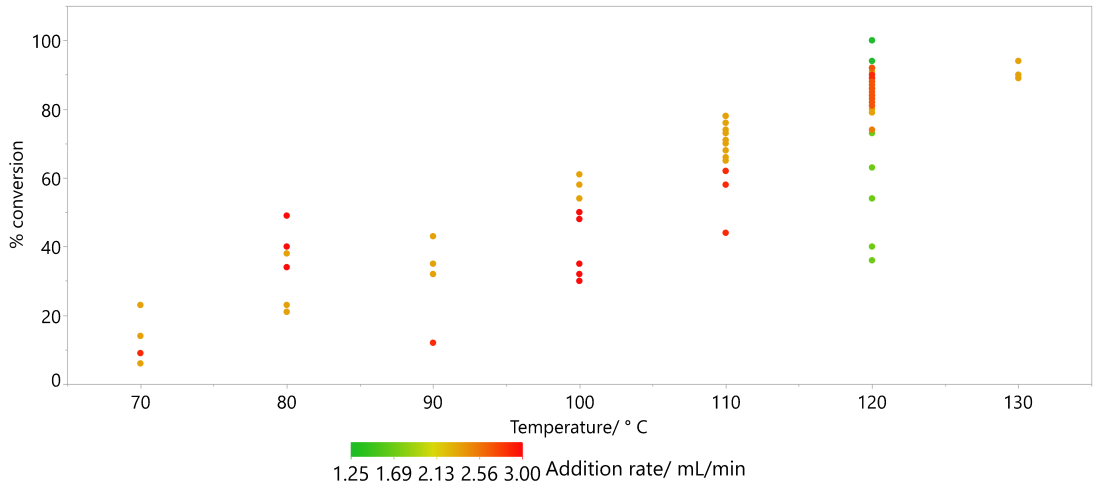

Fig. 14.34 Addition rate *versus* conversion.

Visually, there did not seem to be any correlation between conversion and addition rate. This was examined by creating a fourth and final model. The new model examined temperature, rotation speed, addition rate and the crossings of all of these variables.

The plot of temperature against conversion has become more chaotic, with most data points clustered between 110-120 °C (Fig. 14.35). The overall correlation remains positive.

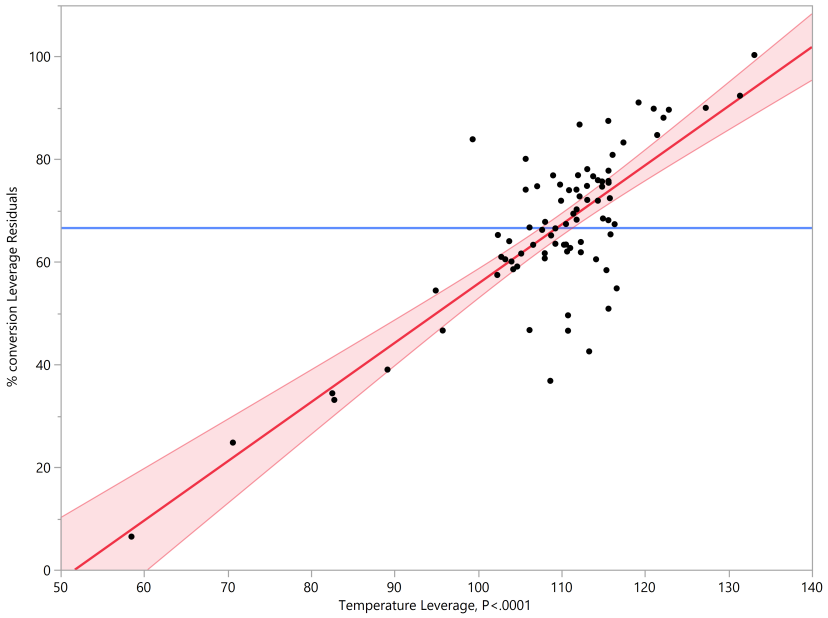

Fig. 14.35 Temperature *versus* conversion in model 4.0.

Similarly, the plot of rotation speed *versus* concentration has also become more chaotic: in this case, almost any trace of correlation has disappeared (Fig. 14.36).

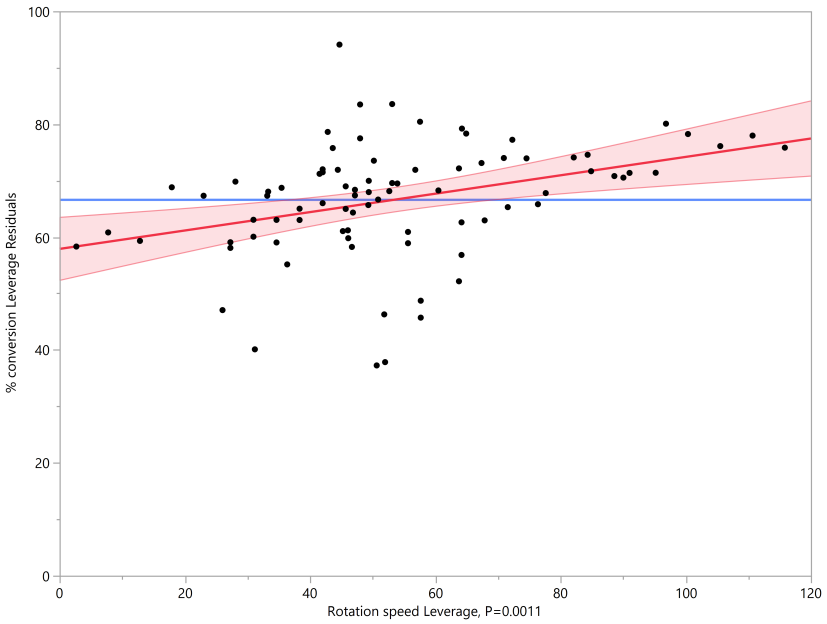

Fig. 14.36 Rotation speed *versus* conversion in model 4.0.

There is little connection between addition rate and conversion (Fig. 14.37).

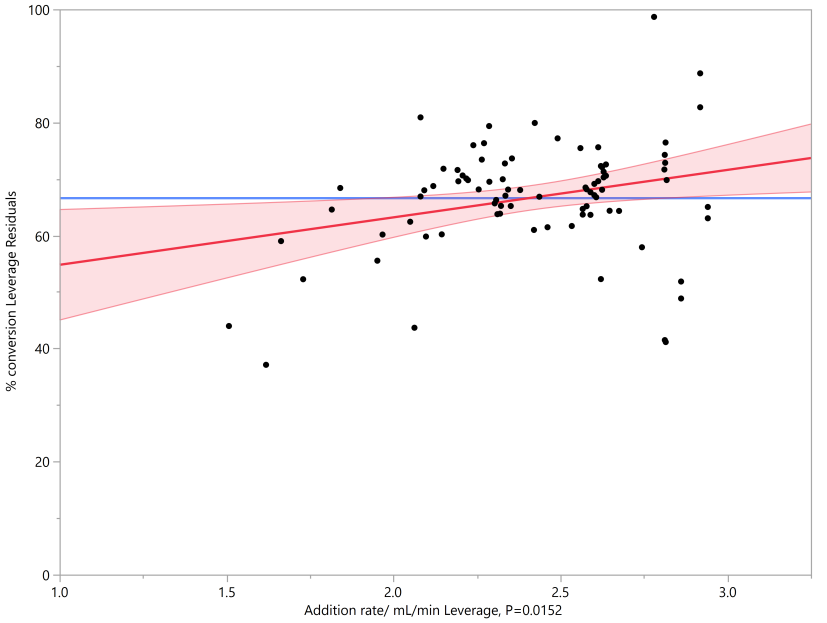

Fig. 14.37 Addition rate *versus* conversion in model 4.0.

Temperature crossed with rotation speed gives little link to conversion (Fig. 14.38).

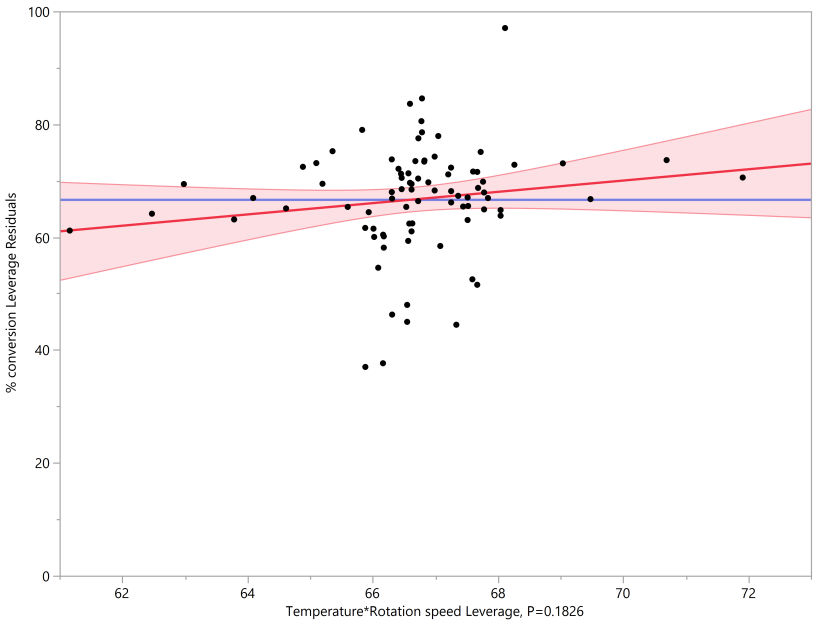

Fig. 14.38 Temperature crossed with rotation speed *versus* conversion in model 4.0.

There is a poor link between crossed temperature/ addition rate and conversion (Fig. 14.39).

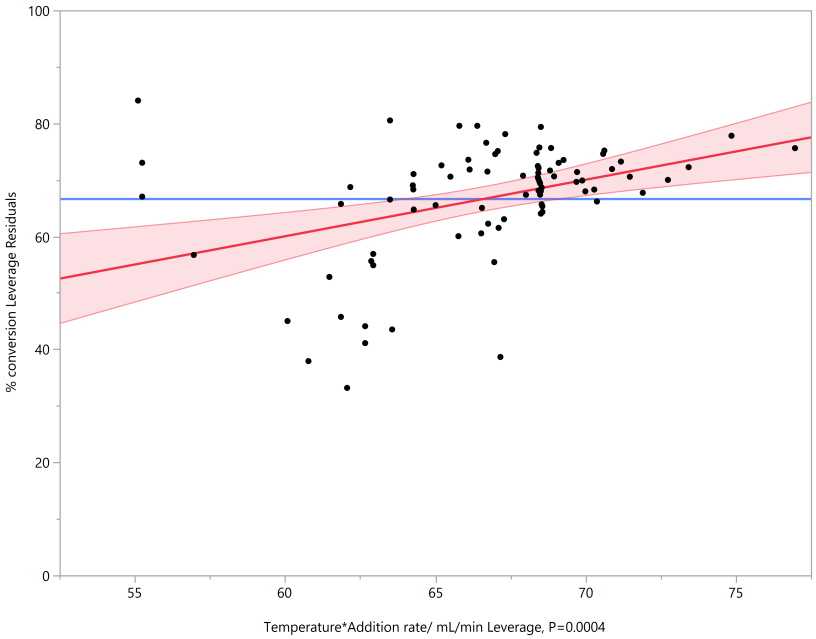

Fig. 14.39 Temperature crossed with addition rate *versus* conversion in model 4.0.

Similarly, there is a weak correlation between crossed rotation speed/ addition rate and conversion (Fig. 14.40).

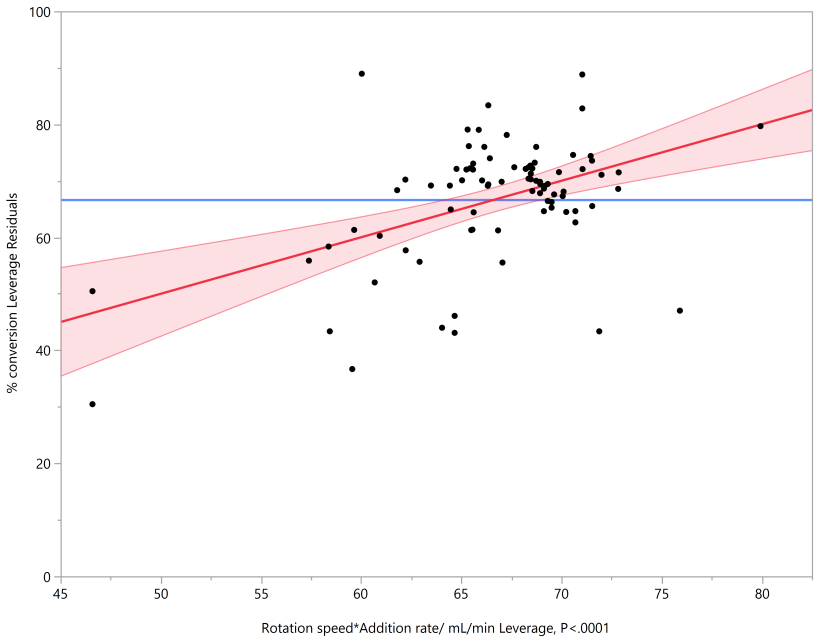

Fig. 14.40 Rotation speed crossed with addition rate *versus* conversion in model 4.0.

Finally, the three variables crossed together against conversion show little to no link between each of these factors (Fig. 14.41).

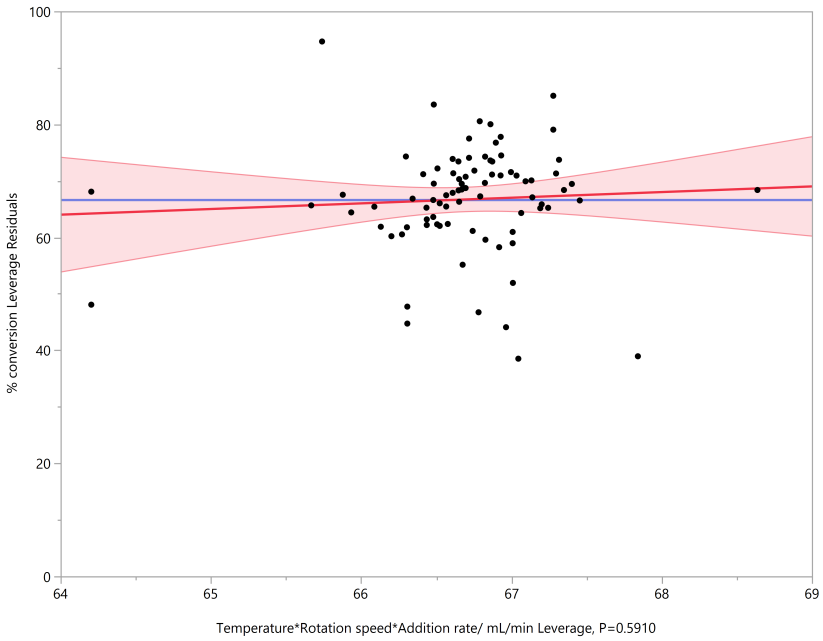

Fig. 14.41 Temperature crossed with rotation speed and addition rate *versus* conversion in model 4.0.

The three variables do not seem to work together or have a strong effect on each other. The accuracy of the model is still good, but with a looser fit than seen before (Fig. 14.42).

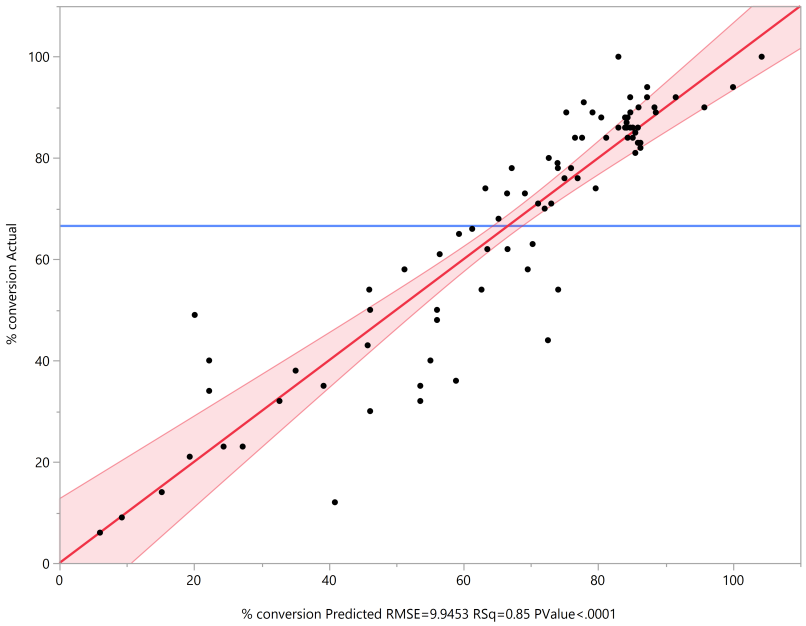

Fig. 14.42 Accuracy of model 4.0.

In order to run experiments for longer, the 100 mL dropping funnel was exchanged for a modified 500 mL dropping funnel comprising a narrowed tap, to fit the tubing required to feed through the rotary drive into the work-tube.

Several tests were conducted to examine whether this affected the size of the drops formed, and the behaviour of the addition rate at different filling volumes (Fig. 14.43).

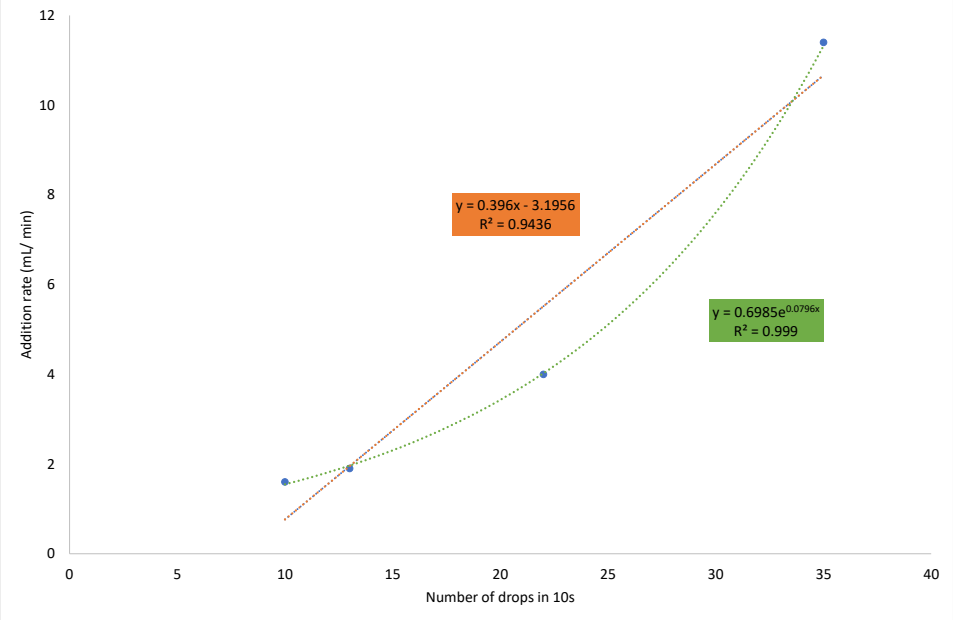

Fig. 14.43 Number of drops in 10 seconds *versus* addition rate.

Two lines of best fit were calculated and their equations are shown on the graph. The orange equation is linear, but does not fit the data as well as the exponential line of best fit (green). It would appear that the size of the drop depends on the addition rate. Compared to the 100 mL dropping funnel where the average drop size was 0.169 mL, the drops from the 500 mL dropping funnel are larger at 0.396 mL, using the gradient of the linear line of best fit (Fig. 14.44).

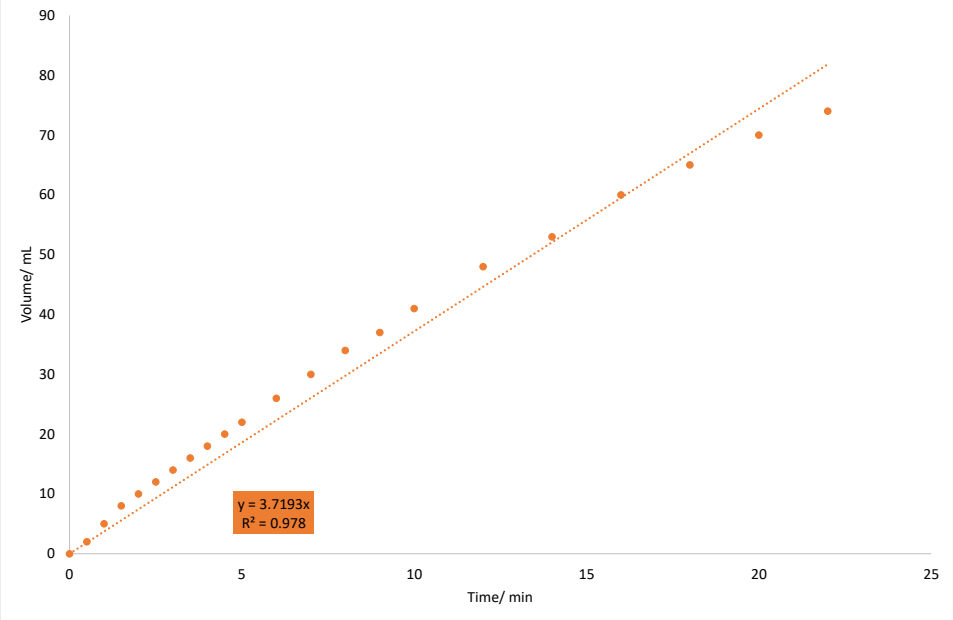

Fig. 14.44 Time *versus* volume for the 500 mL dropping funnel.

The addition rate over time remains approximately constant since the data fits a linear model. It could appear that there are two linear regions with different gradients (Fig. 14.45).

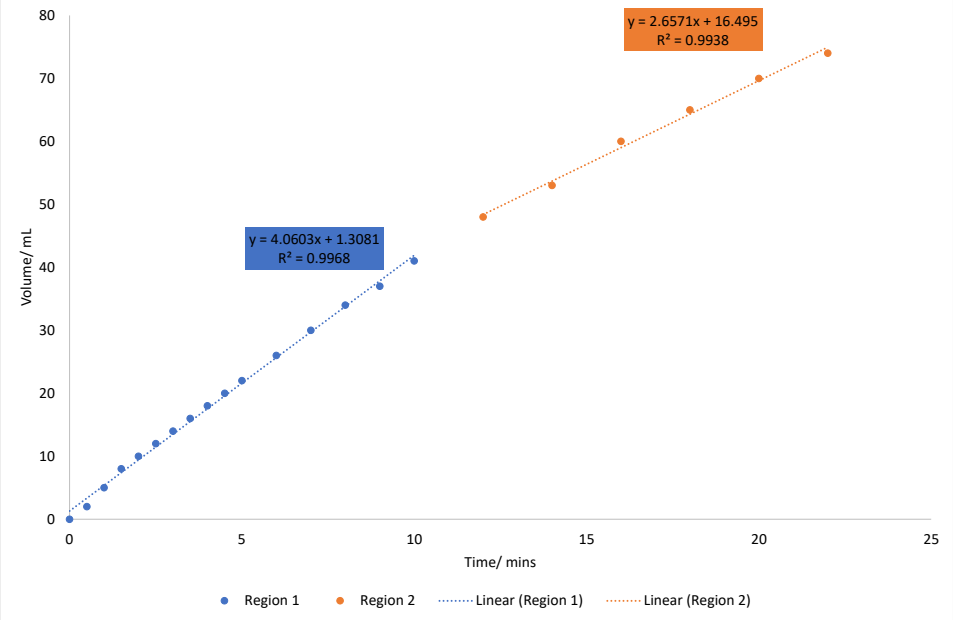

Fig. 14.45 Time *versus* volume for the 500 mL dropping funnel, split into two regions.

The steeper gradient of 4.06 mL min^{-1} up to 10 mins implies that addition is faster when the dropping funnel is fuller. As it empties, the addition rate slows to 2.66 mL min^{-1}.

A further observation was made during these experiments that different amounts of precipitation were observed in quenched samples even when they were shown to have the same percentage conversion by ^{1}H NMR spectroscopy. A hypothesis was that the degree of precipitation depended on the volume of water added to the crude solution as an anti-solvent. To test this, seven experiments were performed by adding varying quantities of water to vials containing the crude solution. The reactions were performed at a concentration of malic acid in sulfuric acid of 3.73 mol dm^{-3}, with a conversion of approx. 90% by ^{1}H NMR spectroscopy. They were allowed to precipitate overnight, filtered and dried *in vacuo* to give different amounts of crude coumalic acid. The results are summarised below (Fig. 14.46).

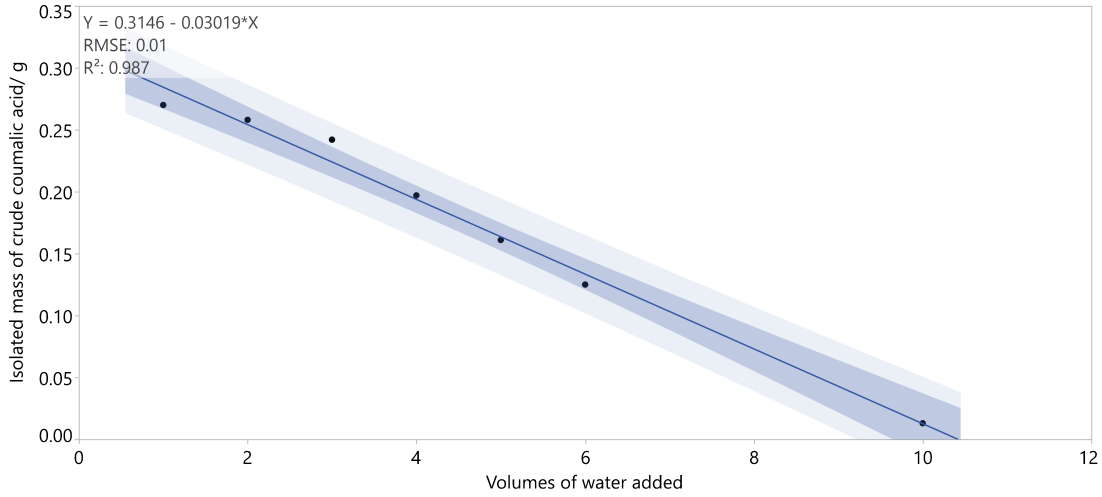

Fig. 14.46 Volumes of water added *versus* isolated mass of coumalic acid.

There is an approximately linear relationship between the volumes of water added and the amount of coumalic acid isolated. As the amount of water added increases, the isolated mass of coumalic acid decreases. There is no precipitation when water is not added. As a general rule, one volume of water was added to the crude solution to obtain the highest recovery of coumalic acid (>50%).

14.12 Extended operation

To test the robustness of the process over longer reaction times, excess stock solution was prepared for an 8-hour run.

The settings used for the 8-hour run were 120 °C (with an overnight pre-equilibrium stage) and 60 rpm. As per the time-course experiment, stock solution was sent through the reactor for 15 mins before collection began.

The total volume collected (1444 mL) was quenched with an equal volume of H_2O and was allowed to precipitate overnight. Filtration and drying *in vacuo* gave the crude material in 65% yield (285.7 g). Efficiency calculations were performed (see below).

14.13 Efficiency calculations

An extended version of the table first seen in Section 13.6 is now presented below (Table 14.3).

Table 14.3 Throughputs for various syntheses of coumalic acid.

Reference	Throughput/ g h^{-1}
Wiley *et al.*[16]	17.6
Ashworth *et al.*[17]	11.8
Kraus *et al.*[19]	0.13
Batch (based on Kaminski *et al.*[18])	6.7
Vapourtec flow process	11.2
HeRo reactor	35.7

The HeRo reactor is capable of throughput efficiencies greater than double that which has been previously claimed to be achievable in batch.

Several assumptions have been made to enable calculation of the reactor volume of the HeRo reactor. These are:

- The solution is homogeneous. This is known to be inaccurate, because significant gas production is observed during the reaction.
- The film thickness is constant at 2 mm.
- The rivulet width is constant at 5 mm.
- Only a single helix is produced.
- The number of turns in the helix is 15.
- The rise of the helix in one revolution is 40 mm.
- Helical behaviour is observed for the full 600 mm of the work-tube.

The rivulet has been treated as though it is a ribbon which can be unfurled to give a cuboid (dimensions: path length x 2 mm x 5 mm). The path length can be found *via* the following calculation shown in Eqn. 14.11:

$$Pathlength, D = N\sqrt{H^2 + (2\pi r)^2} + (600 - L_h) = 15\sqrt{40^2 + (2\pi 18)^2} = 1.8 \text{ m} \tag{14.11}$$

Therefore the volume of the rivulet (and thus the volume of the reactor), shown in Eqn. 14.12 is:

$$Volume = 1.8 \text{ m} \cdot 2 \times 10^{-3} \text{ m} \cdot 5 \times 10^{-3} \text{ m} = 1.8 \times 10^{-5} \text{ m}^3 \tag{14.12}$$

Thus, the space-time yield of the HeRo process, calculated from the 8 h experiment is found by the following calculation shown in Eqn. 14.13:

$$Space - time\ yield = \frac{0.2857 \text{ kg}}{1.8 \times 10^{-5} \text{ m}^3 \cdot 8 \text{ h}} = 1980 \text{ kg m}^{-3} \text{ h}^{-1} \tag{14.13}$$

This is more than 3.5 times than the space-time yield of the Vapourtec® process, and approx. 36 times the space-time yield of the most efficient batch process. These results are summarised below (Table 14.4).

Table 14.4 Throughputs and space-time yields for various syntheses of coumalic acid.

Reference	Throughput/ g h^{-1}	Space-time yield/ kg m^{-3} h^{-1}
Wiley *et al.*[16]	17.6	55.1
Ashworth *et al.*[17]	11.8	37.1
Kraus *et al.*[19]	0.13	1.5
Batch (based on Kaminski *et al.*[18])	6.7	6.7
Masterflex-pumped flow process	11.2	560
HeRo reactor	35.7	1980

14.14 Chemical engineering implications

At this point, a meeting was held with Prof Philip Gaskell and Dr Lian Gan (School of Engineering and Computer Science, Durham University). The reactor design and construction were discussed, as were the data collection procedures. In engineering terms, the process can be described as a rivulet wetting the surface of a rotating heated inclined cone. There are two phases (liquid and gaseous) and it can be considered as an evaporation process due to the gas production. The current set-up is too complex to model, and the helical behaviour of the rivulet depends on too many variables.

An alternative reactor design was proposed by Prof Gaskell which transforms the set-up into a thin-film problem which is easier to calculate and model. A central roller made of materials which are chemically compatible with concentrated sulfuric acid (for example: ceramic, glass, steel core with a glass coating, etc.) would be surrounded by fixed external heaters (infra-red). The solution of malic acid in conc. H_2SO_4 would be delivered to the surface of the roller, and it would travel through the heated arc-path before being collected when the reaction is complete, possibly by scraping the film from the roller surface (Fig. 14.47).

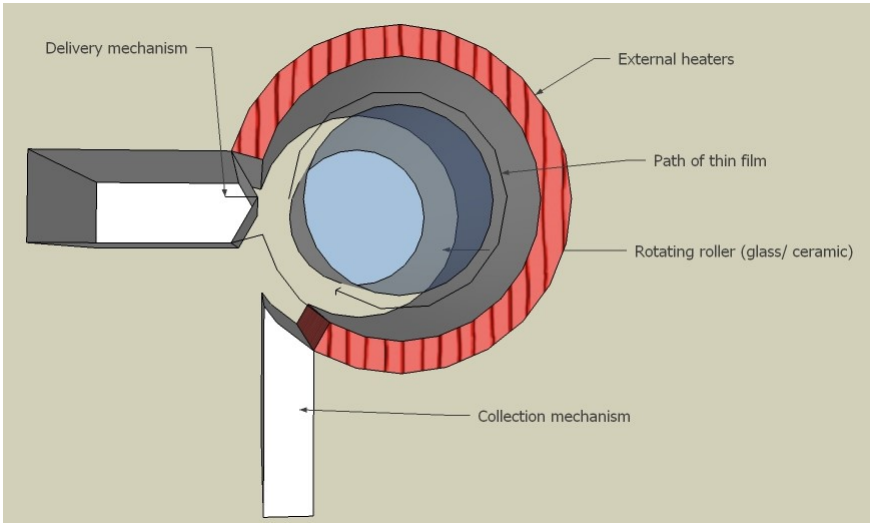

Fig. 14.47 Diagram of the proposed rotating roller reactor.

The temperature, rotation speed, film thickness and roller diameter would be optimised to achieve the maximum possible conversion/ yield and throughput. The length of the roller gives the possibility of performing this reaction on extremely large scales. Similarly, increasing the number of rollers would scale the reaction up even further; this can be seen in the suggested double roller system below (Fig. 14.48).

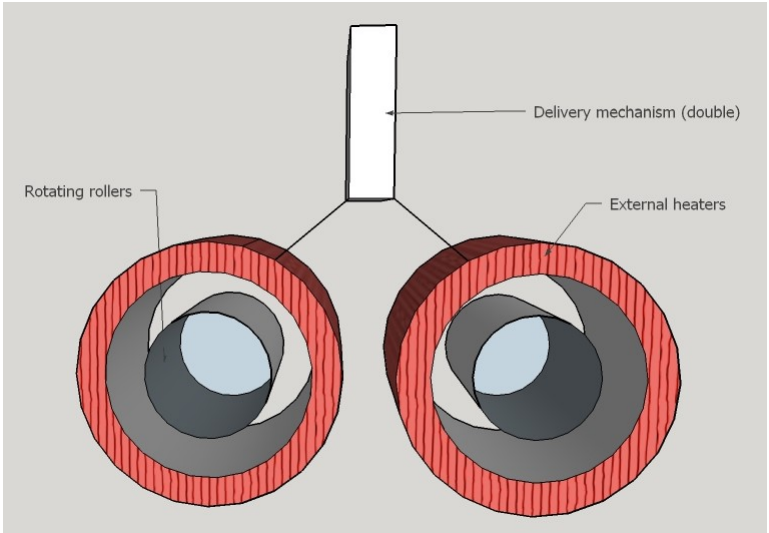

Fig. 14.48 Diagram of the proposed double rotating roller reactor.

14.15 Conclusions

A new type of flow reactor has been developed, which we have nicknamed the 'HeRo' reactor. It consists of a heated rotating work-tube held at an angle into which starting materials are dropped. The product is collected at the bottom.

We have used it to develop an intensified process for the synthesis of coumalic acid. It is more efficient in terms of throughput and space-time yield than any existing batch process, or the small-scale Vapourtec-based flow process that we have developed above. It has a lot of promise for future investigations.

Chapter 15

Derivatising Methyl Coumalate in Diels-Alder Reactions

The field of molecular electronics is rapidly expanding. Terphenyls are a class of compounds with applications in this area, but there are problems with the current literature syntheses. Even trace amounts of metals can disrupt their activity. An alternative is the use of inverse electron demand Diels-Alder reactions, with methyl coumalate as an electron-poor diene. An electron-rich dienophile such as an alkyne is required.

15.1 Diels-Alder reactions with methyl coumalate

Retrosynthetic analysis of terphenyls implies a synthetic route from methyl coumalate and dialkynes (Scheme 15.1).

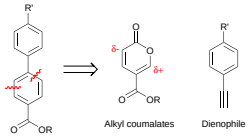

Scheme 15.1 Retrosynthetic analysis of terphenyls.

1,3-Diethynylbenzene as a dienophile

Two dienthynyls were chosen to attempt the Diels-Alder reaction under microwave irradiation conditions. Following a literature procedure, *tert*-butanol was used as an additive.[61,62] The first reaction used 1,3-diethynylbenzene as a substrate with methyl coumalate (Scheme 15.2). As an initial experiment, methyl

coumalate was used in a lower ratio than required for the double Diels-Alder reaction.

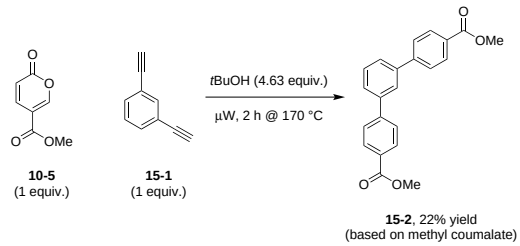

Scheme 15.2 Diels-Alder reaction of methyl coumalate and 1,3-diethynylbenzene.

Gas formation was observed at the end of the reaction, and the pressure inside the microwave vial had increased significantly during the reaction. This is due to decarboxylation. The product was isolated in low yield.

1,4-Diethynylbenzene as a dienophile

Similar conditions were applied to the 1,4-isomer of diethynylbenzene (Scheme 15.3), again with methyl coumalate as the limiting reagent.

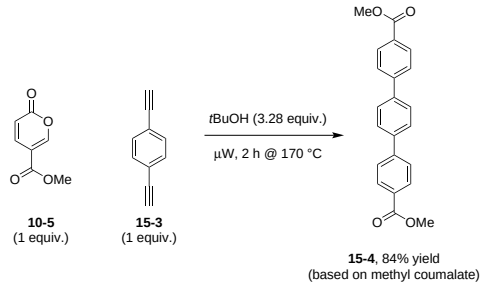

Scheme 15.3 Diels-Alder reaction of methyl coumalate and 1,4-diethynylbenzene.

The product was isolated in moderate yield.

15.2 Conclusions

These reactions require optimisation before they could be used more widely, but these are good examples as proof of concept. There are some benefits to this procedure: the use of the microwave gives efficient heating and a relatively short reaction time for what is typically regarded as a relatively difficult Diels-Alder reaction. This assists in reducing decomposition and side-products.

Optimisation could include altering the ratio between methyl coumalate and the diethyne, changing the amount of *tert*-BuOH additive, and alter the duration

and temperature of the microwave heating conditions. The work-up could be investigated, because both products are very insoluble in almost all common solvents. Once optimised, a wider range of substrates could be screened.

Chapter 16

Conclusions

Coumalic acid and its derivatives are valuable intermediates in organic synthesis, and can be obtained from malic acid. Other starting materials such as methyl-3,3-dimethoxypropionate were also tested, as were acid catalysts such as triflic acid, iron trichloride, and heteropoly acids. Ultimately, the combination of malic acid and concentrated sulfuric acid was the most promising for transfer into flow.

We have developed a flow process based on the Vapourtec reactor to synthesise coumalic acid and methyl coumalate from malic acid in conc. sulfuric acid. This has removed some of the problems associated with the difficult batch process, such as gas production and foaming. However, the pumping speed (and therefore throughput) was limited by the high viscosity of the sulfuric acid solution.

A new reactor design used a gravity feed to avoid the dependence on pumping of this viscous solution. We nicknamed this the 'HeRo' reactor, and it consists of a heated rotating work-tube held at an angle into which starting materials are dropped. We have employed the reactor to develop an intensified process for the synthesis of coumalic acid. The process was more efficient in terms of throughput and space-time yield than any existing batch or flow process.

Methyl coumalate has been used with two dialkynes in test Diels-Alder reactions. These triphenyl products have applications in molecular electronics, which requires multi-phenyls as components. This metal-free synthesis has several advantages over existing literature routes.

Chapter 17

Future Work

The next steps in developing this process include developing an industry-friendly reactor based on the prototype HeRo reactor built here. This would allow coumalic acid to be synthesised on a much larger scale, making it much more readily available as a starting material for other reactions.

The Vapourtec process was telescoped to include a methylation step. This has not yet been attempted with the HeRo reactor, but is likely to be logistically relatively simple.

Derivatisations based on the Diels-Alder reaction have a lot of scope for development and improvement. The two reactions shown here were first attempts, and act as a proof of concept which requires optimisation of the reaction conditions. Other dienophiles can be considered as well.

Chapter 18

Experimental

18.1 Coumalic acid, Compound 10-2

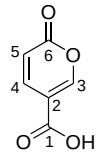

Chemical Formula: $C_6H_4O_4$
Exact Mass: 140.01

Batch procedure:

Malic acid (50.0 g, 373 mmol) was charged to a 250 mL RBF fitted with a stirrer bar. Concentrated sulfuric acid (100 mL, 1880 mmol) was charged to the RBF. The resulting slurry was heated at 90 °C with slow stirring for 6 h, during which time significant foaming was observed. The orange solution was allowed to cool to RT, then poured onto ice (400 mL), and stored in the freezer overnight. Formation of a yellow precipitate was observed. After filtration and washing with H_2O, the wet solid was air-dried at approx. 50 °C before drying under vacuum. The crude material was isolated as a pale yellow solid.

Isolated yield: 12.7 g (90.7 mmol, 49%)
^{1}H NMR (700 MHz, d_6−DMSO): δ/ppm 6.37 (1 H, dd, J = 9.8, 1.1 Hz, H2), 7.77 (1 H, dd, J = 9.7, 2.6 Hz, H3), 8.49 (1 H, dd, J = 2.6, 1.1 Hz, H5);
^{13}C NMR (176 MHz, d_6−DMSO): δ/ppm 112.5 (C4), 115.0 (C2), 143.0 (C3), 159.3 (C5), 160.4 (C1), 164.7 (C6).
IR (neat) ν = 2958.0 (O-H, br w), 1699.8 (C=O, s), 1544.5 (m), 1404.5 (m), 1226.3 (C-O, s), 1130.1 (m), 1097.3 (C-O, s), 952.1 (m), 847.8 (m), 772.8 (s),

617.9 (m), 526.7 (m) cm^{-1}.
LC-MS: R_t = 0.92 min, m/z 138.9 $[M\text{-}H]^-$; HR-MS calculated for $C_6H_3O_4$ at 139.0031, found 139.0020 (Δ = -7.9 ppm). Decomposition by 150.0 °C (MeOH).
Reference[18]

18.2 Methyl coumalate, Compound 10-5

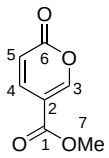

Chemical Formula: $C_7H_6O_4$
Exact Mass: 154.03

One-pot, two-step batch procedure from malic acid:

Malic acid (125.0 g, 933 mmol) was charged to a 1 L RBF fitted with a stirrer bar. Concentrated H_2SO_4 (250 mL, 465 mmol) was slowly charged to the RBF, and the resulting slurry was heated to 90 °C for 3 h, during which time frothing was observed. The solution was cooled to RT, then lowered into an ice bath. MeOH (160 mL, 3960 mmol) was charged dropwise over 15 mins. The solution was then heated at 90 °C for a further 2.5 h. The solution was allowed to cool to RT, then poured over ice and left overnight. Precipitation of the product was not observed. The orange solution was extracted with H_2O and DCM (100 mL x 3). The organic fractions were combined, and the volume reduced *in vacuo* to give the crude product as a yellow solid. Recrystallisation from EtOAc gave the product as a pale yellow solid in two crops, which were dried *in vacuo*.

Isolated yield: 19.130 g (124 mmol, 27%)
^{1}H NMR (700 MHz, $CDCl_3$): δ/ppm 3.87 (3 H, s, H7), 6.33 (1 H, dd, J = 9.8, 1.1 Hz, H2), 7.77 (1 H, dd, J = 9.8, 2.6 Hz, H3), 8.29 (1 H, dd, J = 2.6, 1.1 Hz, H5);
^{13}C NMR (126 MHz, $CDCl_3$): δ/ppm 52.4 (C7), 111.9 (C4), 115.3 (C2), 141.6 (C3), 158.1 (C5), 159.8 (C1), 163.4 (C6).
IR (neat) ν = 1706.4 (C=O, s), 1544.8 (w), 1440.4 (m), 1298.8 (m), 1238.0 (s), 1084.6 (C-O, m), 948.1 (m), 839.1 (m), 815.6 (m), 773.2 (s), 630.0 (w) cm^{-1}.
LC-MS: R_t = 1.04 min, m/z 155.3 $[MH]^+$; HR-MS calculated for $C_7H_7O_4$ at 155.0344, found 155.0347 (Δ = +1.9 ppm).
Melting point: 65.4-69.0 °C (EtOAc).
Reference[17]

18.3 Ethyl 2-oxo-2H-pyran-5-carboxylate - Ethyl coumalate, Compound 10-7

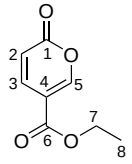

Chemical Formula: $C_8H_8O_4$
Exact Mass: 168.04

Procedure:

Coumalic acid (2.603 g, 14.8 mmol) was charged to a 50 mL RBF fitted with a stirrer bar, followed by EtOH (4.35 mL, 74.4 mmol) and conc. H_2SO_4 (5 mL, 93 mmol). The solution was heated at 90 °C for 3 h, at which point it was allowed to cool to RT before pouring over ice. Formation of brown, oily droplets was observed. Extraction with DCM (10 mL x 3)/H_2O (10 mL x 3)/NaCl (10 mL x 3), combination of the organic layers, drying over Na_2SO_4 and concentrating *in vacuo* gave the crude product as an orange oil.

Isolated yield: 1.650 g (9.82 mmol, 53%)
^{1}H NMR (700 MHz, d_6−DMSO): δ/ppm 1.26 (3 H, t, J = 7.1 Hz, H8), 4.25 (2 H, q, J = 7.1 Hz, H7), 6.41 (1 H, dd, J = 9.8, 1.1 Hz, H2), 7.80 (1 H, dd, J = 9.8, 2.7 Hz, H3), 8.56 (1 H, dd, J = 2.6, 1.1 Hz, H5);
^{13}C NMR (126 MHz, d_6−DMSO): δ/ppm 14.5 (C8), 61.6 (C7), 112.0 (C4), 115.2 (C2), 142.5 (C3), 159.6 (C5), 160.2 (C1), 163.2 (C6).
IR (neat) ν = 1751.3 (C=O, m), 1713.3 (C=O, s), 1288.1 (C-O, s), 1234.5 (C-O, s), 1078.2 (C-O, s), 770.3 (m) cm^{-1}.
LC-MS: R_t = 2.37 min, m/z 169.0 $[MH]^+$; HR-MS calculated for $C_8H_9O_4$ at 169.0501, found 169.0498 (Δ = -1.8 ppm).
Reference[63]

18.4 Propan-2-yl 2-oxo-2H-pyran-5-carboxylate - Isopropyl coumalate

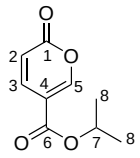

Chemical Formula: $C_9H_{10}O_4$
Exact Mass: 182.06

Procedure:

Coumalic acid (2.608 g, 14.8 mmol) was charged to a 50 mL RBF fitted with a stirrer bar, followed by IPA (5.7 mL, 74.4 mmol) and conc. H_2SO_4 (5 mL, 93 mmol). The solution was heated at 90 °C for 3 h, at which point it was allowed to cool to RT before pouring over ice. Formation of brown, oily droplets was observed. Extraction with DCM (10 mL x 3)/H_2O (10 mL x 3)/NaCl (10 mL x 3), combination of the organic layers, drying over Na_2SO_4 and concentrating *in vacuo* gave the crude product as a dark brown oil. Purification by column chromatography (Hex: EtOAc 1: 1) gave the product as a brown oil.

Isolated yield: 1.576 g (8.66 mmol, 44%)
^{1}H NMR (700 MHz, d_6−DMSO): δ/ppm 1.26 (6 H, d, J = 6.3 Hz, H8), 5.05 (1 H, h, J = 6.3 Hz, H7), 6.39 (1 H, d, J = 10.9 Hz, H2), 7.78 (1 H, dd, J = 9.8, 2.7 Hz, H3), 8.52 (1 H, dd, J = 2.7, 1.1 Hz, H5);
^{13}C NMR (126 MHz, d_6−DMSO): δ/ppm 22.0 (C8), 69.3 (C7), 112.2 (C4), 115.2 (C2), 142.5 (C3), 159.5 (C5), 160.1 (C1), 162.7 (C6).
IR (neat) ν = 1754.8 (C=O, m), 1712.5 (C=O, s), 1289.2 (C-O, s), 1234.7 (C-O, m), 1076.9 (C-O, s), 772.9 (m) cm^{-1}.
LC-MS: R_t = 2.61 min, m/z 183.5 $[MH]^+$; HR-MS calculated for $C_9H_{11}O_4$ at 183.0657, found 183.0668 (Δ = +6.0 ppm).
No literature data available.

18.5 Hexyl 2-oxo-2H-pyran-5-carboxylate - Hexyl coumalate

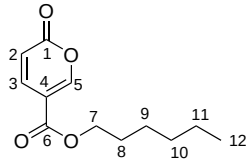

Chemical Formula: $C_{12}H_{16}O_4$
Exact Mass: 224.10

Procedure:

Coumalic acid (2.609 g, 14.8 mmol) was charged to a 50 mL RBF fitted with a stirrer bar, followed by 1-hexanol (9.3 mL, 74.4 mmol) and conc. H_2SO_4 (5 mL, 93 mmol). The solution was heated at 90 °C for 3 h, then allowed to cool to RT before pouring over ice. Formation of brown, oily droplets was observed. Extraction with DCM (10 mL x 3)/H_2O (10 mL x 3)/NaCl (10 mL x 3), combination of the organic layers, drying over Na_2SO_4 and concentrating *in vacuo* gave the crude product as a dark brown oil. Purification by column chromatography (Hex: EtOAc 1: 1) gave the product as a brown oil.

Isolated yield: 2.790 g (12.4 mmol, 64%)
^{1}H NMR (700 MHz, d_6−DMSO): δ/ppm 0.82-0.85 (3 H, m, H12), 1.14-1.30 (8 H, m, H8+9+10+11), 4.19 (2 H, t, J = 6.6 Hz, H7), 6.40 (1 H, d, J = 10.9 Hz, H2), 7.79 (1 H, d, J = 12.4 Hz, H3), 8.55 (1 H, s, H5);
^{13}C NMR (176 MHz, d_6−DMSO): δ/ppm 14.3 (C12), 22.4 (C8/9/10/11), 26.4 (C8/9/10/11), 28.5 (C8/9/10/11), 31.3 (C8/9/10/11), 65.4 (C7), 111.9 (C4), 115.2 (C2), 142.4 (C3), 159.6 (C5), 160.1 (C1), 163.6 (C6).
IR (neat) ν = 1756/9 (C=O, s), 1289.4 (C-O, s), 1234.4 (C-O, m), 1082.0 (C-O, s), 772.2 (m) cm^{-1}.
LC-MS: R_t = 3.53 min, m/z 225.5 $[MH]^+$; HR-MS calculated for $C_{12}H_{17}O_4$ at 225.1127, found 225.1129 (Δ = +0.9 ppm).
No literature data available.

18.6 Octyl 2-oxo-2H-pyran-5-carboxylate - Octyl coumalate

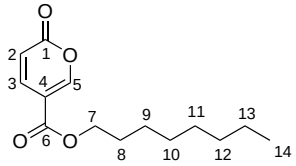

Chemical Formula: $C_{14}H_{20}O_4$
Exact Mass: 252.14

Procedure:

Coumalic acid (2.604 g, 14.8 mmol) was charged to a 50 mL RBF fitted with a stirrer bar, followed by 1-octanol (11.7 mL, 74.4 mmol) and conc. H_2SO_4 (5 mL, 93 mmol). The solution was heated at 90 °C for 3 h, at which point it was allowed to cool to RT before pouring over ice. Formation of brown, oily droplets was observed. Extraction with DCM (10 mL x 3)/H_2O (10 mL x 3)/NaCl (10 mL x 3)/Et_2O (10 mL x 3), combination of the organic layers, drying over Na_2SO_4 and concentrating *in vacuo* gave the crude product as a brown oil which was not purified further due to the co-elution of octanol with the product.

Isolated yield: 7.502 g (29.8 mmol, 160% crude yield)
^{1}H NMR (400 MHz, d_6-DMSO): δ/ppm 0.84-0.86 (15 H, m, H8-14), 4.22 (2 H, t, J = 6.6 Hz, H7), 6.44 (1 H, d, J = 10.9 Hz, H2), 7.82 (1 H, dd, J = 9.8, 2.7 Hz, H3), 8.59 (1 H, dd, J = 2.7, 1.1 Hz, H5).
IR (neat) ν = 1761.4 (C=O, m), 1724.3 (C=O, s), 1290.5 (C-O, s), 1235.3 (C-O, s), 1084.4 (C-O, s), 773.1 (m) cm^{-1}.
No literature data available.

18.7 Decyl 2-oxo-2H-pyran-5-carboxylate - Decyl coumalate

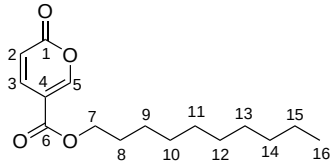

Chemical Formula: $C_{16}H_{24}O_4$
Exact Mass: 280.17

Procedure:

Coumalic acid (2.610 g, 14.8 mmol) was charged to a 50 mL RBF fitted with a stirrer bar, followed by 1-decanol (14.2 mL, 74.4 mmol) and conc. H_2SO_4 (5 mL, 93 mmol). The solution was heated at 90 °C for 3 h, at which point it was allowed to cool to RT before pouring over ice. Formation of brown, oily droplets was observed. Extraction with Et_2O (10 mL x 3)/NaCl (10 mL x 3), combination of the organic layers, drying over Na_2SO_4 and concentrating *in vacuo* gave the crude product as a brown oil which was not purified further due to the co-elution of decanol with the product.

Isolated yield: 8.030 g (28.7 mmol, 154% crude yield)
^{1}H NMR (400 MHz, d_6-DMSO): δ/ppm 0.88-0.91 (19 H, m, H8-16), 4.25-4.31 (2 H, m, H7), 6.36 (1 H, dd, J = 9.8, 1.1 Hz, H2), 7.81 (1 H, dd, J = 9.8, 2.6 Hz, H3), 8.31 (1 H, dd, J = 2.6, 1.1 Hz, H5).
IR (neat) ν = 1761.1 (C=O, m), 1724.4 (C=O, s), 1290.1 (C-O, s), 1234.9 (C-O, m), 1083.0 (C-O, s), 772.8 (m) cm^{-1}.
No literature data available.

18.8 $H_5PMo_{10}V_2O_{40} \cdot xH_2O$

Procedure:[60]

$NaVO_3$ (24.4 g, 200 mmol) was charged to a 1 L RBF fitted with a stirrer bar. H_2O (100 mL) was added to the RBF, and stirring begun, heating to reflux for 1 h with a Vigreux column. Na_2HPO_4 (7.1 g, 50 mmol) was dissolved in H_2O (100 mL), and the resulting solution was added to the RBF. The mixture was allowed to cool to RT, and conc. H_2SO_4 (5 mL) was added to the solution, upon which the colour changed from pale yellow to very dark red. $Na_2MoO_4 \cdot 2\,H_2O$ (121.0 g, 500 mmol) was dissolved in H_2O (200 mL), and the solution transferred to a dropping funnel fitted to the RBF. The solution was added dropwise over 20 mins, and the mixture was stirred at RT for 1 h. Conc. H_2SO_4 (85 mL) was added dropwise over 30 mins and an exotherm of 15 °C was observed. The solution was extracted with Et_2O which produced 3 layers: the lowest and fluorescent layer was the hetereopoly etherate. The middle layer was aqueous, and the top layer was the organic layer. The bottom layer was collected, and the Et_2O allowed to evaporate slowly. The product was a complicated dark red crystalline mixture.

Isolated yield: 33.8 g
^{31}P NMR (162 MHz, d_6-DMSO): δ/ppm -1.08, -2.89, -3.08, -3.33, -3.73, -4.06, -4.19, -4.59 ppm.
LC-MS: R_t = 0.23 min, m/z 873 (ES^-).
Reference[60]

18.9 Ethyl 3,3-dimethoxy-2-methylbutyrate

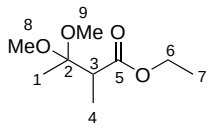

Chemical Formula: $C_9H_{18}O_4$
Exact Mass: 190.12

Procedure:

Ethyl 2-methylacetoacetate (15.2 mL, 108 mmol) was charged to a 3-necked 250 mL RBF fitted with a stirrer bar, condenser and two septa. MeOH (30 mL, 743 mmol) was charged to the RBF to give an orange solution. Trimethylorthoformate (15.5 mL, 151 mmol) was charged to the RBF, followed by concentrated H_2SO_4, whereupon the solution turned yellow. The solution was heated at reflux for 4.5 h, turning dark in colour. The reaction was allowed to cool to RT, then cooled in an ice bath for 15 mins. The mixture was quenched by pouring into an aqueous solution of KOH (0.3 g KOH in 150 mL H_2O), then cooled in an ice bath for 5 mins. The solution was extracted with Et_2O (30 mL), then the combined organic layers were rinsed with brine (20 mL), dried over Na_2SO_4 and filtered. Removal of the solvent *in vacuo* gave the crude product as an orange oil.

Isolated yield: 18.1 g (95.3 mmol, 88%)
^{1}H NMR (700 MHz, $CDCl_3$): δ/ppm 1.13 (3 H, d, J = 7.2 Hz, H4), 1.24 (3 H, t, J = 7.1 Hz, H7), 1.34 (3 H, s, H1), 2.93 (1 H, q, J = 7.1 Hz, H3), 3.15 (3 H, s, H8), 3.21 (3 H, s, H9), 4.13 (2 H, qq, J = 7.0, 3.7 Hz, H6);
^{13}C NMR (126 MHz, $CDCl_3$): δ/ppm 12.9 (C4), 14.1 (C7), 17.4 (C1), 44.8 (C3), 47.8 (C8), 48.4 (C9), 60.3 (C6), 102.2 (C2), 173.6 (C5).
IR (neat) ν = 2982.3 (w), 1732.7 (C=O, s), 1456.4 (w), 1373.5 (w), 1197.2 (C-O, s), 1123.0 (C-O, s), 1052.1 (C-O, s), 873.9 (m) cm^{-1}.
Reference[64]

18.10 Dimethyl 1,1':3',1"-terphenyl-4,4"-dicarboxylate, Compound 15-2

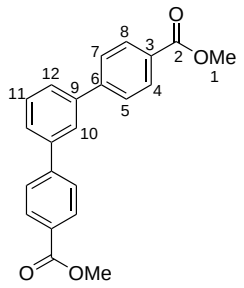

Chemical Formula: $C_{22}H_{18}O_4$
Exact Mass: 346.12

Procedure:[61,62]

Methyl coumalate (0.156 g, 1.01 mmol) and 1,3-diethynylbenzene (0.14 mL, 1.00 mmol) were charged to a microwave vial fitted with a stirrer bar, followed by *t*-BuOH (0.343 g, 4.21 mmol). The vial was capped, sealed and heated to 170 °C for 2 h with 5 mins pre-stirring in the microwave. The high pressure was slowly released, and H_2O (2 mL) and EtOH (2 mL) were added to the vial. Precipitation occurred, forming clumps of a dark orange solid. After filtration and drying *in vacuo*, the crude product was obtained as a dark orange solid.

Isolated yield: 0.037 g (0.11 mmol, 22%)
^{1}H NMR (700 MHz, $CDCl_3$): δ/ppm 3.93 (6 H, d, J = 6.1 Hz, H1), 7.41 (1 H, t, J = 7.8 Hz, H11), 7.51 (1 H, dt, J = 7.1, 1.3 Hz, H12), 7.59 (1 H, dt, J = 7.8, 1.4 Hz, H12), 7.63 (2 H, d, J = 8.6 Hz, H4/5/7/8), 7.71 (1 H, d, J = 8.5 Hz, H4/5/7/8), 7.74 (1 H, t, J = 1.5 Hz, H10), 8.10 (2 H, d, J = 8.6 Hz, H4/5/7/8), 8.13 (1 H, d, J = 8.5 Hz, H4/5/7/8);
^{13}C NMR (176 MHz, $CDCl_3$): δ/ppm 52.2 (C1), 122.8 (C), 127.0 (C4/5/7/8), 127.1 (C4/5/7/8), 127.7 (C12), 128.9 (C11), 130.14 (C4/5/7/8), 130.15 (C4/5/7/8), 130.9 (C10), 131.6 (C12), 140.2 (C), 144.5 (C), 166.8 (C2).
IR (neat) ν = 1712.7 (C=O, s), 1431.6 (m), 1278.4 (C-O, s), 1191.4 (m), 1109.7 (s), 765.2 (s), 700.0 (m) cm^{-1}.
Melting point: decomposition by 100.0 °C (AcOH), literature = 192 °C (AcOH).
Reference[65]

18.11 Dimethyl 1,1':4',1"-terphenyl-4,4"-dicarboxylate, Compound 15-4

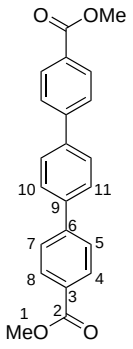

Chemical Formula: $C_{22}H_{18}O_4$
Exact Mass: 346.12

Procedure:[61,62]

Methyl coumalate (0.154 g, 1.00 mmol) and 1,4-diethynylbenzene (0.14 mL, 1.00 mmol) were charged to a microwave vial fitted with a stirrer bar, followed by *t*-BuOH (0.243 g, 3.28 mmol). The vial was capped, sealed and heated to 170 °C for 2 h with 5 mins pre-stirring in the microwave. The high pressure was slowly released, and H_2O (2 mL) and EtOH (2 mL) were added to the vial. Precipitation occurred, generating brown flakes. After filtration and drying *in vacuo*, the crude product was obtained as a multi-coloured brown solid, which was highly insoluble.

Isolated yield: 0.147 g (0.42 mmol, 84%)
^{1}H NMR (700 MHz, d_6-DMSO): δ/ppm 3.86 (6 H, s, H1), 7.81-7.88 (8 H, m, H5+7+10+11), 8.03 (4 H, dd, J = 14.5, 8.4 Hz, H4+8);
IR (neat) ν = 1718.9 (C=O, s), 1432.7 (m), 1274.7 (C-O, s), 1193.3 (m), 1109.9 (s), 829.0 (s), 762.1 (s) cm^{-1}.
Melting point: decomposition by 280.0 °C (DMF), literature = 315 °C (DMF).
Reference[66]

References

[1] P. Anastas and J. Warner, *Green Chemistry Theory and Practice*, OUP, 2000.

[2] A. Corma, S. Iborra and A. Velty, *Chemical Reviews*, 2007, **107**, 2411–2502.

[3] R. A. Sheldon, *Green Chemistry*, 2014, **16**, 950–963.

[4] T. Werpy and G. Petersen, *Top Value Added Chemicals from Biomass Volume I*, United States Department of Energy technical report, 2004.

[5] P. M. Delaney, J. E. Moore and J. P. A. Harrity, *Chemical Communications*, 2006, 3323–3325.

[6] P. M. Delaney, D. L. Browne, H. Adams, A. Plant and J. P. A. Harrity, *Tetrahedron*, 2008, **64**, 866–873.

[7] J. D. Kirkham, P. M. Delaney, G. J. Ellames, E. C. Row and J. P. A. Harrity, *Chemical Communications*, 2010, **46**, 5154–5156.

[8] J. J. Lee and G. A. Kraus, *Green Chemistry*, 2014, **16**, 2111–2116.

[9] G. A. Kraus, G. R. Pollock III, C. L. Beck, K. Palmer and A. H. Winter, *RSC Advances*, 2013, **3**, 12721–12725.

[10] J. J. Lee and G. A. Kraus, *Tetrahedron Letters*, 2013, **54**, 2366–2368.

[11] M. W. Smith and S. A. Snyder, *Journal of the American Chemical Society*, 2013, **135**, 12964–12967.

[12] M. Feng and X. Jiang, *Chemical Communications*, 2014, **50**, 9690–9692.

[13] W. R. Gutekunst and P. S. Baran, *Journal of the American Chemical Society*, 2011, **133**, 19076–19079.

[14] W. R. Gutekunst, R. Gianatassio and P. S. Baran, *Angewandte Chemie International Edition*, 2012, **51**, 7507–7510.

[15] H. von Pechmann, *Annalen der Chemie*, 1891, **264**, 261–309.

[16] R. H. Wiley and N. R. Smith, *Organic Synthesis*, 1963, **4**, 201–202.

[17] I. W. Ashworth, M. C. Bowden, B. Dembofsky, D. Levin, W. Moss, E. Robinson, N. Szczur and J. Virica, *Organic Process Research and Development*, 2003, **7**, 74–81.

[18] T. Kaminski and G. Kirsch, *Journal of Heterocyclic Chemistry*, 2008, **45**, 229–234.

[19] G. A. Kraus, *WO2014189926A1*, 2014.

[20] J. H. Boyer and W. Schoen, *Organic Synthesis*, 1956, **36**, 44.

[21] K. C. Nicolaou, S. A. Snyder, T. Montagnon and G. Vassilikogiannakis, *Angewandte Chemie International Edition*, 2002, **41**, 1668–1698.

[22] P. M. Delaney, J. E. Moore and J. P. A. Harrity, *Chemical Communications*, 2006, 3323–3325.

[23] P. M. Delaney, D. L. Browne, H. Adams, A. Plant and J. P. A. Harrity, *Tetrahedron*, 2008, **64**, 866–873.

[24] J. D. Kirkham, P. M. Delaney, G. J. Ellames, E. C. Row and J. P. A. Harrity, *Chemical Communications*, 2010, **46**, 5154–5156.

[25] J. J. Lee and G. A. Kraus, *Green Chemistry*, 2014, **16**, 2111–2116.

[26] G. A. Kraus, G. R. Pollock III, C. L. Beck, K. Palmer and A. H. Winter, *RSC Advances*, 2013, **3**, 12721–12725.

[27] J. J. Lee and G. A. Kraus, *Tetrahedron Letters*, 2013, **54**, 2366–2368.

[28] M. W. Smith and S. A. Snyder, *Journal of the American Chemical Society*, 2013, **135**, 12964–12967.

[29] M. Feng and X. Jiang, *Chemical Communications*, 2014, **50**, 9690–9692.

[30] W. R. Gutekunst and P. S. Baran, *Journal of the American Chemical Society*, 2011, **133**, 19076–19079.

[31] W. R. Gutekunst, R. Gianatassio and P. S. Baran, *Angewandte Chemie International Edition*, 2012, **51**, 7507–7510.

[32] J. M. Tour, *Accounts of Chemical Research*, 2000, **33**, 791–804.

[33] D. Astruc, E. Boisselier and C. Ornelas, *Chemical Reviews*, 2010, **110**, 1857–1959.

[34] I. V. Kozhevnikov and K. I. Matveev, *Applied Catalysis*, 1983, **5**, 135–150.

[35] M. Misono and N. Nojiri, *Applied Catalysis*, 1990, **64**, 1–30.

[36] I. V. Kozhevnikov, S. Kulikov, N. G. Chukaeva, A. T. Kirsanov, A. B. Letunova and V. I. Blinova, *Reaction Kinetics and Catalysis Letters*, 1992, **47**, 59–64.

[37] Y. Izumi, K. Matsuo and K. Urabe, *Journal of Molecular Catalysis*, 1983, **18**, 299–314.

[38] A. Aoshima, S. Tonomura and S. Yamamatsu, *Polymers for Advanced Technologies*, 1990, **2**, 127–132.

[39] I. V. Kozhevnikov, A. Sinnema, A. J. A. Van Der Weerdt and H. van Bekkum, *Journal of Molecular Catalysis A Chemistry*, 1997, **120**, 63–70.

[40] H. Soeda, T. Okuhara and M. Misono, *Chemistry Letters*, 1994, **23**, 909–912.

[41] P. Dupont and F. Lefebvre, *Journal of Molecular Catalysis A Chemistry*, 1996, **114**, 299–307.

[42] I. V. Kozhevnikov, *Chemical Reviews*, 1998, **98**, 171–198.

[43] M. Tani, T. Sakamoto, S. Mita, S. Sakaguchi and Y. Ishii, *Angewandte Chemie International Edition*, 2005, **44**, 2586–2588.

[44] T. Yokota, S. Fujibayashi, Y. Nishiyama, Y. Ishii and S. Sakaguchi, *Journal of Molecular Catalysis A Chemistry*, 1996, **114**, 113–122.

[45] K. I. Tamaso, Y. Hatamoto, S. Sakaguchi, Y. Obora and Y. Ishii, *Journal of Organic Chemistry*, 2007, **72**, 3603–3605.

[46] S. Fujibayashi, K. Nakayama, M. Hamamoto, S. Sakaguchi, Y. Nishiyama and Y. Ishii, *Journal of Molecular Catalysis A Chemistry*, 1996, **110**, 105–117.

[47] M. Hamamoto, K. Nakayama, Y. Nishiyama and Y. Ishii, *Journal of Organic Chemistry*, 1993, **58**, 6421–6425.

[48] R. Neumann and A. M. Khenkin, *Chemical Communications*, 2006, 2529–2538.

[49] M. Lissel, H. J. in de Wal and R. Neumann, *Tetrahedron Letters*, 1992, **33**, 1795–1798.

[50] C. Venturello, E. Alneri and M. Ricci, *Journal of Organic Chemistry*, 1983, **48**, 3831–3833.

[51] S. Sakaue, T. Tsubakino, Y. Nishiyama and Y. Ishii, *Journal of Organic Chemistry*, 1993, **58**, 3633–3638.

[52] S. Sakaue, Y. Sakata, Y. Nishiyama and Y. Ishii, *Chemistry Letters*, 1992, 289–292.

[53] T. Oguchi, Y. Sakata, N. Takeuchi, K. Kaneda, Y. Ishii and M. Ogawa, *Chemistry Letters*, 1989, 2053–2056.

[54] Y. Ishii, H. Tanaka and Y. Nishiyama, *Chemistry Letters*, 1994, 1–4.

[55] S. Sakaguchi, S. Watase, Y. Katayama, Y. Sakata, Y. Nishiyama and Y. Ishii, *Journal of Organic Chemistry*, 1994, **59**, 5681–5686.

[56] Y. Ishii, K. Yamawaki, T. Ura, H. Yamada, T. Yoshida and M. Ogawa, *Journal of Organic Chemistry*, 1988, **53**, 3587–3593.

[57] Y. Ishii and Y. Sakata, *Journal of Organic Chemistry*, 1990, **55**, 5545–5547.

[58] Y. Sakata and Y. Ishii, *Journal of Organic Chemistry*, 1991, **56**, 6233–6235.

[59] S. Maeda, Y. Obora and Y. Ishii, *European Journal of Organic Chemistry*, 2009, 4067–4072.

[60] G. A. Tsigdinos and C. J. Hallada, *Inorganic Chemistry*, 1968, **7**, 437–441.

[61] K. Kranjc and M. Kocevar, *Collection of Czechoslovak Chemical Communications*, 2006, **71**, 667–678.

[62] F. Effenberger and T. Ziegler, *Chemische Berichte*, 1987, **120**, 1339–1346.

[63] C. R. Engel, A. F. de Krassny, A. Bélanger and G. Dionne, *Canadian Journal of Chemistry*, 1973, **51**, 3263–3271.

[64] F. Orsini and S. Rinaldi, *Tetrahedron: Asymmetry*, 1997, **8**, 1039–1048.

[65] S. Banfi, F. Montanari, G. Pozzi and S. Quici, *Tetrahedron*, 1994, **50**, 9025–9036.

[66] T. W. Campbell, *Journal of the American Chemical Society*, 1960, **82**, 3126–3128.

Part III

The Darzens Reaction in Flow

Chapter 19

Literature Review

19.1 Introduction

Overview of the Darzens reaction

The Darzens condensation is a well-established synthetic tool to form α,β-epoxy esters and their derivatives. It involves the reaction of a carbonyl compound with an α-halo ester in the presence of a base to form a halohydrin-type intermediate. A subsequent ring closure forms the glycidic ester (Scheme 19.1). There are many methods for the formation of epoxides, but the Darzens reaction involves a non-oxidative mechanism to give epoxides bearing electron-withdrawing groups.[1]

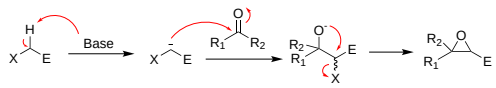

Scheme 19.1 General form of the Darzens condensation.

Although named after Auguste Darzens, the reaction was first reported in 1892 by Emil Erlenmeyer,[2] who combined benzaldehyde and ethyl chloroacetate with sodium to form ethyl β-phenyl-α,β-epoxy propionate, a glycidic ester (Scheme 19.2).

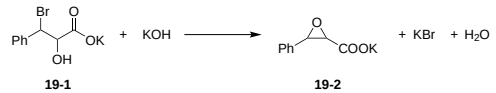

Scheme 19.2 An example of Erlenmeyer's work on epoxide formation.

Darzens later generalised this to become the classically known condensation, with his early defining work on the reaction demonstrating the breadth of modification and adaptation that can be tolerated,[3–12] which in turn has led it to be considered as an important non-oxidative method for the synthesis of epoxides. Risinger summarised the historical developments of the reaction in 1961.[13]

The broad synthetic scope of the reaction can be ascribed to the variety of possible reaction conditions and wide tolerance of functional groups.[14] Although originally the enolate was formed from simple esters, many alternative substituents have subsequently been shown to be amenable. This expansion to a more generalised reaction has ensured its continuing relevance, with a wide variety of different solvents and bases providing effective conditions for the reaction. The use of α,α-dihalogen epoxy esters has expanded the scope of its usage considerably.[15–18] The aza-Darzens reaction has also been reported in the formation of the nitrogen equivalent of the epoxide, the aziridine,[1] but this will not be reported on in any detail in this review.

Perhaps one of the most promising advances in the use of the reaction in recent years has been in the greater control of stereoisomers and in the development of the asymmetric reaction.[19] Potential uses of a catalytic asymmetric Darzens reaction are far-reaching, particularly within pharmaceutical chemistry.[20] However, we know of no examples of syntheses of pharmaceutical compounds that currently use the catalytic asymmetric Darzens reaction.

Although this short literature review will focus primarily on the usages of the reaction within the pharmaceutical industry, it is important to note that epoxides are also found in natural products such as the mosquito pheromone of *Culex pipiens fatigans* (Fig. 19.1).[21]

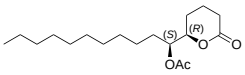

19-3

Fig. 19.1 Pheromone of *Culex pipiens fatigans*.

Mechanism of the Darzens reaction

It should be noted that no definitive mechanism for the Darzens reaction has yet been established, despite its long synthetic lifetime and extensive research.

However, it is known that the reaction proceeds *via* a carbanion intermediate.[22] Alternative mechanisms *via* a carbene or ketene have been considered,[23–26] but ultimately discarded.[22,27–29] The mechanism is thought to proceed *via* an aldol-like nucleophilic addition of the carbanion to a carbonyl compound, followed by an internal S_N2-like cyclisation to form the epoxide (Scheme 19.3).

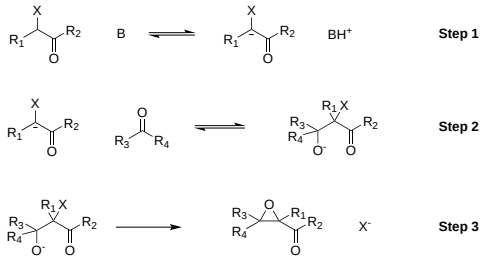

Scheme 19.3 The generally-accepted mechanism of the Darzens reaction.

19.2 The classical Darzens reaction

The versatility of the Darzens condensation has facilitated its incorporation into the industrial synthesis of a number of pharmaceuticals throughout the 20$^{\text{th}}$ century. Presently the reaction does not seem to be considered a primary method for epoxide formation, and this is reflected in the limited number of recent examples. Whether this is due to shortcomings of the reaction, or the existence of superior alternatives will be explored in this section.

The traditional form of the reaction has been successfully implemented into industrial scale syntheses, most notably with its involvement in the one-carbon homologation stages of both vitamin A and ibuprofen. Additionally, a more recent example made use of the Darzens condensation in an alternative method to synthesise (±)-epiasarinin.

Boots synthesis of ibuprofen

In the 1960s, whilst searching for a drug to treat rheumatoid arthritis, the Boots Company discovered and patented the compound ibuprofen (2-(4-methylpropyl)phenylpropanoic acid).[30] The process for their synthesis of ibuprofen is known as the 'Boots synthesis', and consists of six steps, including a Darzens condensation (Scheme 19.4).[31] Ibuprofen is classified as a non-steroidal anti-inflammatory drug (NSAID) and is used to relieve pain, inflammation and fever. The starting material for the synthesis is isobutylbenzene.

The role of the Darzens reaction is as part of a homologation step which is achieved in the formation and subsequent opening of the oxirane ring. The glycidic ester is formed in a classical Darzens synthesis. The ester then undergoes saponification to generate a carboxylic acid, which is followed by a ring-opening step and subsequent decarboxylation (Scheme 19.4).

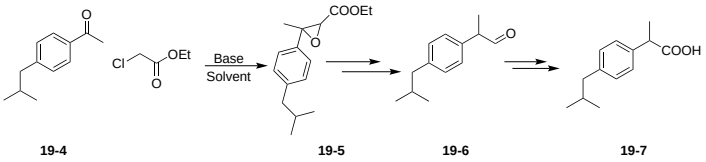

Scheme 19.4 Ring-opening and decarboxylation in the synthesis of ibuprofen.

The expiration of the ibuprofen patent has led to the Boots synthesis falling out of favour. The original process was relatively atom-inefficient and has been replaced by a 'green synthesis' developed by BHC[32] (now BASF), with a much greater atom economy: Boots reported an atom econommy of 40% whilst BHC reports 77%. Part of the atomic inefficiency can be attributed to the Darzens reaction stage, as almost all of the atoms used are not present in the final structure.

Hoffmann-La Roche synthesis of vitamin A

Vitamin A and other retinoid compounds have found a variety of medical applications, particularly in combating vitamin A deficiency in children from developing countries.[33]

Both the Hoffmann-La Roche and Boots syntheses use the Darzens reaction in mechanistically similar ways except for the migration of the carbon-carbon double bond in β-ionone in the Hoffmann-La Roche mechanism (Scheme 19.5).[34] The ability to convert a β-ionone to a β-C14 aldehyde[35] has allowed the synthesis of a number of other retinoid derivatives.[36,37]

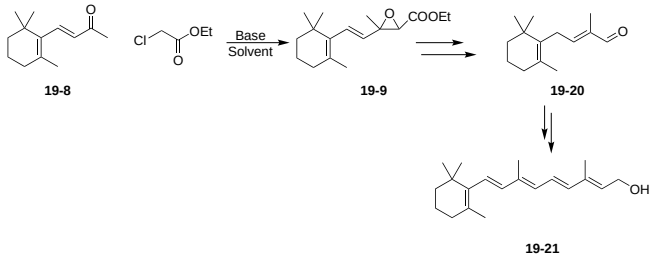

Scheme 19.5 Ring opening and decarboxylation in vitamin A synthesis.

The Hoffmann-La Roche reaction is still considered to be an efficient method of producing vitamin A. However, in recent decades there has been a growth in the number of alternative methods suitable for the industrial synthesis of vitamin A.[38] For example, the BASF protocol utilises an ylid-based reaction in place of a Darzens condensation in addition to an alternative route to the β-ionone.

Steel synthesis of (±)-epiasarinin

Epiasarinin is a furofuran-containing lignan-based natural product with anti-viral, anti-oxidant, anti-cancer and immunosuppressant biological activities.[39] The Steel synthesis describes an enantioselective method to synthesise the pharmaceutical, although the stereochemistry achieved by the Darzens reaction is irrelevant as the stereochemical information is later lost. Unusually, the electron-withdrawing group was an α,β-unsaturated ester.[39] Once formed, the epoxide is employed in a conrotatory ring opening, followed by a disrotatory cyclisation forming *cis*-dihydrofuryl ester (Scheme 19.6).

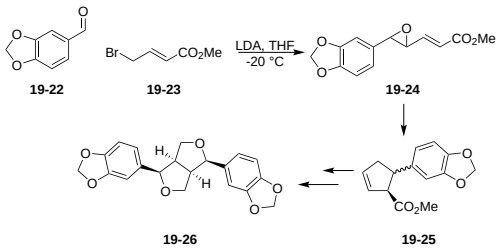

Scheme 19.6 Darzens condensation in the synthesis of (±)-epiasarinin.

Originally the intention of the authors was to use an olefin peroxidation followed by a Wadsworth-Emmons reaction with the epoxide formed to synthesise the glycidic ester. This was unsuccessful, which was thought to be due to the electron-donating effect of the substituents on the aryl group which promoted a ring-opening reaction. The Darzens reaction avoided this problem by forming the desired epoxide in a single step. The Darzens reaction was significantly more high-yielding than model studies for the epoxy formation predicted.

19.3 The asymmetric Darzens reaction

In recent years the desire for single enantiomer pharmaceuticals has expanded considerably due to a greater understanding of the marked difference in biological properties that each isomer may possess. Therefore, the use of synthesis routes with the ability to furnish selectively only the desired isomer has become a key strategy in the production of many new pharmaceuticals.[40] Modern advances within the Darzens condensation have brought about a greater asymmetric capacity, enabling stereoselective and stereospecific approaches, with the former using catalysts and the latter chiral auxiliaries or reagents.

Chiral auxiliaries offer a method of selectively producing single enantiomers, through their addition to the starting reagents in stoichiometric amounts to create diastereotopic products. These can in turn be separated with greater ease than is

possible with enantiomers. This is a particularly powerful tool in the asymmetric Darzens condensation due to the relative simplicity in which the auxiliaries can be incorporated into the starting reagents. The method has been applied in a number of variations.

Synthesis of diltiazem hydrochloride

Diltiazem is a non-dihydropyridine calcium channel blocker used to treat hypertension, angina and some arrhythmias. The (2*S*,3*S*) diastereoisomer has been identified as the most potent[41,42] and consequently the pharmaceutical is marketed as a single enantiomer. The earliest opportunity to access the single enantiomer is at the glycidic ester stage. Schwartz *et al.* used a chiral auxiliary strategy to furnish the desired enantiomer as the major product in 54% yield (Scheme 19.7).[43] The procedure was successfully scaled up to gram and kilogram scales. The diastereomeric products were easily separated on the basis of their differing solubilities, and the chiral auxiliary was recyclable using a straightforward base-mediated hydrolysis.

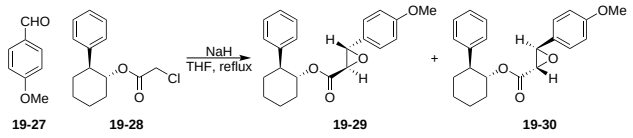

Scheme 19.7 Darzens condensation in the synthesis of diltiazem hydrochloride.

Importantly, this reaction does not produce the *cis*-epoxides in observable amounts. Essentially the stereochemical information is retained following a ring opening reaction with the thiol group to form the enantiomerically pure product (Scheme 19.8). A suggested mechanism is reported for the opening of the oxirane ring.

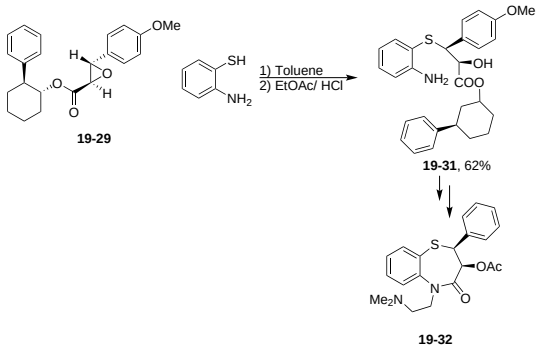

Scheme 19.8 Ring opening of the epoxide formed in the Darzens condensation during the synthesis of diltiazem.

It is proposed that the thiol group acts as a weak acid which protonates the epoxide, assisting the ring-opening. This is facilitated by the *p*-anisyl group and the intermediate quinone methide cation which both stabilise the configuration through electron donation from the ring. Since no chiral inversion occurs, an S_N2-type mechanism cannot be in operation but instead an S_N1-type reaction must be taking place. It is proposed that the rate of reaction between the thiol anion and cation must be greater than the anion migration, which is why the thiol anion's attack is only observed from one face.

Synthesis of (+)-mefloquine hydrochloride

Mefloquine is an anti-malarial drug but unfortunately it exhibits some serious side effects. It is typically manufactured and administered as a racemic mixture. However, (+)-mefloquine is at least 1.5 times more active than the (−)-enantiomer and also is less associated with the commonly reported side effects.

Another recent example of the usage of chiral auxiliaries can be seen in the synthesis of (+)-mefloquine hydrochloride, where the stereochemistry of the product was established early in the synthesis through the use of an asymmetric Darzens reaction (Scheme 19.9).[44]

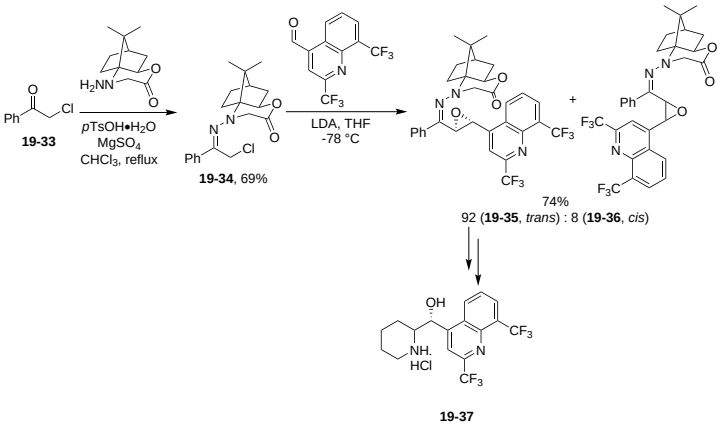

Scheme 19.9 Darzens condensation in the synthesis of (+)-mefloquine hydrochloride.

The synthesis reports a high diastereotopic selectivity (84% ee) for the desired *trans*-glycidic ester by using *N*-amino cyclic carbamate chiral auxiliaries. Furthermore, separating the minor *cis*-epoxide from the product was achieved easily by silica gel chromatography. The *trans*-epoxide was isolated and transformed to (+)-mefloquine hydrochloride by a series of steps.

Synthesis of SK&F 104353

SK&F 104353 is a leukotriene D_4 antagonist used in the potential treatment of bronchial asthma. A synthetic strategy *via* the glycidic amide was proposed by Aggarwal *et al.*[45] The use of camphor-derived sulfonium amides has proven to be a particularly effective enantioselective method in glycidic amide synthesis. Whilst this could be considered to be an ylid epoxidation, it can also be considered to be a derivation of the Darzens condensation.

The reaction is reported to proceed to the epoxide in excellent e.e. (up to 99%) with yields as high as 90%. Both the purity of the sulfonium salt diastereomer and the temperature of the reaction influence the selectivity and yield. The temperature affects only the enantioselectivity and not the yield, with -20 °C to -50 °C giving the best results. The preparation of the chiral auxiliary was achieved in 3 steps from (+)-camphor. The subsequent Darzens reaction is performed as a one-pot process with the catalyst and potassium hydroxide in ethanol (Scheme 19.10). Addition and removal of the auxiliary occurs *in situ*.

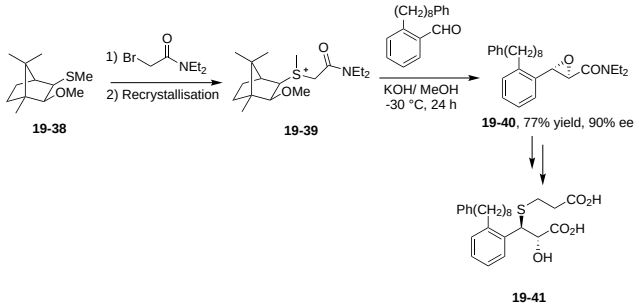

Scheme 19.10 Darzens condensation in the synthesis of SK&F 104353.

The reaction favours the *trans*-isomer in all observed reactions, but a better understanding of the mechanism and enantioselectivity is required. A proposed mechanism proceeds *via* reversible betaine formation, with the subsequent C-C bond rotation being the enantio-differentiating step.

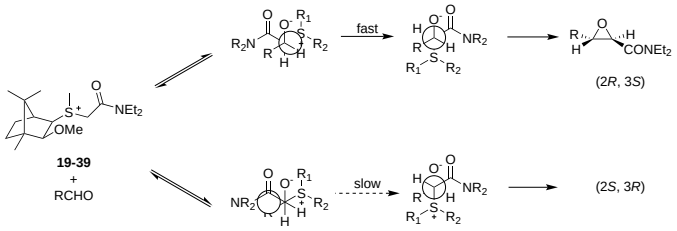

Scheme 19.11 Reversible betaine formation followed by the enantio-differentiating step in the synthesis of SK&F 104353.

19.4 The catalytic asymmetric Darzens reaction

The catalytic asymmetric Darzens reaction is an enantioselective approach to the preparation of glycidic esters and derivatives. Both homogeneous- and heterogeneous-catalysed reactions have been reported with high levels of enantiomeric selectivity. Phase transfer catalysis is heterogeneous, and offers operational simplicity, milder conditions and inexpensive, environmentally benign reagents and solvents as benefits. These advantages make this route particularly appealing in the pursuit of green chemistry. In addition, these positive traits make the development of the reaction especially useful in the pharmaceutical industry.

The catalytic asymmetric reaction has been reviewed elsewhere[19] and so will not be examined in detail here. Instead, a brief summary of the developments will be given, starting with homogeneous catalysis before moving to heterogeneous reactions.

Bovine serine albumin was the first homogeneous catalyst used in the asymmetric reaction by Colonna *et al.*[46] Lewis acid-Brønsted base catalysis,[47] chiral titanium complexes[48] and chiral zirconium complexes[49] have since been more recently used.

Makosza *et al.*[50,51] were the first to use phase-transfer catalysis in the Darzens reaction. They and later groups used crown ethers as catalysts.[52,53] Other major families of catalysts used for phase-transfer Darzens reactions include ephedrinium and cinchona-derived salts, although they operate by very different mechanisms.[19] For example, the Arai group has used chiral quaternary ammonium salts derived from cinchonine[54–59] in the syntheses of α,β-epoxyketones and α,β-epoxysulfones. More recently, they have started employing a BINOL-derived bis ammonium salt as a more effective catalyst with a greater substrate tolerance.[60]

As many of these advances in this area have occurred relatively recently, few examples therefore currently exist of the catalytic asymmetric Darzens reaction as used in pharmaceutical synthesis.[61]

19.5 Advantages and disadvantages of the Darzens reaction

Whilst demonstrating the versatility of this potential method of epoxide synthesis, this overview has also highlighted some of the major issues with its adaptability.

From the various potential and actual uses of the condensation in pharmaceutical synthesis it is clear that there are several limitations to the reaction. The mechanism, particularly with respect to selectivity, has not yet been absolutely established despite various studies and proposals. The lack of understanding has made selective reactions difficult to design.

The lack of stereoselectivity in the classical Darzens condensation means that it is only of use when the stereochemistry of the product is unimportant. Although great strides have been made in the development of a catalytic asymmetric reaction and various other methods of enantiomeric control, this remains problematic, with only very specific routes providing high enantioselectivity. Additionally, the use of chiral auxiliaries brings its own problems: for example, access to the enantiomerically pure auxiliary precursor, the addition of two extra synthetic steps, and subsequent yield reduction.

These methods frequently require expensive starting materials which can be challenging to prepare. Whilst yields are frequently high, the atom economy of the reaction is very poor. This is only exacerbated by the use of chiral auxiliaries. There is potential for side reactions such as self-condensation of the carbonyl compounds and formation of halohydrins,[62] which may lead to reduced yields.

The reaction has the advantage of being able to provide a multitude of synthetic products through its derivations – however, alternatives to the Darzens condensation such as organocatalytic epoxidation[63] have been observed with greater selectivity and easier preparation. Therefore, despite the ability to use the Darzens condensation in a large range of epoxide formations, it remains a challenge to optimise it for industrial-scale procedures.

However, there are still some advantages to the Darzens reaction. It can be incorporated into a wide range of different synthetic routes. Whilst the traditional variant of the reaction has found the most usage, notably in one-carbon homologation, the asymmetric condensation has far greater potential.

Generally the traditional Darzens reaction offers a direct and scalable method in epoxide synthesis. The relatively inexpensive and easily accessible reagents and the acceptance of electron withdrawing groups on the epoxides are also additional advantages. The conditions of chiral auxiliary asymmetric Darzens reactions tend to be very similar to those of the traditional reaction, as once the auxiliary is incorporated into the reagents, the reaction can proceed under classical conditions. The subsequent removal of the chiral auxiliary also tends to be simple. Chiral auxiliary reactions offer significant advantages in providing enantiospecific products. Additionally, the separation of the diastereoisomers is typically straightforward.

Although the variety of the possible substituents has allowed for the synthesis of an abundance of different epoxides, perhaps the most promising advances are in

the asymmetric Darzens reaction. Specifically, the efforts in enantioselective catalysts offer an opportunity for exploitation, especially within the pharmaceutical industry.

Further development of asymmetric heterogeneous catalysis offer several advantages over the homogeneous route in the pursuit of green chemistry, even though it is as-yet under-developed. The use of milder reaction conditions whilst avoiding toxic metal-based catalysts is particularly appealing.

19.6 Conclusions

Ultimately, the future of the Darzens reaction lies in whether the catalytic asymmetric potential can be refined so as to be scalable in pharmaceutical synthesis. The current limitations are preventing the reaction finding use in the synthesis of many bioactive compounds. Unless these are addressed, methods such as the Juliá-Colonna synthesis[64] will take precedence as a more successfully selective methodology.

Chapter 20

Project Aims

The objectives of this project are as follows:

- To replicate a batch procedure for the Darzens reaction
- To develop a continuous flow protocol for the Darzens reaction
- To use this flow procedure to synthesise an industrially useful intermediate e.g. a precursor to ibuprofen

From the literature perspective, it can be seen that the Darzens reaction is somewhat capricious, with conditions varying widely depending on the substrate used. The first step is to successfully perform a relevant batch reaction, and to use these results to inform the adaptation of the batch procedure into continuous flow.

Some changes are likely to be made on translating from batch to flow. The scope of this flow procedure will be examined with a range of benzaldehydes. Additional investigation of industrially relevant examples in a multi-step synthesis of compounds such as ibuprofen or vitamin A will also be considered.

Chapter 21

Results and Discussion

21.1 Preliminary batch experiments and early flow attempts

Ibuprofen

According to Shasun Pharmaceuticals, they have used the Darzens reaction in the synthesis of an intermediate towards ibuprofen on a commercial scale.* No conditions or data were available, but the general reaction scheme is as shown (Scheme 21.1).

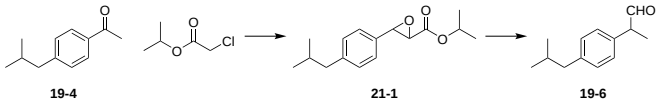

Scheme 21.1 Shasun synthesis of an ibuprofen intermediate.

Batch attempts at the Darzens reaction of isobutylacetophenone

The first experiments conducted in batch were with isobutylacetophenone and ethyl chloroacetate, with sodium ethoxide as the base (Scheme 21.2).[65] Several attempts were made, starting with milder heating conditions and moving to higher temperatures (10-15 °C to RT; 10-15 °C to 85 °C; reflux in EtOH).

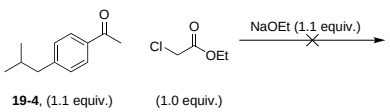

Scheme 21.2 Attempted Darzens reactions with isobutylacetophenone and ethyl chloroacetate.

*In correspondence with Prof Ian R. Baxendale

The ^{1}H NMR spectrum indicated the presence of unreacted ethyl chloroacetate, indicating that the base used was not strong enough to fully deprotonate the ethyl chloroacetate.

Freshly-prepared NaOEt was made by reacting sodium in dry ethanol. When the reaction was attempted again, a conversion of 39% from starting material was observed in the ^{1}H NMR spectrum (Scheme 21.3).

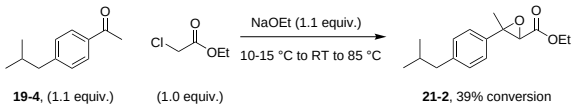

Scheme 21.3 Attempted Darzens reactions with isobutylacetophenone and ethyl chloroacetate and freshly-prepared sodium ethoxide.

Flow attempts at the Darzens reaction of isobutylacetophenone

With the somewhat-successful batch reaction in hand, efforts were made to translate it into flow. Reactions were next carried out in a Vapourtec E-MedChem® reactor system using the in-built peristaltic pumps.

The first attempt used a 10 mL FEP reactor at 90 °C with a flow rate of 0.100 mL min^{-1} (Scheme 21.4).

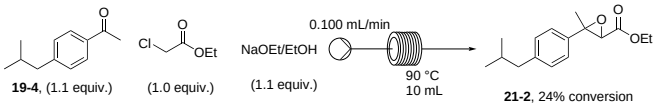

Scheme 21.4 First flow attempt at the Darzens reaction with isobutylacetophenone.

A conversion of 24% to the product was observed by ^{1}H NMR spectroscopy.

The flow rate was increased to 0.500 mL min^{-1}, and then the temperature increased to 100 °C. These changes led to a slight decrease in the overall conversions (Scheme 21.5).

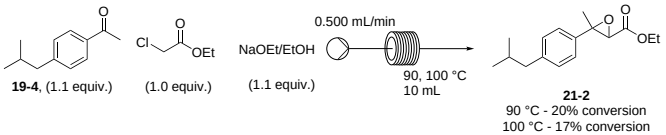

Scheme 21.5 Screening temperatures and flow rates for the Darzens reaction in flow with isobutylacetophenone.

To try and increase the conversion, a second 10 mL reactor coil was added, and the flow rate reduced back to 0.100 mL min^{-1}, giving a residence time of approx. 200 mins (Scheme 21.6).

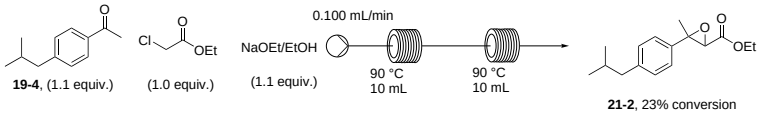

Scheme 21.6 Attempted Darzens reaction with isobutylacetophenone in flow with two 10 mL coil reactors at 90 °C.

Unfortunately this did not make a difference to the conversion.

Next, the first reactor temperature was set to 25 °C, and the second held at the higher temperature of 90 °C (Scheme 21.7).

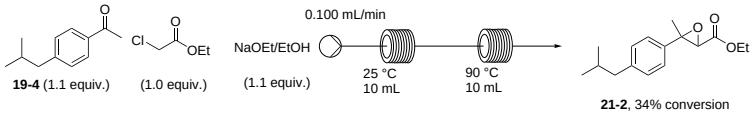

Scheme 21.7 Attempted Darzens reaction with isobutylacetophenone in flow with two 10 mL coil reactors, one at 25 °C and the second at 90 °C.

This gave a modest increase to the conversion.

At this point, isobutylacetophenone was ruled out as a substrate, as it was thought that it was proving too difficult for the deprotonated ethyl chloroacetate to attach into the ketone carbonyl system.

Vitamin A

There are more published protocols and precedent for the successful synthesis of the C_{14} aldehyde in the synthesis of vitamin A, starting from $\beta-$ionone. As an example, the Hoffmann-La Roche synthesis of vitamin A is shown above (Scheme 19.5).[34] The Hoffmann-La Roche reaction is still considered to be an efficient method of producing vitamin A.

Batch attempts at the Darzens reaction of $\beta-$ionone

The first attempt performed aimed to replicate the Isler procedure of 1947 (Scheme 21.8).[34]

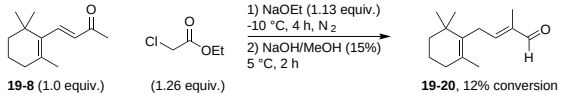

Scheme 21.8 Isler synthesis of the aldehyde.

The conversion was measured by ^{1}H NMR spectroscopy, using the aldehyde peak in the 9.0-9.5 ppm region. The majority of the mixture was the $\beta-$ionone starting material, unlike the literature procedure which reported a yield of 80%.

Flow attempts at the Darzens reaction of $\beta-$ionone

The first flow attempt at synthesising the C_{14} aldehyde mimicked the Isler batch procedure. $\beta-$Ionone and ethyl chloroacetate were pre-mixed, followed by the addition of NaOEt/EtOH. A white precipitate was formed, and the solution turned a pale yellow, before the slurry was pumped into the Polar Bear® reactor held at -10 °C (Scheme 21.9), with no conversion of starting materials observed by ^{1}H NMR spectroscopy.

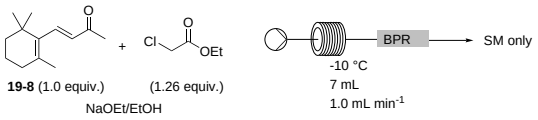

Scheme 21.9 Attempted flow Isler synthesis of the aldehyde.

The second attempt used a re-calculated quantity of NaOEt, based on the need for additional base in the form of NaOH (Scheme 21.10).

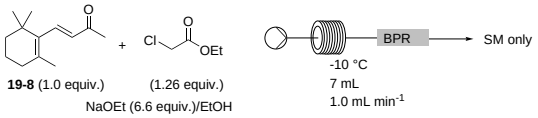

Scheme 21.10 Attempted flow Isler synthesis of the aldehyde.

There were some issues with the pump blocking with precipitated NaCl when run at 0.1 mL min^{-1}. Only $\beta-$ionone was observed by ^{1}H NMR spectroscopy.

The same reaction was attempted at -10 °C, followed by a second pass through a 7 mL reactor housed on a Polar Bear Plus® reactor held at +5 °C (Scheme 21.11).

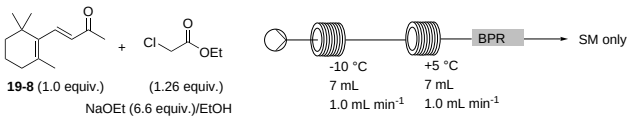

Scheme 21.11 Attempted flow Isler synthesis of the aldehyde.

There was no observable colour change, and only $\beta-$ionone was observed by ^{1}H NMR spectroscopy.

The next approach was to split up the starting material components, placing the base in a separate channel to allow for pre-cooling of the starting materials before mixing with the sodium ethoxide (Scheme 21.12).

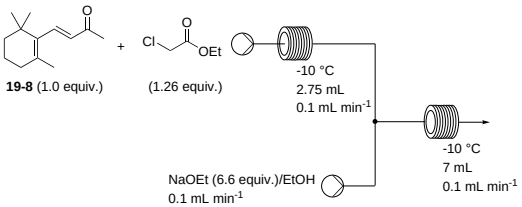

Scheme 21.12 Attempted flow Isler synthesis of the aldehyde.

The crude mixture was split into two 2.5 mL portions. NaOH was added to the first, which was stirred at room temperature. No change was observed.

The second sample was sent through the flow reactor again at a higher temperature before extraction and work-up. The material isolated was a yellow-brown oil, and ^{1}H NMR spectroscopy indicated an absence of aldehyde, as well as the presence of the $\beta-$ionone starting material and other impurities.

Identifying the source of the problem

A series of deprotonation and quenching experiments were performed on ethyl chloroacetate to determine whether it was the initial deprotonation step by the base, or the subsequent aldol-like addition into the carbonyl which was the issue.

Sodium ethoxide in EtOH was added to ethyl chloroacetate at -10 °C and stirred for 30 mins. D_2O was used to quench the solution. Insufficient base (0.5 equiv.) was used so that a mixture could be seen in the ^{1}H NMR spectrum, performed in d_6-DMSO (Scheme 21.13) .

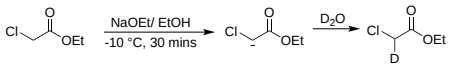

Scheme 21.13 Determination of deprotonation of ethyl chloroacetate by NaOEt in EtOH.

Integration of the ^{1}H spectrum indicated approx. 76% deuteration (although there was only enough NaOEt to deprotonate 45%). Therefore, the deprotonation step was deemed not to be the problematic step in the Darzens reaction.

It would appear that the second, aldol-like addition into the carbonyl is the problem. If it were the ring-closing, epoxide-forming step, the protons from the ester of ethyl chloroacetate would appear in the ^{1}H NMR spectrum, but they do not.

Non-Isler Darzens reactions with $\beta-$ionone

Since all of the attempts at the Darzens reaction of $\beta-$ionone with ethyl chloroacetate using the Isler conditions failed, other literature conditions were considered.

The first of these was from a recent patent and required *N*-methyl-2-pyrrolidone in sub-stoichiometric amounts (Scheme 21.14).[66]

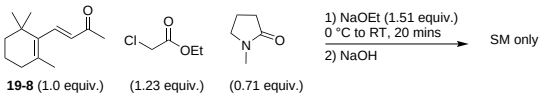

Scheme 21.14 Attempted Darzens synthesis of C_{14} aldehyde.

The only material isolated was $\beta-$ionone by ^{1}H NMR spectroscopy.

The second attempt was from the same patent, using NaOMe instead of NaOEt, and still using *N*-methylpyrrolidone (Scheme 21.15).

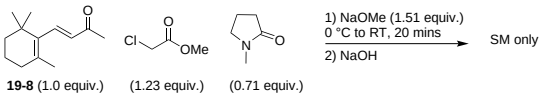

Scheme 21.15 Attempted Darzens synthesis of C_{14} aldehyde.

Again, by ^{1}H NMR spectroscopy, only $\beta-$ionone was isolated.

Finally, a flow reaction with $\beta-$ionone, ethyl chloroacetate and sodium methoxide was attempted,[67] with a telescoped batch step after to add the NaOH/MeOH (Scheme 21.16).

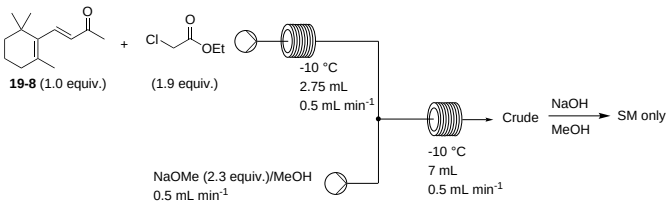

Scheme 21.16 Attempted Darzens synthesis of C_{14} aldehyde.

Again, $\beta-$ionone was the only material isolated according to ^{1}H NMR spectroscopy.

Benzaldehyde

Since it was thought that the addition to the carbonyl was the problem, similar reactions were attempted using benzaldehyde as a more reactive carbonyl functionality.

The first literature procedure[68] performed employed methyl chloroacetate (2 equiv.) and sodium methoxide (2 equiv.) in MeOH at 0 °C. However, only benzaldehyde was isolated.

A second modified literature procedure[69] used ethyl chloroacetate (2 equiv.) and sodium methoxide (1.5 equiv.). Again, ^{1}H NMR spectroscopy indicated that only benzaldehyde was isolated.

Finally, a flow reaction using benzaldehyde, ethyl chloroacetate and sodium methoxide was attempted (Scheme 21.17).

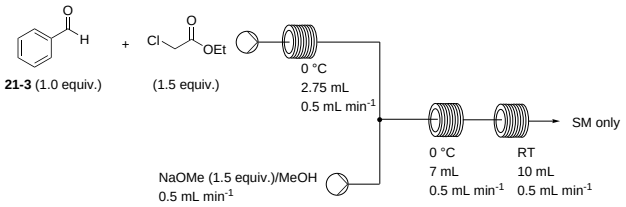

Scheme 21.17 Attempted flow Darzens reaction between benzaldehyde and ethyl chloroacetate.

Benzaldehyde and ethyl chloroacetate were both present by ^{1}H NMR spectroscopy.

21.2 Breakthrough batch reaction

The first batch Darzens reaction that could be described as successful used KO^{t}Bu in *t*-BuOH as the base, following the work of Bachelor *et al.*[22] Benzaldehyde and methyl chloroacetate were used as the starting materials, and the resulting white slurry was stirred at room temperature for 2 h (Scheme 21.18).

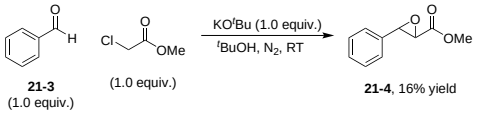

Scheme 21.18 Synthesis of the epoxy ester from benzaldehyde.

After purification by column chromatography, the epoxy ester was isolated as a mixture of diastereomers, in the ratio 2.7:1. The major diastereomer was identified as the *cis* isomer, based on *J*-values in the ^{1}H NMR spectrum and confirmation data from the NOESY spectrum. Both the ratio and assignment are in agreement with the literature.[22]

It was examined whether evaporation of *t*-BuOH was necessary for a successful aqueous work-up. It was concluded that this was only important on a larger scale, and so therefore a simple Et_2O/H_2O work-up is sufficient, and enables rapid extraction when screening flow reactions.

21.3 Benzaldehyde reactions in flow

Several possibilities for transferring the batch reaction to flow were identified. These included a two-pump system, where the aldehyde and methyl chloroacetate

are pre-mixed before being pumped to mix with the base stream. A preferred option was a three-pump system, which separated the carbonyl and chloroacetate streams. For simplicity, the 2-pump system was considered first. Many factors were identified that could alter the conversion to product. These are described and examined in detail below.

Several potential issues were identified with changing from a batch reaction to a flow process. The batch reaction was performed under N_2 in anhydrous conditions, but it was not known how crucial this was. Additionally, when adding the basic solution to the starting materials, a viscous white slurry formed rapidly which may cause blockages in flow. Finally, the melting point of *t*-BuOH is 25 °C, which imposes a limit on the lower temperature range that can be screened.

Full conversion was only observed when benzaldehyde and methyl chloroacetate were mixed together without additional *tert*-butanol. Results at higher dilutions were not very reproducible, but show an approximate trend that as concentration decreases, so does the conversion (Table 21.1). Running the reaction at high concentrations can cause problems with blocking (if not engineered for) due to the formation of a solid as the two reacting streams mix.

Table 21.1 Effect of substrate concentration on conversion of benzaldehyde to epoxide.

Entry	Dilution of BA+MCA	Concentration of BA/ mol dm^{-3}	Flow rates mL min^{-1}	Pressure/ bar	Outcome[a]
1	Neat	-	B = 0.200; C = 1.000	10	100%
2	1:1	9.84	B = 0.200; C = 1.000	10	Blockage - not resolved
3	1:2	4.92	0.500	3.0	57%
4	1:2	4.92	1.00	5.0	39%
5	1:2	4.92	1.00	5.7	57%
6	1:2	4.92	1.50	7.2	58%
7	1:3	3.28	0.500	3.5	43%
8	1:3	3.28	1.00	6.0	80%
9	1:3	3.28	1.00	5.8	78%
10	1:3	3.28	1.50	5.5	57%
11	1:5	1.97	1.00	3.5	63%

[a] % conversion estimated by ^{1}H NMR spectroscopy

There is not a strong correlation between absolute flow rate and conversion (Fig. 21.1).

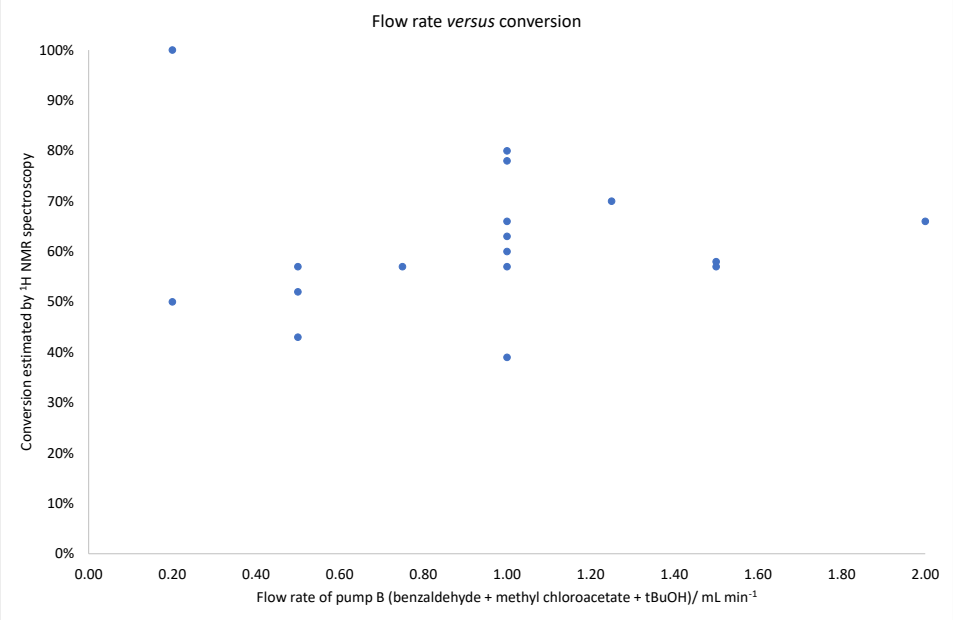

Fig. 21.1 The effect of flow rate on conversion.

Several combinations of flow rates of different streams were examined, and the results are shown below (Fig. 21.2).

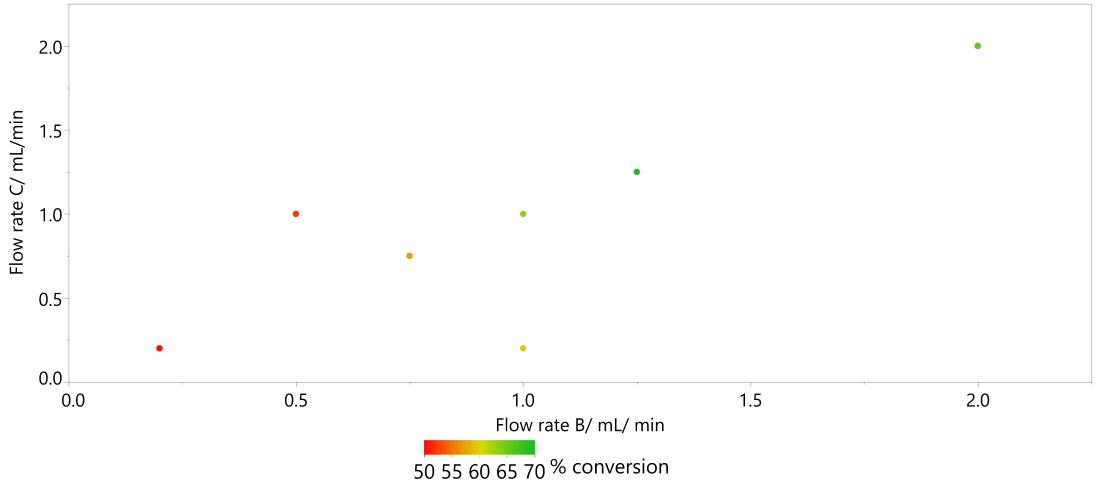

Fig. 21.2 The effect of flow rate on conversion.

There is no obvious relationship between the ratio of flow rates of streams. The higher flow rates give slightly higher conversions, and also allow more material to be processed and so are more efficient.

Reactions cannot be run below 25 °C due to the low freezing point of *tert*-butanol. Two further experiments were performed to examine the effect of in-

creasing the temperature on the percentage conversion, and the results are summarised below (Fig. 21.3).

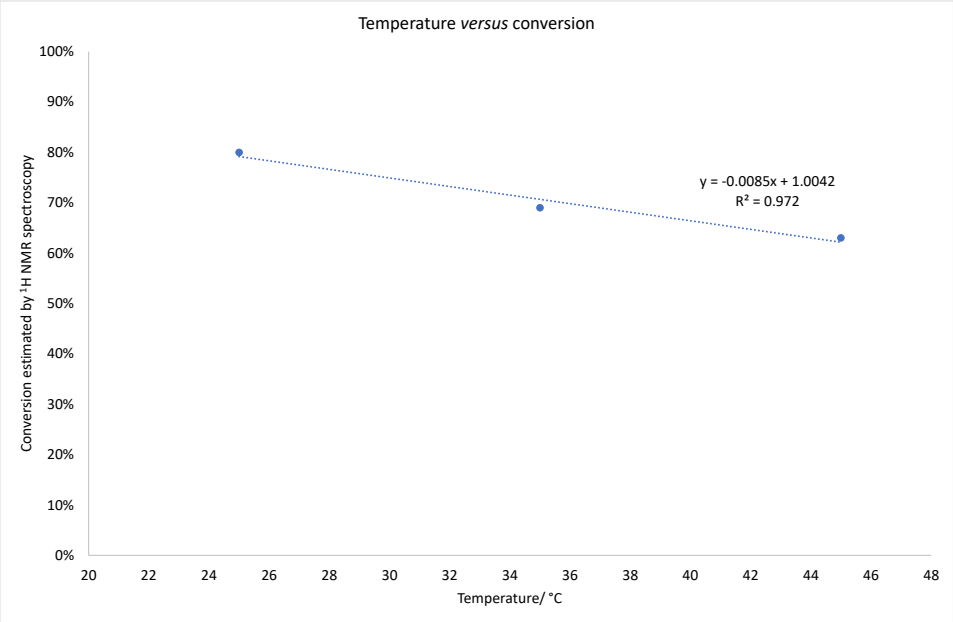

Fig. 21.3 The effect of temperature of the reactor on conversion.

The percentage conversion decreased as the temperature was increased. This was likely to be due to the increased formation of side-products due to reactions of the epoxide product. Discolouration of the product stream was observed, to orange rather than white or pale yellow.

The pressure of the reactions performed was observed, and plotted against conversion (Fig. 21.4).

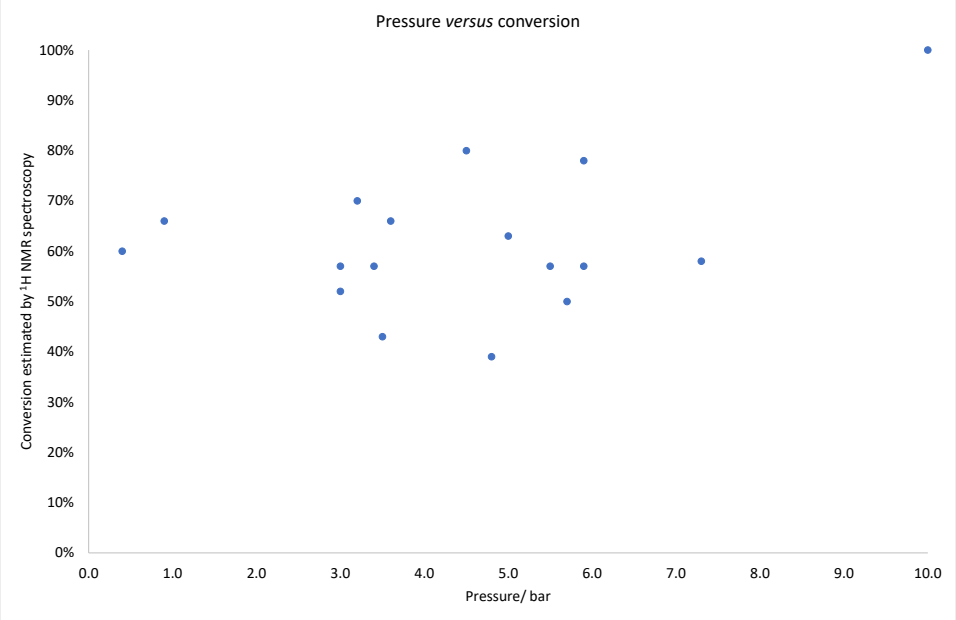

Fig. 21.4 The effect of pressure on conversion.

There does not seem to be a connection between pressure and conversion.

When using the standard narrow tubing, blocking at the T-piece was common. Changing to a Y-piece reduced this problem. The conversion was investigated after mixing, before entering the reactor coil, since it was thought that the coil may be unnecessary. It was found that there was little difference in conversion between experiments where measurements were taken before and after the reactor coil, and so the coil was removed. The effect of the tubing length post-mixing was investigated below.

Narrow-bore tubing had previously been used but caused severe problems with precipitation, over-pressure and blocking. The tubing post-mixing was exchanged for wider-bore tubing (inner diameter = 5.0 mm) which would reduce the likelihood of blockages, and may lead to improved mixing.

This wider-bore tubing was obtained in several pre-cut lengths, and these were tested with benzaldehyde, running neat or diluted in *t*-BuOH (Fig. 21.5).

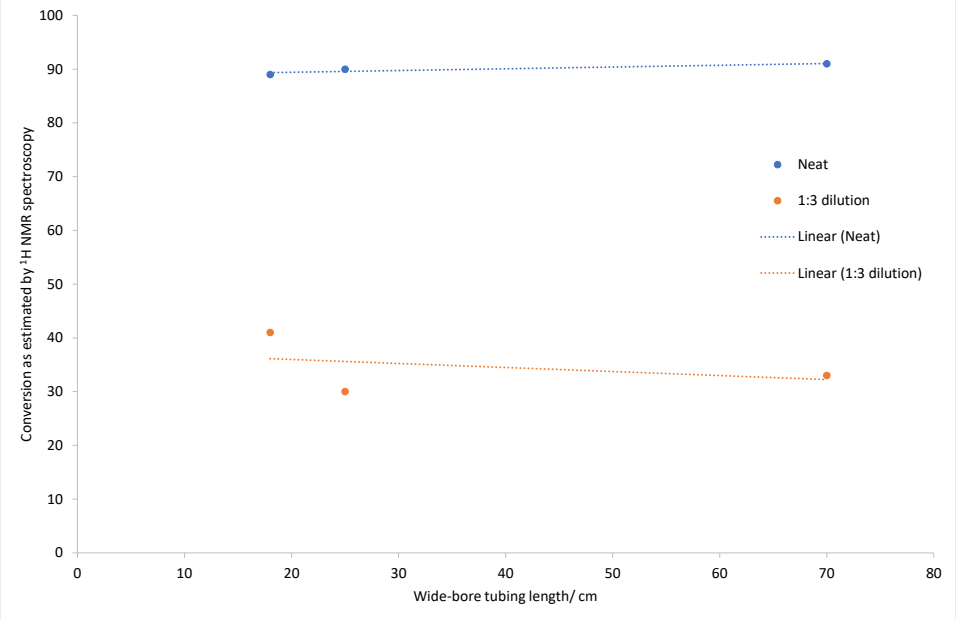

Fig. 21.5 The effect of tube dimensions on conversion.

The conversion of benzaldehyde was > 90 % when run neat; the length of the wider-bore tubing did not have a large impact on this result.

21.4 Isobutylbenzaldehyde reactions in flow

Initially, the flow rates for pumps **B** (isobutylbenzaldehyde and methyl chloroacetate) and **C** (KO^{t}Bu and *t*-BuOH) were set equal, and the absolute flow rate was varied to see if this had any effect on conversion (Fig. 21.6 and Fig. 21.7). The impact was small (if not negligible), which is somewhat surprising because a slower flow rate gives a longer residence time and thus a larger window for reaction to occur, but with poorer mixing.

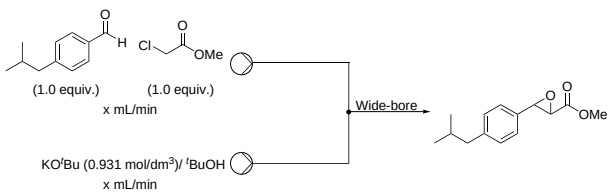

Fig. 21.6 The effect of flow rate on conversion of isobutylbenzaldehyde.

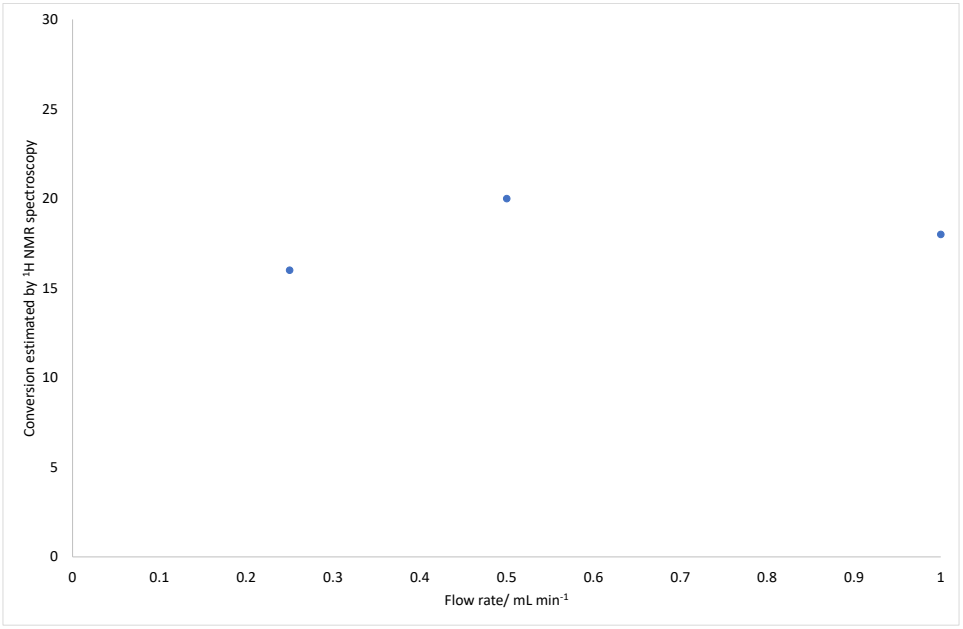

Fig. 21.7 The effect of changing the absolute flow rate on conversion.

Next, the relative flow rates of pumps **B** (isobutylbenzaldehyde and methyl chloroacetate) and **C** (KO^{t}Bu and t-BuOH) were changed. The results are plotted in the graph below (Scheme 21.19 and Fig. 21.8).

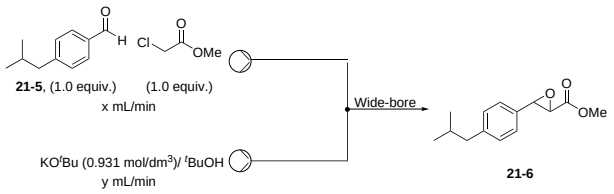

Scheme 21.19 The effect of relative flow rate on conversion of isobutylbenzaldehyde.

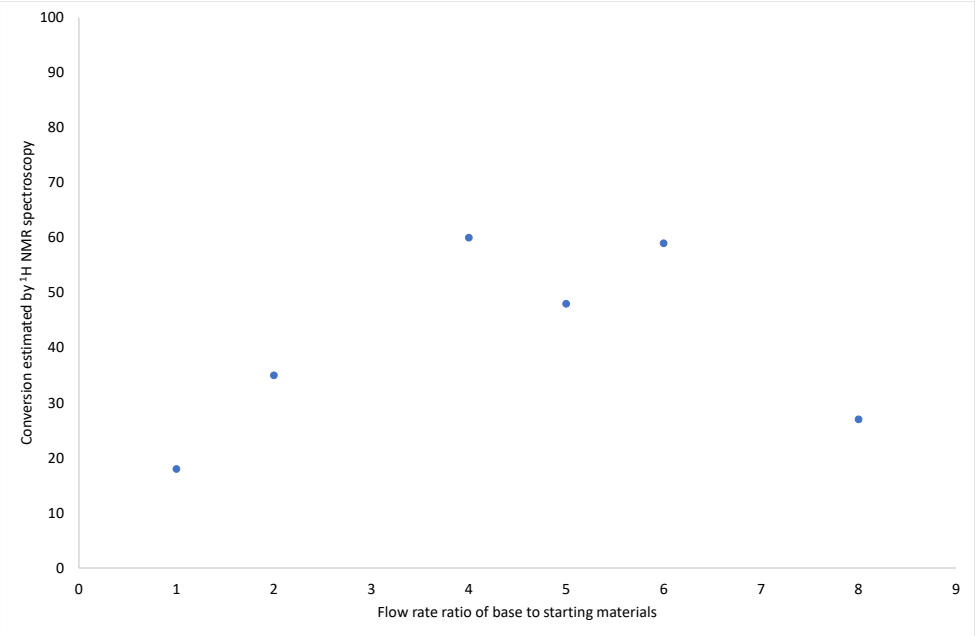

Fig. 21.8 Effect of changing the flow rate ratios on conversion.

It would seem that there are two competing effects occurring. In the first half (ratios up to 1:4), as the flow rate of the base increases, conversion also increases approximately linearly. However, in the second half of the graph (ratios above 1:6), a sharp decrease in conversion is observed. This is thought to be due to the increasing volume of *t*-BuOH and hence a higher dilution. It has previously been observed that this reaction gives its highest conversions at high concentrations, and so this is not surprising. The 1:5 flow rate ratio was also tested, but the conversion observed was not the maximum expected. The reason for this is not yet known.

21.5 Utilising a 3-pump system

To test whether polymerisation of methyl chloroacetate was occurring under these conditions, it was mixed with base and without substrate (Scheme 21.20).

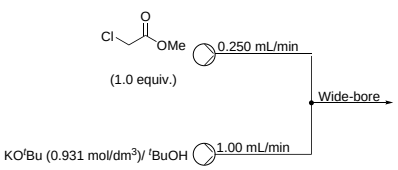

Scheme 21.20 Mixing methyl chloroacetate and the base.

Some side-product formation was observed. One possible route for side-product formation is shown below (Scheme 21.21).

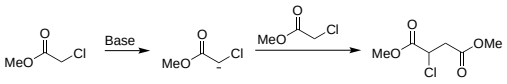

Scheme 21.21 Possible side-product formation from the reaction of methyl chloroacetate with itself (wide bore: inner diameter = 5.0 mm).

Three mixing combinations between isobutylbenzaldehyde or benzaldehyde, methyl chloroacetate and potassium *tert*-butoxide were considered. Mixing the base and methyl chloroacetate gave the worst conversion, presumably because the methyl chloroacetate started reacting with itself before it began reacting with the aldehyde (Scheme 21.22).

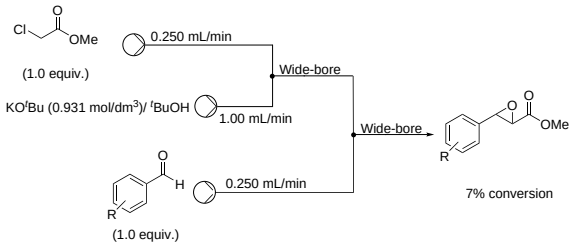

Scheme 21.22 3-pump arrangement, with pre-mixing of methyl chloroacetate and the base (wide bore: inner diameter = 5.0 mm).

There was little difference between mixing methyl chloroacetate and isobutylbenzaldehyde (Scheme 21.23), and mixing isobutylbenzaldehyde and the base (Scheme 21.24).

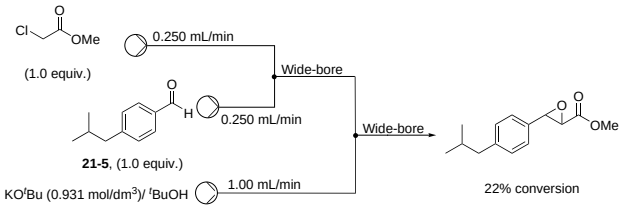

Scheme 21.23 3-pump arrangement, with pre-mixing of methyl chloroacetate and isobutylbenzaldehyde.

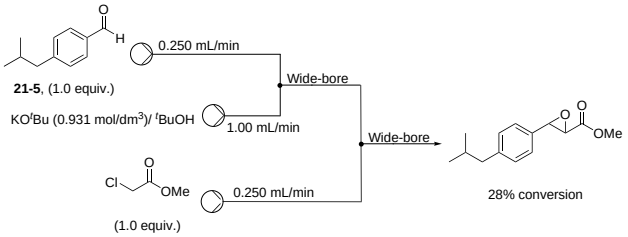

Scheme 21.24 3-pump arrangement, with pre-mixing of isobutylbenzaldehyde and the base.

Finally, two injections of base were sequentially mixed with methyl chloroacetate and isobutylbenzaldehyde (Scheme 21.25).

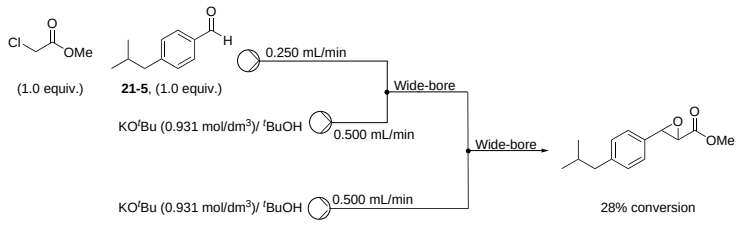

Scheme 21.25 3-pump arrangement, with two injections of the base.

This did not improve the conversion, and so it can be concluded that the low conversion is not due to the availability of base. These results are summarised in the table below (Table 21.2).

Table 21.2 Effect of changing the pumping system layout.

Entry	Pump system	Outcome[a]
1	Scheme 21.22 (Benzaldehyde)	8%
2	Scheme 21.22 (IBBA)	7%
3	Scheme 21.23 (IBBA)	22%
4	Scheme 21.24 (IBBA)	28%
5	Scheme 21.25 (IBBA)	28%

[a] % conversion estimated by ^{1}H NMR spectroscopy

The three-pump systems considered did not give an advantage in conversion over the other two-pump systems. They do, however, allow aldehydes to be changed easily so that rapid screening is possible.

21.6 Substrate screening

A range of readily-available benzaldehydes were tested under the same conditions (Scheme 21.26). Of these, *p*-nitrobenzaldehyde was a solid at room temperature,

and would not dissolve in methyl chloroacetate or *t*-BuOH. Therefore for this initial screening, only benzaldehydes which are liquids at room temperature were considered. The results are summarised below (Table 21.3).

Scheme 21.26 General flow diagram for testing a variety of aldehydes in the Darzens reaction in flow.

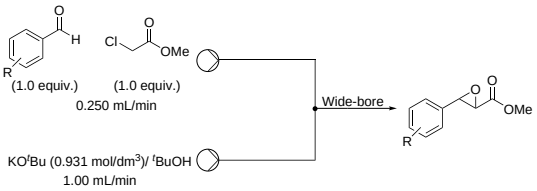

Entry	Starting material	Outcome[a]
1	Isobutylbenzaldehyde	18%
2	*p*-Methoxybenzaldehyde	19%
3	*m*-Methoxybenzaldehyde	21%
4	*o*-Methoxybenzaldehyde	15%
5	*p*-Bromobenzaldehyde	47%
6	*m*-Bromobenzaldehyde	37%
7	*o*-Bromobenzaldehyde	65%
8	*m*-Fluorobenzaldehyde	> 95%
9	*o*-Trifluoromethylbenzaldehyde	68%
10	*o*-Methylbenzaldehyde	50%

[a] % conversion estimated by ^{1}H NMR spectroscopy

The resulting epoxide exhibits *cis/ trans* isomerism, as illustrated by the benzaldehyde-derived epoxide shown below (Fig. 21.9).

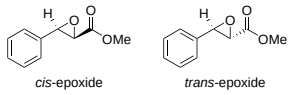

Fig. 21.9 *cis*- and *trans*-epoxides of benzaldehyde.

The epoxide products were separated from the aldehyde starting material by preparative HPLC, and the *cis*/*trans* ratios were determined by ^{1}H NMR spectroscopy. The results are summarised below (Table 21.4).

Table 21.4 Isomer ratios of epoxides prepared by the Darzens reaction.

Entry	Starting material	*cis*	*trans*
1	*p*-Isobutylbenzaldehyde	1	2.2
2	*p*-Methoxybenzaldehyde	1	1.4
3	*m*-Methoxybenzaldehyde	1	1.8
4	*o*-Methoxybenzaldehyde	1	1.8
5	*m*-Bromobenzaldehyde	1	2.5
6	*o*-Bromobenzaldehyde	1	2.4
7	*m*-Fluorobenzaldehyde	1	3.1
8	*o*-Trifluoromethylbenzaldehyde	1	6.8
9	*o*-Methylbenzaldehyde	1	4.4
10	Benzaldehyde	1	2.5

In all cases except the trifluoromethyl-substituted epoxide, the *trans* isomer is the major component. This is in line with the literature observation that steric interactions are minimised between the substituent groups on the epoxide when they are *trans* to each other.[22] However, the stereochemistry and mechanism of this reaction are not straightforward or well-understood. There are several series of compounds in which to consider trends (Table 21.5). The methoxy-substituted compounds show an increasing preference for the *trans* isomer as the methoxy group is moved closer around the ring to the epoxide. There is little difference for the bromo-substituted *meta* and *ortho* compounds. For the four *ortho*-substituted compounds, the picture is complicated: for example, the ratios do not tally with A-values for these substituents, used here as a measure of steric bulk.[70]

Table 21.5 Isomer ratios of epoxides compared to A-values.

Starting material	*cis*	*trans*	A-value
p-Methoxybenzaldehyde	1	1.4	0.6
m-Methoxybenzaldehyde	1	1.8	
o-Methoxybenzaldehyde	1	1.8	
m-Bromobenzaldehyde	1	2.5	0.38
o-Bromobenzaldehyde	1	2.4	
m-Fluorobenzaldehyde	1	3.1	0.15
o-Trifluoromethylbenzaldehyde	1	6.8	2.1
o-Methylbenzaldehyde	1	4.4	1.7

The picture is a little clearer for the *meta*-substituted epoxides: as the steric bulk increases, the preference for the *trans*- over the *cis*-epoxide weakens; this is the reverse of what may be predicted on the basis of A-values alone. This reinforces the notion that the stereochemistry of the Darzens reaction is not simple or easy to predict.

21.7 Isobutylbenzaldehyde in the synthesis of ibuprofen

Ibuprofen and derivatives can be reached from isobutylbenzaldehyde according to the following synthetic route,[71] although acetophenone is a more common starting material (Scheme 21.27).

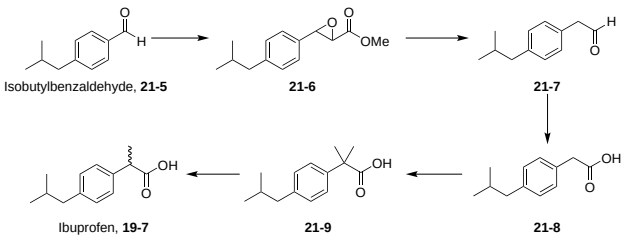

Scheme 21.27 Synthetic route from isobutylbenzaldehyde to ibuprofen.

This project has synthesised the first intermediate by the Darzens reaction in flow, enabling access to ibuprofen. The continuous flow process will require further optimisation.

Chapter 22

Conclusions

The three aims outlined at the beginning of this project will be examined here.

As expected from the literature review, the batch Darzens reaction is troublesome. Early attempts to achieve the Darzens reaction in batch started from isobutylacetophenone and β-ionone, and met with very limited success. Changing to benzaldehyde with a *tert*-butoxide base gave the first epoxide product, albeit in low yield.

This benzaldehyde batch reaction was translated into flow, and led to the discovery that mixing and concentration were the two most important factors. The use of wide-bore tubing and a T-piece gave some mixing, but there is room for improvement. The flow rates, temperature and pressure of the reaction were less important with this substrate. Changing to isobutylbenzaldehyde, the concentration and flow rate had two conflicting effects. The mixing is still crucial. Although it gives medium to low yields, the main advantages of this flow procedure over the batch process is that the residence time is many times lower (minutes rather than hours). A wider range of aromatic benzaldehydes was screened through this flow process, with the conversion highly dependent on the substrate. The viscosity of the benzaldehyde seems to be important in determining the quality of the mixing.

There is literature precedent for converting isobutylbenzaldehyde to ibuprofen. The one-carbon homologated aldehyde of isobutylbenzaldehyde can be formed from the Darzens glycidic ester intermediate. This epoxide intermediate was reached *via* the flow process described herein. Conversions were typically low, but the rapid reaction time means that viable quantities of material could be reached in a similar amount of time to the batch process.

Chapter 23

Future Work

The continuous flow Darzens reaction has had some success, but would benefit from further optimisation, particularly in improving the mixing of streams.

Other substrates, such as heteroaromatic aldehydes, or other carbonyl compounds could be rapidly screened using this set-up. Purification by preparative HPLC is sufficient on a fairly small scale, but will not be sustainable on larger quantities of material. Refining the chromatographic purification would be advisable if the process were scaled up.

The ibuprofen synthesis could be completed from the epoxide intermediate to comprehensively demonstrate the value of this process. This is a good example of how flow chemistry can be used to synthesise valuable organic compounds.

Whilst not a resounding success, this project demonstrates the first example of the Darzens reaction in flow. It has great potential which has yet to be fully explored.

Chapter 24

Experimental

24.1 General procedure A

The aromatic aldehyde (1 equiv.) and methyl chloroacetate (1 equiv.) are pre-mixed in a vial. A stock solution of KO^{t}Bu in t-BuOH (10% by mass) is prepared. The aldehyde/ methyl chloroacetate mixture is passed through the Vapourtec peristaltic pump (1.0 mL min^{-1}, RTP) and mixes with the base (1.0 mL min^{-1}, RTP) in a wide-bore T-piece. The viscous, white slurry formed by their exothermic mixing passes through wide-bore tubing and is collected. The work-up consists of an aqueous/Et_2O extraction, followed by removal of the solvent *in vacuo* to give the crude product.

24.2 Methyl 3-phenylglycidate, Compound 21-4

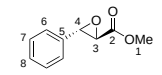

Chemical Formula: $C_{10}H_{10}O_3$
Exact Mass: 178.06

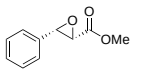

Chemical Formula: $C_{10}H_{10}O_3$
Exact Mass: 178.06

Procedure:

Benzaldehyde (1.45 mL, 14.1 mmol) and methyl chloroacetate (1.25 mL, 13.9 mmol) were charged to a 100 mL RBF fitted with a stirrer, septum and nitrogen balloon. KO^{t}Bu (1.63 g, 14.1 mmol) was dissolved in *t*-BuOH (15.0 mL), and the solution was charged dropwise over 15 mins to the benzaldehyde mixture. Immediate formation of a white precipitate was observed, and the solution became a viscous slurry. The slurry was swirled at RT for 2 h. The *t*-BuOH was removed *in vacuo*, and the residue was extracted with Et_2O/H_2O. The organic layer was washed with NaCl(aq), H_2O, dried over Na_2SO_4 and concentrated *in vacuo* to give the crude product as a pale yellow oil in 30% crude yield. The oil was purified by flash column chromatography (Hex:EtOAc 80:20 to Hex:EtOAc 98:2) to give the product as a mixture of diastereomers, in the ratio 1:2.5 (*cis*:*trans*).

Isolated yield: 0.386 g (2.168 mmol, 16%)

Major diastereomer (*trans*)

^{1}H NMR (700 MHz, $CDCl_3$): δ/ppm 3.52 (1 H, d, J = 1.7 Hz, H3), 3.83 (3 H, s, H1), 4.10 (1 H, d, J = 1.7 Hz, H4), 7.28-7.41 (5 H, m, H6-8);
^{13}C NMR (126 MHz, $CDCl_3$): δ/ppm 52.6 (C3), 56.6 (C1), 58.0 (C4), 125.8 (C6), 128.7 (C7/8), 129.0 (C7/8), 134.9 (C5), 168.7 (C2).

Minor diastereomer (*cis*)

^{1}H NMR (700 MHz, $CDCl_3$): δ/ppm 3.55 (3 H, s, H1), 3.84 (1 H, d, J = 4.6 Hz, H3), 4.26 (1 H, d, J = 4.6 Hz, H4), 7.28-7.41 (5 H, m, H6-8);
^{13}C NMR (126 MHz, $CDCl_3$): δ/ppm 52.0 (C1), 55.8 (C3), 57.5 (C4), 126.6 (C6), 128.1 (C7/8), 128.5 (C7/8), 132.8 (C5), 168.7 (C2).

Both diastereomers together

IR (neat) ν = 1749.6 (C=O, s), 1439.5 (m), 1291.6 (m), 1206.3 (C-O, s), 1183.2 (m), 758.3 (m), 695.6 (s), 599.1 (m), 516.4 (m) cm^{-1}.
LC-MS: R_t = 2.78 min, m/z 357.6 $[2M+H]^+$; HR-MS calculated for $C_{20}H_{21}O_6$ at 357.1338, found 357.1336 (Δ = -0.6 ppm).

Reference[72]

24.3 3-[4-(2-Methylpropyl)phenyl]oxirane-2-carboxylate, Compound 21-6

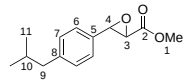

Procedure:

General procedure A. The ratio of *trans* to *cis* isomers was 2.2:1.

cis-Methyl 3-(4-isobutylphenyl)oxirane-2-carboxylate

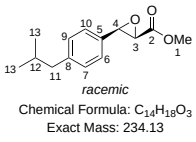

^{1}H NMR (700 MHz, $CDCl_3$): δ/ppm 0.87 (6 H, d, J = 6.4 Hz, H13), 1.78-1.89 (1 H, m, H12), 2.45 (2 H, d, J = 7.1 Hz, H11), 3.64 (3 H, s, H1), 4.45 (1 H, d, J = 6.5 Hz, H3), 5.10 (1 H, d, J = 6.4 Hz, H4), 7.13 (2 H, d, J = 7.8 Hz, H7+9), 7.26 (2 H, d, J = 7.8 Hz, H6+10);
^{13}C NMR (176 MHz, $CDCl_3$): δ/ppm 22.3 (C13), 30.1 (C12), 45.1 (C11), 52.9 (C1), 62.9 (C3), 74.5 (C4), 126.3 (C6+10), 129.3 (C7+9), 135.3 (C8), 142.4 (C5), 168.4 (C2).
LC-MS: R_t = 4.04 min, m/z 469.3 $[2M+H]^+$; HR-MS calculated for $C_{28}H_{37}O_6$ at 469.2590, found 469.2597 (Δ = +1.5 ppm).

trans-Methyl 3-(4-isobutylphenyl)oxirane-2-carboxylate

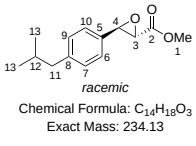

^{1}H NMR (700 MHz, $CDCl_3$): δ/ppm 0.88 (6 H, d, J = 6.6 Hz, H13), 1.84 (1 H, dt, J = 13.3, 6.7 Hz, H12), 2.46 (2 H, d, J = 7.2 Hz, H12), 3.52 (1 H, s, H3), 3.81 (3 H, s, H1), 4.06 (1 H, s, H4), 7.13 (2 H, d, J = 7.8 Hz, H7+9), 7.26 (2 H, d, J = 8.0 Hz, H6+10);

^{13}C NMR (176 MHz, $CDCl_3$): δ/ppm 22.3 (C13), 30.2 (C12), 45.1 (C11), 52.5 (C1), 56.6 (C3), 58.0 (C4), 125.6 (C6+10), 129.4 (C7+9), 132.1 (C8), 142.8 (C5), 168.7 (C2).

Literature data not available.

24.4 Methyl 3-(4-methoxyphenyl)oxirane-2-carboxylate

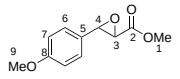

Chemical Formula: $C_{11}H_{12}O_4$
Exact Mass: 208.07

Procedure:

General procedure A. The ratio of *trans* to *cis* isomers was 1.4:1.

cis-Methyl 3-(4-methoxyphenyl)oxirane-2-carboxylate

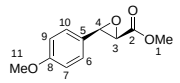

racemic
Chemical Formula: $C_{11}H_{12}O_4$
Exact Mass: 208.07

^{1}H NMR (400 MHz, $CDCl_3$): δ/ppm 3.70 (3 H, s, H1/11), 3.83 (3 H, s, H1/11), 4.45 (1 H, d, J = 6.7 Hz, H3), 5.11 (1 H, d, J = 6.7 Hz, H4), 6.91 (2 H, d, J = 8.8 Hz, H6/7/9/10), 7.38 (2 H, d, J = 8.5 Hz, H6/7/9/10);
^{13}C NMR (101 MHz, $CDCl_3$): δ/ppm 53.5 (C1), 61.4 (C11), 68.7 (C3), 76.4 (C4), 125.8 (C5), 128.6 (C6/7/9/10), 129.7 (C6/7/9/10), 131.9 (C6/7/9/10), 136.9 (C8), 169.0 (C2).
LC-MS: R_t = 2.89 min, m/z 250.1 $[M+MeCN+H]^+$.

trans-Methyl 3-(4-methoxyphenyl)oxirane-2-carboxylate

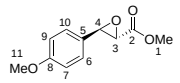

racemic
Chemical Formula: $C_{11}H_{12}O_4$
Exact Mass: 208.07

^{1}H NMR (400 MHz, $CDCl_3$): δ/ppm 3.54 (1 H, d, J = 1.8 Hz, H3), 3.84 (3 H, s, H1/11), 3.85 (3 H, s, H1/11), 4.07 (1 H, d, J = 1.8 Hz, H4), 6.92 (2 H, d, J = 8.8 Hz, H6/7/9/10), 7.24 (2 H, d, J = 8.7 Hz, H6/7/9/10);
^{13}C NMR (101 MHz, $CDCl_3$): δ/ppm 52.6 (C1), 55.4 (C11), 56.6 (C3), 58.0 (C4), 114.2 (C6/7/9/10), 126.7 (C5), 127.2 (C6/7/9/10), 160.3 (C8), 168.8 (C2).
LC-MS: R_t = 2.83 min, m/z 250.1 $[M+H]^+$.

Reference[73]

24.5 Methyl 3-(3-methoxyphenyl)oxirane-2-carboxylate

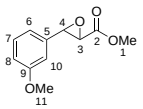

Chemical Formula: $C_{11}H_{12}O_4$
Exact Mass: 208.07

Procedure:

General procedure A. The ratio of *trans* to *cis* isomers was 1.8:1.

cis-Methyl 3-(3-methoxyphenyl)oxirane-2-carboxylate

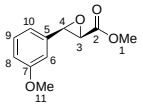

racemic

Chemical Formula: $C_{11}H_{12}O_4$
Exact Mass: 208.07

^{1}H NMR (700 MHz, $CDCl_3$): δ/ppm 3.70 (3 H, s, H1), 3.80 (3 H, s, H11), 4.46 (1 H, d, J = 6.1 Hz, H3), 5.13 (1 H, d, J = 6.1 Hz, H4), 6.86 (1 H, dd, J = 8.2, 2.5 Hz, H6/8/10), 6.90-6.96 (2 H, m, H6/8/10), 7.27 (1 H, t, J = 7.9 Hz, H9);
^{13}C NMR (176 MHz, $CDCl_3$): δ/ppm 53.0 (C1), 55.3 (C11), 62.7 (C3), 74.2 (C4), 112.0 (C6/8/10), 114.3 (C6/8/10), 118.7 (C6/8/10), 129.6 (C9), 139.7 (C5), 159.7 (C7), 168.4 (C2).
LC-MS: R_t = 2.70 min, m/z 250.1 $[M+MeCN+H]^+$; HR-MS calculated for $C_{13}H_{16}NO_4$ at 250.1079, found 250.1088 (Δ = +3.6 ppm).

trans-Methyl 3-(3-methoxyphenyl)oxirane-2-carboxylate

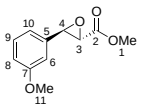

racemic

Chemical Formula: $C_{11}H_{12}O_4$
Exact Mass: 208.07

^{1}H NMR (700 MHz, $CDCl_3$): δ/ppm 3.49 (1 H, d, J = 1.7 Hz, H3), 3.79 (3 H, s, H11), 3.82 (3 H, s, H1), 4.07 (1 H, d, J = 1.6 Hz, H4), 6.79 (1 H, s, H6), 6.88 (2 H, t, J = 8.3 Hz, H8+10), 7.27 (1 H, d, J = 7.9 Hz, H9);
^{13}C NMR (176 MHz, $CDCl_3$): δ/ppm 52.6 (C1), 55.3 (C11), 56.4 (C3), 57.9 (C4), 110.8 (C6), 114.7 (C8/10), 118.2 (C8/10), 129.7 (C9), 136.5 (C5), 159.9

(C7), 168.6 (C2).
LC-MS: R_t = 2.90 min, m/z 250.1 $[M+MeCN+H]^+$.

Literature data not available.

24.6 Methyl 3-(2-methoxyphenyl)oxirane-2-carboxylate

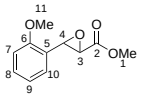

Chemical Formula: $C_{11}H_{12}O_4$
Exact Mass: 208.07

Procedure:

General procedure A. The two diastereomers were not separated from the starting material. The ratio of *trans* to *cis* isomers was 1.8:1.

Major diastereomer (*trans*)

^{1}H NMR (400 MHz, $CDCl_3$): δ/ppm 3.42 (1 H, d, J = 1.8 Hz, H3), 3.81 (3 H, s, H11), 3.83 (3 H, s, H1), 4.43 (1 H, d, J = 1.7 Hz, H4), 6.86-6.94 (1 H, m, H7/8/9/10), 7.27-7.31 (3 H, m, H7/8/9/10).

Minor diastereomer (*cis*)

^{1}H NMR (400 MHz, $CDCl_3$): δ/ppm 3.73 (3 H, s, H1), 3.84 (3 H, s, H11), 4.83 (1 H, d, J = 4.4 Hz, H3), 5.47 (1 H, d, J = 4.4 Hz, H4), 6.86-6.94 (1 H, m, H7/8/9/10), 7.13 (1 H, dd, J = 7.6, 1.7 Hz, H7/8/9/10), 7.27-7.31 (1 H, m, H7/8/9/10).

Reference[74]

24.7 Methyl 3-(3-bromophenyl)oxirane-2-carboxylate

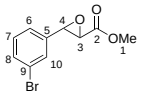

Chemical Formula: $C_{10}H_9BrO_3$
Exact Mass: 255.97

Procedure:

General procedure A. The ratio of *trans* to *cis* isomers was 2.5:1.

cis-Methyl 3-(3-bromophenyl)oxirane-2-carboxylate

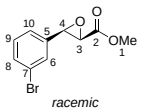

racemic
Chemical Formula: $C_{10}H_9BrO_3$
Exact Mass: 255.97

^{1}H NMR (700 MHz, $CDCl_3$): δ/ppm 3.73 (3 H, s, H1), 4.43 (1 H, d, J = 5.7 Hz, H3), 5.14 (1 H, d, J = 5.7 Hz, H4), 7.23 (1 H, t, J = 7.9 Hz, H9), 7.30 (1 H, d, J = 7.2 Hz, H8/10), 7.46 (1 H, d, J = 8.7 Hz, H8/10), 7.55 (1 H, s, H6);
^{13}C NMR (176 MHz, $CDCl_3$): δ/ppm 53.2 (C1), 62.3 (C3), 73.5 (C4), 122.7 (C7), 125.1 (C8/10), 129.6 (C6), 130.0 (C9), 131.8 (C8/10), 140.4 (C5), 168.1 (C2).

trans-Methyl 3-(3-bromophenyl)oxirane-2-carboxylate

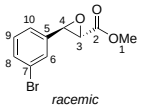

racemic
Chemical Formula: $C_{10}H_9BrO_3$
Exact Mass: 255.97

^{1}H NMR (700 MHz, $CDCl_3$): δ/ppm 3.47 (1 H, d, J = 1.7 Hz, H3), 3.82 (3 H, s, H1), 4.06 (1 H, d, J = 1.6 Hz, H4), 7.17-7.26 (2 H, m, H8/9/10), 7.42 (1 H, s, H6), 7.45-7.49 (1 H, m, H8/9/10);
^{13}C NMR (176 MHz, $CDCl_3$): δ/ppm 52.7 (C1), 56.6 (C3), 57.0 (C4), 122.8 (C7), 124.5 (C8/9/10), 128.7 (C6), 130.2 (C8/9/10), 132.1 (C8/9/10), 137.2 (C5), 168.2 (C2).

Literature data not available.

24.8 Methyl 3-(2-bromophenyl)oxirane-2-carboxylate

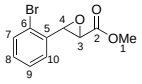

Chemical Formula: $C_{10}H_9BrO_3$
Exact Mass: 255.97

Procedure:

General procedure A. The ratio of *trans* to *cis* isomers was 2.4:1.

cis-Methyl 3-(2-bromophenyl)oxirane-2-carboxylate

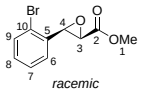

racemic

Chemical Formula: $C_{10}H_9BrO_3$
Exact Mass: 255.97

^{1}H NMR (700 MHz, $CDCl_3$): δ/ppm 3.85 (3 H, s, H1), 4.79 (1 H, d, J = 2.8 Hz, H3), 5.65 (1 H, d, J = 2.6 Hz, H4), 7.20 (1 H, t, J = 7.7 Hz, H8), 7.38 (1 H, t, J = 8.0 Hz, H7), 7.53 (1 H, d, J = 8.0 Hz, H9), 7.63 (1 H, d, J = 6.4 Hz, H6);
^{13}C NMR (176 MHz, $CDCl_3$): δ/ppm 53.4 (C1), 60.1 (C3), 72.1 (C4), 121.3 (C10), 127.4 (C7), 129.5 (C6), 129.9 (C8), 132.6 (C9), 137.3 (C5), 169.1 (C2).

trans-Methyl 3-(2-bromophenyl)oxirane-2-carboxylate

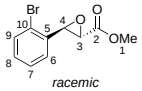

racemic

Chemical Formula: $C_{10}H_9BrO_3$
Exact Mass: 255.97

^{1}H NMR (700 MHz, $CDCl_3$): δ/ppm 3.36 (1 H, d, J = 1.8 Hz, H3), 3.85 (3 H, s, H1), 4.37 (1 H, d, J = 1.6 Hz, H4), 7.19-7.24 (2 H, m, H6+8), 7.31 (1 H, t, J = 7.5 Hz, H7), 7.55 (1 H, dd, J = 8.0, 0.9 Hz, H9);
^{13}C NMR (176 MHz, $CDCl_3$): δ/ppm 52.7 (C1), 55.9 (C3), 57.7 (C4), 122.7 (C10), 126.3 (C6), 127.7 (C7), 130.0 (C8), 132.5 (C9), 134.7 (C5), 168.3 (C2).
LC-MS: R_t = 3.30 min, m/z 298 $[M+MeCN+H]^+$; HR-MS calculated for $C_{12}H_{13}NO_3Br$ at 298.0079, found 298.0081 (Δ = +0.7 ppm).

Reference[75]

24.9 Methyl 3-(3-fluorophenyl)oxirane-2-carboxylate

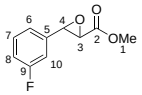

Chemical Formula: $C_{10}H_9FO_3$
Exact Mass: 196.05

Procedure:

General procedure A. The ratio of *trans* to *cis* isomers was 3.1:1.

trans-Methyl 3-(3-fluorophenyl)oxirane-2-carboxylate

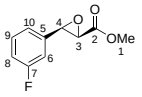

racemic
Chemical Formula: $C_{10}H_9FO_3$
Exact Mass: 196.05

^{1}H NMR (400 MHz, $CDCl_3$): δ/ppm 3.50 (1 H, d, J = 1.7 Hz, H3), 3.85 (3 H, s, H1), 4.12 (1 H, d, J = 1.7 Hz, H4), 6.96-7.38 (4 H, m, H6,8-10);
^{19}F NMR (376 MHz, $CDCl_3$): δ/ppm -112.2 (F9) ppm.
LC-MS: R_t = 2.34 min, m/z 197.2 $[MH]^+$.

Reference[76]

24.10 Methyl 3-[2-(trifluoromethyl)phenyl]oxirane-2-carboxylate

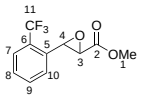

Chemical Formula: $C_{11}H_9F_3O_3$
Exact Mass: 246.05

Procedure:

General procedure A. The ratio of *trans* to *cis* isomers was 1:6.75.

trans-Methyl 3-[2-(trifluoromethyl)phenyl]oxirane-2-carboxylate

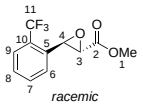

racemic

Chemical Formula: $C_{11}H_9F_3O_3$
Exact Mass: 246.05

^{1}H NMR (400 MHz, $CDCl_3$): δ/ppm 3.85 (3 H, s, H1), 4.59 (1 H, d, J = 3.1 Hz, H3), 5.73 (1 H, d, J = 3.0 Hz, H4), 7.49 (1 H, t, J = 7.7 Hz, H6/7/8/9), 7.60-7.75 (2 H, m, H6/7/8/9), 7.93 (1 H, d, J = 8.0 Hz, H6/7/8/9);
^{19}F NMR (376 MHz, $CDCl_3$): δ/ppm -100.0 (F11).

Literature data not available.

24.11 Methyl 3-(2-methylphenyl)oxirane-2-carboxylate

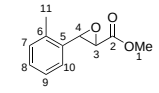

Chemical Formula: $C_{11}H_{12}O_3$
Exact Mass: 192.08

Procedure:

General procedure A. The two diastereomers were not separated from the starting material. The ratio of *trans* to *cis* isomers was 4.4:1.

Major diastereomer (*trans*)

^{1}H NMR (400 MHz, $CDCl_3$): δ/ppm 2.40 (3 H, s, H11), 3.43 (1 H, d, J = 1.9 Hz, H3), 4.24 (1 H, d, J = 1.8 Hz, H4), 7.10-7.29 (4 H, m, H6-9).

Minor diastereomer (*cis*)

^{1}H NMR (400 MHz, $CDCl_3$): δ/ppm 2.39 (3 H, s, H11), 3.67 (3 H, s, H1), 4.58 (1 H, d, J = 6.1 Hz, H3), 5.42 (1 H, d, J = 6.1 Hz, H4), 7.10-7.29 (4 H, m, H6-9).

Reference[68]

References

[1] *Aziridines and Epoxides in Organic Synthesis*, ed. A. K. Yudin, Wiley-VCH, Weinheim, 2006.

[2] E. Erlenmeyer, *Annalen der Chemie*, 1892, **271**, 137–180.

[3] G. Darzens, *Comptes Rendus de l'Académie des Sciences C*, 1904, **139**, 1214–1217.

[4] G. Darzens, *Comptes Rendus de l'Académie des Sciences C*, 1905, **141**, 766–768.

[5] G. Darzens, *Comptes Rendus de l'Académie des Sciences C*, 1906, **142**, 214–215.

[6] G. Darzens, *Comptes Rendus de l'Académie des Sciences C*, 1906, **142**, 714–715.

[7] G. Darzens, *Comptes Rendus de l'Académie des Sciences C*, 1907, **144**, 1123–1124.

[8] G. Darzens, *Comptes Rendus de l'Académie des Sciences C*, 1907, **145**, 1342–1343.

[9] G. Darzens, *Comptes Rendus de l'Académie des Sciences C*, 1910, **150**, 1243–1245.

[10] G. Darzens, *Comptes Rendus de l'Académie des Sciences C*, 1910, **151**, 758–759.

[11] G. Darzens and H. Rost, *Comptes Rendus de l'Académie des Sciences C*, 1911, **152**, 443–436.

[12] G. Darzens and J. Sejourné, *Comptes Rendus de l'Académie des Sciences C*, 1911, **152**, 1105–1107.

[13] G. E. Risinger, *Ph.D. thesis*, Iowa State University, 1961.

[14] T. Rosen, in *Comprehensive Organic Synthesis*, ed. B. Trost and I. Fleming, Pergamon, Oxford, 1st edn., 1991, vol. 2, pp. 409–439.

[15] V. A. Mamedov, V. G. Malaev, F. G. Sibgatullina, I. A. Nuretdinov and Y. P. Kitaev, *Bulletin of the Academy of Sciences of the USSR Division of Chemical Science*, 1992, **41**, 438–441.

[16] V. A. Mamedov, V. L. Polushina, F. F. Mertsalova and I. A. Nuretdinov, *Bulletin of the Academy of Sciences of the USSR Division of Chemical Science*, 1992, **41**, 170–171.

[17] V. A. Mamedov, I. A. Litvinov, O. N. Kataeva, I. K. Rizvanov and I. A. Nuretdinov, *Monatshefte fuer Chemie*, 1994, **125**, 1427–1435.

[18] V. A. Mamedov, E. A. Berdnikov, I. A. Litvinov and L. G. Kuz'mina, *Russian Chemical Bulletin*, 1995, **44**, 1247–1251.

[19] P. Bako, Z. Rapi and G. Keglevich, *Current Organic Synthesis*, 2014, **11**, 361–376.

[20] W. J. Choi and C. Y. Choi, *Biotechnology and Bioprocess Engineering*, 2005, **10**, 167–179.

[21] L. Guo-Qiang, X. Hai-Jian, W. Bi-Chi, G. Guong-Zhong and Z. Wei-Shan, *Tetrahedron Letters*, 1985, **26**, 1233–1236.

[22] F. W. Bachelor and R. K. Bansal, *Journal of Organic Chemistry*, 1968, **34**, 3600–3604.

[23] C. A. Maryanoff, K. L. Sorgi and A. M. Zientek, *Journal of Organic Chemistry*, 1994, **59**, 237–239.

[24] R. F. Pratt and T. C. Bruice, *Journal of the American Chemical Society*, 1970, **92**, 5956–5964.

[25] J. Hine, *Journal of the American Chemical Society*, 1950, **72**, 2438–2445.

[26] W. V. E. Doering and A. Kentaro Hoffman, *Journal of the American Chemical Society*, 1954, **76**, 6162–6165.

[27] H. E. Zimmerman and L. Ahramjian, *Journal of the American Chemical Society*, 1960, **82**, 5459–5466.

[28] D. J. Dagli, P.-S. Yu and J. Wemple, *Journal of Organic Chemistry*, 1975, **40**, 3173–3178.

[29] M. Ballester and D. Perez-Blanco, *Journal of Organic Chemistry*, 1958, **23**, 652.

[30] S. Adams, *Journal of Clinical Pharmacology*, 1992, **32**, 317–323.

[31] J. S. Nicholson and S. Sanders Adams, *Phenyl Propionic Acids*, Boots Pure Drug Company Technical Report US3385886, 1968.

[32] D. D. Lindley, T. A. Curtis, T. R. Ryan, E. M. de la Garza, C. B. Hilton and T. M. Kenesson, *Process for the produdction of 4'-isobutylacetophenone*, Hoechst Celanese Corporation Technical Report US5068448, 1990.

[33] E. Mayo-Wilson, A. Imdad, K. Herzer, M. Y. Yakoob and Z. A. Bhutta, *BMJ*, 2011, **343**, d5094.

[34] O. Isler, W. Huber, A. Roneo and M. Kofler, *Helvetica Chimica Acta*, 1947, **30**, 1911–1927.

[35] N. A. Milas, S. Warren Lee, E. Sakal, H. C. Wohlers, N. S. Macdonald, F. X. Grossi and H. F. Wright, *Journal of the American Chemical Society*, 1948, **70**, 1584–1591.

[36] O. Isler, *Pure and Applied Chemistry*, 1979, **51**, 447–462.

[37] P. B. S. Dawadi and J. Lugtenburg, *Molecules*, 2010, **15**, 1825–1872.

[38] G. L. Parker, L. K. Smith and I. R. Baxendale, *Tetrahedron*, 2016, **72**, 1645–1652.

[39] D. J. Aldous, A. J. Dalencon and P. G. Steel, *Organic Letters*, 2002, **4**, 1159–1162.

[40] L. A. Nguyen, H. He and C. Pham-Huy, *International Journal of Biomedical Science*, 2006, **2**, 85–100.

[41] R. Sato, K. Sakamoto, J. Yamazaki and T. Nagao, *European Journal of Pharmacology*, 2002, **434**, 125–131.

[42] S. Ikeda, J.-I. Oka and T. Nagao, *European Journal of Pharmacology*, 1991, **208**, 199–205.

[43] A. Schwartz, P. B. Madan, E. Mohacsi, J. P. O'Brien, L. J. Todaro and D. L. Coffen, *Journal of Organic Chemistry*, 1992, **57**, 851–856.

[44] J. D. Knight, S. J. Sauer and D. M. Coltart, *Organic Letters*, 2011, **13**, 3118–3121.

[45] V. K. Aggarwal, G. Hynd, W. Picoul and J. L. Vasse, *Journal of the American Chemical Society*, 2002, **124**, 9964–9965.

[46] R. Annunziata, S. Banfi and S. Colonna, *Tetrahedron Letters*, 1985, **26**, 2471–2474.

[47] S.-I. Watanabe, R. Hasebe, J. Ouchi, H. Nagasawa and T. Kataoka, *Tetrahedron Letters*, 2010, **51**, 5778–5780.

[48] W.-J. Liu, B.-D. Lv and L.-Z. Gong, *Angewandte Chemie*, 2009, **48**, 6625–6628.

[49] L. He, W.-J. Liu, L. Ren, T. Lei and L.-Z. Gong, *Advanced Synthesis and Catalysis.*, 2010, **352**, 1123–1127.

[50] A. Jonczyk, A. Kwast and M. Makosza, *Journal of the Chemical Society, Chemical Communications*, 1977, 902–903.

[51] M. Fedorynski, K. Wojciechowski, Z. Matacz and M. Makosza, *Journal of Organic Chemistry*, 1978, **43**, 4682–4684.

[52] C. Kimura, K. Kashiwaya, K. Murai and H. Katada, *Industrial and Engineering Chemistry Product Research and Development*, 1983, **22**, 118–120.

[53] E. V. Dehmlow and J. Kinnius, *Journal fuer Praktische Chemie*, 1995, **337**, 153–155.

[54] S. Arai, T. Ishida and T. Shioiri, *Tetrahedron Letters*, 1998, **39**, 8299–8302.

[55] S. Arai and T. Shioiri, *Tetrahedron Letters*, 1998, **39**, 2145–2148.

[56] S. Arai, Y. Shirai, T. Ishida and T. Shioiri, *Tetrahedron*, 1999, **55**, 6375–6386.

[57] S. Arai, Y. Shirai, T. Ishida and T. Shioiri, *Chemical Communications*, 1999, 49–50.

[58] S. Arai and T. Shioiri, *Tetrahedron*, 2002, **58**, 1407–1413.

[59] S. Arai, Y. Suzuki, K. Tokumaru and T. Shioiri, *Tetrahedron Letters*, 2002, **43**, 833–836.

[60] S. Arai, K. Tokumaru and T. Aoyama, *Tetrahedron Letters*, 2004, **45**, 1845–1848.

[61] H. Hamamoto, V. A. Mamedov, M. Kitamoto, N. Hayashi and S. Tsuboi, *Tetrahedron: Asymmetry*, 2000, **11**, 4485–4497.

[62] M. E. Krafft, S. J. R. Twiddle and J. W. Cran, *Tetrahedron Letters*, 2011, **52**, 1277–1280.

[63] Y.-N. Xuan, H.-S. Lin and M. Yan, *Organic and Biomolecular Chemistry*, 2013, **11**, 1815–1817.

[64] B. M. Adger, J. V. Barkley, S. Bergeron, M. W. Cappi, B. E. Flowerdew, M. P. Jackson, R. McCague, T. C. Nugent and S. M. Roberts, *Journal of the Chemical Society, Perkin Transactions 1*, 1997, 3501–3507.

[65] K. Kogure, H. Koyama and K. Nakagawa, *US3959349A*, 1976.

[66] J. Stangl and C. Stritt, *WO2007031286A1*, 2007.

[67] J. D. Surmatis, J. Maricq and A. Ofner, *Journal of Organic Chemistry*, 1958, **23**, 157–162.

[68] C. Wei, J. Ling, H. Shen and Q. Zhu, *Molecules*, 2014, **19**, 8067–8079.

[69] D. Wilcke and T. Bach, *Organic and Biomolecular Chemistry*, 2012, **10**, 6498–6503.

[70] J. A. Hirsch, in *Table of Conformational Energies*, John Wiley Sons, Inc., 1967, pp. 199–222.

[71] M. A. Windsor, D. J. Hermanson, P. J. Kingsley, S. Xu, B. C. Crews, W. Ho, C. M. Keenan, S. Banerjee, K. A. Sharkey and L. J. Marnett, *ACS Medicinal Chemical Letters*, 2012, **3**, 759–763.

[72] F. W. Bachelor and R. K. Bansal, *Journal of Organic Chemistry*, 1968, **34**, 3600–3604.

[73] D. Wilcke and T. Bach, *Organic and Biomolecular Chemistry*, 2012, **10**, 6498–6503.

[74] R. P. Polniaszek and S. E. Belmont, *Synthetic Communications*, 1989, **19**, 221–232.

[75] P. L. Minin and J. C. Walton, *Organic and Biomolecular Chemistry*, 2004, **2**, 2471–2475.

[76] J. Li, J. Li, Y. Xu, Y. Wang, L. Zhang, L. Ding, Y. Xuan, T. Pang and H. Lin, *Natural Product Research*, 2016, **30**, 800–805.

Appendices

Appendix A

Raw data from the HeRo reactor

Run	Batch	Concentration	Temperature	Diameter of work tube	Rotation speed	Drops per se	Production ri	% conversion	Addition rate/ mL/min
1	A	3.73	30	44	7			6	
2	A	3.73	60	44	7			6	
3	A	3.73	90	44	7			12	
4	A	3.73	105	44	7			17	
5	A	3.73	108	44	7			7	
6	A	3.73	123	44	7			11	
7	A	3.73	130	44	7			4	
8	A	3.73	133	44	7			17	
9	A	3.73	137	44	7			57	
10	A	3.73	140	44	7			19	
11	A	3.73	143	44	7			7	
12	A	3.73	147	44	7				
13	A	3.73	125	44	14			26	
14	A	3.73	123	44	14			51	
15	A	3.73	125	44	14			53	
16	A	3.73	125	44	7			31	
17	A	3.73	125	44	7		7.5	14	
18	A	3.73	125	44	14		7.5	17	
19	A	3.73	125	44	14		4.3	28	
20	A	3.73	125	44	21		4.3	6	
21	A	3.73	115	44	14		6	4	
22	A	3.73	115	44	14		10	11	
23	A	3.73	120	36	7		1.56	33	
24	A	3.73	120	36	14			59	
25	A	3.73	120	36	21			66	
26	A	3.73	120	36	28			65	
27	A	3.73	120	36	35			59	
28	A	3.73	120	36	0		5.56	6	
29	A	3.73	120	36	7		4	11	
30	A	3.73	120	36	14		3.45	19	
31	A	3.73	120	36	21		2.94	33	
32	A	3.73	120	36	28		2.63	37	

Run	Batch	Concentration	Temperature	Diameter of work tube	Rotation speed	Drops per se	Production ri	% conversion	Addition rate/ mL/min
33	A	3.73	120	36	35		1.92	47	
34	A	3.73	120	36	7	1		29	1.689
35	A	3.73	120	36	14	1		45	1.689
36	A	3.73	120	36	21	1		28	1.689
37	A	3.73	120	36	28	1			1.689
38	A	3.73	120	36	35	1			1.689
39	A	3.73	120	36	7	1.5		9	2.5335
40	A	3.73	120	36	14	1.5		11	2.5335
41	A	3.73	120	36	21	1.5		7	2.5335
42	A	3.73	120	36	28	1.5		14	2.5335
43	B	7.46	120	36	0	1.1		2	1.8579
44	B	7.46	120	36	7	1.1		6	1.8579
45	B	7.46	120	36	14	1.1		7	1.8579
46	B	7.46	120	36	21	1.1		14	1.8579
47	B	7.46	120	36	28	1.1		14	1.8579
48	B	7.46	120	36	35	1.1		12	1.8579
49	B	7.46	120	36	7	0.4	0.84	11	0.6756
50	B	7.46	120	36	14	0.4	0.79	18	0.6756
51	B	7.46	120	36	21	0.4	0.58	15	0.6756
52	B	7.46	120	36	28	0.4	0.57	12	0.6756
53	B	7.46	120	36	35	0.4	0.48	14	0.6756
54	B	7.46	120	36	7	1.8	3	7	3.0402
55	B	7.46	120	36	14	1.8	3.33	7	3.0402
56	B	7.46	120	36	21	1.8	3	9	3.0402
57	B	7.46	120	36	28	1.8	3.33	7	3.0402
58	B	7.46	120	36	35	1.8	2.67	9	3.0402
59	B	7.46	120	36	7	0.9	1.46	11	1.5201
60	B	7.46	120	36	14	0.9	1.24	15	1.5201
61	B	7.46	120	36	21	0.9	1.09	15	1.5201
62	B	7.46	120	36	28	0.9	1.02	23	1.5201
63	B	7.46	120	36	35	0.9	0.91	17	1.5201
64	A	3.73	120	36	35	1	1.94	40	1.689

Run	Batch	Concentration	Temperature	Diameter of work tube	Rotation speed	Drops per se	Production ri	% conversion	Addition rate/ mL/min
65	A	3.73	120	36	42	1	1.56	36	1.689
66	A	3.73	120	36	49	1	1.3	54	1.689
67	A	3.73	120	36	56	1	1.13	73	1.689
68	A	3.73	120	36	63	1	0.97	63	1.689
69	A	3.73	120	36	70	1	0.88	54	1.689
70	C	3.73	70	36	20	1.4		6	2.3646
71	C	3.73	70	36	40	1.4		14	2.3646
72	C	3.73	70	36	60	1.4		23	2.3646
73	C	3.73	80	36	20	1.4		21	2.3646
74	C	3.73	80	36	40	1.4		23	2.3646
75	C	3.73	80	36	60	1.4		38	2.3646
76	C	3.73	90	36	20	1.4		32	2.3646
77	C	3.73	90	36	40	1.4		35	2.3646
78	C	3.73	90	36	60	1.4		43	2.3646
79	C	3.73	100	36	20	1.4		54	2.3646
80	C	3.73	100	36	40	1.4		58	2.3646
81	C	3.73	100	36	60	1.4		61	2.3646
82	C	3.73	110	36	20	1.4		65	2.3646
83	C	3.73	110	36	40	1.4		74	2.3646
84	C	3.73	110	36	60	1.4		78	2.3646
85	C	3.73	120	36	20	1.4		80	2.3646
86	C	3.73	120	36	40	1.4		89	2.3646
87	C	3.73	120	36	60	1.4		91	2.3646
88	C	3.73	130	36	20	1.4		90	2.3646
89	C	3.73	130	36	40	1.4		94	2.3646
90	C	3.73	130	36	60	1.4		89	2.3646
91	C	3.73	110	36	30	1.4		66	2.3646
92	C	3.73	110	36	50	1.4		68	2.3646
93	C	3.73	110	36	70	1.4		73	2.3646
94	C	3.73	110	36	80	1.4		71	2.3646
95	C	3.73	120	36	30	1.4		79	2.3646
96	C	3.73	120	36	50	1.4		84	2.3646

Run	Batch	Concentration	Temperature	Diameter of work tube	Rotation speed	Drops per se	Production ri	% conversion	Addition rate/ mL/min
97	C	3.73	120	36	70	1.4		89	2.3646
98	C	3.73	120	36	80	1.4		88	2.3646
100	D	3.73	120	36	85	0.7		86	1.1823
101	D	3.73	120	36	90	0.7		92	1.1823
102	D	3.73	120	36	95	0.7		92	1.1823
103	D	3.73	120	36	100	0.7		90	1.1823
104	D	3.73	120	36	105	0.7		94	1.1823
105	D	3.73	120	36	110	0.7		100	1.1823
106	D	3.73	120	36	85	0.7		100	1.1823
107	D	3.73	110	36	85	1.4		70	2.3646
108	D	3.73	110	36	90	1.4		71	2.3646
109	D	3.73	110	36	95	1.4		78	2.3646
110	D	3.73	110	36	100	1.4		76	2.3646
111	D	3.73	110	36	105	1.4		78	2.3646
112	D	3.73	110	36	110	1.4		76	2.3646
113	D	3.73		36					
114	D+E	3.73		36					
115	E	3.73		36					
116	E	3.73	120	36	100	1.7		84	2.8713
117	E	3.73	120	36	80	1.7		84	2.8713
118	E	3.73	120	36	60	1.7		89	2.8713
119	E	3.73	120	36	40	1.7		90	2.8713
120	E	3.73	110	36	100	1.7		62	2.8713
121	E	3.73	110	36	80	1.7		62	2.8713
122	E	3.73	110	36	60	1.7		58	2.8713
123	E	3.73	110	36	40	1.7		44	2.8713
124	E	3.73	90	36	40	1.7		12	2.8713
125	E	3.73	70	36	40	1.7		9	2.8713
126	E	3.73		36					
127	E	3.73		36					
128	F	3.73	80	36				28	

Run	Batch	Concentration	Temperature	Diameter of work tube	Rotation speed	Drops per se	Production ri	% conversion	Addition rate/ mL/min
129	F	3.73	80	36				26	
130	F	3.73	80	36				15	
131	F	3.73	80	36				25	
132	F	3.73	80	36				29	
133	F	3.73	80	36				15	
134	F	3.73	80	36				32	
135	F	3.73	80	36				33	
136	F	3.73	80	36				19	
137	F	3.73	100	36		1.8		56	3.0402
138	F	3.73	100	36				67	
139	F	3.73	100	36				48	
140	F	3.73	100	36				73	
141	F	3.73	100	36				75	
142	F	3.73	100	36				69	
143	F	3.73	120	36	70			81	
144	F	3.73	120	36	70			76	
145	F	3.73	120	36	70			70	
146	F	3.73	100	36				77	
147	F	3.73	100	36				79	
148	F	3.73	100	36					
149	F	3.73	120	36	40	1.5		74	2.5335
150	F	3.73	120	36	40			77	
121	F	3.73	120	36	40			75	
152	F	3.73	120	36	70			50	
153	F	3.73	120	36	70			54	
154	F	3.73	120	36	70			49	
155	F	3.73	120	36	100			77	
156	F	3.73	120	36	100			70	
157	F	3.73	120	36	100			81	
158	G	3.73	120	36	100		0	21	
159	G	3.73	120	36	100	1.4	0.5	58	2.3646
160	G	3.73	120	36	100	1.4	1	69	2.3646

Run	Batch	Concentration	Temperature	Diameter of work tube	Rotation speed	Drops per se	Production ri	% conversion	Addition rate/ mL/min
161	G	3.73	120	36	100	1.4	2	82	2.3646
162	G	3.73	120	36	100	1.4	3	89	2.3646
163	G	3.73	120	36	100	1.4	5	82	2.3646
164	G	3.73	120	36	100	1.4	10	86	2.3646
165	G	3.73	120	36	100	1.4	15	95	2.3646
166	G	3.73	120	36	50			88	
167	G	3.73	120	36	50			83	
168	G	3.73	120	36	90			89	
169	G	3.73	120	36	90			84	
170	G	3.73	120	36	70			89	
171	G	3.73	120	36	70			82	
172	G	3.73	120	36	100			85	
173	G	3.73	120	36	100			87	
174	G	3.73	100	36	50	1.8		48	3.0402
175	G	3.73	100	36	50	1.8		50	3.0402
176	G	3.73	100	36	60	1.8		32	3.0402
177	G	3.73	100	36	60	1.8		35	3.0402
178	G	3.73	100	36	90	1.8		30	3.0402
179	G	3.73	100	36	90	1.8		50	3.0402
180	G	3.73	80	36	50	1.8		40	3.0402
181	G	3.73	80	36	50	1.8		34	3.0402
182	G	3.73	80	36	60	1.8		49	3.0402
183	G	3.73	80	36	60	1.8			3.0402
184	G	3.73	80	36	90	1.8			3.0402
185	G	3.73	80	36	90	1.8			3.0402
186	G	3.73	100	36	100	1.4		11	2.3646
187	G	3.73	100	36	100	1.4			2.3646
188	G	3.73	100	36	100	1.4		40	2.3646
189	G	3.73	100	36	100	1.4		40	2.3646
190	G	3.73	100	36	100	1.4		51	2.3646
191	G	3.73	100	36	100	1.4		32	2.3646
192	G	3.73	100	36	100	1.4		64	2.3646

Run	Batch	Concentration	Temperature	Diameter of work tube	Rotation speed	Drops per se	Production r	% conversion	Addition rate/ mL/min
193	G	3.73	100	36	100	1.4		75	2.3646
194	G	3.73	80	36	100	1.8		6	3.0402
195	G	3.73	80	36	100	1.8		6	3.0402
196	G	3.73	80	36	100	1.8		4	3.0402
197	G	3.73	80	36	100	1.8			3.0402
198	G	3.73	80	36	100	1.8		30	3.0402
199	G	3.73	80	36	100	1.8		30	3.0402
200	G	3.73	80	36	100	1.8		32	3.0402
201	G	3.73	80	36	100	1.8		37	3.0402
202	H	3.73	120	36	10	1.6		83	2.7024
203	H	3.73	120	36	10	1.6		82	2.7024
204	H	3.73	120	36	15	1.6		83	2.7024
205	H	3.73	120	36	15	1.6		86	2.7024
206	H	3.73	120	36	20	1.6		81	2.7024
207	H	3.73	120	36	20	1.6		85	2.7024
208	H	3.73	120	36	25	1.6		86	2.7024
209	H	3.73	120	36	25	1.6		84	2.7024
210	H	3.73	120	36	30	1.6		86	2.7024
211	H	3.73	120	36	30	1.6		92	2.7024
212	H	3.73	120	36	35	1.6		88	2.7024
213	H	3.73	120	36	35	1.6		84	2.7024
214	H	3.73	120	36	37	1.6		86	2.7024
215	H	3.73	120	36	37	1.6		87	2.7024
216	H	3.73	120	36	40	1.6		86	2.7024
217	H	3.73	120	36	40	1.6		88	2.7024

Appendix B

% Conversion data and calculations from the HeRo reactor

Run	MA integral	CA integral	Coumalic acid integral * 2	Total = MA + 2CA	% conversion = 2CA/ (MA + 2CA) * 100
1	1	0.03	0.06	1.06	6
2	1	0.03	0.06	1.06	6
3	1	0.07	0.14	1.14	12
4	1	0.1	0.2	1.2	17
5	1	0.04	0.08	1.08	7
6	1	0.06	0.12	1.12	11
7	1	0.02	0.04	1.04	4
8	1	0.1	0.2	1.2	17
9	1	0.65	1.3	2.3	57
10	1	0.12	0.24	1.24	19
11	1	0.04	0.08	1.08	7
12	X		0		
13	1	0.18	0.36	1.36	26
14	1	0.53	1.06	2.06	51
15	1	0.57	1.14	2.14	53
16	1	0.22	0.44	1.44	31
17	1	0.08	0.16	1.16	14
18	1	0.1	0.2	1.2	17
19	1	0.19	0.38	1.38	28
20	1	0.03	0.06	1.06	6
21	1	0.02	0.04	1.04	4
22	1	0.06	0.12	1.12	11
23	1	0.25	0.5	1.5	33
24	1	0.72	1.44	2.44	59
25	1	0.96	1.92	2.92	66
26	1	0.92	1.84	2.84	65
27	1	0.72	1.44	2.44	59
28	1	0.03	0.06	1.06	6
29	1	0.06	0.12	1.12	11
30	1	0.12	0.24	1.24	19
31	1	0.25	0.5	1.5	33
32	1	0.29	0.58	1.58	37

Run	MA integral	CA integral	Coumalic acid integral * 2	Total = MA + 2CA	% conversion = 2CA/ (MA + 2CA) * 100
33	1	0.45	0.9	1.9	47
34	2.89	0.6	1.2	4.09	29
35	1	0.41	0.82	1.82	45
36	1	0.19	0.38	1.38	28
37	X		0		
38	X		0		
39	1	0.05	0.1	1.1	9
40	1	0.06	0.12	1.12	11
41	1	0.04	0.08	1.08	7
42	1	0.08	0.16	1.16	14
43	1	0.01	0.02	1.02	2
44	1	0.03	0.06	1.06	6
45	1	0.04	0.08	1.08	7
46	1	0.08	0.16	1.16	14
47	1	0.08	0.16	1.16	14
48	1	0.07	0.14	1.14	12
49	1	0.06	0.12	1.12	11
50	1	0.11	0.22	1.22	18
51	1	0.09	0.18	1.18	15
52	1	0.07	0.14	1.14	12
53	1	0.08	0.16	1.16	14
54	1	0.04	0.08	1.08	7
55	1	0.04	0.08	1.08	7
56	1	0.05	0.1	1.1	9
57	1	0.04	0.08	1.08	7
58	1	0.05	0.1	1.1	9
59	1	0.06	0.12	1.12	11
60	1	0.09	0.18	1.18	15
61	1	0.09	0.18	1.18	15
62	1	0.15	0.3	1.3	23
63	1	0.1	0.2	1.2	17
64	1	0.34	0.68	1.68	40

Run	MA integral	CA integral	Coumalic acid integral * 2	Total = MA + 2CA	% conversion = 2CA/ (MA + 2CA) * 100
65	1	0.28	0.56	1.56	36
66	0.64	0.37	0.74	1.38	54
67	0.41	0.55	1.1	1.51	73
68	1	0.86	1.72	2.72	63
69	0.71	0.42	0.84	1.55	54
70	1	0.03	0.06	1.06	6
71	1	0.08	0.16	1.16	14
72	1	0.15	0.3	1.3	23
73	1	0.13	0.26	1.26	21
74	1	0.15	0.3	1.3	23
75	1	0.31	0.62	1.62	38
76	1	0.23	0.46	1.46	32
77	1	0.27	0.54	1.54	35
78	1	0.38	0.76	1.76	43
79	1	0.58	1.16	2.16	54
80	1	0.68	1.36	2.36	58
81	1	0.78	1.56	2.56	61
82	1	0.94	1.88	2.88	65
83	1	1.44	2.88	3.88	74
84	1	1.8	3.6	4.6	78
85	1	1.98	3.96	4.96	80
86	1	4.24	8.48	9.48	89
87	1	5.29	10.58	11.58	91
88	1	4.51	9.02	10.02	90
89	1	7.51	15.02	16.02	94
90	1	4.13	8.26	9.26	89
91	1	0.96	1.92	2.92	66
92	1	1.06	2.12	3.12	68
93	1	1.34	2.68	3.68	73
94	1	1.25	2.5	3.5	71
95	1	1.93	3.86	4.86	79
96	1	2.58	5.16	6.16	84

Run	MA integral	CA integral	Coumalic acid integral * 2	Total = MA + 2CA	% conversion = 2CA/ (MA + 2CA) * 100
97	1	4.1	8.2	9.2	89
98	1	3.82	7.64	8.64	88
99	X		0		
100	1	3.17	6.34	7.34	86
101	1	5.425	10.85	11.85	92
102	1	5.64	11.28	12.28	92
103	1	4.27	8.54	9.54	90
104	1	7.69	15.38	16.38	94
105	0	1	2	2	100
106	0	1	2	2	100
107	1	1.14	2.28	3.28	70
108	1	1.195	2.39	3.39	71
109	1	1.735	3.47	4.47	78
110	1	1.585	3.17	4.17	76
111	1	1.73	3.46	4.46	78
112	1	1.555	3.11	4.11	76
113	1	0.78	1.56	2.56	61
114	1	0.88	1.76	2.76	64
115	1	1.79	3.58	4.58	78
116	1	2.55	5.1	6.1	84
117	1	2.72	5.44	6.44	84
118	1	4.21	8.42	9.42	89
119	1	4.33	8.66	9.66	90
120	1	0.83	1.66	2.66	62
121	1	0.8	1.6	2.6	62
122	1	0.7	1.4	2.4	58
123	1	0.39	0.78	1.78	44
124	1	0.07	0.14	1.14	12
125	1	0.05	0.1	1.1	9
126					
127					
128	1	0.19	0.38	1.38	28

Run	MA integral	CA integral	Coumalic acid integral * 2	Total = MA + 2CA	% conversion = 2CA/ (MA + 2CA) * 100
129	1	0.18	0.36	1.36	26
130	1	0.09	0.18	1.18	15
131	1	0.17	0.34	1.34	25
132	1	0.2	0.4	1.4	29
133	1	0.09	0.18	1.18	15
134	1	0.23	0.46	1.46	32
135	1	0.25	0.5	1.5	33
136	1	0.12	0.24	1.24	19
137	1	0.63	1.26	2.26	56
138	1	1.02	2.04	3.04	67
139	1	0.46	0.92	1.92	48
140	1	1.32	2.64	3.64	73
141	1	1.54	3.08	4.08	75
142	1	1.09	2.18	3.18	69
143	1	2.07	4.14	5.14	81
144	1	1.58	3.16	4.16	76
145	1	1.19	2.38	3.38	70
146	1	1.66	3.32	4.32	77
147	1	1.69	3.38	4.38	77
148			0		
149	1	1.46	2.92	3.92	74
150	1	1.63	3.26	4.26	77
151	1	1.51	3.02	4.02	75
152	1	0.5	1	2	50
153	1	0.58	1.16	2.16	54
154	1	0.49	0.98	1.98	49
155	1	1.64	3.28	4.28	77
156	1	1.14	2.28	3.28	70
157	1	2.09	4.18	5.18	81
158	1	0.13	0.26	1.26	21
159	1	0.68	1.36	2.36	58
160	1	1.1	2.2	3.2	69

Run	MA integral	CA integral	Coumalic acid integral * 2	Total = MA + 2CA	% conversion = 2CA/ (MA + 2CA) * 100
161	1	2.34	4.68	5.68	82
162	1	3.92	7.84	8.84	89
163	1	2.31	4.62	5.62	82
164	1	3.13	6.26	7.26	86
165			0	0	95
166	1	3.61	7.22	8.22	88
167	1	2.37	4.74	5.74	83
168	1	3.89	7.78	8.78	89
169	1	2.64	5.28	6.28	84
170	1	4.01	8.02	9.02	89
171	1	2.34	4.68	5.68	82
172	1	2.83	5.66	6.66	85
173	1	3.34	6.68	7.68	87
174	1	0.46	0.92	1.92	48
175	1	0.5	1	2	50
176	1	0.24	0.48	1.48	32
177	1	0.27	0.54	1.54	35
178	1	0.21	0.42	1.42	30
179	1	0.51	1.02	2.02	50
180	1	0.34	0.68	1.68	40
181	1	0.26	0.52	1.52	34
182	1	0.48	0.96	1.96	49
183			0	0	
184			0	0	
185			0	0	
186	1	0.06	0.12	1.12	11
187			0	0	
188	1	0.33	0.66	1.66	40
189	1	0.33	0.66	1.66	40
190	1	0.52	1.04	2.04	51
191	1	0.24	0.48	1.48	32
192	1	0.87	1.74	2.74	64

Run	MA integral	CA integral	Coumalic acid integral * 2	Total = MA + 2CA	% conversion = 2CA/ (MA + 2CA) * 100
193	1	1.52	3.04	4.04	75
194	1	0.03	0.06	1.06	6
195	1	0.03	0.06	1.06	6
196	1	0.02	0.04	1.04	4
197			0	0	
198	1	0.21	0.42	1.42	30
199	1	0.21	0.42	1.42	30
200	1	0.23	0.46	1.46	32
201	1	0.29	0.58	1.58	37
202	1	2.44	4.88	5.88	83
203	1	2.28	4.56	5.56	82
204	1	2.38	4.76	5.76	83
205	1	3.14	6.28	7.28	86
206	1	2.13	4.26	5.26	81
207	1	2.91	5.82	6.82	85
208	1	2.98	5.96	6.96	86
209	0.77	2.07	4.14	4.91	84
210	1	3.07	6.14	7.14	86
211	1	5.8	11.6	12.6	92
212	1	3.79	7.58	8.58	88
213	1	2.54	5.08	6.08	84
214	1	2.99	5.98	6.98	86
215	1	3.49	6.98	7.98	87
216	1	3.12	6.24	7.24	86
217	1	3.52	7.04	8.04	88
218	1	1.24	2.48	3.48	71
219	1	1.32	2.64	3.64	73
220	1	0.77	1.54	2.54	61
221	1	1.51	3.02	4.02	75
222 X			0		
223	1	1.81	3.62	4.62	78
224 X			0		

Run	MA integral	CA integral	Coumalic acid integral * 2	Total = MA + 2CA	% conversion = 2CA/ (MA + 2CA) * 100
225	X	-			
226	X		0		
227	0.89	0.71	1.42	2.31	61
228	X		0		
229	1	1.02	2.04	3.04	67
230	X		0		
231	1	1.03	2.06	3.06	67
232	X		0		
233	1	2.17	4.34	5.34	81
234	X		0		
235	1	2.07	4.14	5.14	81
236	X		0		